An integrated approach to ciprofloxacin susceptibility analysis and high-throughput bacterial phenotyping in *Salmonella*

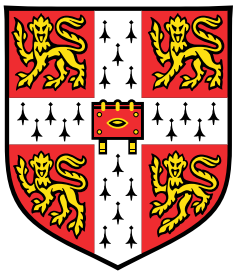

Sushmita Sridhar

Wellcome Sanger Institute; Department of Medicine
University of Cambridge

This dissertation is submitted for the degree of
Doctor of Philosophy

Downing College September 2020

Declaration

I hereby declare that except where specific reference is made to the work of others, the contents of this dissertation are original and have not been submitted in whole or in part for consideration for any other degree or qualification in this, or any other university. This dissertation is my own work and contains nothing which is the outcome of work done in collaboration with others, except as specified in the text and Acknowledgements. This dissertation contains fewer than 60,000 words excluding appendices, bibliography, footnotes, and tables.

Sushmita Sridhar
September 2020

Acknowledgements

The world is full of obvious things which nobody by any chance ever observes.

- Sherlock Holmes, *The Hound of the Baskervilles*

Sherlock Holmes was no microbiologist, but this quote seems to ring true for biology. If I have learned anything during my PhD, it is to how to be a more critical observer of microbiological phenomena and follow those observations with hypotheses, experiments and analysis. It goes without saying that I have benefited from an incredible amount of support and encouragement during this process, first and foremost from an incredible set of supervisors: Gordon Dougan, Stephen Baker, and Nick Thomson. In particular, thanks to Doog for the conception of a challenging and stimulating project, always having an eye on the bigger picture, and being available anytime for a 'quick chat'. It has been a privilege to be in your group, and I cannot have asked for a better mentor. Thanks to Steve Baker for suggesting several of the (most time-consuming) experiments, all of which were incredibly useful. Thanks also for your boundless enthusiasm for discussing science and your unstinting support and leadership during the SARS-CoV-2 testing. Thanks to Nick Thomson for support at Sanger and critical high-level project advice and feedback at various intervals. I also owe an enormous thanks to Stanley Falkow, my first microbiology mentor.

I have been incredibly fortunate in my colleagues, many of whom have helped with various aspects of my project, from scientific discussions to protocol optimization. Thanks to Derek Pickard for helping generate mutant derivatives, optimize protocols, perform experiments, and data analysis support. I have learned so much from you, and it has been a pleasure to work with you in the lab. Thanks also to Sally Forrest, who has been indispensable in optimizing *Salmonella* imaging on the Opera Phenix and discussing data, and who is one of

the most thoughtful scientists I know. I am also grateful to Josefin Bartholdson Scott, Ben Warne, and Mailis Maes for considerable assistance in early project design and pioneering many of the high-content imaging protocols. A massive thank you to Sandra Van Puyvelde, who helped me develop my project, taught me phylogenetic analyses, and who has been instrumental in acquiring ST313 isolates for this work. It has been so much fun thinking through hypotheses and experiments with you, and your mentorship and friendship have been a highlight of my PhD. I am also thankful for the guidance and mentorship of Christine Boinett, who taught me TraDIS data analysis and provided considerable insight into my RNA-seq findings, as well as much laughter over Skype on Wednesday mornings.

Many of the bacterial isolates and methods used in this work were obtained or generated in collaboration with others. Special thanks to Jan Jacobs and Liselotte Hardy at the Institute of Tropical Medicine, Antwerp, and Octavie Lunguya at the National Institute for Biomedical Research, Democratic Republic of Congo, for providing many of the *S.* Typhimurium isolates. Additional thanks to Florian Marks, Hyonjin Jeon, and Ursula Panzner at the International Vaccine Institute and Rob Kingsley at the Quadram Institute for *S.* Typhimurium isolates. The *S.* Typhimurium D23580 TraDIS library used in this study was generated by Moataz Abd El Ghany (University of Sydney) and validated by Edna Ondari (Swiss Tropical and Public Health Institute). Organoid experiments were conducted by Emily Lees. Thanks to Dave Goulding and Claire Cormie for performing electron microscopy on various isolates. Thanks to Kirill Tsyganov and Rhys Dunstan at Monash University as well as Victoria Offord at Sanger for help with transcriptomic analyses. Thanks to Sally Kay for lab support and Pathogen Informatics for bioinformatic support at Sanger.

I am also thankful for an incredible group of friends, in Cambridge and across the world. In particular, Elsa Kentepozidou, Hannah Currant, Harald Vöhringer, Gal Horesh, Tapoka Mkandawire, and Emily Hoyt. Thanks to Uttara Parthap and Sarah Kaewert for many laughs and adventures, and Emily Lees, who has been a friend, colleague, mentor, and biscuit co-conspirator, all wrapped into one. Thanks to Oliwia Baney, Natalie Rich, and Miguel Boluda, who have provided much motivation from abroad. Thanks to the Queens' College Grad Choir and Cambridge University Ceilidh Band for keeping me grounded.

Finally, I could not have done this without the unconditional love and support of my family. Thanks in particular to my dad for helping format this thesis. To my sister Sunita, brother-in-law Shavi, and parents Viji and Sridhar—you inspire me. Thank you for everything.

Abstract

An integrated approach to ciprofloxacin susceptibility analysis and high-throughput bacterial phenotyping in *Salmonella*

Sushmita Sridhar

Antimicrobial resistance is a growing threat across the world. *Salmonella* are Gram-negative, motile, rod-shaped bacteria that are transmitted through the faecal-oral route and invade the small intestine to cause self-limiting gastroenteritis or invasive, systemic disease. Invasive non-typhoidal *Salmonella* are a significant cause of bacterial infection globally, and the ST313 lineage of *Salmonella* Typhimurium are responsible for much of the burden of salmonellosis in sub-Saharan Africa. In recent years, there has been a drastic rise in multidrug resistance within this lineage, including fluoroquinolone resistance, a first line antimicrobial against invasive *Salmonella* species. In this thesis, I have explored the response of *Salmonella* Typhimurium (*S.* Typhimurium) to ciprofloxacin, a fluoroquinolone, using a combination of methodologies. In particular, this work was targeted at better understanding ciprofloxacin susceptibility in invasive non-typhoidal *S.* Typhimurium in sub-Saharan Africa. I began by assessing growth of *S.* Typhimurium in the presence of ciprofloxacin, finding that *S.* Typhimurium is capable of growth in concentrations of ciprofloxacin above the minimum inhibitory concentration (MIC). I have developed high-content imaging methodologies to screen *Salmonella* grown in the presence of ciprofloxacin. These morphological data suggest that there may be heterogeneous subpopulations with differential responses to ciprofloxacin, which was supported by studying the bacterial transcriptional response, and this may influence survival during ciprofloxacin treatment and interactions with host cells. Additionally, ciprofloxacin exposure triggers a bacterial stress response that appears to be distinct from responses generated by other stressors. Finally, I have investigated the genomic and phenotypic differences of a larger set of related *S.* Typhimurium ST313 isolates with

an array of susceptibilities to ciprofloxacin. High-content screening has shown that isolates appear to differ in their morphological signature depending on their genetic makeup. Together these data suggest that the study of the bacterial response to ciprofloxacin and integration of genotyping and phenotyping could significantly enhance our understanding of antimicrobial resistance and help guide appropriate antimicrobial usage.

Table of contents

List of figures **xix**

List of tables **xxv**

1 Introduction **1**

1.1 The global burden of infectious diseases including *Salmonella* 1

1.1.1 Definition of *Salmonella enterica* by classical phenotyping and genotyping using MultiLocus Sequence Typing (MLST) 2

1.1.2 Burden of all *Salmonella* serovars 4

1.1.3 Brief description of *S*. Typhi and *S*. Paratyphi 5

1.1.4 Burden of non-typhoidal *Salmonella* 7

1.1.5 Host distribution and transmission of *S*. Typhimurium 8

1.1.6 Phylogeny of *S*. Typhimurium 9

1.1.7 Disease presentation and treatment of *S*. Typhimurium in humans . 10

1.1.8 Human infection by *S*. Typhimurium 11

1.2 Invasive non-typhoidal *Salmonella* compared to other non-typhoidal strains, an overview 12

1.2.1 Global distribution of iNTS 14

1.2.2 Disease presentation and treatment of iNTS 16

1.2.3 Risk factors for iNTS disease 16

1.2.4 Genetic factors characterizing/influencing *S*. Typhimurium iNTS . . 18

1.2.5 Phylogeny of iNTS 19

1.3 iNTS in sub-Saharan Africa 19

1.3.1 *S*. Typhimurium ST313 as major contributors to iNTS 20

1.3.2 Brief description of *S*. Enteritidis 20

1.3.3 iNTS surveillance in Africa 21

1.3.4 Phylogeny of *S*. Typhimurium ST313s 22

1.3.5 Genetic and phenotypic characteristics of ST313 reference strain D23580 24

1.4 AMR in *Salmonella* 26

1.4.1 WHO R&D 'directive' on FQR *Salmonella* 27

1.4.2 How AMR is assessed in clinical settings 28

1.4.3 Distribution of fluoroquinolone usage 29

1.4.4 FQR in *S*. Typhi and Paratyphi 30

1.4.5 FQR in *S*. Typhimurium 32

1.4.6 Other AMR profiles in invasive *S*. Typhimurium 33

1.4.7 iNTS vaccines 35

1.5 Fluoroquinolone mechanism of action and resistance 36

1.5.1 Mechanism of action of fluoroquinolones in Gram-negative bacteria 37

1.5.2 Chromosomal resistance to ciprofloxacin in Gram-negative bacteria 38

1.5.3 Plasmid-mediated resistance by *qnr* to ciprofloxacin in Gram-negative organisms 39

1.5.4 Other genes involved in resistance 40

1.5.5 Mechanisms of resistance found in African *S*. Typhimurium ST313 41

1.5.6 Pharmacokinetics/pharmacodynamics of ciprofloxacin 42

1.6 Observation of disconnect between phenotypic and genotypic resistance . . 42

1.6.1 Observation of phenotypic heterogeneity in ST313s 43

1.6.2 'Adaptive resistance' and desensitization to antimicrobials 47

1.6.3 Lack of understanding of additional factors involved in FQR in *S*. Typhimurium 49

1.7 Summary 53

2 Materials and Methods **55**

2.1 Bacterial isolates 55

2.1.1 Growth medium and growth conditions 55

2.1.2 Ciprofloxacin susceptibility testing by MIC ETEST 55

2.2 Time kill curves 56

2.2.1 Ciprofloxacin-degradation kill curves 56

2.3 Spontaneous *gyrA* mutant generation and validation 57

2.4 *S.* Typhimurium D23580 bacteria grown for 24 h in ciprofloxacin medium for whole genome sequencing 57

2.5 Whole genome sequencing: library creation and sequencing 58

2.6 Read mapping, variant detection, and SNP analysis 58

2.7 Opera Phenix confocal phenotyping of bacteria 59

2.7.1 Opera Phenix microscopy phenotyping of *S.* Typhimurium bacteria during ciprofloxacin exposure 59

2.7.2 Opera Phenix phenotyping of *S.* Typhimurium ST313 isolates after ciprofloxacin exposure 60

2.7.3 Opera Phenix image analysis 60

2.8 RNA extractions and RNA sequencing 62

2.8.1 RNA extractions from 4 ‘pilot’ isolates under 2x MIC ciprofloxacin exposure 63

2.8.2 RNA extractions of *S.* Typhimurium D23580 under parallel treatment conditions 64

2.8.3 Sucrose gradient separation of ciprofloxacin-treated D23580 64

2.8.4 RNA extractions from *S.* Typhimurium D23580 after sucrose gradient separation 66

2.9 RNA sequencing analysis 66

2.9.1 RNA sequencing analysis of gradient-separated bacteria 66

2.10 Light microscopy of gradient-separated *S.* Typhimurium D23580 bacteria . 67

2.11 Generation of *S.* Typhimurium D23580 single-gene knockout derivatives . . 67

2.12 TraDIS screen on time kill curves of ciprofloxacin-exposed *S.* Typhimurium D23580 68

2.13 TraDIS screen on *S.* Typhimurium D23580 injected into intestinal organoids 69

2.14 Phylogenetic analysis 70

2.14.1 SNP analysis of *S.* Typhimurium ST313 isolates 70

2.15 Pangenome analysis 71

2.16 *In silico* AMR analysis 72

2.17 Biofilm growth conditions 72

2.18 Scanning electron microscopy (SEM) of bacteria grown under stress conditions 73

3 Development of high-content imaging of individual bacteria 75

3.1 Introduction 75

3.2 Optimization of bacterial adhesion for imaging 77

3.3 Optimization of staining for *S.* Typhimurium 80

3.4 Development of an *S.* Typhimurium analysis pipeline 82

3.5 Imaging of antimicrobial-treated bacteria 84

3.6 Discussion 88

4 Characterization of growth dynamics of *S.* Typhimurium following ciprofloxacin exposure 91

4.1 Introduction 91

4.2 Ciprofloxacin susceptibilities of the *S.* Typhimurium isolates 93

4.3 Phenotypic assessment of ciprofloxacin MIC and growth dynamics 94

4.4 Microscopic visualization of isolates exposed to ciprofloxacin 100

4.5 Generation of spontaneous *gyrA* mutations in D23580 and SL1344 107

4.6 Investigation of SNPs involved in desensitization to ciprofloxacin 109

4.7 Discussion 112

5 Investigation of transcriptional response of *Salmonella* Typhimurium under ciprofloxacin exposure 115

5.1 Introduction 115

5.2 Comparative transcriptomics of four *S.* Typhimurium isolates 117

5.3 Investigation of specificity of D23580 transcriptional response to ciprofloxacin 124

5.4 Investigation of transcriptional effect of *gyrA* mutation in *S.* Typhimurium D23580 129

5.5 Transcriptional profile of density-separated D23580 upon ciprofloxacin exposure 131

5.6 Discussion 137

6 TraDIS analysis of *S.* Typhimurium D23580 during ciprofloxacin exposure and infection of intestinal organoids 141

6.1 Introduction 141

6.2 *S.* Typhimurium D23580 transposon mutant library quality control 145

6.3 Required genes in *S.* Typhimurium D23580 after exposure to ciprofloxacin . 147

6.4 *S.* Typhimurium D23580 genes required for the invasion of intestinal organoids 155

6.5 Discussion 156

7 Investigation of genomic and phenotypic characteristics of selected *S.* Typhimurium ST313 isolates with a range of ciprofloxacin susceptibilities 161

7.1 Introduction 161

7.2 Genomic analyses of 108 selected African *S.* Typhimurium isolates 165

7.3 Small-scale high content imaging screen of ciprofloxacin-exposed *S.* Typhimurium ST313 isolates 172

7.4 Assessment of two distinct biofilm morphotypes in *S.* Typhimurium ST313 lineages. 183

7.5 Discussion 187

8 Developing and implementing a SARS-CoV-2 testing workflow in a CL2 research laboratory for screening and viral sequencing 191

8.1 Introduction 191

8.2 A blueprint for the implementation of a validated approach for the detection of SARS-CoV-2 in clinical samples in academic facilities. 193

8.3 Screening of healthcare workers for SARS-CoV-2 highlights the role of asymptomatic carriage in COVID-19 transmission. 194

8.4 Effective control of SARS-CoV-2 transmission between healthcare workers during a period of diminished community prevalence of COVID-19. 194

8.5 Rapid implementation of SARS-CoV-2 sequencing to investigate cases of health-care associated COVID-19: a prospective genomic surveillance study. 195

8.6 Secondary pneumonia in critically ill ventilated patients with COVID-19. . 195

9 Future directions 197

9.1 Further development of genotype-phenotype investigations 197

9.2 Effects of ciprofloxacin on *Salmonella* invasion of host cells 199

9.3 Interaction of *S.* Typhimurium with additional antimicrobials 201

References 203

References for COVID-19 **263**

Appendix A Supplementary Materials and Methods **267**

Appendix B Supplementary Information to Chapter 3 **277**

List of figures

1.1 Radial phylogeny of *S*. Typhimurium. 10

1.2 *Salmonella* invasion strategies of the intestine. 13

1.3 iNTS disability-adjusted life years (DALYs)/100k. 15

1.4 African *S*. Typhimurium ST313 sub-lineage II.1 in context of other African invasive *S*. Typhimurium. 25

1.5 Structure of the fluoroquinolone ciprofloxacin. 36

1.6 Mechanisms of fluoroquinolone resistance. 39

2.1 Assembly of sucrose gradient columns. 65

3.1 High content bacterial imaging and analysis workflow. 76

3.2 Comparison of Opera Phenix plates for *S*. Typhimurium imaging. 78

3.3 Optimization of fixation and temperature conditions for *S*. Typhimurium adhesion. 79

3.4 Comparison of *S*. Typhimurium SL1344 adhesion on 11 coatings and uncoated wells. 80

3.5 Quantification of bacterial single cells adhered to coated plates. 81

3.6 Optimization of staining for *S*. Typhimurium. 82

3.7 Analysis pipeline steps to identify and segment bacterial objects. 83

3.8 Linear classification of bacteria into three categories. 84

3.9 Phenotyping on the Opera Phenix of *S*. Typhimurium after 2 h antimicrobial exposure. 85

3.10 Assessment of ciprofloxacin-treated *S*. Typhimurium after Opera Phenix imaging. 87

4.1 Geographic origin and phylogeny of four chosen *S*. Typhimurium isolates in a global context. 93

4.2 Example of a ciprofloxacin MIC ETEST. 96

4.3 Ciprofloxacin 24 h Time Kill Curves of four *S*. Typhimurium isolates. . . . 97

4.4 TKC measurement of ciprofloxacin sustainability. 99

4.5 Bacteria grown in ciprofloxacin show desensitization over following 24 h. . 100

4.6 Confocal imaging of *S*. Typhimurium D23580 over 24 h of ciprofloxacin exposure. 101

4.7 Confocal microscopy of ciprofloxacin sustainability after 24 h. 102

4.8 Single bacteria per well over 24 h of ciprofloxacin exposure. 104

4.9 *S.* Typhimurium bacterial length over 24 h in total single cell and 4x MIC treated population. 105

4.10 Scanning electron microscopy of *S.* Typhimurium D23580 at 2 and 8 h, 0x or 2x ciprofloxacin MIC exposure. 106

4.11 Characterization of *S.* Typhimurium SL1344 and D23580 spontaneous *gyrA* mutants. 108

4.12 SNP analysis of *S.* Typhimurium D23580 bacteria grown for 24 h in culture medium containing ciprofloxacin. 111

5.1 Heatmaps of differentially expressed genes upon 2 h of 2x ciprofloxacin MIC exposure. 118

5.2 Chromosome maps of differentially expressed genes of the four isolates upon 2 h of 2x ciprofloxacin MIC exposure. 119

5.3 Chromosome maps of differentially expressed genes of the four *S.* Typhimurium isolates after 2 h of 2x ciprofloxacin MIC exposure 121

5.4 Heatmaps of differentially expressed genes upon 8 h of 2x ciprofloxacin MIC exposure. 123

5.5 Chromosome maps of differentially expressed genes of the four *S.* Typhimurium isolates after 8 h of 2x ciprofloxacin MIC exposure. 125

5.6 Time kill curves of D23580Δ*sulA* and D23580 WT. 126

5.7 Heatmaps of differential expression of *S.* Typhimurium D23580 exposed to four different conditions. 127

5.8 Differential expression of *S.* Typhimurium D23580 chromosomal genes in response to four treatments. 128

5.9 Differential expression of D23580**gyrA* relative to *S.* Typhimurium D23580 WT after 2 h. 130

5.10 Differential expression of *S.* Typhimurium D23580 WT and D23580**gyrA* ciprofloxacin-treated relative to NT after 2 h growth. 132

5.11 Schematic of sucrose density gradient fractionation. 133

5.12 Light microscopy of *S.* Typhimurium D23580 separated by density fractionation. 134

5.13 Differential expression of *S.* Typhimurium D23580 bacteria separated by sucrose gradients following 2 h growth. 135

5.14 Chromosome maps of differentially expressed genes of ciprofloxacin-treated *S.* Typhimurium D23580 after sucrose density gradient separation. 136

5.15 Network analysis of genes highly downregulated in ciprofloxacin-treated *S.* Typhimurium D23580 within 60% sucrose gradient relative to 50% sucrose gradient. 137

6.1 Sequencing strategy for TraDIS. 143

6.2 Difference in coverage of matched reads of transposon library with known transposon tag depending on the mismatch threshold used. 146

6.3 Assessment of *S.* Typhimurium D23580 essential genes based on TraDIS. . 148

6.4 Schematic of experiment measuring exposure of *S.* Typhimurium D23580 transposon mutant library to 2x MIC ciprofloxacin. 149

6.5 Venn diagrams of genes required for increase or decrease of ciprofloxacin susceptibility in *S.* Typhimurium D23580 at 2, 10.25, or 24 h post-exposure. 150

6.6 Metabolic pathways implicated by genes required for *S.* Typhimurium D23580 increased ciprofloxacin susceptibility at 2, 10.25, and 24 h post-exposure. . 153

6.7 Chromosome maps of *S.* Typhimurium D23580 genes implicated in increased and decreased susceptibility to 2x MIC ciprofloxacin using TraDIS. 154

6.8 Schematic of organoid invasion experiment using *S.* Typhimurium D23580 transposon insertion library. 155

7.1 Phylogenetic trees of global and 108 selected African *S.* Typhimurium isolates. 166

7.2 Comparison of SNPs in coding regions found in an DCS lineage of ST313 and 82 selected *S.* Typhimurium ST313 isolates. 169

7.3 Choice of 24 *S.* Typhimurium ST313 isolates and workflow for high-content imaging. 173

7.4 Number of analysed *S.* Typhimurium ST313 bacteria analysed per well across three replicates. 174

7.5 SYTOX Green mean fluorescence intensity for each of the 24 *S.* Typhimurium ST313 isolates. 176

7.6 Measurement of the length-to-width ratio across isolates and ciprofloxacin treatments of 24 imaged *S.* Typhimurium ST313 isolates. 177

7.7 Measurement of the DAPI radial relative deviation across isolates and ciprofloxacin treatments of 24 imaged *S.* Typhimurium ST313 isolates. . . . 179

7.8 Measurement of the CSA threshold compactness 60% across isolates and ciprofloxacin treatments of 24 imaged *S.* Typhimurium ST313 isolates. . . . 180

7.9 Principal component analysis of morphological parameters of 24 *S.* Typhimurium ST313 isolates following 0 or 1 μg/ml ciprofloxacin treatment. . 182

7.10 Principal component analysis of morphological parameters of 5 *S.* Typhimurium ST313 isolates with "intermediate" ciprofloxacin susceptibility following four different ciprofloxacin treatments. 183

7.11 Colony morphotypes of *S.* Typhimurium bacteria grown under biofilm-forming conditions. 184

7.12 Scanning electron microscopy and phylogeny of selected *S.* Typhimurium ST313 lineage II and lineage II.1 isolates grown under biofilm-forming conditions. 186

List of tables

2.1 *S.* Typhimurium isolates and respective ciprofloxacin MIC linked concentrations used to generate growth curves. 56

2.2 Preparation of *S.* Typhimurium D23580 and VNS20081 cultures for imaging. 61

2.3 Treatment conditions for *S.* Typhimurium D23580 and D23580**gyrA*. . . . 64

2.4 Primer sequences for gene knockouts. 68

2.5 Components of RDAR agar plates (1 L). 72

2.6 Isolates for RDAR growth and SEM. 73

3.1 *Z*'-statistics for the 20 most important parameters to distinguish between ciprofloxacin-treated (2x MIC) and non-treated *S.* Typhimurium. 88

4.1 Ciprofloxacin susceptibility of four *S.* Typhimurium isolates. 94

4.2 *In silico* AMR analysis of four *S.* Typhimurium isolates. 95

6.1 Genes associated with increased ciprofloxacin susceptibility in common across time points. 151

7.1 Coding SNPs found in highest MIC isolates compared to lower MIC isolates. 170

7.2 Drug-associated genes containing SNPs amongst ST313 isolates. 170

A.1 All *S.* Typhimurium isolates used in this thesis 272

A.2 *S.* Typhimurium ST313 isolates phenotyped on Opera Phenix 272

B.1 Final plate coatings chosen for isolates used in Opera Phenix imaging. 277

B.2 Gram-negative rods analysis pipeline (Harmony v4.9). 277

B.3 Antimicrobials and determined MICs used for Opera Phenix imaging optimization. 277

B.4 *Z*' statistics of S. Typhimurium D23580 treated for 2 h with 2x MIC ciprofloxacin versus no treatment. 287

1. Introduction

1.1 The global burden of infectious diseases including *Salmonella*

In economically developed regions of the world, infectious diseases are sometimes considered a problem of the past. Clearly infections such as the common cold, influenza, travellers-associated and healthcare-associated occur but the burden and impact are somewhat restricted compared to 50 years ago. However, infectious diseases remain a significant cause of morbidity and mortality across the globe, particularly in resource restricted settings such as Lower and Middle Income Countries (LMICs). According to the Global Burden of Disease Study 2017, the global incidence of communicable diseases, including TB, malaria, and HIV/AIDS, is on the order of 25 billion cases[1]. Two other leading causes of infectious disease associated with significant health impact are lower respiratory infections and diarrhoeal episodes. There are on the order of two million deaths per year from bacterial infections[2].

Of those, approximately 1.4 million global cases are attributed to diarrhoeal disease, still a significant problem in much of the world, particularly in children[3]. It is estimated that there were an estimated 6.29 billion diarrhoeal episodes in 2017, with an approximated 1.16 billion cases in children under 5 years, although this estimate is difficult to accurately assess[1,4].

Many of these infections occur in settings where healthcare and access to clean water is limited, and there are severe repercussions on longer term health and economic productivity[1]. It is estimated that in LMICs, the 842,000 deaths that are estimated to occur annually from diarrhoeal disease are attributable to a lack of clean water, sanitation and hygiene[5]. Of diarrhoeal diseases, in 2015 the leading cause of mortality from diarrhoeal disease was estimated to be rotavirus, followed by *Shigella* spp and *Salmonella* spp[1,3]. The 2015 Global Burden of Disease Study found diarrhoeal disease to be the ninth leading cause of death globally, and the fourth leading cause of death in children under 5 years, accounting for 499,000 child deaths[3].

1.1.1 Definition of *Salmonella enterica* by classical phenotyping and genotyping using MultiLocus Sequence Typing (MLST)

Salmonella species are a major contributor to systemic and diarrhoeal disease, with approximately 15 million systemic cases and 95.1 million diarrhoeal cases each year[1,3]. *Salmonella* form a group of Gram-negative, foodborne, rod-shaped bacteria that can invade the small intestine to cause limited or, more rarely, systemic infections. They were first described by the scientist Daniel E. Salmon in 1855. *Salmonella* are classified into two species: *Salmonella bongori* (*S. bongori*), which comprises 22 serovars and *Salmonella enterica* (*S. enterica*), which comprises six subspecies and at least 2650 serovars[6–8]. Serovars are traditionally defined using specific antisera. Isolates of serovars within both of these species can infect humans, but serovars within *S. enterica* remain more significant in causing human disease; *S. bongori* is primarily associated with the colonisation of reptiles[9].

Classically, the identification of *Salmonella* serotypes has been done using slide agglutination with specific antisera to distinguish between key surface antigens present on the surfaces of the different serovars. This typing of *Salmonella* can distinguish a serovar predominantly on the basis of the antigenicity of lipopolysaccharide (LPS) O antigen and flagellar antigens (phases 1 and 2 of H antigen, respectively), as described by the White-Kauffman-Le Minor scheme first developed in 1934[6]. There are at least 64 and 114 variants of the O and H antigens, respectively. Several O antigen types may be present on the cell surface of an isolate in conjunction, whereas only one flagellar variant is usually expressed at a time. Agglutination reactions are conducted by mixing the isolate being tested with the specific antisera against the O (encoded by genes including *rfb*) or H (flagella subunit encoded by *fliC* or *fljB*) antigens. In a surveillance setting or a reference laboratory, a large array of O and H antisera is normally used to type the *Salmonella* after culturing. For example, *Salmonella enterica* subspecies *enterica* Typhimurium (*S*. Typhimurium) is reported as 1,4,[5],12;i;1,2, which means that it is in subspecies I of *S. enterica* and it expresses O antigens 4, 12, and sometimes 5[6]. It is "i" for Phase 1 Flagellar (H) antigen and 1,2 for Phase 2 H antigen. The White-Kauffman-Le Minor scheme also includes capsular typing (K), which only applies to a small subset of serovars that harbour this type of surface antigen. *S*. Paratyphi C, *S*. Dublin, and *S*. Typhi isolates can express the Vi polysaccharide, a capsular antigen associated with immunogenicity and virulence[10–13].

More recently, the system of MLST has been advocated as a replacement of serological and biochemical characterizations to distinguish between *S. enterica* on the basis of DNA sequence and the associated evolutionary relatedness[14]. This method groups isolates within a given ST if they share identical alleles for a set of housekeeping genes, and isolates are placed within an ST-based clonal complex if they differ in one or two alleles[6,14,15].

Within *S. enterica*, the over 2500 serovars fit within six subspecies: subspecies I (ssp. I) *enterica*, ssp. II *salamae*, ssp. IIIa *arizonae*, ssp. IIIb *diarizonae*, ssp. IV *houtenae*, ssp. VI *indica*. The vast majority of serovars (approximately 1500) are classified within ssp. I *enterica*, causing over 99% of human and animal infections. Subspecies were previously distinguished from each other on the basis of general phylogeny and biochemical characteristics. O antigens are a key saccharide component of LPS on the surface of the *Salmonella* cell. While the composition differs between serovars, the O-antigen chain is comprised of a main branch of repeating units of sugars, which may contain branching sugars[16–18]. *Salmonella* can express LPS of differing composition and length on their surface, which can impact immune detection. This is an important factor for the development of *Salmonella* vaccines, as the diversity of LPS lengths and accessibility at the bacterial cell surface may compromise the utility of LPS as a suitable antibody target. There are additional characteristics that may be used to distinguish within serovars, including the phage types that may infect and lyse a given strain and other physical and biochemical properties, but these will not be considered further here.

S. enterica serovars and isolates can be arbitrarily further classified into two groupings; typhoidal and non-typhoidal on the basis of disease presentation. Typhoidal *Salmonella* are mainly the serovars Typhi and Paratyphi (A, B, C). Isolates of these serovars are associated with invasive systemic infections classically referred to as typhoid or enteric fever. Isolates of *S*. Typhi and *S*. Paratyphi A only cause a serious typhoid-like infection in humans and are consequently referred to as human-restricted. Isolates of *S*. Typhi and *S*. Paratyphi C can express Vi antigen, whereas *S*. Paratyphi A and B isolates normally do not. Further, *S*. Paratyphi B is actually a complex serovar and, like *S*. Paratyphi C, is now infrequently isolated globally compared to *S*. Typhi and *S*. Paratyphi[19–22].

Other typhoidal serovars can cause a typhoid-like disease in other animals. For instance, *Salmonella enterica* subspecies *enterica* serovar Gallinarum is host-restricted to chickens and causes a chicken typhoidal systemic disease. Interestingly, many host-restricted serovars

have genetically degraded genomes in that they have accumulated inactivated genes known as pseudogenes, and this factor may contribute to their host-restricted phenotype[23,24].

The majority of other serovars fall into the non-typhoidal classification. These include the classical serovars *S*. Typhimurium and *S*. Enteritidis. Isolates of these serovars are predominantly associated with localised gastroenteric disease, but this is not a strict definition as most disease-associated serovars can cause fully invasive infections in some circumstances. Also, in sub-Saharan Africa, isolates of *S*. Typhimurium and *S*. Enteritidis are a common cause of invasive disease[25]. Thus, the typhoidal/non-typhoidal classification is useful but not absolute.

1.1.2 Burden of all *Salmonella* serovars

As a single group of bacteria, *Salmonella* are a leading cause of bacterial infections globally, with approximately 167 million cases each year. The United States Centers for Disease Control estimates that 1.35 million cases arise annually in the United States, causing 26,500 hospitalizations and 420 deaths[26]. *S*. Typhi and *S*. Paratyphi, the leading causes of enteric fever, cause approximately 14.3 million cases and 135,900 deaths annually and are responsible for approximately 76% of enteric fever cases[27].

Together, *S*. Typhi and *S*. Paratyphi are referred to as typhoidal *Salmonella*, and they disproportionately affect people in LMICs, where prevalence is high. This burden is regarded as being highest in South and Southeast Asia, where the incidence rate may be between 200 and 700 cases per 100,000. However, as more studies are undertaken on typhoid in Africa there is an increasing recognition that the disease is very common in some parts of this continent[28,29]. In comparison, in higher income countries, the incidence rate is fewer than 15 cases per 100,000. Globally, there has been a considerable decline in typhoidal disease from 25.9 million cases in 1990 to 14.3 million cases in 2017; however, the burden is still significant. This is particularly true in South Asia, which accounts for 10.3 million (72%) of the 14.3 million cases[27].

Of the global cases of typhoidal *Salmonella*, it is estimated that 76.3% (10.9 million) were infections of *S*. Typhi, and 3.4 million were infections of *S*. Paratyphi. Demographically,

the incidence is highest amongst children between 5 and 9 years in high-incidence regions, followed by children between 1 and 4 years[27]. The fatality rate varies, though is highest in children and the elderly at up to 1.6%, with 17.2% of total deaths in children under 5 years, and 59.3% of total deaths in children under 15 years. The fatality rate is highest in South Asia, followed by sub-Saharan Africa[27]. However, data are sparse from many regions of the world, particularly Oceania and central sub-Saharan Africa, so the true burden of typhoid and paratyphoid fever may be higher than currently estimated[27]. There are also significant problems with the diagnosis of typhoid, which requires well founded laboratories for the gold standard approach of blood culture[19,30,31]. Serological assays are largely unreliable, in part due to the marketing of kits with poor specificity and sensitivity[30,32].

In contrast to typhoidal *Salmonella*, non-typhoidal *Salmonella* cause approximately 153 million cases each year[26]. These cases can be divided into non-typhoidal gastroenteritis and non-typhoidal invasive disease, which have strikingly different distribution, incidence, and fatality rates. CDC figures estimate that the highest rates of non-typhoidal *Salmonella* in US travellers abroad occur in Africa, with an incidence of 25.8 cases per 100,000 air travellers. Invasive non-typhoidal *Salmonella* infections caused by a variety of serovars are responsible for conservatively 534,600 cases and 77,500 deaths annually, or less conservatively 3.4 million cases and 618,316 deaths[33,34]. Because of insufficient surveillance in regions with the highest burdens, it is difficult to assess the true number of cases. Finally, infections localized to the gastrointestinal tract are responsible for nearly 94 million cases and 155,000 deaths annually[4].

1.1.3 Brief description of *S*. Typhi and *S*. Paratyphi

While the focus of this thesis is on non-typhoidal *Salmonella* (NTS) and specifically *S*. Typhimurium, it is important to distinguish NTS from *S*. Typhi and *S*. Paratyphi, the leading causes of enteric fever. Unlike most non-typhoidal infections, *S*. Typhi and Paratyphi cause systemic disease, characterized by lengthy high fevers, headaches, and general malaise, and if left untreated, can be debilitating or deadly. The two infections are difficult to distinguish from each other clinically but more insight has recently been acquired through human challenge studies[35]. These infections are highly associated with poor water supply and sanitation and are found predominantly in LMICs in South and Southeast Asia and sub-Saharan Africa.

Typhoid fever is largely managed using antimicrobials, and the three first-line antimicrobials to treat *S*. Typhi were chloramphenicol, ampicillin, and trimethoprim-sulfamethoxazole, followed by fluoroquinolones, third-generation cephalosporins, and azithromycin[36]. However, the choice of antimicrobial usage shows significant regional variation and in Asia the fluoroquinolones have until recently been the predominant drug of choice[37,38].

South and East Asia have a significant burden of Paratyphi A cases, with nearly 30% of all typhoidal *Salmonella* cases in India and Nepal and above 60% in China being of this serovar[27,35,39]. The number of cases of *S*. Typhi and *S*. Paratyphi is proportionally much lower than that of non-typhoidal *Salmonella* (NTS) globally; however, mortality from systemic infections is much higher when compared with overall NTS. Antimicrobial resistance (AMR) is becoming a key influencer in both typhoidal and non-typhoidal *Salmonella* disease. The incidence rates vary between serovars and by region, but the challenge of AMR is increasing[40–42].

Genomically, *S*. Typhi and *S*. Paratyphi are distinct from their non-typhoidal relatives and each other. They belong to *Salmonella* enterica subsp. I. *Salmonella* Typhi has O-antigen type O9-12, phase 1 flagellin type H:d, and is normally positive for the capsular Vi antigen. *S.* Typhi and *S.* Paratyphi have undergone extensive pseudogenization when compared with other broader host-range *Salmonella* serovars, thought to be a sign of host-adaption and restriction that have occurred more recently[43]. They share approximately 90% of their genomes with non-typhoidal *Salmonella* serovars, and *S*. Typhi contains on average around 200 pseudogenes, many due to early stop codons or frame-shift mutations. The reference *S*. Typhi CT18 genome is comprised of approximately 4599 coding sequences and encodes the Vi antigen, which is responsible for the production of capsule[44]. Phylogenetically, *S*. Typhi and *S*. Paratyphi sit separately from other serovars of *S*. enterica, with long branches between each other as well. *S*. Typhi is distinguished from *S*. Paratyphi by its Vi capsular profile; dominant serovars of *S*. Paratyphi do not show a capsular phenotype[45]. The severity of typhoid and paratyphoid fever justify the attention they have received; however, non-typhoidal *Salmonella* infections also present a significant burden to many parts of the world. Recent human challenge studies have been conducted using both *S*. Typhi and *S*. Paratyphi[20,46,47]. These have provided significant information on the in-volunteer evolution of these diseases and aspects of their pathogenesis, immunology and vaccinology[48,49]. Clearly, the two diseases have different temporal and bacteriological signatures, for example the patterns of bacteraemia differ significantly[47,50]. However, such studies were conducted in healthy

volunteers in England and with specific bacterial isolates, so they may not be completely representative of disease in the field.

1.1.4 Burden of non-typhoidal *Salmonella*

There is still a considerable burden of disease caused by non-typhoidal *Salmonella* (NTS) serovars, and it is a major cause of bacterial diarrhoea[4]. Of these, serovars *S*. Typhimurium and *S*. Enteritidis are responsible for over 50% of *Salmonella* infections worldwide[51]. Globally, non-typhoidal *Salmonella* is responsible for approximately 94 million cases of gastroenteritis (self-limiting diarrhoea) and 535,000 cases of invasive disease[4,33]. Estimates suggest that 86% of non-typhoidal infections are foodborne[4]. In the developed world, transmission of non-typhoidal *Salmonella* occurs by consumption of food or water contaminated with animal faeces. Undercooked eggs are a common source of infection by *S*. Enteritidis in particular[52–54]. Direct interaction with infected animals, and in some cases, direct contact with infected humans are also involved[55]. In addition, because the two predominant serovars of human illness *S*. Typhimurium and *S*. Enteritidis are broadly host-generalists, they can be transmitted from other animals, causing isolated cases.

Outbreaks in the developed world largely occur through food contamination in the supply chain and, while serious, these are typically self-resolving infections. Consequently, as the vast majority of gastrointestinal *Salmonella* infections are foodborne, they do not disproportionately affect a given demographic. Non-typhoidal serovars can cause invasive disease in the developed world. In the US, it is understood that approximately 7% of non-typhoidal *Salmonella* cases are invasive although these are primarily in immunocompromised hosts, and are responsible for only a small proportion of deaths[56].

In contrast, in parts of the developing world, non-typhoidal *Salmonella* serovars causes considerable invasive in addition to non-invasive disease. According to the GBD 2017 Non-Typhoidal *Salmonella* Invasive Disease Collaborators, the highest burden of invasive non-typhoidal *Salmonella* (iNTS) occurs in sub-Saharan Africa, where there are endemic serovars, predominantly *S*. Typhimurium, *S*. Enteritidis, *S*. Dublin, and *S*. Isangi[33]. There is also a considerable burden of iNTS in Southeast Asia, particularly amongst immunocompromised patients, e.g. in Vietnam[33,57]. Estimates of the incidence rate vary considerably, with a recent

analysis from the GBD 2017 Non-Typhoidal *Salmonella* Invasive Disease Collaborators estimating 535,000 cases and 77,500 deaths of iNTS in 2017, while an earlier analysis from Ao *et al.* in 2010 estimated 3.4 million cases and 618,316 deaths in 2010[33,34]. These infections disproportionately affect children under 5 years, similar to typhoidal *Salmonella*, and immunocompromised and malnourished populations. The burden is particularly high in those with co-morbidities of HIV, malaria, and sickle-cell disease[34,58–62].

1.1.5 Host distribution and transmission of *S.* Typhimurium

Of the many non-typhoidal serovars, *S.* Typhimurium is one of the most reported, causing a large percentage of gastrointestinal and invasive illnesses; hence the focus of this work on *S.* Typhimurium. *S.* Typhimurium is classically regarded as a host-generalist, meaning that it can infect a number of different species. The name "Typhimurium" refers to the typhoid-like systemic illness it causes in mice. Transmission, as for all other *Salmonella* species, is predominantly via the faecal-oral route, and the bacteria can be transferred between species through the ingestion of contaminated food and water and poor hygiene. *S.* Typhimurium foodborne infection is particularly associated with consumption of contaminated pork, beef, fruits and vegetables[63–65]. In the developed world, another mode of transmission is from domestic pets to humans. In humans, it is predicted that approximately 100 bacteria must be ingested to cause disease after passage through the acidic stomach environment[66,67]. In animals other than humans, *S.* Typhimurium readily transmits faecal-orally and causes infection, thus enhancing soil contamination[68]. While it is largely a gastrointestinal organism in humans, it may cause more widespread illness in other species, such as pneumonia in calves[69].

Interestingly, while the canonical understanding of *S.* Typhimurium transmission is that it occurs mostly through zoonoses, genomic studies of animal and human isolates especially of invasive *S.* Typhimurium from the same geographic areas in LMICs have shown that the animal samples can cluster separately from human ones[57,70,71]. This suggests that, in fact, transmission of *S.* Typhimurium is occurring more commonly between humans. The role of human-to-human transmission has been investigated in sub-Saharan Africa[72,73]. However, such research has not yet been able to definitively show what the reservoir for human-specific

S. Typhimurium infection is, what the transmission chain looks like, or what the contribution is of factors including food, water, or direct contact with infected animals and humans[74,75].

1.1.6 Phylogeny of *S*. Typhimurium

S. Typhimurium is a relatively diverse serovar of *Salmonella*, consisting of many sequence types that are distributed globally across many species. On the phylogenetic tree of *S*. enterica subspecies I, *S*. Typhimurium sits apart from other serovars, with approximately 40,000 – 60,000 SNPs divergence from its most recent common ancestor. Indeed, the serovar shows substantially more strain diversity at the isolate level than do many other serovars. While there is considerable diversity within *S*. Typhimurium, isolates have on average only acquired 400-600 SNPs, which accrues to an average nucleotide identity of 99.99%[76,77]. While some STs exhibit a broad host range, such as ST19 including DT104 (definitive type 104), others such as ST313 and ST34 look to have adapted to infecting certain species. Due to the prevalence and diversity of *S*. Typhimurium isolates, there has not been a recent comprehensive phylogenetic analysis of all *S*. Typhimurium STs, and differentiation between STs is largely assigned using MLST classification. The core genome of *Salmonella* is regarded to comprise approximately 3496 genes[78]. However, there is also additional diversity in the pan genome, and this is generally ignored when calculating SNP differences.

S. Typhimurium currently harbours 12 known STs, of which 9 form a single clonal complex. The central ST of the main clonal complex is ST19, and the other eight STs in this complex each have one allelic difference from ST19. ST19 is the most frequent ST isolated globally, and with the other eight STs in the complex, comprises the vast majority of *S*. Typhimurium isolates[7,79,80]. The three STs that sit outside of the clonal complex are ST36, ST40, and ST207.

While many of these sequence types, including ST19, are host-generalists, there are some that are more host-restricted. This includes pigeon-specific STs like ST98 and the human-associated ST34 and ST313[57,81,82]. Disease caused by ST19 isolates are reported globally, but there appears to be less geographic distribution of some of the other STs. For instance, ST36 is found widely in India, but it is less prevalent elsewhere; in contrast, ST34 appears to have found a distinct niche in humans in Southeast Asia[83,57]. The predominant clade of

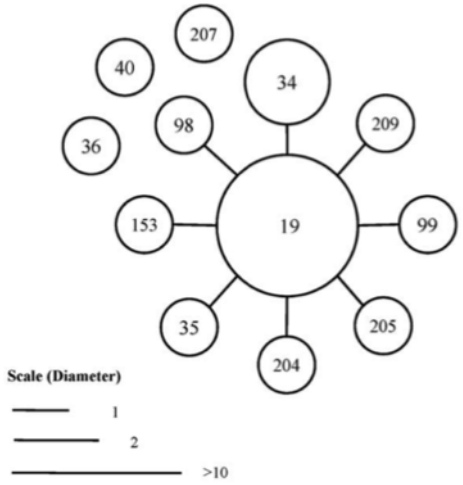

Figure 1.1 Radial phylogeny of *S*. Typhimurium. Phylogenetic organization of *S*. Typhimurium sequence types, adapted from Lan *et al.*, 2009[7].

ST313 has diverged substantially from ST19 and is found primarily in sub-Saharan Africa, although there have been isolates from Brazil and the UK, which predominantly cause gastroenteritis. Interestingly, isolates from the different geographic regions have distinct genotypes and phenotypes[84,85]. Clearly, there may be significant sampling bias in some of these associations and phenotypic links, and further work is required to obtain a fuller picture.

1.1.7 Disease presentation and treatment of *S.* Typhimurium in humans

S. Typhimurium infections in healthy humans typically presents as gastroenteritis, characterized by diarrhoea, stomach cramps, fever, and sometimes vomiting, with 5% of otherwise-healthy patients developing secondary bacteraemia[55]. These symptoms generally begin between six hours and six days after exposure to contaminated food or water and can last between four and seven days[55]. If there are no complications, the infection is self-limiting and resolves without intervention within a week. However, complications can arise in those with weakened immune systems—children under five, elderly, and immunocompromised individuals. This may occur in between 2 and 45% of patients with *Salmonella* gastroenteritis. In these cases, the bacteria can spread beyond the gastrointestinal tract, causing more systemic illness, including meningitis and septic arthritis, requiring intervention[86].

In severe cases, CDC guidelines recommend antimicrobial treatment, with patients administered broad-spectrum antimicrobials until any AMR data is obtained. For antimicrobial susceptible invasive *S*. Typhimurium infection, standard treatment includes fluoroquinolones, azithromycin, and third generation cephalosporins[87].

Invasive lineages of *S*. Typhimurium often cause more systemic disease in immunocompromised hosts, resulting in symptoms with some resemblance to those seen in typhoid and paratyphoid—high fever, general malaise, and headaches. Importantly, cases of invasive *Salmonella* are not always characterized by diarrhoea. As a result, iNTS is often confused with other diseases causing similar symptoms including malaria and typhoid, and cases may be misdiagnosed and mistreated as a result[88,59].

1.1.8 Human infection by *S*. Typhimurium

Depending on the *Salmonella* serovar and severity of infection, the distribution and diffusion of bacteria may vary. The focus here will be on *S*. Typhimurium, though most clinically relevant non-typhoidal *Salmonella* serovars may have the broadly similar initial interactions with the human host[89]. Bacteria are ingested orally and pass through the acidic stomach environment by deploying an acid tolerance response to enter the small intestine[90]. Once established on the surface of epithelial cells in the gut, which is dependent on the level of colonization restriction from the microbiome and the ability to pass through the mucous layer, they employ a type three secretion system (T3SS) encoded on the *Salmonella* Pathogenicity Island I (SPI-1). This initial interaction can trigger a gut inflammation, modulate host cytoskeleton arrangement, and the bacteria can enter cells[89,91–93]. Work is still ongoing to understand the mechanisms *Salmonella* employ to breach the lumen, but it is known that they can readily enter gut enterocytes, microfold (M) cells, and roving dendritic cells.

In the case of enterocytes, the bacteria can actively trigger host cytoskeleton remodelling, creating a membrane ruffle that enables bacterial entry[94,95]. In enterocytes, *Salmonella* are shunted by the cell into a membrane-enclosed vacuole, called a *Salmonella*-containing vacuole (SCV). Intracellular survival and replication are facilitated by virulence-associated factors encoded by genes within *Salmonella* Pathogenicity Island-2 (SPI-2) and other chromosomal loci[96–98]. This compartment is co-opted by the bacteria as a niche to hide and

potentially replicate in, and both the host and bacteria battle to exert influence on the fate of the SCV.

Salmonella can modulate host endocytic trafficking to limit SCV fusion with the lysosomal compartment, thus avoiding degradation[99–101]. In some cases, the SCV transcytoses to the basolateral membrane of the enterocyte, where it may be phagocytosed by dendritic cells, neutrophils, or macrophages. Enterocytes containing a high burden of *Salmonella* may also undergo apoptosis, resulting in their uptake by phagocytic cells and the dissemination of the bacteria[102,103]. In the case of direct entry into M cells, a type of specialized gut cell that *Salmonella* can invade at significant levels, the mechanism of entry is less clear. It appears that bacteria are able to penetrate these antigen-sampling cells without the aid of the T3SS, although they still modulate the host cytoskeleton, and the process may involve dynamin[104,105].

A further cell type exploited for entry are CD18+ dendritic cells that periodically traverse the lumen to monitor and sample antigens in the mucosa. Bacteria are phagocytosed by the dendritic cells, which then re-enter lamina propria, and the bacteria can then replicate within the dendritic cells[106,107]. Once in phagocytes, bacteria may trigger rapid or delayed pyroptosis, an inflammatory programmed cell death, thus facilitating further bacterial dissemination within and outside of the intestinal environment[108]. Notably, all of the interactions that occur between the host and *Salmonella* are enabled by a diverse set of virulence factors, many of them effector proteins produced by the T3SS[97,109–112]. Additionally, key host factors are adapted to control *Salmonella* infections[113–117].

1.2 Invasive non-typhoidal *Salmonella* compared to other non-typhoidal strains, an overview

Over the past 60 years, there has been an emergence of sub-lineages of non-typhoidal *Salmonella* that more frequently cause invasive disease (iNTS), with some similarities to infections caused by *S*. Typhi or Paratyphi[119]. These invasive *Salmonella* infections have been observed extensively in sub-Saharan Africa and to a more limited extent in Southeast Asia[57,82]. Due to high levels of malaria, HIV, and malnutrition that cause an immuno-

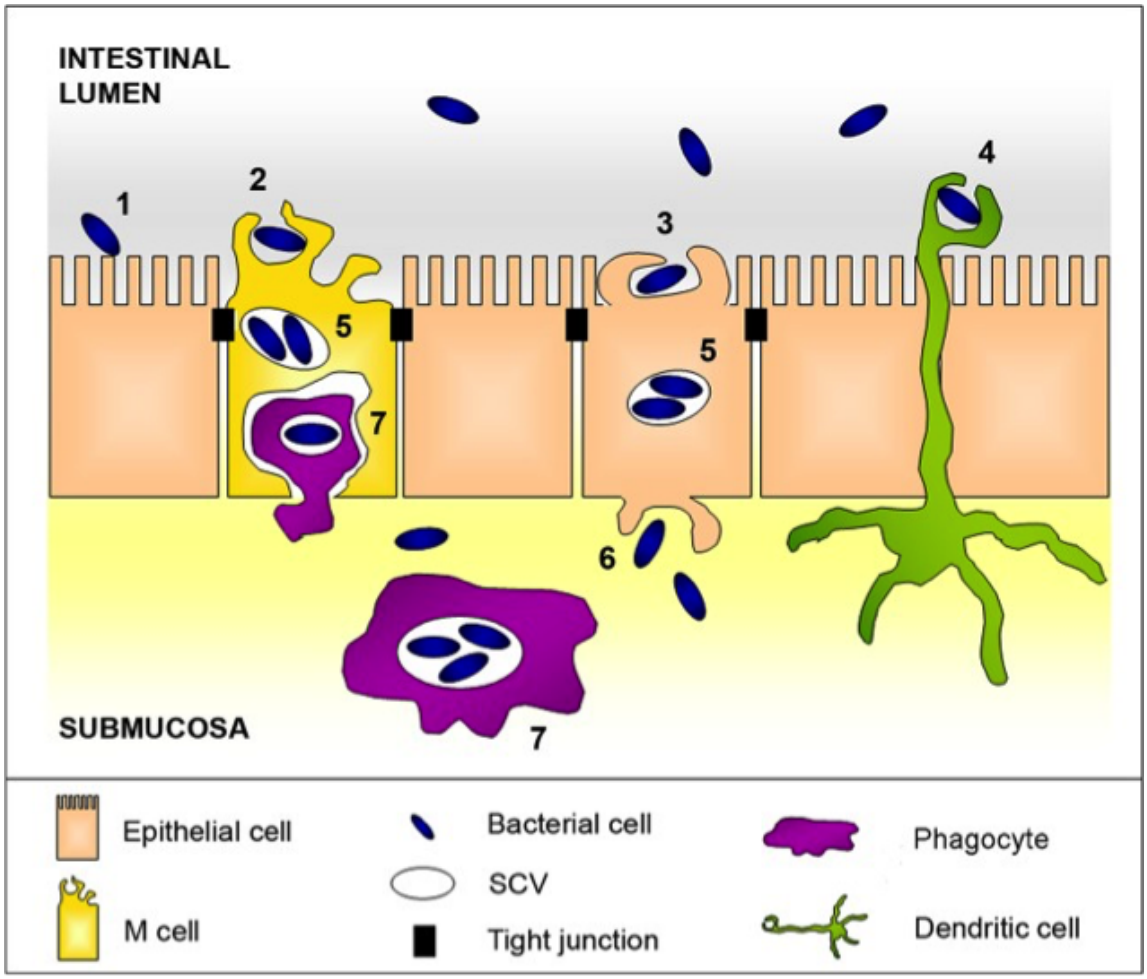

Figure 1.2 *Salmonella* invasion strategies of the intestine. *Salmonella* bacteria are able to enter the intestinal epithelium through multiple mechanisms, with and without uptake by immune cells. Adapted from Fabrega and Vila, 2013[118].

compromised state, infection with iNTS poses a serious risk with high mortality in those parts of the world where these conditions predominate, specifically in sub-Saharan Africa where *Salmonella* is one of the leading causes of mortality from bacterial disease [120,36,121]. While NTS can be invasive, this typically happens in only 8% of global cases [55]. However, certain serotypes, namely S. Dublin, Cholerasuis, Enteritidis, and Typhimurium are broadly also associated more frequently with invasive disease compared to other non-typhoidal serovars. Within these 'more invasive' serovars, specific sub-lineages that are genotypically and phenotypically distinct are potentially more likely to be invasion-associated.

1.2.1 Global distribution of iNTS

While iNTS occurs in the developed world, it is a more serious and pervasive problem in sub-Saharan Africa and parts of Asia. The burden of iNTS has been difficult to ascertain due to a general lack of effective surveillance, resources, and misdiagnosis. In particular, Latin America is severely lacking in surveillance of bacteraemia including iNTS, and it is unknown how severe a problem it is there [119]. iNTS is often mistaken for malaria, typhoid, or other bacterial infections, as they may all co-present to healthcare facilities in the same geographical regions [122–126]. The highest burden of iNTS occurs in sub-Saharan Africa and is predominantly caused by *S*. Typhimurium, which is responsible for 48% of cases across 33 countries [127]. Within Africa, surveillance has historically been better in Eastern and Central Africa, where there is a high level of invasive *S*. Typhimurium. In sub-Saharan Africa, iNTS is at least as great a problem as typhoid fever, and it is a persisting problem that is highly correlated with HIV infection, malaria, and malnutrition [88,128,129].

Worryingly, there is a rise in drug resistance associated with iNTS infection in sub-Saharan Africa, exacerbating the problem. Current and historic surveillance indicates that there is a spectrum of disease incidence across sub-Saharan Africa, with 8% and 45% of community-acquired bacteraemia due to iNTS in South Africa and the Democratic Republic of the Congo (DRC), respectively. The incidence of iNTS disease in sub-Saharan Africa was estimated to be two million cases in 2010. The region with the next highest incidence is Europe at 763,191 cases, largely due to higher prevalence in Eastern Europe [34].

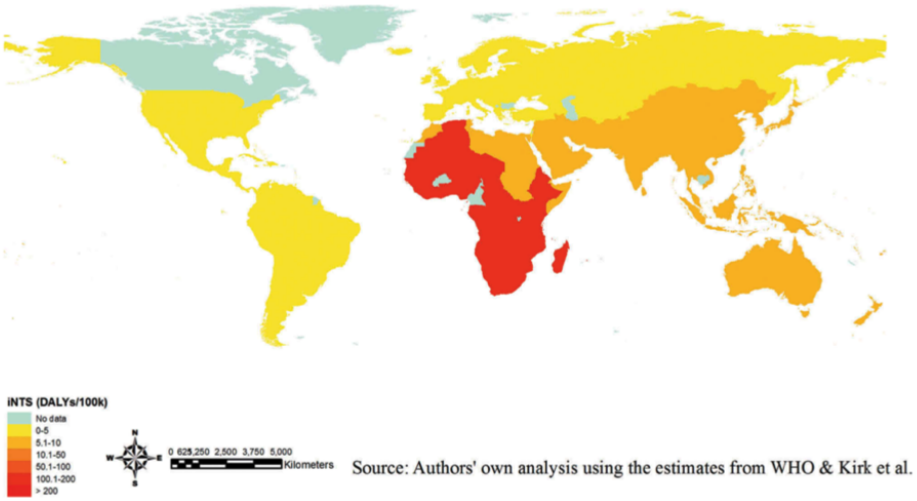

Figure 1.3 iNTS disability-adjusted life years (DALYs)/100k. iNTS infections have a distributed impact on DALYs globally, with the greatest burden in sub-Saharan Africa. Adapted from Balasubramanian *et al.*, 2019[130].

In South and Southeast Asia, regions with high levels of diarrheal disease, iNTS has not been found to be as common, particularly when compared to the incidence of typhoid and paratyphoid fever. There are high levels of *Salmonella* found in Southeast Asia, and a recent study on sepsis in Indonesia, Vietnam, and Thailand has documented that 2.7% of sepsis patients are positive for iNTS[131]. *S.* Typhimurium is the most common serovar associated with iNTS in South and Southeast Asia, and ST19 and ST34 are the two major *S.* Typhimurium STs responsible. Many of the cases of iNTS in Southeast Asia have been associated with HIV infection, as in Africa[57,131]. While surveillance for iNTS is not as widespread in some parts of Asia as in Africa, the burden of iNTS disease, despite a similar case fatality rate, seems to be lower in this region. In South Asia, there is a similar lack of data, though there are some reports concerning cases of invasive disease in India, suggesting that there may be higher levels of infection than reported in at least some regions[132].

In Latin America, a region that has particularly sparse epidemiological data on bacteraemia, there is likely to be some iNTS, though lower than in sub-Saharan Africa. It may be that data is available at a local and country level on this continent but this has so far not been broadly reported. A single surveillance study in Colombia identified 4,010 *S. enterica* samples isolates from blood and faeces over a six-year period, a far lower number of cases than that found in Africa[133]. ST313 found in Brazil appear to be genetically distinct from African ST313 and cause mostly gastroenteritis[119,130,85].

1.2.2 Disease presentation and treatment of iNTS

iNTS is acquired through faecal-oral contamination. Linked to the invasive nature of the infection, common clinical symptoms include non-specific markers of febrile illness such as fever, malaise, and headaches. However, beyond these clinical features, disease presentation may vary. A study of Malawian adults with iNTS found many to have bacteraemia, fever, and splenomegaly[134]. Another study has found that one-third of adults with iNTS present with respiratory symptoms[88]. It is less common for patients to present with diarrhoea compared to normal non-typhoidal *Salmonella* infections; diarrhoea occurs in approximately 35% of children and 46% of adults, based on multiple studies from Eastern and Central Africa[59,75,88,135–137,121]. In some cases, young children, typically younger than those with nonfocal disease, may present with meningitis, and the mortality rate from this complication is high, at approximately 50%, and subsequent neurological sequelae are found in approximately half of recovered patients[60,135,138,139].

As iNTS is most prevalent in low-resource settings, patients may not have access to healthcare facilities, and even if they do, there is a chance of misdiagnosis and inability to access the appropriate medication. iNTS is a severe illness, and initial treatment is broad-spectrum antimicrobials, such as the fluoroquinolone ciprofloxacin, until any drug resistance is confirmed. In response to high levels of multidrug resistance (MDR), ceftriaxone is now the standard treatment for undifferentiated sepsis in much of Africa[140]. In low-resource settings, it is unlikely that such rigorous testing is undertaken to diagnose the infection, subsequently test for AMR, and administer the appropriate antimicrobials. Depending on the region, access to broad spectrum antimicrobials like ciprofloxacin may be minimal. Due to the complications of misdiagnosis, and the time and resources involved to culture bacteria, antimicrobials may be arbitrarily administered, if at all.

1.2.3 Risk factors for iNTS disease

In acute iNTS cases, particularly in coinfections with malaria, HIV, malnutrition, and sickle cell disease, the prognosis is poor, and there is up to a 30% mortality rate in those with malaria. Much research has been done on the effects of malaria on iNTS infection, particularly in sub-Saharan Africa where the malaria burden is high. Studies have shown that

macrophages are hampered in their oxidative burst function by the presence of Plasmodium parasites, and complement mediated killing of bacteria is also reduced by consumption of complement[141–143]. Moreover, malaria disease appears to inhibit phagocyte recruitment to sites of bacterial infection, thus facilitating bacterial dissemination. Interestingly, this may be mediated through the induction of IL-10, an anti-inflammatory cytokine, as a component of the immune response to malaria, and this is likely consequently a side effect of a suppression of the inflammatory response to the bacteria as well[25,144,145].

HIV is another common risk factor for iNTS infection, particularly amongst adults in Africa and Vietnam. In Africa, approximately 95% of adults and 20% of children with iNTS patients are positive for HIV, and a study from Vietnam reported that 73% of patients with iNTS from *S*. Typhimurium ST34 were positive for HIV[57,88]. HIV results in a loss of CD4+ T cells, which increases susceptibility to iNTS by depleting the inflammatory response to *Salmonella*[146]. This loss subsequently fails to sufficiently activate bacteria-infected phagocytic cells, allowing for greater infiltration by bacteria in the initial infection and the potential for recurrent infection[82]. In addition, mucosal Th17 cells are also depleted during early HIV infection, resulting in poor initial response to an iNTS infection thus enabling it to spread more easily[147,148].

Malnutrition is another significant risk factor for iNTS infection in Africa due to reduced immune function in malnourished individuals and a leakier gut barrier[149]. Malnourished children additionally have lower levels of complement, and neutrophils have been shown to have lower activity in clearing bacteria[150,151]. These problems are potentially further exacerbated by a weaker inflammatory response, leading to insufficient recruitment of immune cells to the site of infection, and a lower overall humoral immune response, which delays recovery from infection[152,153]. In African children in iNTS endemic areas, sickle cell disease may also be a significant risk factor, causing significant immune dysregulation[154]. It is hypothesized that complement-mediated bacterial killing is severely restricted in patients with sickle cell disease, as is neutrophil oxidative burst, limiting the clearing of infection[155].

1.2.4 Genetic factors characterizing/influencing *S.* Typhimurium iNTS

While the majority of cases of iNTS are caused by *S.* Typhimurium, a serovar that can infect multiple species, an interesting characteristic of invasive serovars is their adaptation to a more human-specific niche. The most prominent example of this is *S.* Typhimurium ST313, a lineage that is the largest contributor to iNTS. Recent data from Ghana showed that the *Salmonella* isolated from human patients were genetically distinct from those isolated from the environment[156]. Comparative analysis of multiple ST313 and ST19 genomes have shown pseudogenization of some genes in ST313 that may equip the bacteria for a more host-adapted lifestyle[157,158]. It is known that the genomes of *S.* Typhi and *S.* Paratyphi A also display this characteristic—a more 'streamlined' and smaller genome that is potentially adapted to a human-specific lifestyle.

Experiments with ST313 *S.* Typhimurium have shown that, compared to ST19, they have an enhanced ability to infect macrophages and greater resistance to killing[157,159]. The prophage BTP1 in ST313 encodes a glycosyltransferase operon (gtr), which modifies LPS length. It is hypothesized that is may contribute to the increased invasiveness of ST313[160]. Furthermore, the ST313 genomes can harbour a single nucleotide polymorphism (SNP) in the promoter of gene *pgtE*, encoding outer membrane protease PgtE. PgtE is involved in resistance to certain antimicrobial peptides and the human complement cascade. The SNP in the promoter region of *pgtE* upregulates expression of PgtE, enhancing the ability to evade the human immune response and survive extracellularly in a host[161].

In contrast, ST34, which are a cause of iNTS in Southeast Asia, do not show this marked pseudogenization profile but do have a wide set of AMR signatures and unique flagellar characteristics[57]. A significant proportion of ST34 isolates from Vietnam are monophasic in terms of their flagellar expression. *S.* Typhimurium ST19 are normally biphasic, able to independently express the genes *fliC* and *fljB* that encode flagellar subunits. Dependent on environmental conditions, the *Salmonella* can undergo phase switching to alternate which flagellar protein is expressed[162,163]. However, the ancestral ST34 clone is monophasic, whereas a more recent set of Vietnamese ST34 clones are biphasic, having reacquired the *fljBA* operon containing *fliC* and *fljB* through a transposition event[57]. *In vitro* work in human macrophages and induced human gut organoids (iHOs) has shown that there are significant

differences in invasion between monophasic and biphasic *S*. Typhimurium ST34 isolates (Lees *et al.*, unpublished). This, combined with multidrug resistance (MDR), has likely enabled these isolates to thrive in this setting.

1.2.5 Phylogeny of iNTS

As previously mentioned, the four serovars most commonly causing iNTS are *S. enterica* Typhimurium, Enteritidis, Dublin, and Cholerasuis, although there is regional and temporal variation. While the isolates that cause iNTS do fit within the phylogenetic structure of their parent clades, they often form sub-structure in the phylogenetic tree, as evidenced by their cladal genetic differences. However, as a broader category, iNTS phylogeny has not been well studied due to the fact that iNTS isolates fall within multiple serovars, and these are not typically studied as a unit. The phylogeny of the dominant serovars that are associated with invasive disease, most prominently *S*. Typhimurium, is much better understood. *S*. Typhimurium ST313 is a major cause of iNTS, particularly in sub-Saharan Africa where it accounts for approximately reported 40% of cases[119].

1.3 iNTS in sub-Saharan Africa

Sub-Saharan Africa has the highest burden of invasive non-typhoidal *Salmonella*, based on the epidemiological data that has been reported to date. iNTS has emerged as a common causes of bacteraemia and is now considered to be the leading cause of bacterial-related morbidity and mortality in many parts of the region. This is in part to a significant reduction in the burden of *Neisseria meningitidis*, thanks in part to vaccination programmes in the northern "Meningitis Belt," targeting *N. meningitidis* A using a conjugate vaccine[164,165]. iNTS have adapted to the niche of the immunocompromised individuals, primarily those who are malnourished or have HIV or malaria. Given its rise in prominence and high rates of mortality in the region, iNTS and in particular *S*. Typhimurium ST313, warrants greater attention.

1.3.1 *S.* Typhimurium ST313 as major contributors to iNTS

iNTS has risen in prominence in recent years as surveillance and awareness of blood stream infections has increased. This has led to a better understanding of the serovars and sequence types that contribute most to the iNTS burden. In sub-Saharan Africa, where the iNTS burden is the highest, *S.* Typhimurium ST313 are responsible for the many cases. Interestingly, although African ST313 can cause both gastroenteritis and invasive disease, it is associated with more iNTS than NTS[119,166]. In Africa, approximately 40% of iNTS infections are routinely caused by ST313, and the next most common serovar is *S.* Enteritidis, which appears to cause approximately 12% of the iNTS, followed by S. Dublin at 11%[36,119]. Burden of disease estimations have not been calculated exclusively for ST313, but there have been many independent studies in various parts of Africa, particularly sub-Saharan Africa, documenting the proportion of ST313 cases of all *S. enterica* cases. These studies have provided evidence that ST313 is widespread across Africa and constitutes a major percentage of iNTS cases.

Comprehensive whole genome sequence-based analysis of 129 iNTS isolates across seven countries in sub-Saharan Africa, isolated between 1988 and 2010, found that 93% were ST313[82]. A study of 29 iNTS isolates from HIV-infected adults with fever in Mozambique found that 100% analysed by MLST were ST313, which is consistent with high levels of ST313 reported from neighbouring countries[167]. Similarly, longitudinal sampling in the DRC from 2007-2011 revealed that 96% of the *S.* Typhimurium isolates (79% of total non-typhoidal *S. enterica* isolates) recovered over that period belonged to the ST313 clade[168]. In Western Kenya, a recent study reported that 57.6% of iNTS cases in children under five years of age were caused by *S.* Typhimurium ST313, and 66.7% of iNTS cases in patients above five years of age were caused by ST313[169]. It is as yet unclear why ST313 have become the predominant cause of iNTS in sub-Saharan Africa above other serovars also endemic that have followed similar evolutionary paths. However, host adaptation and multiple antimicrobial resistance likely played a role[80,82].

1.3.2 Brief description of *S.* Enteritidis

While *S.* Enteritidis as a cause of iNTS has received less attention than *S.* Typhimurium, it is responsible for a significant proportion of cases in sub-Saharan Africa[119,170]. *S.* Enteritidis

infections follow a similar trend to *S*. Typhimurium in the developed world. The serovar is regarded as a host-generalist and cases mostly gastroenteritis; in the developing world, especially in sub-Saharan Africa, it is a common cause of invasive disease. Phylogenetically, *S*. Enteritidis is distinct from *S*. Typhimurium. A 2016 study on *S*. Enteritidis phylogeny showed distinct lineages in Africa compared to other parts of the world. In Africa, there are two main lineages of *S*. Enteritidis in circulation and associated with invasive disease, and these display evidence of genome degradation and harbour the virulence-associated plasmid, potentially signals of moving toward a more human host-restricted lifestyle[170].

Based on assessment of a global collection of 675 *S*. Enteritidis genomes, these two lineages appear to segregate on a geographic basis, rather than the temporal basis that defines ST313 lineages. One *S*. Enteritidis lineage is concentrated in West Africa and is distinct from the lineage found in Central and Eastern Africa, and both of these lineages were associated with AMR to at least one antimicrobial[170]. Further analysis of these genomes revealed that the two African-specific lineages appear to have split from the global epidemic clade and expanded in Africa after 1945 based on assessment of the most recent common ancestor. This timeline matches with the expansion of *S*. Typhimurium ST313 in Africa in association with the HIV pandemic and a newly emerging HIV-positive immunosuppressed population[88,171]. Similar to African *S*. Typhimurium ST313, African *S*. Enteritidis show evidence of genome reduction associated with a greater restriction to a human-associated lifestyle and higher invasiveness[170].

1.3.3 iNTS surveillance in Africa

There remains a significant gap in surveillance of iNTS disease globally. However, in the past decade, some regions of Africa have received more attention and surveillance because of the rising awareness that iNTS is a significant problem. The Typhoid Fever Surveillance in Africa Program (TSAP), administered by the International Vaccine Institute (IVI) collected data on bacterial infections, especially typhoid and iNTS, across thirteen sites in ten sub-Saharan African countries from 2010 to 2014. The countries included were: Senegal, Guinea-Bissau, Burkina Faso, Ghana, Sudan, Ethiopia, Kenya, Tanzania, Madagascar, and South Africa. These sites and countries were chosen on the basis of previously identified cases of typhoid fever, and field sites had already been established for other purposes. Importantly, these sites

were in a mixture of high and low population density areas. Of the 568 blood bacterial isolates collected in TSAP, 17% were found to be NTS, and 40% of those were *S*. Typhimurium[128].

While the TSAP study has ended, there are ongoing follow-up studies being conducted in Africa to continue surveillance of bacterial infections. This coincides with the roll-out of the typhoid conjugate vaccine and associated data collection in some countries. The Severe Typhoid in Africa (SETA) Program, also conducted by IVI has collected additional data on typhoid fever and other bacterial infections, particularly iNTS, following on from the TSAP study. However, SETA has concentrated on six sub-Saharan African countries: Ghana, Ethiopia, the DRC, Nigeria, Madagascar, and Burkina Faso, to identify *Salmonella* infections as the cause of fever in pre-determined regions and enrol patients for samples from multiple body sites and potential longer-term follow up studies[172].

Independently, the Institute of Tropical Medicine in Antwerp, Belgium has collected longitudinal data on and isolates from bloodstream infections in the DRC and Burkina Faso. Within-country surveillance also occurs in Kenya, largely administered by the Kenya Medical Research Institute (KEMRI). Surveillance conducted at KEMRI was instrumental in recognizing iNTS as a major cause of illness in sub-Saharan Africa, especially in HIV-positive patients[173,174]. While there is still incomplete surveillance in Africa, there is a much more comprehensive understanding of the endemicity of iNTS, and further surveillance will better elucidate the picture.

1.3.4 Phylogeny of *S*. Typhimurium ST313s

Many of the *S*. Typhimurium isolates associated with invasive *Salmonella* disease in sub-Saharan Africa fall into the lineage ST313[82]. This MLST branches off from the dominant ST19 type that is a common cause of salmonellosis in other parts of the world. Phylogenetic analysis based on whole genome sequences has shown that the ST313 in Africa have evolved into two distinct lineages—lineages 1 and 2[80,82]. Isolates in both lineage 1 and 2 are normally MDR, while isolates in lineage 2 have also acquired an additional resistance to chloramphenicol, an antimicrobial that was in common use while lineage II ST313 were emerging[80,82]. ST313 reference strain D23580 differs from ST19 reference strain LT2 by a number of SNPs, and these differences include 20 genes affected by four large deletions, 77

pseudogenes that could be characterized, and significant plasmid and prophage differences[80]. There are also additional pangenome differences.

Within the ST313 clade, there is considerable ongoing evolution, with recent genomic analysis revealing further changes in the AMR profile and phylogenetic structure. ST313 isolates from the 1990s and early 2000s clustered as a single lineage, forming ST313 lineage I, and isolates within this cluster were susceptible to the antimicrobial chloramphenicol[80,175]. The *S.* Typhimurium ST313 lineage II branched off later than lineage I and harboured chloramphenicol resistance, acquired very early on by this lineage. Bayesian (BEAST) analysis of 129 iNTS isolates in the context of a global collection of *S.* Typhimurium date the emergence of lineage I and II independent of one another $\sim$60 and $\sim$43 years ago, respectively, and the majority of ST313 cases from the mid-1990s onwards have been caused by lineage II bacteria[82].

Isolates from both lineages contain two Tn*21*-like transpositional elements, which appear to have independently arisen in the two lineages. While lineage I and lineage II cluster more closely with each other than with any other *S.* Typhimurium, there are distinct differences that separate them. Epidemiological data suggest that lineage II arose in response to widespread chloramphenicol usage, as lineage II is characterized by chloramphenicol resistance, whereas lineage I isolates are susceptible. Ongoing surveillance of iNTS in sub-Saharan Africa suggest that lineage I has been outcompeted by lineage II. With the increase in samples that have been sequenced in the past five years, it is now obvious that there is considerable substructure within the phylogenetic tree of ST313, and there is a significant sub-lineage emerging in the DRC that has extensive drug resistance.

Phylogenetic analysis by Van Puyvelde *et al.* of all available sequenced African ST313 have provided greater resolution of where and how ST313 is evolving, with a particular focus on the newly-identified sub-lineage II.1[176]. This sub-lineage (ST313 II.1), which branches off from lineage II, is defined by extended spectrum beta-lactamase production, azithromycin resistance, and an IncHI2 plasmid beyond the existing MDR profile of ST313. This sub-lineage has so far been responsible for > 10% of *S.* Typhimurium cases in the central region of the DRC; however, this outbreak illustrates the ongoing changes and evolution in ST313 and the ability of this lineage to adapt to antimicrobial exposure. Further investigations in the Congo region have found additional evolution related to decreased ciprofloxacin susceptibility. These isolates appear to form yet another sub-lineage (II.2) and may be responsible for a

significant number of cases of iNTS (Van Puyvelde, personal communication). It is likely that ST313 will continue to evolve in response to new or different treatment regiments used regionally.

1.3.5 Genetic and phenotypic characteristics of ST313 reference strain D23580

The best-characterized isolate amongst ST313 lineage II is D23580, which has been sequenced to completion and is used as a reference strain. D23580 was isolated from a febrile patient in Malawi in 2004 during an MDR outbreak of iNTS in Blantyre, Malawi and has since been extensively analysed[80]. AMR in D23580 is largely plasmid-mediated, encoded within a 117 kbp plasmid pSLT-BT, conferring resistance to chloramphenicol, ampicillin, streptomycin, sulphonamide, and trimethoprim. It also carries three other smaller plasmids, pBT1, pBT2, and pBT3, none of which carries known resistance genes. pSLT-BT shares significant homology with pSLT found in SL1344[177,178]. Beyond its MDR profile, D23580 is considerably different from ST19 strains, namely reference isolate SL1344. D23580 diverges from SL1344 by 856 core SNPs across the chromosome and also possesses a distinct array of prophages, which may influence virulence and survival[179]. D23580 has lost function of the gene *sseI*, a type III-secreted effector important in virulence and *ratB*, which is implicated in intestinal persistence in mice. There are also large blocks of deletions in a set of genes of unknown functions: STM1549-1553, and a loss of allantoin metabolism, which are similarly absent in *S*. Typhi[80]. These convergent changes with *S*. Typhi, a known invasive bacterium, suggest a shift towards a more human-host adapted lifestyle. Interestingly, while lineage I ST313 isolates show some signs of genome degradation in the form of pseudogenization, they do not share some of the novel chromosomal deletions present in lineage II isolates[80,82].

As D23580 has been fully sequenced and the genome annotated, it has been used extensively in the laboratory to explore the differences between ST313 and ST19. Metabolically, D23580 has lost the ability to ferment melibiose, has a lower utilization of L-tartaric acid and dihydroxyacetone, has some preference for alternative carbon sources, can ferment inositol, can use the butylene glycol pathway to make pyruvate, is able to survive on citrate as a carbon source, and has a lower utilization of purine and pyrimidine as phosphorous sources[180,157]. With regards to stress, D23580 has a greater resistance to human serum

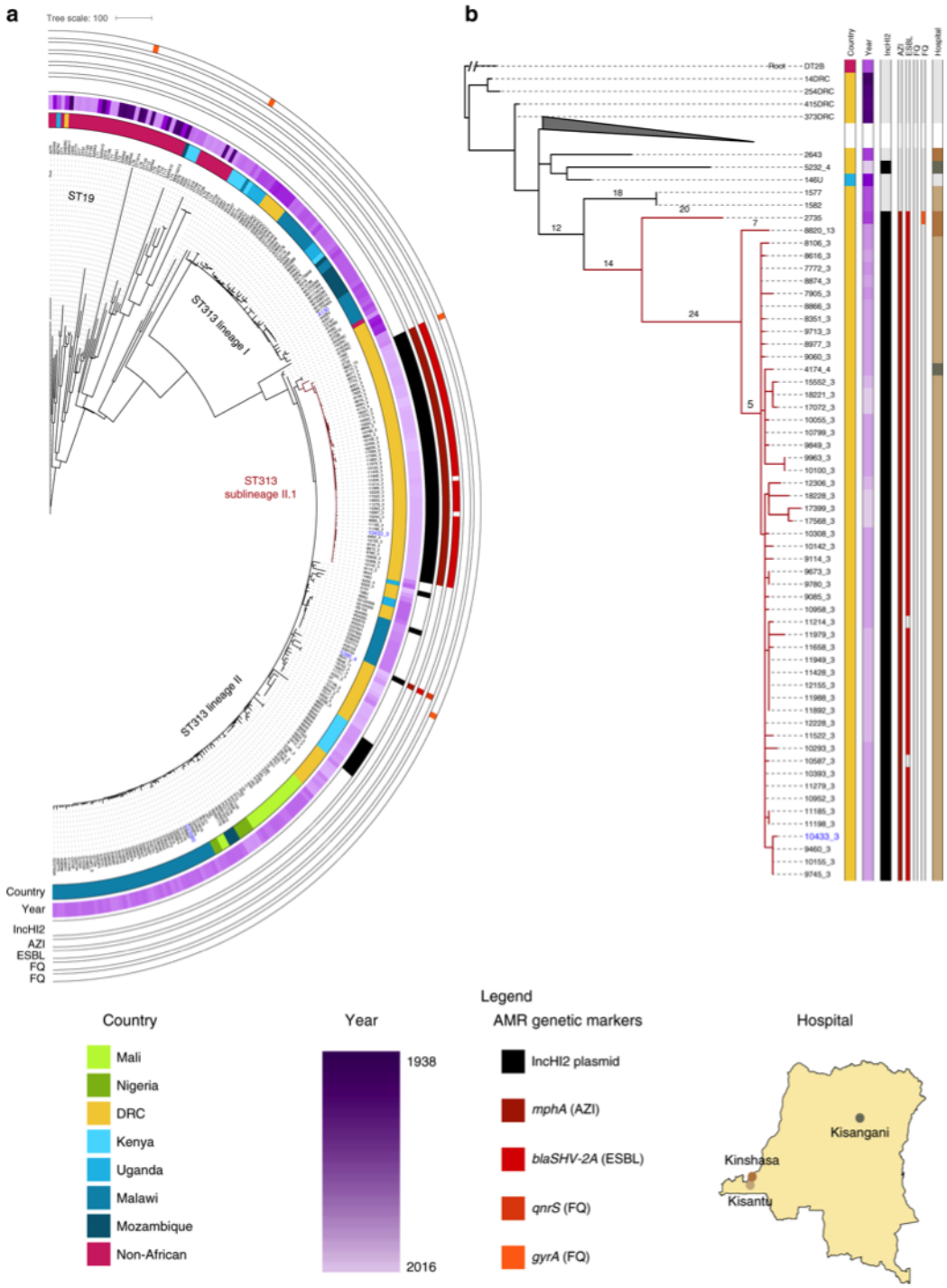

Figure 1.4 African *S.* Typhimurium ST313 sub-lineage II.1 in context of other African invasive *S.* Typhimurium (a) and independently (b). ST313 lineage II contains considerable sub-structure in its phylogeny, including recently-described lineage II.1 found in the DRC. From Van Puyvelde *et al.*, 2019[176].

killing, a higher tolerance to acid stress, a distinct and reduced biofilm morphology, and decreased survival in dry conditions[157,161,181–183]. In vitro comparisons with ST19 strains have shown that D23580 more readily invades and replicates inside macrophages; however, studies of epithelial cell invasion have produced contradictory results. In macrophages, D23580 and other ST313 lineage II isolates appear to cause less inflammation, which may account for greater intracellular survival[157,159,182,184,185].

Animal experiments have also been used to confirm and elucidate differences between ST313 and ST19 isolates: in mice, experiments have shown that D23580 disseminates from the gut more readily than SL1344, and there are higher levels of bacteraemia, alongside a less inflammatory response[158,180,184,186]. While other isolates have been subjected to long-read sequencing to the same depth as D23580 and have been experimented on, D23580 continues to be the best-described ST313 lineage II isolate.

1.4 AMR in *Salmonella*

AMR in bacterial pathogens has become a critical concern in recent years, with an increasing number of microorganisms exhibiting resistance to a spectrum of drug treatments. This is particularly concerning as there are few new antimicrobials being discovered or developed, and there is a dearth of vaccines to address the myriad of bacterial infections[2,187]. This presents a serious threat to the global community, as the rise in MDR, resistance to more than three classes of antimicrobials, may make even routine surgeries and hospital treatments an opportunity for bacterial infection. Moreover, these AMR organisms pose a great concern to immunocompromised and at-risk populations in the developing world, where there has been a sharp rise in MDR and more invasive infections, in large part due to indiscriminate use of antimicrobials[187].

In *Salmonella* species, the distribution of MDR is varied depending on the geography and serovars. In some parts of the world, notably Southeast Asia, where access to antimicrobials is easy, there are extremely high levels of MDR. In contrast, where access to antimicrobials is lower, as is the case in much of sub-Saharan Africa, the acquisition of MDR in *Salmonella* is generally slower. Similarly, in much of the developed world, particularly in parts of Europe that have rigorous antimicrobial stewardship, AMR in *Salmonella* is lower. However, there

has been a noticeable overall increase in drug resistance in *Salmonella* species globally to many of the first-line broad-spectrum antimicrobials, and it is likely only a matter of time before AMR further increases. The degree of AMR in *Salmonella* species is also dependent on the serovar. Regions with high endemicity of typhoid and paratyphoid, which require antimicrobial intervention, have much higher levels of drug resistance.

The H58 clade of *S*. Typhi, an MDR clade that has become the dominant clone globally, expanded at least in part because of its ability to outcompete other antimicrobial susceptible clones[188–190]. In regions where there is particularly high antimicrobial usage, H58 has acquired further AMR, including resistance to azithromycin, one of the last treatment options for MDR *S*. Typhi. This has resulted in an ongoing outbreak of extremely drug resistant (XDR) *S*. Typhi first reported in Hyderabad, Pakistan[191]. Similarly, there are ongoing outbreak of MDR *S*. Typhi in sub-Saharan Africa[190,192–194]. Combined with poor healthcare infrastructure and treatment, this outbreak has the potential to expand and acquire further AMR. This then has a knock-on effect on other bacteria found in the environment. Although iNTS serovars may not naturally carry as much plasmid-mediated AMR as *S*. Typhi, if they coexist in the same environment, as is the case in parts of the developing world, particularly in sub-Saharan Africa, then the potential for horizontal transfer of AMR genes increases.

1.4.1 WHO R&D 'directive' on FQR *Salmonella*

In 2017, the World Health Organization (WHO) issued a priority list of antimicrobial-resistant tuberculosis and other bacterial pathogens, listing the infections that had concerning levels of drug resistance. The 20 bacterial pathogens and 25 patterns of resistance acquisition of greatest concern were determined using ten criteria: mortality, health-care burden, community burden, prevalence of resistance, 10-year trend of resistance, transmissibility, preventability in the community setting, preventability in the health-care setting, treatability, and pipeline[187]. The pathogens and resistance mechanisms chosen were categorized based on their criticality—critical, high, and medium priorities. Notably, of these, Gram-negative bacteria were a more critical concern than Gram-positives, and fluoroquinolone resistant (FQR) *Salmonella* species fell within the "Priority 2: high" category. This categorization was made on a multitude of factors, and for non-typhoidal *Salmonella*, some of the key factors were mortality, transmissibility, and likelihood for alternative treatment or vaccine

development[187]. This directive from the WHO has helped clarify which antimicrobials need to be most actively conserved for emergency use and how to prioritize research and development into novel therapeutics.

1.4.2 How AMR is assessed in clinical settings

The gold-standard for antimicrobial susceptibility testing (AST) is broth microdilution measurements, which involves growing bacteria in a standardized set of antimicrobial concentration over a designated period of time[195,196]. However, this method is time intensive and laborious, and most clinical laboratories assess antimicrobial susceptibility using antimicrobial disk diffusion tests or minimum inhibitory concentration (MIC) test strips. Disk diffusion, or Bauer-Kirby, testing works by placing a disk containing a defined concentration of an antimicrobial on an agar plate inoculated evenly with $\sim$1-2 x 10^8 colony forming units of bacteria/millilitre and subsequently measuring the zone of bacterial growth inhibition that occurs after overnight incubation. This method is widely-used due to the ease, standardization, and reliability of the assay and relatively low cost of antimicrobial disks[195,197,198]. MIC test strips operate on the same principal of a zone of inhibition, although in this case, incrementally more concentrated antimicrobial is dotted along the underside of a plastic strip. After the strip is placed on an agar plate inoculated evenly with bacteria, the level at which bacterial growth is no longer inhibited is determined to be the MIC. Disk diffusion tests remain the cheapest option, so they are the ones most commonly used in the field, although they are considered less reliable and to generate slightly lower MICs than do the MIC test strips[199]. They are considered less reliable in part because they are more difficult to interpret. A caveat with any MIC test that involves reading the result is that results may vary depending on the stringency of the 'reader', and it becomes very important to maintain consistency of how the results are read and interpreted.

Yet another method that has gained widespread use and acceptance in recent years is the automated Vitek System, which uses reagent cards containing minute quantities of antimicrobials pre-loaded. Bacterial culture at a specified optical density are added to the plastic cards, and a machine measures the turbidity of the culture under antimicrobial exposure after a period of incubation. These data are then outputted as a report, specifying whether bacteria

are above or below the breakpoint for the given antimicrobial, and whether that corresponds to a susceptible, intermediate, or resistant phenotype[195].

There are two institutional bodies that determine MIC "breakpoints" for any given antimicrobial based on levels of susceptibility of groups of bacteria. This is updated every couple of years to reflect changes in antimicrobial susceptibility. One such organization is the Clinical and Laboratory Standards Institute (CLSI), an international voluntary organization accredited by the American National Standards Institute, which collates reported data from clinicians and laboratories to advise appropriate breakpoints for antimicrobial usage[200,201]. The other is the European Committee on Antimicrobial Susceptibility Testing (EUCAST). While these are both accepted, the breakpoints for given bacteria for specific antimicrobials may vary because they use different metrics to assess levels of resistance, which may lead to inconsistencies between how an infection is treated[202,203]. While breakpoints determined from both organizations are accepted and recommended by the WHO, they do not necessarily align, which may be problematic in determining whether a patient should be treated with a certain drug on the basis of AST[202].

1.4.3 Distribution of fluoroquinolone usage

Fluoroquinolones are one of the most widely-used classes of antimicrobials, given their ability to function on both Gram-positive and Gram-negative bacteria. Amongst fluoroquinolones, one of the most widely-used is ciprofloxacin, a second-generation fluoroquinolone. In the developed world, it is commonly prescribed to travellers for traveller's diarrhoea and is the first line empirical treatment for an invasive infection in hospitals[204,205]. A study of antimicrobial use in 2004 in the United States and European Union found that fluoroquinolones were heavily used as a first-line treatment for outpatient respiratory tract infections in the United States[206]. For ciprofloxacin, the defined daily doses per 1000 inhabitants per day (DID) was 0.97% in the United States compared to a range of 0.17% (Croatia) - 1.81% (Portugal)[206]. In the developing world, usage of fluoroquinolones is highly correlated with access, and this differs across regions. The highest use of fluoroquinolones is in South and Southeast Asia where fluoroquinolones are accessible from a pharmacy without prescription and are widely used by patients as self-medication.

A study of paediatric patients presenting with diarrhoea in Ho Chi Minh City, Vietnam between 2014 and 2016 found that over 66.7% of admitted patients were administered fluoroquinolones, and in many cases, this was prior to determination of the infection[207]. A study conducted in Singapore between 2006 and 2008 found that there was a steady increase in ciprofloxacin administration amongst hospital inpatients, from 317.87 to 448.76 defined daily doses per 1000 inpatient-days over the two-year period. Compared to the other classes of antimicrobials tracked in this study, fluoroquinolone usage increased the most[208]. A study of AMR and antimicrobial prescription in regions of South Asia and Africa for *Escherichia coli* (*E. coli*) infection found that in three South Asian study sites (Pakistan, India, and Bangladesh), 60% of the antimicrobials administered to patients presenting with dysentery were ciprofloxacin. In contrast, for cases of watery diarrhoea, ciprofloxacin was given approximately 10% of the time in Pakistan and Bangladesh, compared to 60% of the time in India[209]. In Africa, the same study found that ciprofloxacin usage was much lower, with ciprofloxacin accounting for 0-10% of prescribed antimicrobials for either diarrhoea or dysentery[209]. There is insufficient data about fluoroquinolone usage in Africa, although there is still distribution and use of fluoroquinolones, particularly for the treatment of typhoid and other bacteraemia, for which ciprofloxacin is one of the primary treatment options. There is some data showing widespread usage of antimicrobials in livestock, and this heavy usage, ranging from 77.6% in Nigeria to 100% in certain countries throughout Africa, may allow bacteria to develop resistance in the environment that then adversely affect patients[210].

1.4.4 FQR in *S.* Typhi and Paratyphi

AMR, including fluoroquinolone resistance (FQR), is a considerable problem in *S.* Typhi and *S.* Paratyphi[19,211,212]. After fluoroquinolones were introduced, cases of fluoroquinolone-resistant *S.* Typhi and *S.* Paratyphi became apparent in the 1990s and 2000s[212–214]. At that time, there were still significant numbers of FQ-susceptible isolates, and this was the case through the mid-2000's. However, after fluoroquinolones became an established treatment for *S.* Typhi, there has been an increasing trend of FQR on top of existing MDR. The H58 (genotype 4.3.1) lineage of *S.* Typhi are often MDR, for example by carrying incH1 plasmids, which contain multiple resistance genes, and many of the isolates sequenced also have decreased fluoroquinolone susceptibility due to chromosomal and sometimes plasmid-mediated resistance[188]. In some cases, susceptibility still exists to later-generation fluoroquinolones,

such as the fourth-generation fluoroquinolone gatifloxacin[215,216]. However, given the prevalence of fluoroquinolone usage and the pressure bacteria are under to develop resistance, there is an evolution of resistance amongst typhoidal *Salmonella* against fluoroquinolones and the likelihood is that resistant strains are at least as fit fluoroquinolone susceptible ones[217]. A recent outbreak of XDR *S*. Typhi in Pakistan not only displayed resistance to the three first-line treatments but also had a decreased susceptibility to fluoroquinolones, marked by carriage of plasmid-mediated resistance gene *qnrS*, which has complicated the treatment strategy[191]. Interestingly, *S*. Typhi seems much more adept than *S*. Typhimurium at acquiring plasmid-mediated FQR. In the face of XDR *S*. Typhi, azithromycin and ceftazidime have been used successfully for FQR, although there are limited reports of resistance of azithromycin-resistant *S*. Typhi[218]. In Africa, there has been an increase in MDR *S*. Typhi, marked by a decreased ciprofloxacin susceptibility[219,220]. These outbreaks further validate the need for wider vaccination efforts in areas with endemic *S*. Typhi.

Vaccines against *S*. Typhi and *S*. Paratyphi

Recent efforts to control the spread of *S*. Typhi, especially in light of the increase in multidrug resistance, have focused on wider vaccination efforts. There are currently two broadly licensed vaccines against *S*. Typhi; an oral live attenuated Ty21a and inactivated parenteral Vi capsular polysaccharide vaccine, which have been used in at-risk populations and travellers but do not provide full immunity[221,222]. The Ty21a vaccine is administered in three doses and is largely used by travellers visiting endemic *S*. Typhi areas. The efficacy of this vaccine is 65%, and the vaccine needs to be administered every 3-5 years for continued protection[222,223]. The Vi polysaccharide vaccine, which is administered as one intramuscular injection, has a three-year efficacy of approximately 55%, and a follow-up study has shown ten-year protective antibody levels in approximately half of the immunized population[224,225]. Importantly, neither Ty21a nor the Vi polysaccharide vaccine are approved for use in children under two years of age, a high-risk population[222].

More recently, a typhoid conjugate vaccine (Typbar-TCV) manufactured by Bharat Biotech has undergone clinical trials in Malawi, Bangladesh, and Nepal, regions with high levels of endemic *S*. Typhi. This vaccine shows considerably higher efficacy, with up to 85% protection following immunization of children from nine months to 15 years of age, and it has now been pre-qualified by the WHO for wider trials and usage[226–228]. Pakistan was

one of the first countries to add this vaccine to their national immunization programme in response to the XDR typhoid outbreak, and India has introduced TCV into its childhood immunization programme in Navi Mumbai[229,230]. The IVI is currently implementing studies to continue to evaluate the vaccine and follow up cohorts to understand effects on the *S*. Typhi burden, transmission, and prevalence of other sources of bacteraemia in various sites in Africa. Countries enrolled in Typbar-TCV vaccine trials and administration are Ghana, the DRC, and independently, Bangladesh. The Effect of a novel typhoid conjugate vaccine in Africa: a multicentre study in Ghana and the DRC (THECA) will conduct clinical studies and a mass vaccination campaign, measuring vaccine efficacy[231].

There are no current licensed vaccines in general use against *S*. Paratyphi. There is a significant need for a vaccine against *S*. Paratyphi A, given the high burden in parts of South and Southeast Asia, where the incidence approaches that of *S*. Typhi. There are some vaccine candidates under development and in Phase I and II clinical trials, and more research and testing is needed to determine their efficacy and suitability for routine use[232].

1.4.5 FQR in *S*. Typhimurium

FQR in *S*. Typhimurium is not yet considered as problematic as in *S*. Typhi and *S*. Paratyphi, largely due to the fact that NTS infections generally do not require antimicrobial intervention. However, this situation is changing with the rise in ST313 and other iNTS infections. Epidemiological data suggest that *S*. Typhimurium isolates primarily acquire chromosomal mutations in *gyrA*, and there are scant examples of other chromosomal mutations in *S*. Typhimurium that confer direct FQR, unlike what is found in *S*. Typhi[233,234]. Plasmid-mediated quinolone resistance (PMQR) in *S*. Typhimurium is also significantly less than what is seen in *S*. Typhi, with only one out of 276 isolates of analysed African ST313 isolates from before 2017 displaying a PMQR gene[176]. This likely reflects that fluoroquinolone usage in iNTS is still lower than in typhoidal infections, at least in Africa. However, there are regions that have high levels of FQR, namely South and Southeast Asia where fluoroquinolone usage is high[57,235]. In Vietnam and other nearby Southeast Asian countries, *S*. Typhimurium ST34 exhibit extensive MDR, often with high levels of resistance to fluoroquinolones[236]. Many of these isolates carry multiple mechanisms of resistance to fluoroquinolones and other drugs[131,237,238].

Ciprofloxacin is one of the most commonly used broad-spectrum antimicrobials and is the first-line treatment for invasive salmonellosis in many parts of the world. Over the past several years, the prevalence of *S*. Typhimurium strains with intermediate and complete ciprofloxacin resistance has grown. The patent for ciprofloxacin expired in 2003, and the introduction of affordable generics into Africa has influenced higher usage across the continent[239]. According to CLSI, *Salmonella* are considered sensitive to fluoroquinolones excluding nalidixic acid if the minimum inhibitory concentration is ≤ 0.06 μg/ml of the FQ. Susceptibility is considered intermediate for an MIC of 0.12 - 0.5 μg/ml, and resistance is an MIC of ≥ 1 μg/ml of the FQ[200,240,241].

In African ST313 lineages, there is not yet widespread FQR; however, there has been an observable decrease in ciprofloxacin susceptibility (DCS) over the past decade. This has been notable in the DRC, where there is an ongoing outbreak of DCS ST313 infections with a high degree of MDR (Van Puyvelde *et al.*, in progress). Perhaps because of simultaneous outbreaks of *S*. Typhi and *S*. Typhimurium in the DRC, there is an increased likelihood of bacteria becoming DCS[220] (Van Puyvelde and Dyson, in progress). In particular, DCS has been observed in ST313 lineage II.1 isolates, where substructure in the phylogenetic tree reveal specific branches show a phenotypic and genotypic decrease in ciprofloxacin susceptibility. Most of these isolates do not yet have full resistance to ciprofloxacin and other FQs, but there is the potential for them to acquire further resistance[176].

1.4.6 Other AMR profiles in invasive *S*. Typhimurium

While resistance to fluoroquinolones is one of the most pressing AMR concerns in *S*. Typhimurium because of its importance as a first-line broad-spectrum antimicrobial, it is not the only class of drugs that *S*. Typhimurium clades have shown resistance to. This problem is most worrisome for invasive clades, especially ST313 and ST34 that cause more disease in immunocompromised individuals. Some isolates of ST34 carry an IncHI2 plasmid, which confers drug resistance to: fluoroquinolones, bleomycin, sulphonamides, trimethoprim, kanamycin, streptomycin, chloramphenicol, spectinomycin, florfenicol, hygromycin B, apramycin, beta-lactams, and rifampin, and they may further carry mercury resistance genes[57]. Analysis of ST313 lineage I and II isolates when first sequenced revealed that they had a substantial AMR profile carried by a Tn*21*-like transposition element[82]. Lineage I

isolates lack resistance to chloramphenicol but otherwise carry resistance genes on the pSLT virulence plasmid against cotrimoxazole, ampicillin, and sulphonamide, and trimethoprim. Lineage II isolates carry additional chloramphenicol and streptomycin resistance[80]. Recent analysis of ST313 lineage II and sublineage II.1 isolates have shown that sublineage II.1 also contains an IncHI2 plasmid, named pSTm-ST313-II.1. This plasmid carries genes conferring resistance to chloramphenicol, ampicillin, and trimethoprim/sulfamethoxazole. In XDR sublineage II.1 isolates, there are additional extended spectrum beta-lactamase (ESBL) genes that confer resistance to cephalosporins and plasmid-mediated azithromycin resistance. Sublineage II.1 isolates also carry genes that may confer silver and copper resistance[176]. Importantly, this analysis was conducted on isolates predominantly from the DRC, and it is possible that the AMR profile of ST313 lineage II and other potentially emerging sublineage isolates elsewhere in Africa differ slightly in their AMR makeup.

1.4.6.1 Threat of XDR *S*. Typhimurium ST313

An outbreak of extremely drug-resistant *S*. Typhimurium has recently been documented in the DRC, and this accounts for >10% of all *S*. Typhimurium isolates collected in the Kongo Central Province[176]. Given the trends of resistance already observed, without intervention in antimicrobial stewardship or vaccination, there is a strong likelihood of this occurring more frequently and across a wider geography. One region of significant concern is the DRC, where there are observed incidences of MDR and DCS ST313 and independently of MDR ST313 carrying plasmid-mediated azithromycin resistance, both sets of which are also ESBL positive[176] (Van Puyvelde et al., in progress). There is also an observation of three pan drug resistant ST313 isolates that carry the MDR plasmid pSTm-ST313-II.1 as well as plasmid-mediated azithromycin resistance and either chromosomal or plasmid-mediated DCS.

These two phenotypes of isolates predominate in different geographic regions of the DRC, but given the ease of horizontal transmission occurring and spontaneous DCS arising, there is a number of scenarios that could emerge. One possibility is that a spontaneous chromosomal mutation conferring DCS or even full ciprofloxacin resistance (CR) could arise in the azithromycin-resistant isolates. Or, they could acquire a plasmid-mediated resistance gene conferring CR. Alternatively, bacterial populations that are DCS could acquire a novel azithromycin resistance mutation or acquire plasmid-mediated azithromycin resistance. In

any country, MDR bacteria with DCS and azithromycin resistance pose a considerable threat. The DRC, despite increased surveillance of cases of bacteraemia, is a country ill-equipped to mitigate such an outbreak, making further surveillance and iNTS vaccine initiatives even more necessary. It will be interesting to see how the introduction of the typhoid conjugate vaccine influences the MDR profile and burden of ST313 in the DRC.

1.4.7 iNTS vaccines

Given the burden of iNTS, and specifically *S*. Typhimurium ST313, various entities have begun investigating and developing vaccines against iNTS. While iNTS remains a lesser-known problem globally, it is appreciated as an acute concern in sub-Saharan Africa, and a vaccine against iNTS could make significant differences in child mortality and reduce pressure on antimicrobial usage to treat bacteraemia[25,130]. There are currently efforts underway to develop a vaccine against iNTS that covers *S*. Typhimurium and *S*. Enteritidis, and some of these have performed positively in animal models[242,243,51]. One of the vaccine candidates is a bivalent conjugate vaccine that uses the core and O-antigen polysaccharides of *S*. Typhimurium and *S*. Enteritidis linked to the FliC (Phase I flagellin subunit) protein of each serovar. A second candidate is a live attenuated oral vaccine, which would consist of *S*. Typhimurium and *S*. Enteritidis lacking *guaBA*, *clpP* or *clpX*, and *fljB*, which encode guanine synthesis, flagellar regulation, and flagellar function, respectively. In mice, these attenuated strains have been shown to cause an attenuated response and generate some protection[244].

A third type of vaccine is led by GSK Vaccines for Global Health (GVGH) and uses the Generalized Modules for Membrane Antigens (GMMA) technology for vaccine development. The principle behind this technology is the use of Gram-negative outer membrane particles that are shed from genetically modified bacteria to deliver immune-stimulatory components, namely outer membrane antigens including O-antigen, directly to the immune system[245]. These particles include outer membrane lipids, outer membrane proteins, and soluble periplasmic components, and the bacteria can be genetically modified to shed more or less of these constituents. As these components form part of the bacterial outer membrane, they are highly stimulatory to the human immune system, thus eliciting a measurable protective responses, including a B-cell response and antibody generation against O-antigen and porins[246,247].

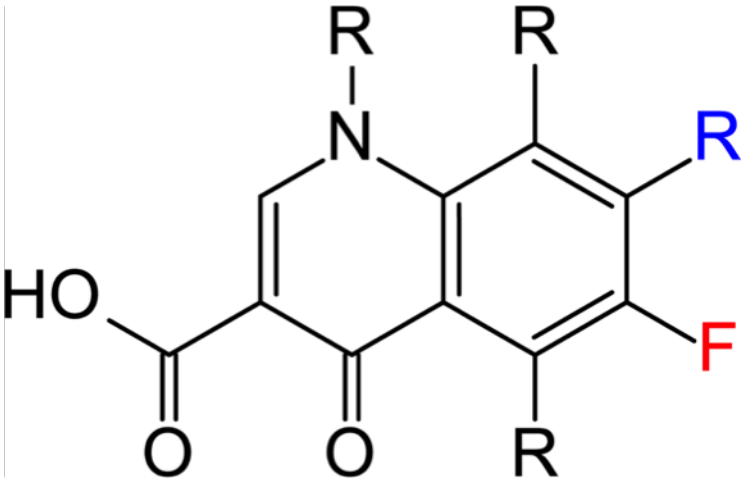

Figure 1.5 Structure of the fluoroquinolone ciprofloxacin. Ciprofloxacin is a fluorinated quinolone that binds to DNA gyrase I and Topoisomerase IV of Gram-negative bacteria.

1.5 Fluoroquinolone mechanism of action and resistance

Fluoroquinolones are a highly successful class of bactericidal antimicrobials because of their action on DNA replication machinery. Quinolones were first discovered in the 1960s, and nalidixic acid, though not strictly a quinolone based on its composition, was the first "quinolone" to be used against bacterial infections. Quinolones are comprised of a two-ringed system involving a nitrogen and a ketone. These were soon superseded by newer generations of fluorinated quinolones, the addition of a fluorine atom attached to the central quinolone ring. There are now four generations of quinolone drugs, with the 'generation' referring to the spectrum of bacteria they are active against[248]. Second generation fluoroquinolones were notable in their activity against Gram-negative bacteria, including *Pseudomonas aeruginosa*, while later generations were capable of treating Gram-positive bacterial infections as well[248,249]. The later generations have a broader spectrum, although there is no systematic measurement of assigning these drugs to a specific generation. Despite the vast number of synthesized fluoroquinolones, not all of them are licensed for human usage by the Food and Drug Administration (FDA) due to levels of toxicity and side effects[250]. As a result, some of the earlier generations of fluoroquinolones, which lack the most toxic effects, are still in use.

1.5.1 Mechanism of action of fluoroquinolones in Gram-negative bacteria

Ciprofloxacin is a second-generation fluoroquinolone bactericidal antimicrobial that acts by binding to bacterial type II topoisomerases DNA gyrase I and Topoisomerase IV in Gram-negative bacteria to disrupt DNA supercoiling. Bacteria supercoil DNA to condense and pack large quantities into the limited intracellular space, and the enzymes DNA gyrase and Topoisomerase IV function by creating temporary DNA breaks to constantly modify the level of supercoiling in response to bacterial needs and environment[251–253]. DNA gyrase I is unique in its involvement in negative supercoiling, a process that can be invoked to relax supercoils in the DNA. This comes into play as bacteria undergo DNA replication and need to release tension that builds in the double-stranded DNA as replication proceeds[254]. DNA gyrase I is an A2B2 heterotetramer comprised of four subunits: two GyrA and two GyrB complexed together. The GyrA subunit is 97 kDa, comprised of an N-terminal domain of 59 kDa and a C-terminal domain of 38 kDa, and the C-terminal domain, which directly interacts with DNA, is involved in substrate recognition and other protein interactions[255]. Topoisomerase IV is a heterotetramer comprised of two repeating units of ParC and ParE, assembled similarly to DNA gyrase. Topoisomerase IV is primarily involved in segregating the catenated DNA rings post-replication.

When bacteria are treated with fluoroquinolones, the drug enters the cell and binds to the interface between the DNA and GyrA or GyrB subunit of DNA gyrase I or ParC of Topoisomerase IV, converting transient double-stranded breaks into permanent ones[253,256,257]. As fluoroquinolones do not inhibit gyrase activity, the initial reaction of bacterial cells is a halt in growth, and cell death occurs when the permanent double-stranded DNA breaks occur.

If there is insufficient fluoroquinolone to bind all the active gyrases, the drug acts as a bacteriostatic antimicrobial. However, if there is an excess of drug compared to binding sites, enough double-stranded breaks overwhelm the SOS response and DNA repair machinery, leading to cell death. In Gram-positive bacteria, the primary target of ciprofloxacin is topoisomerase IV. Despite similarities between human and bacterial topoisomerases, there is a strong preference of fluoroquinolones for prokaryotic topoisomerases, and there appears to be minimal activity of fluoroquinolones against human topoisomerase[258–262].

1.5.2 Chromosomal resistance to ciprofloxacin in Gram-negative bacteria

A key region of the bacterial genome responsible for FQR is known as the quinolone resistance determining region (QRDR)[252,253,263,264]. Mutations in the QRDR within *gyrA*, *gyrB* or *parC* are mainly conserved, with a specific serine substitution, most commonly Ser83Tyr in GyrA, responsible for most resistance in Gram-negative bacteria by reducing the drug binding affinity[252,263]. However, some *Salmonella* isolates with more recent resistance acquisition show mutations at alternative sites within the QRDR (Van Puyvelde, personal communication)[241]. Additionally, there may be other unknown mutations within the chromosome that can contribute to FQR though not within the QRDR.

The degree to which organisms acquire *gyrA*, *gyrB*, *parC*, and *parE* mutations depends on the organism itself. *S*. Typhi isolates have been known to acquire mutations in *gyrA* and *parC* or *parE*, and in many cases a single isolate may carry multiple mutations[191,265]. They typically will not, however, acquire a *parC* or *parE* mutation on its own. This follows *gyrA*, as DNA gyrase appears to be the enzyme more susceptible to poisoning by fluoroquinolones, although there are exceptions to this[265–267]. In contrast, there are few reported cases of *parC* or *parE* mutations in *S*. Typhimurium or other NTS serovars[268]. When mutations arise in *gyrA* in *S*. Typhimurium, some of the most common clinical amino acid substitutions are D87N (aspartic acid to asparagine), S83F (serine to phenyalanine), and S83Y (serine to tyrosine), as these are residues important for quinolone binding[269–273]. There are other amino acid substitutions that may occur within the QRDR, including D87G (aspartic acid to glycine); however, these occur with less frequency in in *S*. Typhimurium. Serine substitutions are thought to be the most common because they disrupt DNA gyrase catalytic activity the least[253,269]. The level of resistance conferred is also dependent upon the specific amino acid change, and this likely explains the preponderance of specific substitutions (Van Puyvelde, personal communication)[272–274].

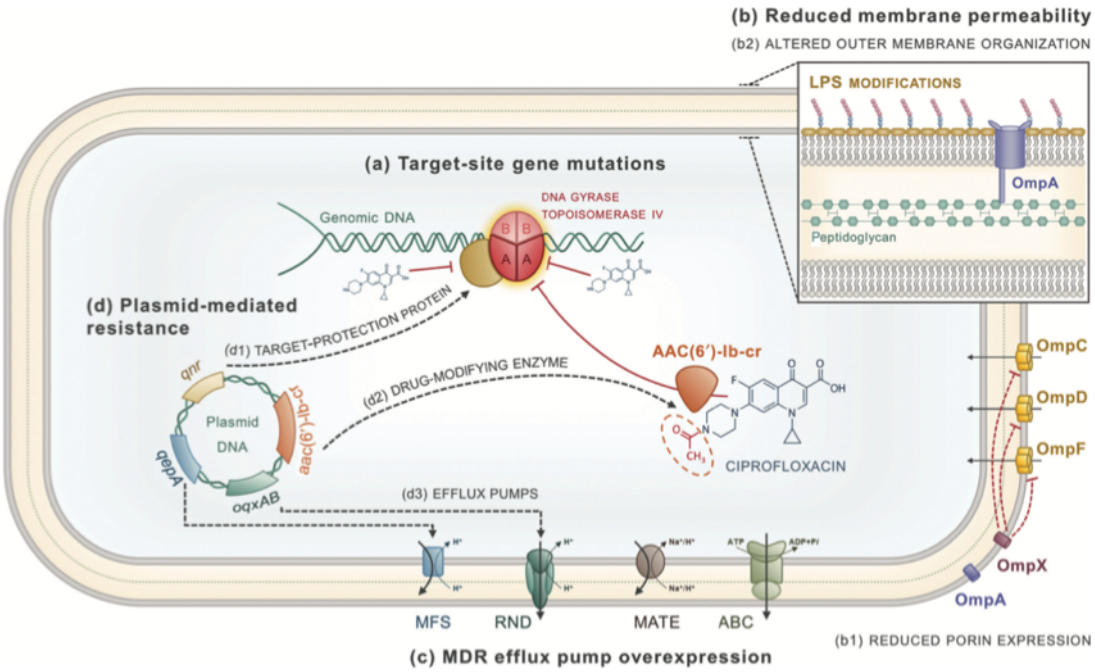

Figure 1.6 Mechanisms of fluoroquinolone resistance. Gram-negative bacteria can employ multiple mechanisms independently or in tandem to resist killing by fluoroquinolones. From Correia *et al.*, 2017[275].

1.5.3 Plasmid-mediated resistance by *qnr* to ciprofloxacin in Gram-negative organisms

In addition to chromosomal mutations in the QRDR, a secondary mechanism of FQR is due to plasmid-mediated quinolone resistance (PMQR). This is currently less common in *S.* Typhimurium, and PMQR is rarely observed independently of chromosomal mutations in the QRDR. However, families of genes known as the *qnr* genes directing the expression of the protein Qnr that can bind to topoisomerase, are responsible for decreasing ciprofloxacin susceptibility in some *Salmonella*[252,253]. The *qnr* genes fit within six different families, which are QnrA, QnrB, QnrS, QnrC, QnrD, and QnrVC, and these proteins of approximately 218 amino acids physically prevent quinolone binding to DNA gyrase and topoisomerase IV[269,276–278]. It has been observed that Qnr proteins are more inhibitory towards ciprofloxacin than nalidixic acid, and *qnrA* has been found to increase the resistance from 12.5-250-fold, while *qnrS* has increased ciprofloxacin resistance by 16-62.5-fold[279–281]. While the presence of *qnr* is understood to elevate the MIC of an organism, it is rare that *qnr* without a chromosomal mutation to DNA gyrase or topoisomerase IV confers decreased

susceptibility to fluoroquinolones[277]. However, there have been a few examples of organisms that have a *qnr* gene on the plasmid but do not have chromosomal resistance[176]. Such cases are highly unusual, and it is not clear why this does not occur more frequently.

1.5.4 Other genes involved in resistance

In addition to *qnr* genes, there are other classes of PMQR genes that are able to break down certain fluoroquinolones and yet other genes that restrict drug entry[282,275]. Gene aac(6')-Ib-cr encodes a bifunctional variant of an aminoglycoside-modifying acetyltransferase. While aac(6')-Ib-cr has primarily been implicated in resistance to aminoglycosides (including kanamycin), two known amino acid substitutions in aac(6')-Ib-cr enable the acetylation of a nitrogen in quinolones, thus reducing the quinolone efficacy and increasing tolerance to fluoroquinolones[275]. Lastly, yet another set of PMQR genes, *oqxAB* and *qepA*, code for a subset of efflux pumps that actively transport fluoroquinolones out of the cells[283]. QepA specifically acts against hydrophilic fluoroquinolones, which includes ciprofloxacin. In contrast, OqxAB acts more broadly against fluoroquinolones and also targets other antimicrobials including tetracycline, chloramphenicol, and trimethoprim[275,278,284,285]. While *oqxAB* and *qepA* are normally not solely responsible for FQR, they can play a key role in reducing drug susceptibility[253]. Of concern is the observation that some PMQR genes may be easily transferred horizontally but have been detected chromosomally, suggesting that these genes may propagate on the plasmid but insert within the chromosome to become fixed in the bacterial population[275,278].

In Gram-negative organisms, there are yet more mechanisms that occur to reduce drug uptake. Because of the LPS barrier in Gram-negative bacteria, drugs are dependent on outer membrane porin channels for cell entry, and bacteria can modulate the size, number, and conductance of porins. Expression of Omp proteins, including OmpF, OmpC, OmpD, and OmpA, controlled by expression of regulator OmpX have been implicated in decreased drug susceptibility. The expression of Omp proteins often occurs in conjunction with an upregulation of efflux pumps, such as AcrAB-TolC, to decrease quinolone uptake and increase efflux. These can be further aided by mutations in Mar, SoxRS and Rob regulons, which can regulate porin, efflux pump expression, and LPS remodelling[252,253,269,286–293].

1.5.5 Mechanisms of resistance found in African *S*. Typhimurium ST313

S. Typhimurium ST313 respond to ciprofloxacin in a similar way to how other Gram-negative bacteria respond. The primary target for ciprofloxacin is *gyrA*, and that is the gene in which the most primary mutations occur. Of the African ST313 isolates that have been analysed, with particular attention to those in sub-lineage II.1 and the emerging sub-lineage II.2 from the DRC, there is considerable variation in the ciprofloxacin MIC as determined by MIC eTest. Of 61 analysed ST313 isolates that have been studied in greater depth, the MICs range from 0.015 (susceptible) to 0.75 (intermediate). Interestingly, the isolate (4930_4) with the lowest MIC harbours a GyrA D87Y substitution, while the isolate (10530_17) with the highest MIC from within this study has an unknown mechanism of DCS (Van Puyvelde, personal communication). There have been documented GyrA substitutions at S83Y, D87N, D87Y, and G81C. Most of the lineage II.2 isolates carrying an S83Y *gyrA* mutation cluster within the MIC range of 0.094 and 0.25. However, even this smaller spectrum is still substantial enough to beg the question of what contributes to these differences. There have also been scant examples of recent isolates carrying a GyrB substitution S464Y, which is within the QRDR (Van Puyvelde, personal communication)[294]. Interestingly, the different substitutions seem to group separately in organisms dispersed on the phylogenetic tree, suggesting that different organisms are capable of withstanding different degrees of mutational stress (Van Puyvelde, personal communication)[176].

There have been at least four examples of a *qnrS* gene carried on the plasmid of an ST313 isolate. The four isolates carrying *qnrS* have all been isolated in the past four years, suggesting that this may be an emerging form of DCS in ST313. Given the ease of horizontal gene transfer, it is highly probable that *qnrS* will become more prevalent in the population over time. The pSTm-ST313-II.1 plasmid also carries *aac* gene, which may influence fluoroquinolone binding[176]. The bias in geographic sampling may mean that there are additional or different resistance mechanisms that have not yet been observed.

1.5.6 Pharmacokinetics/pharmacodynamics of ciprofloxacin

In order to appropriately administer antimicrobials, the rates of absorption, secretion, and excretion(pharmacokinetics) and the effects and mechanisms of uptake (pharmacodynamics) must be assessed. For ciprofloxacin, pharmacokinetic studies undertaken with human volunteers determined that the drug is most efficacious when administered orally twice every 24 hours to achieve a level of perfusion similar to an intravenous dose[295]. 70% of the drug is thought to be bioavailable in adults and 60% is bioavailable in children, and the maximum concentration in the serum is achieved between one and two hours after oral administration[295,296]. In adults, the mean concentration found 12 hours after a 500 mg oral dose is 0.2 μg/ml. For typhoid or infectious diarrhoea, the recommended dose is 500 mg every 12 h for 10 days or 5-7 days, respectively. Ciprofloxacin is a large solute, and after entering the bloodstream, it disperses widely, and tissue concentrations may exceed serum concentrations. The active form of ciprofloxacin is found in multiple tissue locations and secretions, including in the saliva, lymph, sputum, and bile[295]. Despite widespread use of ciprofloxacin, it is still not fully understood how and when cells take up ciprofloxacin and the efficiency of cell absorption. Because *Salmonella* are partly intracellular organisms, this directly affects killing efficiency. Beyond excretion of ciprofloxacin in urine, it has been found that ciprofloxacin is also excreted in sweat, and this has been linked to resistance in *Staphylococcus aureus* resident on the skin within one week of treatment[297].

1.6 Observation of disconnect between phenotypic and genotypic resistance

Thus, when considering phenotype, genotype and phylogeny, not all resistance to the fluoroquinolones in field isolates of *S*. Typhimurium is explained. To fully understanding how bacteria develop decreased susceptibility to stress, including antimicrobials, it is important to recognize the contribution of genetic and epigenetic components. While the primary genetic basis for resistance to ciprofloxacin has been well characterized, there are likely other factors that occur in tandem or instead of that contribute to a decreased susceptibility. This has been observed historically but has not been thoroughly considered or investigated as a substantial contributor to AMR and as a factor that may play a large role in antimicrobial treatment.

Further, there may be species and lineage-specific adaptations that may lead to resistance as some lineages appear more successful in the natural world than others.

1.6.1 Observation of phenotypic heterogeneity in ST313s

The African ST313 clades have been more thoroughly characterized in recent years, and it is known that they are a highly clonal population still undergoing evolution in the context of antimicrobial exposure. While the landscape of DCS has not yet been fully explored, there have been studies looking at genotypic and phenotypic differences between ST313 isolates under serum exposure. These studies stemmed from the observation that highly related ST313 isolates are differentially susceptible to serum killing. Ondari *et al.* exposed six different ST313 lineage II isolates to serum from healthy adults and found that there were three definable phenotypes: susceptible, intermediate, and resistant to antibody-mediated killing. This was an interesting finding because these isolates have few SNP differences, and these known SNPs could not explain the differences in serum susceptibility. Transcriptional analysis of the serum-resistant isolates grown in the presence of serum identified relatively upregulated genes associated with cell surface structures, iron use, and metabolism, while they downregulated genes associated with membrane proteins. These data suggest that there is considerable variation that occurs at the tips of the phylogenetic tree, which may not be due to readily identifiable genetic differences between the isolates[181].

Similarly, ongoing work in ST313s have indicated unique groups of colonial morphotypes when bacteria are grown under biofilm-forming conditions, another form of environmental stress. Bacteria may form biofilms when exposed to harsh environmental conditions. A biofilm is an extracellular matrix composed primarily of polysaccharides, proteins, and extracellular DNA that protect the bacteria from direct assault[298]. Biofilms have been shown to form in various conditions where a community lifestyle is advantageous, such as in adverse conditions outside of a host, on the built environment such as catheters and filters, and as part of the microbiome within hosts[299,300]. D23580 carries mutations that inactivate KatE, a catalase involved in oxidative stress, and BcsG, a cellulose biosynthesis enzyme required for biofilm formation[182]. Together these mutations are implicated in differences in biofilm formation between ST313 and ST19 (lab strain 14028s), but they do not explain variation in biofilm morphotypes within the ST313 sublineage. The genetic basis underlying the

phenotype of varying ST313 biofilm colonial morphotypes has proven elusive, and there may be multiple factors, some of them transcriptional, that explain differences in these morphologies that occur when bacteria are required to form biofilms[176,183].

A further phenotype that has been noticed in *S*. Typhimurium and is under investigation in ST313 isolates is differences in O5 antigen presence or absence, and what that correlates to[301,302]. *S*. Typhimurium is characterized by having O4 and H:I antigens, but not all of *S*. Typhimurium have O5. Interestingly, a recent analysis by Tack *et al.* has identified an increase in O5 negative invasive *S*. Typhimurium, representing 36.9% of the sampled *S*. Typhimurium in the DRC. Notably, there was an increase in O5-negative isolates each year, with much more significant numbers of O5-negative isolates from 2013-onwards[302]. It has previously been shown that variation in O-antigen length can affect macrophage uptake and complement resistance, and a length of > 4 and < 15 repeating units provides greater protection[303]. Furthermore, it appears that O-antigen length is growth phase-dependent, modulated by environmental factors, and this regulation influences serum sensitivity[304]. Additionally, past studies have shown that the presence of O5 plays a significant role in antibody binding and thus host response to infection[18]. In the context of vaccine development that is based on O-antigen specificity and binding, it is essential to understand what these differences in O5 and LPS chain length mean, how they are regulated, and how they can be detected.

1.6.1.1 High-throughput genotyping as method to distinguish between related organisms

Over the past two decades, whole genome sequencing (WGS) has become a powerful method to investigate differences between related organisms, and with the steady decrease in cost of WGS, it has become commonplace to sequence bacterial isolates on a large scale as part of surveillance and to understand population structure. The power of this technology is that it enables detection of minute differences between related organisms, such as SNPs, which may contribute to virulence or drug resistance. This has already been undertaken to great effect in many organisms, including in *S*. Typhimurium ST313. Okoro *et al.* showed significant differences between ST19, ST313 lineage I and ST313 lineage II bacteria using phylogenetic and BEAST analyses to pinpoint nodes of divergence and where in the genome these differences arose[82]. Similarly, Van Puyvelde *et al.* have been able to identify and

investigate a novel sub-lineage of ST313 bacteria that differ from lineage II using WGS of over 500 ST313 isolates. These data have revealed SNP differences and pseudogenization that indicate a greater degree of host-specificity and azithromycin resistance. However, a limitation of WGS, even when it is done for a high volume of samples, is that it cannot provide any insight of how bacteria are behaving in real-time to environmental pressures; it can only provide a prospective snapshot. Additionally, given the transcriptional and post-transcriptional modifications that occur, it is likely that some of the differences in bacterial phenotype cannot be accounted for by the genome sequences alone, and a combination of high-throughput genotyping and high-throughput phenotyping may provide greater insight.

1.6.1.2 Introduction to high-throughput phenotyping to understand AMR

In contrast, phenotyping of organisms allows scientists to examine bacterial behaviour under growth and/or duress to understand any underlying mechanisms of persistence and survival. Historically, this has been done at small scale because of technological limitations. However, with the advent of newer technologies, it is now possible to undertake large high-throughput screens to investigate multiple bacterial isolates simultaneously. There are a few different levels of phenotype that can be measured, and depending on the question, they can be used to great effect. An area of study that could significantly benefit from the use of high-throughput phenotyping is AMR measurement, because present methods of detecting, validating, and applying AMR information are often low-throughput, time-consuming, and often not clinically useful[305,306].

One method of high-throughput phenotyping is RNA sequencing (RNA-seq) of bacteria to investigate the changes in gene expression that occur upon antimicrobial exposure. Such information is extremely useful for determining the conditions under which antimicrobials might be used and concentrations that are effective, and it can be employed to understand nascent resistance mechanisms, especially when linked to genomic information[307]. A limitation of direct measurements on bacteria is that they are growing outside of the context of the host.

A second method is high-throughput metabolic profiling of bacteria. This has been carried out extensively to understand how bacteria respond to different nutrient environments and metabolic pathways associated with biosynthesis, metabolism, virulence, and AMR have

been investigated[308,309]. The power of such a method is that one can use known interactions and phenotypes to help identify unknown interactions based on similarity of patterns. Such phenotyping has been done using the Biolog assay to quantify cellular respiration of bacteria under different metabolic conditions[176,237,310]. This methodology paired with advances in analysis pipelines has opened doors to probing interactions and patterns at greater depth. An example of this is the extensive mapping of the fitness of an *E. coli* mutant library under 324 different conditions, including antimicrobial perturbation, which revealed insights into drug mechanisms and gene essentiality[311]. Another successful example from Yang *et al.* used network modelling and biochemical screening to flag pathways and mechanisms that determine antimicrobial lethality[312].

Yet another powerful method is high-throughput imaging to assess changes in morphology. With high-content microscopes that can clearly image wells of bacteria at high-resolution to distinguish individual bacteria, it is now possible to analyse single bacterial cells. The power of this technology is that it can be harnessed to assess how a given isolate responds to antimicrobial treatment at a given concentration, to study how genotypically similar isolates respond to the same treatment, and to follow antimicrobial treatment over time. While some of these questions have been addressed in the past, the combination of automated high-throughput screening and automated analysis pipelines that can distinguish morphological features allows for a new depth of investigation and understanding. In particular, these advancements enable large-scale assessment of how clinically relevant bacteria respond to standard antimicrobials in a diagnostic context. For example, a screen that can rapidly quantify growth of a clinical sample in the presence of various antimicrobials to help determine the best course of treatment would be valuable in a clinical setting. Some of this information would be obtainable via sequencing and standard laboratory diagnostics; however, observing morphological changes of the bacteria over a period of time would help predict how a given isolate and population might respond over the course of treatment and thus help clarify appropriate dosage and single or combination therapies. Additionally, these technologies can and have been used to screen for novel therapeutics and development of resistance to them as well as track development of resistance to existing antimicrobials[313,314]. Even with low-resolution microscopy, increased analytical power and methodologies have opened doors to gleaning increasing amounts of information from phenotypic data[315].

1.6.2 'Adaptive resistance' and desensitization to antimicrobials

Such phenotyping methods as described above open the door to exploring how bacteria adapt in real-time to an environmental stressor, specifically measuring how they change morphologically over time. This enables the study of adaptive resistance to antimicrobials, a concept that has not yet been as well-characterized as mutational resistance. It is understood that in a heterogeneous culture, given a large enough population of bacteria, there are likely to be some that carry mutational resistance to a given antimicrobial (or other stressor)[316]. However, what is less-well understood is how bacteria can develop resistance, or rather, 'desensitization' to a treatment in a way that is not obviously due to mutation. It has been observed that when bacteria are grown in the presence of theoretically lethal concentrations of antimicrobials, there is typically an initial death phase, which may be followed by a rebound growth phase[317,318]. However, the mechanisms contributing to this phenotype have not been studied in depth. One study proposed that a decoupling of transcription and translation in the cells leads to uncontrolled cellular division, resulting in a surge in bacterial counts after an initial death phase[317]. Overall, while this phenotype has been observed, most have not delved into its significance and the role it may play in bacterial escape of antimicrobial killing[318,319]. It is possible that the explanation for this lies in bacterial desensitization to the antimicrobial via transcriptional means, and part of this may occur from phase variation stochastically during growth or by DNA inversion[320,321]. The serum resistance in ST313 isolates observed by Ondari *et al.* may similarly be explained by this phenomenon, especially as there were no SNPs that accounted for the differences in serum sensitivity and resistance between isolates[181]. However, at the moment that remains unproven.

1.6.2.1 Mechanisms of adaptive resistance to stress in *S.* Typhimurium

Some discussion of adaptive resistance was mentioned earlier when considering the mechanisms of FQR. One of these mechanisms is upregulation of drug efflux pumps and alteration in membrane permeability that help expel drug[322]. This is an example of adaptive resistance because the bacteria have not acquired any mutations during the course of treatment, but they have changed transcription of existing machinery. One prominent mechanism that seems to enhance bacterial survival in the presence of antimicrobials is the induction of prophage. Prophages are latent viral sequences that insert into the genomes of bacteria or

exist as a plasmid and are closely associated with specific serovars. When bacterial growth is normal, these viral genomes passively reside within the bacterial genome and are consistently replicated as part of the bacterial replication process. However, bacterial cell damage initiates viral excision from the bacterial chromosome, and phage replication occurs via the lytic cycle. Viruses replicate and escape the stressed bacterium, and the cycle begins anew in a new host[323]. However, in the context of fluoroquinolone treatment, this process further amplifies the stress (SOS) response of the bacteria. Prophage induction increases transcription of prophage cell division inhibitors *kilR*, *dicB*, *dicC*, and *dicF*, amongst other stress response genes including *abc2*. This process additionally triggers the bacterial SOS response using a *lexA*-dependent pathway, which involves activation of the DNA repair gene *recA* following binding to single-stranded DNA fragments, and the DNA repair processes that follow may enhance bacterial survival under this stress[323–325]. These include upregulation of error-prone DNA polymerases UmuC and UmuD that can replicate DNA more quickly but with less accuracy as well as excision repair proteins UvrAB and the inhibition of cell division by SulA[325].

1.6.2.2 Persistence and tolerance. Differences between persistence, tolerance, and 'adaptive resistance'

Antimicrobial treatment with sub-inhibitory concentrations has been linked to persistence of bacterial populations. Persistence, though a complicated and contentious term, implies survival of bacteria in the presence of a given potentially lethal stressor. The classical understanding of persistent bacteria is that they enter a dormant or less metabolically active form while exposed to the stressor and return to normal function once the stressor has been removed[326,327]. This response is not due to genetic changes in the bacteria but transcriptional ones that allow survival in adverse conditions including antimicrobial exposure by downregulating porins and genes that are involved in drug influx, limiting replication and transcription, reducing metabolism, and the employment of toxin-antitoxin systems[327]. Microscopy of such organisms has revealed that they look morphologically distinct to non-persisters and are able to rebound as a population after the stress has been removed[328,329].

It is important to also mention the concept of drug-tolerant bacteria when discussing persistence. Tolerance to an antimicrobial implies the bacterium's ability to protect themselves during exposure to the drug. Such organisms are able to not only survive but replicate and

expand. One way in which bacteria manage is through the formation of a biofilm. Producing this extracellular matrix shields the bacterial population from contact with the antimicrobial, and these bacteria are phenotypically distinct from bacteria growing planktonically[329,330]. Importantly, these bacteria, other than expending energy and resources in creating the biofilm, do not have to directly respond to the effects of the antimicrobial. However, there are likely costs associated with forming and maintaining a biofilm that may outweigh the benefits of such a strategy.

In light of the costs and benefits each survival strategy requires, it is likely that bacteria employ a system of bet-hedging or gambling to ensure survival of at least part of the population. It has been hypothesized that bacteria use a form of game theory to spread the risk of the entire population dying[331]. This has been termed 'bet-hedging', and in the context of antimicrobial exposure, it is likely that some bacteria form a biofilm to stave off contact with the antimicrobial, some bacteria go into a persister state by downregulating or turning off any non-essential processes, and some directly encounter the antimicrobial[320,330]. One can imagine that one of these strategies may be more successful than the others in a given context. For instance, if the drug exposure is long term, the persister population may not survive because eventually it will need to metabolize nutrients to survive, and it may uptake and be killed by the drug at that point. In an alternative scenario, forming a biofilm may prove too energetically expensive or expose the population to other harm. In yet another scenario, the bacteria directly exposed to the drug may not be able to survive the dosage, or replication in the presence of the antimicrobial may lead to lethal mutations downstream. Given the likelihood of any of these challenges, the strategy of bet-hedging with various populations may help ensure bacterial survival during antimicrobial treatment and may explain phenotypic heterogeneity seen in bacterial populations.

1.6.3 Lack of understanding of additional factors involved in FQR in *S*. Typhimurium

As stated above, it is plausible that bacteria deliberately stratify their response to antimicrobials to enhance survival. However, it is still unclear what the precise and predominating epigenetic strategies are when *S*. Typhimurium are exposed to fluoroquinolones. Beyond mutational resistance, there is insufficient understanding of what phenotypic changes directly

contribute to bacteria resisting killing by fluoroquinolones. It is likely that some combination of strategies is employed, and it is important to know which to implement appropriate FQ usage. In addition, because mutations in *gyrA* are the primary and obvious changes that confer DCS, it is possible that there are concurrent SNP changes that occur in the bacteria that may influence the level of susceptibility but that are not obvious without a deep sequencing analysis. In a changing landscape of ciprofloxacin presence, it is important to understand how those additional factors may play into compounding resistance.

1.6.3.1 Transcriptional response to FQs

As described above, there are significant phenotypic differences between ST313 isolates that appear genetically clonal. One way of probing this further is by investigating transcriptional responses to fluoroquinolones, and this has been done to some extent. Transcriptional studies of bacteria exposed to ciprofloxacin have shown that pathways involved in stress response, solute and drug transport, DNA repair, and phage induction are upregulated, which can increase error-prone DNA replication and bacterial resilience in the face of antimicrobials[332–337]. Li *et al.* showed that in a *Caenorbitans elegans* model with ciprofloxacin-exposed *S*. Typhimurium, many genes involved in the stress response and DNA damage are upregulated. Furthermore, studies in *Salmonella*, *E. coli*, Staphylococcus aureus, and *Acinetobacter baumanii* have shown that stress from fluoroquinolone exposure induces a strong prophage response, and this in turn positively reinforces the bacterial stress response[325,338–340]. Furthermore, work in *A. baumanii* has shown that treatment with colistin results in an upregulation of genes such as *acrB*, *emrB*, and *mexB*, which are involved in drug efflux[341]. While colistin is not a fluoroquinolone, these data may help clarify some of the genes and processes involved in general antimicrobial evasion strategies.

1.6.3.1.1 Overview of bacterial transcriptomics to understand drug resistance

In general, the study of bacterial transcriptomics has begun to gain in popularity as a method to study AMR. This is especially in light of the concern that genomics cannot provide a complete picture of everything that occurs in the bacteria in response to stress. While transcriptomics has not yet been deployed to study and determine AMR in real-time, it can

be a powerful tool in understanding individual genes, networks, and pathways in bacteria that contribute to resistance. As previously mentioned, whole genome sequencing alone cannot capture all of the mechanisms of resistance that bacteria might employ, and transcriptomics can help bridge that gap. This has been demonstrated successfully by Boinett *et al.* in elucidating the many efflux pumps and pathways that colistin-resistant *A. baumanii* use[341]. Similarly, Siqueira *et al.* were able to demonstrate the advantages of combination therapy for MDR *P. aeruginosa* rather than dosing with either meropenem or ciprofloxacin by measuring the transcriptional response of bacteria to the antimicrobial treatments[342]. The advantage of transcriptomics is that if bacteria exposed to antimicrobials are sampled longitudinally or at discrete points during antimicrobial exposure, this can provide considerable insight into how the bacterial population is responding over time to treatment, especially if much of the response is epigenetic rather than genetic.

1.6.3.2 How bacteria respond to antimicrobial exposure longitudinally

Despite the testing that antimicrobials undergo before they are licensed for human use, there is still a dearth of information about how bacteria respond to these antimicrobials, especially over longer periods of time. When antimicrobials are licensed for humans, the majority of assessments involve safety, side effects, and efficacy. However, they do not involve extensive study of the effect on the bacteria being treated, and any studies on antimicrobial efficacy would focus on the impact of the drug within the host. Given the current climate of excess antimicrobials in the environment that are discharged through sewage, in agriculture, and in clinical environments, it becomes essential to understand how bacteria might interact with and develop resistance to antimicrobials independent of the host[343,344]. Considering pathogens like *S.* Typhimurium that can exist in the environment and are transmitted via faecally-contaminated food and water, there is an acute need to explore the interaction with ciprofloxacin outside of the human host. Often, the methodology of studying this involves treating bacteria with an antimicrobial and then measuring growth over a designated period of time. One well-established method is performing growth curves of bacteria in nutrient medium containing the antimicrobial and measuring the optical density (OD600) of the bacteria as a readout for growth[345]. An alternative method that is used extensively to study antimicrobial efficacy is to use time kill curves (TKC) follow bacterial growth dynamics over a period of time and count colony forming units (CFU) at each timepoint[346–348]. Both of these methods provide information on the growth dynamics of bacteria in the presence

of an antimicrobial and can be used to compare against growth dynamics when bacteria are not exposed. Studies of ciprofloxacin treatment of various Gram-negative bacteria have shown that at high (> 1x MIC) concentrations of ciprofloxacin, bacteria are initially killed by the antimicrobial but that there can be subsequent growth after six hours that has not been properly characterized[319,342,349,350]. Additional information can be gleaned using some of the methods discussed previously, including whole genome sequencing, RNA-seq, and microscopy. However, few (if any) of the above techniques are routinely used to describe bacterial growth longitudinally.

Specific to agents that act on DNA replication machinery, it is known that one of the early responses is cellular elongation. This occurs because when ciprofloxacin forms a complex with DNA gyrase and the DNA, this causes permanent double-stranded DNA breaks, which stall DNA replication. The stalling of replication causes a cascade of downstream reactions, specifically triggering the SOS response and DNA repair pathways. One of the effects is the halting of bacterial septation by cell division inhibitor SulA by the inhibition of cell division protein FtsZ[351–353]. As a result, filamentous, elongated bacterial cells form, which have been observed to grow up to 200 μm in length and can contain multiple copies of the chromosome along their length[352,354–357]. It has been observed that these filamentous bacteria can subsequently divide into daughter cells once growth conditions are less adverse, although the dynamics and mechanics of this occurrence are as yet unexplored[358]. There is an urgent need for further understanding of how bacteria can recover from ciprofloxacin exposure and what that means for subsequent resistance.

1.6.3.2.1 Imaging to observe killing over time

In addition to monitoring changes in growth by microbiological assays, key insights into bacterial response to antimicrobials come from morphological changes that can be captured via microscopy. Multiple studies have shown that it is possible to identify bacteria on the basis of their morphology when treated with antimicrobials[359,360]. This is particularly true of ciprofloxacin-treated bacteria due to the clear filamentation that occurs in affected cells. Multiple groups have shown the utility of single-event and time-lapse microscopy to screen for antimicrobial efficacy for specific bacteria, and this technique may also be an important way of identifying and appreciating the contribution of subpopulations to the overall phenotype. For example, Ungphakorn *et al.* were able to demonstrate similar results

between time kill curves and time-lapse microscopy of carbapenemase-producing *Klebsiella pneumoniae* and *E. coli* when treated with various colistin combinations[361]. Additionally, Barrett *et al.* were able to visually track *E. coli* response to high concentrations of ofloxacin and identify septation events in filamentous bacteria and link those morphological changes to error-prone DNA polymerase V UmuDC and activation of the SOS response[362].

1.6.3.2.2 Use of imaging, kill curves, and transcriptomics to tie together phenotype and genotype

Ultimately, to capture the greatest amount of information about and fully understand bacterial response to antimicrobial exposure, it is preferable to combine multiple approaches. With the advent of higher-throughput technologies and techniques, this multi-pronged approach is becoming increasingly feasible. Using multiple technologies, Pribis *et al.* were able to exhibit the role of a bacterial subpopulation of *E. coli* that formed in response to ciprofloxacin-induced stress by cell-sorting bacteria on their morphological characteristics, capturing growth dynamics, and identifying genes that were differentially expressed between ciprofloxacin-exposed and unexposed bacteria[331]. It is expected that more such dynamic workflows will emerge.

1.7 Summary

As fluoroquinolones, particularly ciprofloxacin, continue to be used widely, there is an increasing need to understand how this affects the fitness landscape in *S*. Typhimurium and is driving further AMR. As fluoroquinolones disrupt DNA replication, it is possible that FQR has other impacts on the bacterial cell, potentially modifying metabolism, resistance to heavy metals and other antimicrobials, invasion of host cells, and improving survival in hostile conditions[363–367]. Therefore, it is more important than ever to better understand how clinically-important bacteria are responding to ciprofloxacin.

Thanks to technological advancements, it has become easier in recent years to collect more comprehensive linked genotypic and phenotypic information. Consequently, in this project

we intend to perform a combination of RNA-seq and imaging analysis to develop our understanding of FQR. Multiple studies have shown that it is possible to identify bacteria on the basis of their morphology when treated with antimicrobials[359,360]. This is particularly true of ciprofloxacin-treated bacteria, where bacteria become filamentous and elongated when treated.

Beyond characterising treated versus untreated bacteria, linked imaging and expression analysis, performed on an Opera Phenix high-throughput microscopy platform, enables classification of multiple phenotypes in a stable 96/384-well system. In this system, we can identify live versus dead bacteria and potentially even finer characteristics such as membrane permeability, the bacterial stress response, and analysis of persister populations. The Opera Phenix is normally used to study eukaryotic cells, but it has not previously been validated as a tool to study bacteria, which we hope to do[368,369].

While some transcriptional analysis has been undertaken on the *Salmonella* response to antimicrobials, little RNA-seq analysis has been performed on MDR clinical isolates of *S.* Typhimurium to look at the transcriptional effect of drug treatment, especially comparatively across a variety of isolates and drug conditions[333]. The combination of RNA-seq and high-resolution imaging on isolates could provide considerable insight into the different effects of ciprofloxacin treatment on distinct *S.* Typhimurium isolates growing in a controlled environment. Combining this with growth assays and genomic information may further disentangle bacterial response to ciprofloxacin by distinguishing between genetic and epigenetic features. Ultimately, further insight into *S.* Typhimurium response to ciprofloxacin may help guide future antimicrobial stewardship and development of targeted vaccines, especially against iNTS isolates prevalent in sub-Saharan Africa[51].

2. Materials and Methods

2.1 Bacterial isolates

A combination of *S.* Typhimurium ST19, ST313, and ST34 isolates were used in this study. They are enumerated in **Appendix A, Table 1**. Many of the isolates used were kindly provided by the Institute of Tropical Medicine, Antwerp and the International Vaccine Institute.

2.1.1 Growth medium and growth conditions

Prior to experimentation, all isolates were grown on Isosensitest agar (Oxoid, CM0471) and subjected to ciprofloxacin M.I.C.E. (Oxoid, MA0104F) or ETEST (BioMerieux, 412311) to determine baseline ciprofloxacin susceptibility. Isolates were maintained on Isosensitest agar and streaked fresh weekly from frozen stocks. To prepare for experiments, isolates were always inoculated into 10 ml Isosensitest broth (Oxoid, CM0473) from plates followed by overnight shaking at 37°C for 16-18 h.

2.1.2 Ciprofloxacin susceptibility testing by MIC ETEST

Isolates were streaked from frozen stocks onto Isosensitest plates and grown at 37°C. Three serial streaks on fresh plates were subsequently performed. For M.I.C.E. or ETEST application, a few colonies from each plate were inoculated in $\sim$3 ml PBS and vortexed well to create a slightly cloudy solution. 100 μl of the solution was spotted on Isosensitest plates and spread well before gently laying down the MIC test strip. Inoculated and control plates were incubated overnight at 37°C and then visually analysed. Each *S.* Typhimurium isolate was tested a minimum of two times to ensure an accurate reading.

2.2 Time kill curves

Four *S.* Typhimurium isolates were chosen for the initial time kill curve analysis. These were D23580, SL1344, VNS20081, and 5390_4[80,370,57,176]. Initially, colonies from plates were inoculated into 10 ml of Isosensitest broth and these were shaken at 200 rpm at 37°C overnight. 10 μl of the subsequent culture was then added to 990 μl of 1x PBS to make a 1:100 dilution for the inoculum. 100 μl of this preparation was added to 10 ml of Isosensitest containing different levels (0x, 1x, 2x, 4x MIC) of ciprofloxacin according to the predetermined MIC of each isolate (**Table 2.1**). The starter inoculum was between 1 and 5 x 10^5 CFU/ml. Cultures were incubated shaking at 37°C and aliquots were taken to determine colony forming units (CFU) at 0, 2, 4, 6, 8, and 24 h. For this analysis, serial dilutions were made using samples of each culture, and a total of 50 μl of each dilution was plated using 10 μl spots of inoculum onto L-agar. CFUs were counted and determined as CFU/ml. Means and standard deviations (SD) of three replicates per isolate were calculated.

Table 2.1 *S.* Typhimurium isolates and respective ciprofloxacin MIC linked concentrations used to generate growth curves.

Isolate	0x MIC	1x MIC	2x MIC	4x MIC
D23580	–	0.03 µg/ml	0.06 µg/ml	0.12 µg/ml
SL1344	–	0.015 µg/ml	0.03 µg/ml	0.06 µg/ml
VNS20081	–	1.0 µg/ml	2.0 µg/ml	4.0 µg/ml
5390_4	–	0.5 µg/ml	1.0 µg/ml	2.0 µg/ml

2.2.1 Ciprofloxacin-degradation kill curves

Experiments were performed to determine whether ciprofloxacin was degraded or inactivated during the initial growth curve analysis. Here, the initial 24 h time kill curves were performed as described above. At 24 h, cultures were centrifuged and sterile-filtered through a 0.2 μm membrane, and the filtered medium was transferred to fresh growth tubes. Overnight bacterial cultures were then inoculated at a concentration of 1:10000 to the medium and CFU were determined at 0, 2, 4, 6, 8, and 24 h using conditions identical to those used in the initial growth curve analysis. Note: no additional ciprofloxacin was added to medium.

2.3 Spontaneous *gyrA* mutant generation and validation

To isolate spontaneous nalidixic acid mutant lines from *S.* Typhimurium isolates SL1344 and D23580, bacterial cultures were grown overnight in L-broth, and 100 μl of this was spread onto L-agar containing 100 μg/ml nalidixic acid for initial spontaneous mutant generation. After overnight incubation at 37°C, single colonies that had grown were re-plated on L-agar also containing 100 μg/ml nalidixic acid. Any colonies that were present on these agar plates were then streaked serially onto agar plates harbouring increasing concentrations of nalidixic acid up to 400 μg/ml, then these were switched to plates containing ciprofloxacin, harbouring from 0.1 μg/ml ciprofloxacin up to 1.0 μg/ml ciprofloxacin. Once colonies were able to grow stably on 1.0 μg/ml ciprofloxacin, overnight cultures were grown for genomic DNA purification and were purified using the Promega Wizard DNA Purification Kit (Promega, A1120). The DNA extraction protocol is detailed in **Appendix A**.

Following purification, DNA was PCR-amplified to check for mutations in the *gyrA* gene using primers: 5'-GAGATGGCCTGAAGC-3' for nucleotides 108 to 127 and 5'- TACCGT-CATAGTTATCCA CG -3' for nucleotides 435 to 454, forward and reverse, respectively[371].

2.4 *S.* Typhimurium D23580 bacteria grown for 24 h in ciprofloxacin medium for whole genome sequencing

One of the challenges in the ciprofloxacin growth curve experiments was to determine whether any SNPs or other mutations due to ciprofloxacin exposure had accumulated in the 24 h growth period from the initial inoculum. To determine this bacteria were isolated before and at the end of the culture period, and their DNA was isolated and sequenced. To prepare DNA, bacterial cultures of *S.* Typhimurium D23580 were initially grown overnight in 10 ml of broth. As in the time kill curve experiments, 10 ml of fresh Isosensitest broth containing 0x, 1x, 2x, or 4x ciprofloxacin MIC were inoculated with overnight cultures at 1:10000. Bacteria were grown for 24 h and then DNA was extracted. To ensure that the DNA extracted was not capturing a skewed population and to obtain a comprehensive sequence analysis, DNA was acquired in three ways, as described in detail in **Appendix A**.

After all bacterial pellets were collected, bacterial DNA was extracted using the Promega Wizard DNA Purification kit as described above. DNA was quantified on a Qubit 4 Fluorometer (Q33226) using the Qubit dsDNA HS Assay Kit (Q32851), then frozen at -80°C prior to whole genome sequencing.

2.5 Whole genome sequencing: library creation and sequencing

Library preparation for Illumina sequencing was undertaken at the Wellcome Sanger Institute using automated systems using the IHTP WGS NEB Ultra II library kit.

Libraries were sequenced on an Illumina HiSeq platform (Illumina, San Diego, USA) using standard running protocols, as described in greater detail in **Appendix A**.

2.6 Read mapping, variant detection, and SNP analysis

Illumina adapter content was removed from the reads using Trimmomatic v.0.33. Read mapping was undertaken using the WSI bacterial mapping pipeline, which uses bwa, and reads were assembled using the closest reference strain: D23580 (FN424405.1), SL1344 (FQ312003.1) or VNB151 (LT795114.1)[370,178,57]. samtools mpileup and bcftools were used to create a BCF file. Recombinant genomic regions were virtually masked from the alignment using an in-house script and verified using Gubbins, after which SNP sites were pulled out from the final alignment using snp-sites to generate a VCF file. SNPs were grouped as coding or non-coding using an R script from Van Puyvelde *et al.*, and the SNPs located in coding regions were manually evaluated[176].

2.7 Opera Phenix confocal phenotyping of bacteria

Several different experimental setups were assessed using the Opera Phenix; however, the general methodology was as follows. PerkinElmer CellCarrier-96 Ultra Microplates (PerkinElmer, 6655308) were coated with 50 μl Vitronectin (Stem Cell Technologies, 07180) in CellAdhere Dilution Buffer (Stem Cell Technologies, 07183) at 1:20, and these were incubated overnight at 37°C.

The following day, wells were aspirated and washed 1x with 50 μl CellAdhere buffer and then with 50 μl 1x PBS (Thermo, 10010023). 50 μl of bacteria culture was added to each well and incubated for standardised times to generate sufficient bacteria for imaging. After incubation, bacteria were aspirated from wells, and adherent bacteria were fixed using 50 μl 4% paraformaldehyde (PFA) (Alfa Aesar, J61899) for 10 min. Wells were washed 1x with PBS, and then 50 μl 2% BSA (Fisher Scientific, BP9700-100) in PBS was added to each well and incubated for 20 min at room temperature. BSA was aspirated and replaced with BSA containing either FITC- or Alexa-647-conjugated CSA antibody (BacTrace, 5330-0059; Novus Biologicals, NB110-16952AF647). Subsequent incubation was then for 1 h in the dark. Wells were aspirated and replaced with either 50 μl 1:100 DAPI (Sigma, D9542) or DAPI and 1:200 SYTOX Green (Thermo Fisher, A8- 0626) in HBSS (ThermoFisher, 14025092). The processed plates were incubated for 20 min in the dark, then washed 1x in PBS, which was replaced with 50 μl PBS, and then sealed with a foil seal ready for imaging.

2.7.1 Opera Phenix microscopy phenotyping of *S.* Typhimurium bacteria during ciprofloxacin exposure

S. Typhimurium D23580 and VNS20081 were screened at 2 h intervals over 24 h after ciprofloxacin exposures of 0x, 1x, 2x, and 4x as related to the MIC of each isolate. This was undertaken by inoculating overnight cultures of *S.* Typhimurium D23580 and VNS20081 independently at 1:1000 dilutions (100 μl) in 100 ml Isosensitest broth in a 200 ml flask. The rationale for using a 1:1000 inoculum was the need for greater volumes to concentrate the low CFU samples at early time points, and the aeration is greater in 200 ml flasks. Cultures were collected for imaging from 2 h – 24 h. Because of the low bacterial concentrations at

early timepoints, the amount of culture taken and the degree of concentration was modified per timepoint (**Table 2.2**). At each time point, a final volume of 100 μl of culture was used to fill two wells with 50 μl each, and the plates were incubated static at 37°C for 13 min. As per standard protocol (see section 2.7), the microbial culture was aspirated, then fixed with 4% PFA, and washed with 1x PBS. Wells were refilled with PBS and kept at 4°C until the next time point. At the end of the 24 h experiment, all wells were incubated with 2% BSA, then for 1 h with CSA-Alexa- 647 at 1:1000 in BSA. Wells were aspirated and then incubated with solutions harbouring DAPI and SYTOX Green for 20 min as described above. Wells were washed 1x; plates were sealed and imaged.

2.7.2 Opera Phenix phenotyping of *S.* Typhimurium ST313 isolates after ciprofloxacin exposure

24 *S.* Typhimurium isolates were chosen for screening (**Appendix A, Table 2**). Colonies from plates were inoculated in ∼2 ml Isosensitest broth in a 96-well, deep well plate (Nunc, 260251). The plate was sealed with a gas permeable seal (Sigma, A9224) and incubated shaking at 37°C at 100 rpm for 16-18 h. The following day, a ciprofloxacin-Isosensitest was prepared for inoculation of bacteria at 0.06 μg/ml, 0.25 μg/ml, and 1.0 μg/ml, corresponding to concentrations at which *S.* Typhimurium are considered sensitive, intermediate, or resistant, respectively. An additional aliquot of Isosensitest broth lacking ciprofloxacin was prepared to have a baseline readout. Ciprofloxacin-containing broth was prepared by adding 2x of each concentration to Isosensitest broth to a total volume of 5 ml. 25 μl of these 2x solutions was added to the wells of a pre-coated CellCarrier Ultra plate in duplicate. 25 μl of the overnight cultures were then added to each well. The plate was incubated statically at 37°C for 2 h and then processed for imaging as described in 2.7. For staining, the CSA-Alexa-647 antibody was used 1:1000 in BSA for 1 h. Wells were then incubated with DAPI at 1:100 and SYTOX Green at 1:200 for 20 min, after which the plate was washed and readied for imaging.

2.7.3 Opera Phenix image analysis

Images generated on the Opera Phenix were analysed using the Harmony software (Perkin Elmer). The analysis pipeline was refined from a more general pipeline developed within the

Table 2.2 Preparation of *S.* Typhimurium D23580 and VNS20081 cultures for imaging.

Time point	Isolate/conditions	Preparation
2 h	All	Centrifuged 10 ml (4°C, 4000 rpm, 7 min). Decanted supernatant, transferred pellet to 1.5 ml tube. Centrifuged 1.5 ml tube (23°C, 8000 rpm, 3 min). Aspirated supernatant and resuspended pellet in 100 µl PBS.
4 h	D23580 0x; VNS20081 0x and 1x	From 10 ml as above but resuspended in 250 µl.
4 h	D23580 1x, 2x, 4x; VNS20081 2x, 4x	From 10 ml with final resuspension in 100 µl.
6 h	D23580 1x, 2x, 4x; VNS20081 2x, 4x	From 10 ml with final resuspension in 100 µl.
6 h	D23580 0x; VNS20081 0x, 1x	Plated neat culture.
8 h – 14 h	D23580 1x, 2x, 4x; VNS20081 4x	From 10 ml with final resuspension in 100 µl.
8h – 14 h	D23580 0x; VNS20081 0x, 1x, 2x	Plated neat culture.
16 h	D23580 4x	From 10 ml with final resuspension in 100 µl.
16 h	D23580 0x, 1x, 2x; VNS20081 0x, 1x, 2x, 4x	Plated neat culture.
18 h	All	Plated neat culture.
20 h	D23580 4x	From 10 ml with final resuspension in 100 µl.
20 h	D23580 0x, 1x, 2x; VNS20081 0x, 1x, 2x, 4x	Plated neat culture.
22 h	D23580 4x	From 10 ml with final resuspension in 100 µl.
22 h	D23580 0x, 1x, 2x; VNS20081 0x, 1x, 2x, 4x	Plated neat culture
24 h	D23580 4x	From 10 ml with final resuspension in 100 µl.
24 h	D23580 0x, 1x, 2x; VNS20081 0x, 1x, 2x, 4x	Plated neat culture.

group for Gram-negative bacterial analysis. Inputted images underwent flatfield correction, and images were calculated using the DAPI and FITC channels. The output "Calculated Image" was used to find "Spots" in the image. The population "Spots" was used to select populations by removing border objects. The selected spots were then assessed for area and roundness, and only objects with an area > 1.6 μm were included for downstream analysis; these were labelled "bacteria". Bacteria were assessed for area, roundness, width, length, and the ratio of width to length. Independently and using the DAPI and FITC channels, multiple morphology properties were calculated: symmetry, threshold compactness, axial, radial, profile (width of 4 px), sliding parabola (curvature of 10), and texture SER (scale of 1 px with Kernal normalization). The mean and standard deviation of DAPI intensity was also calculated. By applying a linear classifier to the "bacteria" population, three categories were defined: "Single_cells", "Round_cells", or "Other", and 45 morphology and intensity characteristics were calculated. See **Appendix B, Table B.2** for full pipeline. The output of the Harmony analysis was tabulated by object, and the result table was visualized in R (v 3.6.1).

For the principal component analysis (PCA) conducted on the 24 *S.* Typhimurium ST313 isolates, analysis was performed using base R on the combined three biological replicates of the screen. Initial analysis was performed on all 24 isolates in the non-treated (0 μg/ml) condition. A separate PCA was conducted on all 24 isolates treated with 1 μg/ml ciprofloxacin. Following this, all susceptible isolates were excluded from the dataset, and a PCA was conducted on the 'intermediate' susceptibility isolates separately at each treatment (0, 0.06, 0.25, 1.0 μg/ml ciprofloxacin). The first three principal components of each analysis were visualized in R.

2.8 RNA extractions and RNA sequencing

After bacteria were grown according to experimental specifications, double the volume of RNAProtect Bacteria Reagent (Qiagen, cat no. 76506) was added to cultures and incubated for 10 min. Cultures were centrifuged at 3215 x *g* for 14 m at 4°C. Supernatant was decanted, and the pellets were resuspended in 400 μl Tris buffer (0.25 mM, pH 8.0) containing 10 mg/ml lysozyme, and incubated for 5 min. To this was added 700 μl RLT buffer containing 10 μl β-mercaptoethanol (Sigma, cat no. M6250) per ml, and samples were vortexed well.

1 ml 100% ethanol was immediately added and vortexed well. The Qiagen RNeasy Mini Kit (Qiagen, cat. no. 74104) was subsequently used to process samples. Briefly, samples were loaded onto columns and spun. Columns were washed with 700 μl RW1 Buffer, then 2x with 500 μl RPE Buffer, and eluted in 40 μl RNase-free water. Samples were frozen at -20°C if not immediately processed. Subsequently, samples were treated with DNase I using the Qiagen DNase Kit (Qiagen, cat no. 79254). Outputs of the DNase treatment were treated using phenol-chloroform by first increasing solution volume with RNase-free water to 400 μl. 400 μl of phenol-chloroform-isoamyl alcohol mixture (Sigma, cat. no. 77617) was then added to the samples, mixed by inversion, then centrifuged at 8000 x *g* for 5 min. Supernatant was transferred to a new tube and combined with 400 μl chloroform:isoamyl alcohol 24:1 (Sigma, cat no. C0549). Samples were mixed then centrifuged as above. The supernatant was transferred to a new tube and combined with 1 μl glycogen (Roche, cat no. 10901393001), 40 μl 3M sodium acetate, pH 5.5 (Ambion, cat no. AM9740), and 500 μl ice-cold 100% ethanol. Tubes were mixed by inversion and incubated at -20°C for 30 min before centrifugation at 4°C for 20 min at 16000 x *g*. Supernatant was decanted and replaced with 500 μl ice-cold 70% ethanol and centrifuged at 4°C for 5 minutes at 16,000 x *g*. Ethanol was decanted and pellets were air-dried before resuspension in 50 μl RNase-free water. Samples were frozen at -80°C prior to sequencing. All library preparation and RNA-sequencing were performed at the Wellcome Sanger Institute using standard protocols. Briefly, libraries were made using the NEB Ultra II RNA custom kit (NEB, cat no. E7530S) on an Agilent Bravo WS automation system. RiboZero was added to deplete ribosomal RNA. Libraries were pooled and normalized to 2.8 nM for sequencing. Sequencing was performed on an Illumina HiSeq 4000, using a minimum of two lanes per pool.

2.8.1 RNA extractions from 4 'pilot' isolates under 2x MIC ciprofloxacin exposure

Four *S.* Typhimurium isolates: D23580, SL1344, VNS20081, and 5390_4 were grown as overnight cultures and inoculated at a dilution of 1:1000 in 10 ml Isosensitest broth with and without 2x the MIC ciprofloxacin (see **Table 2.1** for concentrations). After 2 h growth, RNA was extracted from the cultures as described in section 2.8.

2.8.2 RNA extractions of *S.* Typhimurium D23580 under parallel treatment conditions

D23580 and a D23580 *gyrA* mutant derivative (D23580**gyrA*) were grown under standard overnight conditions. Seven different experimental conditions were established for 2 h growth (**Table 2.3**). Bacterial overnight cultures were inoculated by a dilution of 1:1000 in 10 ml Isosensitest set to the treatment condition and grown shaking at 200 rpm at 37°C for 2 h. At 2h, standard RNA extractions were performed.

Table 2.3 Treatment conditions for *S.* Typhimurium D23580 and D23580gyrA*.**

Strain	Treatment	Concentration
D23580	None	None
D23580	Ciprofloxacin	0.5x MIC (0.015 µg/ml)
D23580	Ciprofloxacin	2x MIC (0.12 µg/ml)
D23580	Mitomycin C	1 µg/ml
D23580	Azithromycin	1x MIC (8 µg/ml)
D23580*gyrA	None	None
D23580*gyrA	Ciprofloxacin	0.24x MIC (0.12 µg/ml)

2.8.3 Sucrose gradient separation of ciprofloxacin-treated D23580

To separate subpopulations of bacteria after ciprofloxacin exposure, a sucrose gradient procedure was developed. Bacterial overnight and sub-cultures were grown according to the particular experimental requirements. These cultures were either non-treated or exposed to 2x MIC for ciprofloxacin. As there was relatively low bacterial yield at 2 h, sub-cultures were inoculated 1:100 from overnight cultures into 10 ml of Isosensitest broth either containing 0 μg/ml or 0.06 μg/ml ciprofloxacin. These sub-cultures were incubated while shaking at 200 rpm at 37°C for 2 h. While cultures were growing, fresh sucrose solutions were prepared. The four concentrations of sucrose used were 25%, 50%, 60%, and 70%, and these were made by dissolving sucrose (Sigma, S7903) in 1x PBS (w/v). Solutions were sterile-filtered using 0.2 μm syringe filters (GE Healthcare, 6794-2502). 2 ml of each sucrose concentration was layered from 70% to 25% in open-top ultracentrifuge tubes (Beckman Coulter, 344059) immediately before use (**Figure 2.1**). At 2 h, cultures were removed from incubator and centrifuged for 14 min at 4000 x *g* at 4°C. The supernatant was aspirated off with a stripette (carefully because the pellets were small and unstable), leaving behind a small volume of

medium to avoid aspirating the pellet. Pellets were resuspended in the remaining medium and transferred to 1.5 ml tubes, which were centrifuged at 5000 x *g* for 2 min to re-pellet. The remaining supernatant was removed, and pellets were resuspended in 500 μl PBS. Using a Pasteur pipette, 500 μl of cells was carefully added to the top of the 25% layer of the sucrose column. Gradients were centrifuged for 9 min at 3000 x *g*, 4°C. After centrifugation, gradients were removed:

- There were two visible layers on the gradients loaded with non-treated cultures: 1. within 50% (thick band), 2. ∼60% (very thin band).
- There were three visible layers from the 2x MIC ciprofloxacin treated gradients: 1. within 50% (thin band), 2. within 60% (more distinct, diffuse band), 3. 60-70% interface (distinct but thin band).

The cloudy portion of each layer was carefully removed using a Pasteur pipette, beginning with the lowest-density layer (fresh pipettes were used for each lower layer to avoid mixing the layers).

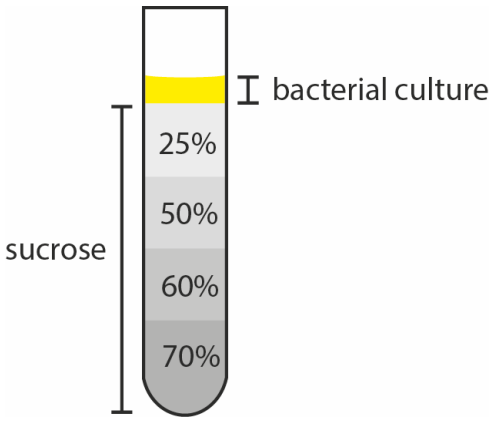

Figure 2.1 Assembly of sucrose gradient columns. Open-top ultra-centrifugation tubes were used to layer four concentrations of sucrose solution, on top of which bacterial cultures were added for sucrose density separation.

2.8.4 RNA extractions from *S.* Typhimurium D23580 after sucrose gradient separation

Subsequent to separation by sucrose gradients, isolated fractions were immediately added to 10 ml bacterial RNAProtect and processed using the standard RNA extraction protocol described above.

2.9 RNA sequencing analysis

Illumina sequence reads from *S.* Typhimurium D23580 and 5390_4 DNA were mapped to the reference D23580 genome (accession number FN424405.1) (Kingsley et al., 2009), VNS20081 was mapped to the sequenced isolate VNB151 (Mather et al., 2018), and SL1344 was mapped to reference sequence SL1344[80,57]. The Wellcome Sanger Institute pipeline tool DEAGO (Differential Expression Analysis Gene Ontology) a wrapper script for DESeq2 was used to determine differential gene expression starting with raw count files[372]. Using DESeq2, a Wald test was performed by comparing data from the treatment condition versus the non-treated equivalent. The p-value cut-off used was 0.05, and $\log_2$ fold change was calculated for treatment condition versus non-treated. Genetic networks and relationships were analysed using PheNetic, and GO terms were generated and compared[373].

Independently, data sets were analysed by the Monash University Bioinformatics Platform in Melbourne, Australia to provide comparative data sets. These data were analysed using the RNAsik pipeline, and differential gene expression comparisons were rendered using the Degust webtool using the limma-voom statistical test[374,375].

2.9.1 RNA sequencing analysis of gradient-separated bacteria

RNA-seq analysis was performed on the bacteria recovered from the gradients. These RNA-sequencing reads were processed using DEAGO as described in section 2.10. Pairwise comparisons were made between conditions:

- 50% fraction non-treated versus 50% fraction treated bacteria
- 50% non-treated versus 60% fraction treated
- 50% treated versus 60% treated
- 50% treated versus 60-70% treated

Heatmaps were made using R package heatmap.2, and other visualizations were performed using ggplot2. Network analysis was undertaken using PheNetic.

2.10 Light microscopy of gradient-separated *S.* Typhimurium D23580 bacteria

S. Typhimurium D23580 bacteria that had been gradient-separated after 2 h ciprofloxacin exposure were prepared for light microscopy to visualize gross morphological differences between non-treated and ciprofloxacin treated bacteria from the sucrose fractions. Bacterial samples were smeared on glass slides and heat-fixed. They were then stained using a standard Gram-staining protocol. Briefly, bacteria were first stained with crystal violet for 30 seconds followed by washing in H_2O for 5 seconds. The slides were then covered in Gram's iodine solution for 1 min before washing. Slides were decolorized by washing in 95% ethanol and acetone, then rinsed in H_2O for 5 seconds. Finally, slides were counterstained using safranin for 30 seconds and washed. After slides were air-dried, images were captured using an oil-immersion lens at 900x – 1000x.

2.11 Generation of *S.* Typhimurium D23580 single-gene knockout derivatives

Five genes identified in the RNA-seq analysis were chosen to be inactivated in *S.* Typhimurium D23580 by making targeted-gene knockouts. These genes were: *ybiI_2*, *sulA*,

malK, *cadA*, and *ddrA*. Targeted gene knockouts were generated using the lamda Red recombinase system[376]. Primer sequences were constructed for each gene (**Table 2.4**). Knockouts were designed and verified as described in **Appendix A**.

Table 2.4 Primer sequences for gene knockouts.

Gene	Forward	Reverse
ybiI_2	TGTGTAGGCTGGAGCTGCTTCG	CATATGAATATCCTCCTTAG
sulA	TGTGTAGGCTGGAGCTGCTTCG	CATATGAATATCCTCCTTAG
malK	TGTGTAGGCTGGAGCTGCTTCG	CATATGAATATCCTCCTTAG
cadA	TGTGTAGGCTGGAGCTGCTTCG	CATATGAATATCCTCCTTAG
ddrA	TGTGTAGGCTGGAGCTGCTTCG	CATATGAATATCCTCCTTAG

2.12 TraDIS screen on time kill curves of ciprofloxacin-exposed *S.* Typhimurium D23580

A previously validated *S.* Typhimurium D23580 Transposon Directed Insertion site Sequencing (TraDIS) library was used for the following experiment[181]. 50 μl of one batch of the total TraDIS library pool ($\sim$ 60000 mutants) was grown overnight in 10 ml of Isosensitest broth containing 15 μg/ml Kanamycin as three independent replicates. A 50 μl aliquot of this input library was separately frozen for genomic DNA processing. Multiple 50 ml tubes were prepared containing either Isosensitest broth or 0.06 μg/ml ciprofloxacin (2x MIC) in 10 ml Isosensitest broth. Three time points were determined for collection: 2 h, 10.25 h, 24 h on the basis of growth dynamics, and because of the potential for low bacterial yield at the earlier two timepoints, 12 tubes were prepared for the 2 h timepoint (6 per treatment condition), and 4 tubes were prepared for the 10.25 h time point (1 tube for non-treated and 3 tubes for 2x MIC). For the 24 h timepoint, only one tube per treatment was required. After $\sim$17.5 h pre-incubation, cultures were diluted 1:100 in PBS, and 100 μl of this was added to the readied testing tubes and incubated shaking at 200 rpm at 37°C. 1 ml of the overnight cultures was also spun down and the pellet frozen at -80°C for genomic DNA extraction. At 2 h post-treatment, sub-cultures were removed from the incubator. 100 μl was removed from a representative tube of non-treated and 2x MIC cultures for plating CFU at dilutions of 10^{-1}, 10^{-2}, and 10^{-3} on agar plates. Plates were incubated at 37°C overnight. The remainder of the sub-cultures were combined for centrifugation. Tubes were centrifuged at 4600 rpm for 20 min at 4°C. Supernatant was decanted, and the residual medium was

used to resuspend the pellet, which was then transferred to a 1.5 ml tube. This tube was centrifuged again at 8000 rpm for 3 min, and the supernatant was removed. The cell pellet was immediately frozen at -80°C. At 10.25 h and 24 h, the above protocol was repeated. Once all time point pellets were harvested, genomic DNA was extracted using the Promega Wizard Genomic DNA Purification Kit, eluted in 50 or 100 μl elution buffer depending on pellet size. Library preparation and sequencing were carried out by the Sequencing Pipelines at the Wellcome Sanger Institute. Similar to Ondari et al., gDNA was fragmented to $\sim$300 bp insert size using an E220 Evolution Sonicator (Covris), and the DNA fragments were end- repaired, A-tailed, and adaptor ligated using an Illumina DNA fragment library preparation kit (NEB Ultra II)[181]. Libraries were enriched by 10-20 PCR cycles using transposon specific primers 5'-ATCCCTATTTAGGTGACACTATAGAAGAGATGTGTA-3' and 3'- TTATGGGTAATACGACTCACTATAGGGAGATGTGTA-5'. Enriched libraries were purified by Agencourt AMPure XP beads and quantified using the Agilent DNA1000 chip. Libraries were sequenced on a HiSeq 2500 as 42 bp single reads across 2 lanes. Reads were processed using Bio::TraDIS toolkit v1.132190[377]. Reads were first filtered for the transposon tag sequence TAAGAGACAG. The filtered reads were mapped against the D23580 reference genome using SMALT, and transposon insertion sites and indices were calculated for each gene. Due to low percentage of genes mapped using the default settings, reads were mapped using a less stringent matching cut-off for the transposon tags. Gene essentiality (under-represented genes) was assessed by evaluating genes for which there were 0 or 1 insertions. Log_2 fold changes in mutant abundance between input pool and output were calculated using tradis_comparison.R within the Bio::TraDIS tookit. Pairwise contrasts were performed on treated versus non-treated bacteria for each time point.

2.13 TraDIS screen on *S.* Typhimurium D23580 injected into intestinal organoids

Intestinal organoids were prepared as described previously by Lees *et al.*, 2019[378]. Using the same *S.* Typhimurium D23580 TraDIS library, 50 μl of the library was inoculated in 10 ml LB containing 15 μg/ml Kanamycin and incubated shaking at 37°C overnight. The following day, the bacterial concentration was adjusted to a multiplicity of infection of 10:1 in 1 ml PBS. For each biological replicate, 60 organoids were microinjected with bacteria

and incubated at 37°C for 90 minutes. The detailed protocol of organoid injections and processing is in **Appendix A**. The organoids were lysed, and serial dilutions were performed and plated to calculate CFU and grow bacteria for TraDIS screening. CFU were plated on L-agar plates and incubated at 37°C overnight. The following day, CFU were enumerated, and colonies were collected for DNA extractions, as described in section 2.3.

Sequencing and analysis were performed as in section 2.13, including running the pipeline with default and relaxed transposon tag matching criteria.

2.14 Phylogenetic analysis

108 *S.* Typhimurium previously sequenced isolates were selected to represent global *S.* Typhimurium with an emphasis on ST313 isolates[176]. S. Paratyphi A270 was used as an outgroup for the phylogenetic analysis. Following BCF file generation as described in section 2.6, a pseudo-genome was generated by substituting uncertain sites in the reference genome base calls with an "N". Prophage and recombinant regions of the genome were informatically removed as described in section 2.8, after which snp-sites was used to extract SNP sites to create a maximum likelihood phylogeny. 1000 bootstraps were performed using RAxML with the substitution model GTRCAT to generate a tree with supported nodes[379]. The tree was visualized using iTOL[380].

2.14.1 SNP analysis of *S.* Typhimurium ST313 isolates

Based on a prior analysis of a *S.* Typhimurium ST313 lineage with decreased ciprofloxacin susceptibility (DCS), a SNP comparison was performed on isolates within the lineage that had greatest and least ciprofloxacin susceptibility (Van Puyvelde, personal communication). Isolates were compared as two discrete groups: those with greater and lesser DCS, and only SNPs that were either present or absent amongst all isolates in a given group were included. The coding SNPs were analyzed using an R script from Van Puyvelde *et al.*, as performed previously in section 2.6, to determine whether they were non-synonymous or synonymous and the codon position[176].

The SNPs in the 82 *S.* Typhimurium ST313 isolates contained within the 108 selected *S.* Typhimurium were independently compared following the methods described in section 2.6, mapped to isolate D23580. As before, coding SNPs were analyzed to determine synonymous or non-synonymous mutation and codon position. These SNPs were then compared against those from the DCS lineage above to determine overlap of specific SNPs, and these SNPs were manually evaluated in greater detail. The overlapping SNPs were used as the basis for defining manual functional groups that relevant SNPs might belong to. To determine functional groups of SNPs found within the 82 *S.* Typhimurium ST313 isolates, a text-based search was executed on the annotation for each gene containing a SNP. All SNPs found in a functional group of interest were concatenated into a single text file, and duplicates were removed. SNPs in genes involved in drug transport were manually evaluated in greater detail.

2.15 Pangenome analysis

Pangenome analysis tool Roary was used to generate a pangenome from annotated assemblies of the selected 108 *S.* Typhimurium isolates using the default settings and percentage identity of 90%[381]. To perform a pangenome-wide association study, isolates were scored for presence or absence of a chosen trait and evaluated using Scoary (Brynildsrud, 2016). The first trait was susceptibility, and isolates were determined based on ciprofloxacin MIC to have 'intermediate' susceptibility (1) or or 'susceptible' susceptibility (0). Isolates with unknown ciprofloxacin MICs were excluded from the analysis. Scoary was executed to evaluate whether gene clusters were trait-specific.

The second trait tested for was known *gyrA* mutation or *qnrs* presence or absence. Isolates with a known *gyrA* mutation or *qnrs* were scored with a 1, and those without were scored 0, based on in silico AMR analysis (see section 2.15). *gyrB*, *parC*, or *parE* mutations were excluded from the analysis because these are uncommon in *S.* Typhimurium isolates. Scoary was executed for this trait, and gene clusters for this trait were evaluated manually.

2.16 *In silico* AMR analysis

Antibiotic resistance genes were identified from the assemblies of the Illumina sequence data using ariba v 2.11.1 with CARD database 1.1.8[382,383]. ResFinder was also used to verify ariba results and to further identify resistance genes on plasmids by direct uploading of contig files to the ResFinder web browser[384].

2.17 Biofilm growth conditions

Tryptone, yeast extract, and agar were combined with MilliQ water to 1 L and autoclaved (see **Table 2.5**). After sufficient cooling, Coomassie Blue and Congo Red were added to the melted agar and gently mixed. Plates were poured with ∼20 ml agar per plate. Plates were left for 2-4 hours to dry and then sealed in parafilm and stored at 4°C in the dark until use. Selected isolates (see **Table 2.6**) were grown overnight (16-18 h) from plates in 10 ml Isosensitest broth with shaking at 200 rpm at 37°C. 10 μl of culture was added to 990 μl 1x PBS and vortexed well. 5 μl of each isolate was spotted on each plate with a maximum of 6 spots per plate. Plates were left on bench until dry, then sealed with parafilm and incubated at 27°C without inversion for a minimum of 72 h. Colonies were subsequently taken directly for SEM analysis.

Table 2.5 Components of RDAR agar plates (1 L).

Reagent	Supplier	Quantity
Tryptone	Difco, 211921	10 g
Yeast Extract	Difco, 212750	5 g
Agar	Difco, DF0812	15 g
Coomassie Brilliant Blue	VWR, 0615-10G	2 ml of 10 mg/ml stock
Congo Red, Indicator Grade	Acros Organics, 110501000	2 ml of 20 mg/ml stock

Table 2.6 Isolates for RDAR growth and SEM.

Isolate	RDAR morphology (red/smooth or white/smooth)
D23580	Red/smooth
2643	Red/smooth
10018	White/smooth
1577	White/smooth
2735	Red/smooth
10433_3	White/smooth
9266_3	Red/smooth
8429_3	White/smooth
2101	White/smooth
6549_3	Red/smooth

2.18 Scanning electron microscopy (SEM) of bacteria grown under stress conditions

In one experiment, *S.* Typhimurium D23580 cultures were treated with 0x or 2x MIC equivalents of ciprofloxacin, grown for 2 h or 8 h in shaking liquid cultures at 37°C, 200 rpm, and then plated on Isosensitest plates. Following colonial growth, bacteria were processed for SEM.

In an independent experiment, bacteria were grown under biofilm-forming conditions as specified in section 2.16 above. Sections of each colony were then selected by Dave Goulding and Claire Cormie for SEM processing at the Wellcome Sanger Institute, as described in **Appendix A**.

3. Development of high-content imaging of individual bacteria

3.1 Introduction

While there have been many recent startling advances in the field of bacterial genomics, it is arguable that there has not yet been a similar revolution in bacterial phenotyping. The phenotyping of clinical bacterial isolates relies primarily on empirical bacterial culture on agar plates, which in some cases is linked to rapid diagnostic tests, for example a urine dipstick[385]. Current assessment of minimum inhibitory concentrations of a drug to asses AMR in patients is largely performed by the use of semi-automated systems such as VITEK, or disk diffusion/ETESTs to measure the zone of inhibition of bacterial growth on a plate. While these strategies paired with genomic analysis can detect resistance in the overall population, they do not consider fluctuations within a bacterial population and likelihood of subtle mechanisms of drug evasion. To begin to tackle the deficiency in higher throughput microbial phenotyping, and potentially to obtain a faster and more accurate readout of bacterial behaviour under antimicrobial pressure, we investigated the use of high throughput microscopy for bacterial phenotyping.

With the advent of more powerful microscopy technologies, it is now possible to visualize and measure individual bacteria at high resolution to assess morphological characteristics. High-content imaging (HCI) is the combined technologies of high-resolution, high-throughput automated microscopy with automated analysis pipelines to derive meaning from the imaging data[386,387]. The ability to study individual bacteria and record changes allows for not only the assessment of bacterial response to antimicrobials but also the ability to screen novel compounds for efficacy and/or impact. Imaging has been used widely as a strategy to screen for drug impact on the behaviour of eukaryotic cells, and in theory similar principles can now be applied to antibacterial drug screening[388–392]. HCI has previously been used to study intracellular pathogens such as *Mycobacterium tuberculosis* and *Salmonella* species[393–397]. However, much of this work has been conducted looking at intracellular bacterial dynamics, and the screening of individual bacteria at scale is a much more recent phenomenon[398,399].

The strategy of imaging bacteria at high-throughput builds upon existing low-throughput strategies of capturing and analysing bacteria by microscopy. An assay for bacterial cytological profiling (BCP) has been developed in recent years by Pogliano and colleagues, facilitating the identification of morphological changes of bacteria after antimicrobial perturbation[359,400]. They used confocal microscopy to distinguish between bacteria exposed to five different classes of antimicrobials and subsequent image analysis could separate them into distinct clusters based on the drug mechanism of action[359,401]. Importantly, they showed that such imaging and analysis was applicable across multiple bacterial species, including *E. coli*, *Acinetobacter baumanii*, and *Staphylococcus aureus*[360,401–405].

Independently, there have been many efforts over the years to image bacteria individually and track movement and population expansion, particularly inside host cells[406,407]. However, one drawback with current low-throughput methodologies is that they require a pre-existing understanding of the phenotype in question to follow a discrete population or behaviour. In contrast, an agnostic approach to capturing all possible populations and phenotypic variants using HCI would be an important step towards better understanding bacterial population-level dynamics.

Based on the existing body of work on bacterial phenotyping, we wanted to optimize conditions and protocols to enable high-content bacterial phenotyping using an Opera Phenix (Perkin Elmer). The Opera Phenix is a dual spinning disk confocal microscope capable of acquiring images using four lasers and four cameras simultaneously, minimizing background fluorescence and time taken to capture images (Perkin Elmer). These features are vital for imaging bacteria because of their small size and the need to distinguish between individuals. In this study, we aimed to develop a methodology to simultaneously screen thousands of individual bacteria under a variety of conditions and further develop robust analysis pipelines to distinguish bacterial morphologies, following a consistent workflow (**Figure 3.1**).

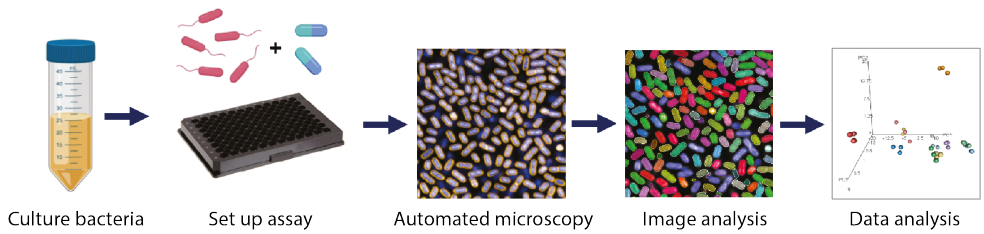

Figure 3.1 High content bacterial imaging and analysis workflow. A set of protocols was developed to culture bacteria, prepare samples for imaging, perform automatic microscopy and image analysis, and undertake analysis of the imaging data.

We further aimed to screen multiple bacterial isolates in tandem by comparing any morphological characteristics while growing in media or under challenge with antimicrobials. We hypothesized that it would be possible to distinguish between bacteria on the basis of their phenotypic characteristics after sufficient optimization of imaging and analysis parameters to specifically quantify trends in bacterial growth dynamics. We selected three distinct and clinically relevant bacterial species on which to optimize HCI and image analysis using the Opera Phenix: *Staphylococcus aureus* (Gram-positive), *Klebsiella pneumoniae* (Gram-negative, non-motile), and *Salmonella* Typhimurium (Gram-negative, motile). In line with the specific interest in *Salmonella* biology of the work described in this thesis and the particular challenges associated with imaging *Salmonella*, I undertook a more comprehensive optimization for *S*. Typhimurium, which will be the focus of this chapter.

3.2 Optimization of bacterial adhesion for imaging

Unlike low-throughput confocal microscopy, in which bacteria are typically placed on slides for single time point analysis, imaging on the Opera Phenix is conducted in 96- or 384-well plates. Thus, the first challenge was in optimizing the adhesion of bacteria, particularly motile ones, to the plastic ultra-thin-bottomed plates. Because motile *S*. Typhimurium D23580 did not adhere well to the plate plastic, we began by testing two types of thin-bottomed-plates, centrifuging *S.* Typhimurium D23580 bacteria onto the plates and exploring adhesion by coating plates with a variety of materials. Our initial panel of coatings included thin rat-tail collagen and *Salmonella*-specific antisera O4 and H:i to bind the surface lipopolysaccharide and/or flagella (**Figure 3.2**).

We found that although there were negligible visual differences between the two plate types (Cell Carrier versus Cell Carrier Ultra), it was necessary to coat the plates to have enough bacteria for imaging and analysis (**Figure 3.2 A, B**). Additionally, we found that initially, it was necessary to gently centrifuge *S*. Typhimurium D23580 bacteria onto the plates. However, none of the three initial well coatings bound sufficient numbers of bacteria for downstream visualization and analysis, so further optimization was required.

As bacterial adhesion was poor even with coating and centrifugation, we attempted to optimize other parts of the adhesion process. We hypothesized that fixation of motile bacteria

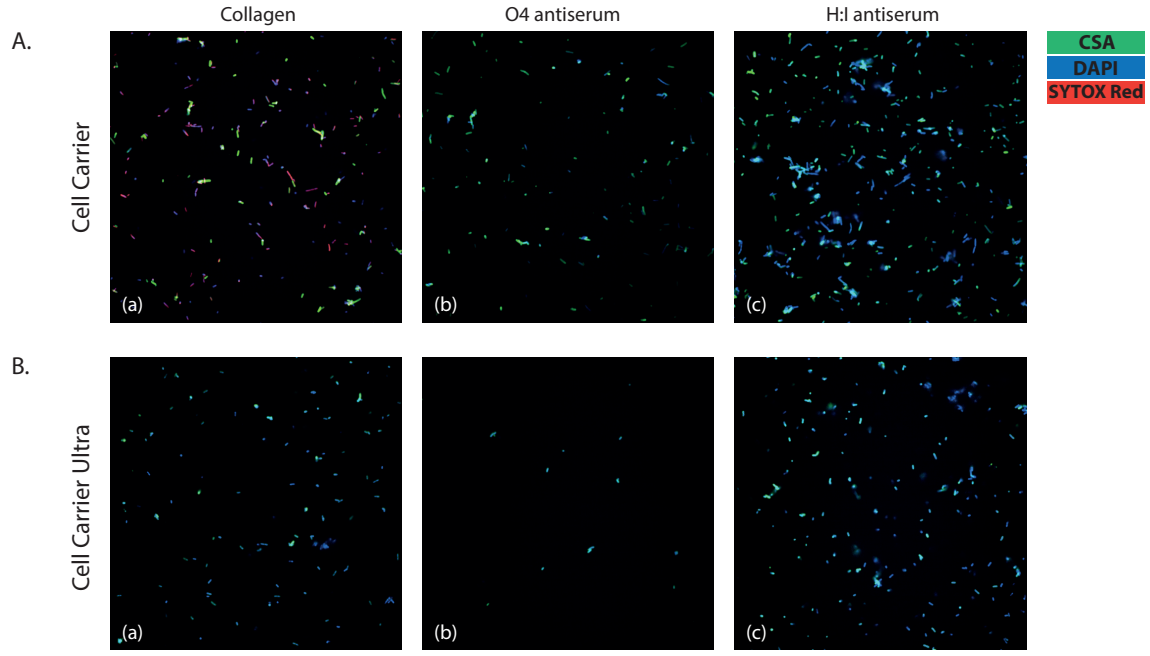

Figure 3.2 Comparison of Opera Phenix plates for *S*. Typhimurium imaging. Bacteria plated on Cell Carrier (**A**) or Cell Carrier Ultra (**B**) plates with coating of (a) collagen, (b) O4 antiserum or (c) H:i antiserum.

prior to addition to the plate might enhance adhesion because flagellar movement would be restricted. Thus, we compared bacteria fixed after plating and centrifugation (**Figure 3.3 A (a)**) with bacteria fixed in tubes and subsequently plated and centrifuged (**Figure 3.3 A (b)**).

However, this resulted in bacterial clumping, leading to blurred images. We next attempted to increase bacterial adhesion by centrifuging bacteria onto the plate at 4°C, hypothesizing that the bacteria would be less motile and therefore adhere better. Here, we centrifuged *S*. Typhimurium at either room temperature (**Figure 3.3 B (a)**) or at 4°C (**Figure 3.3 B (b)**). We found that while there was marginal improvement with centrifugation at 4°C, there were still very few bacteria in each field, and the image quality was poorer with the 4°C treatment.

Given the challenges associated with adhering *S*. Typhimurium to plates, we subsequently identified a set of 11 plate coatings that have previously been used to bind eukaryotic cells to surfaces[408–414]. We systematically screened binding of the three bacterial species of interest, including *S*. Typhimurium SL1344, to these coatings and compared the quality of images and number of adhered bacteria (**Figure 3.4, 3.5**).

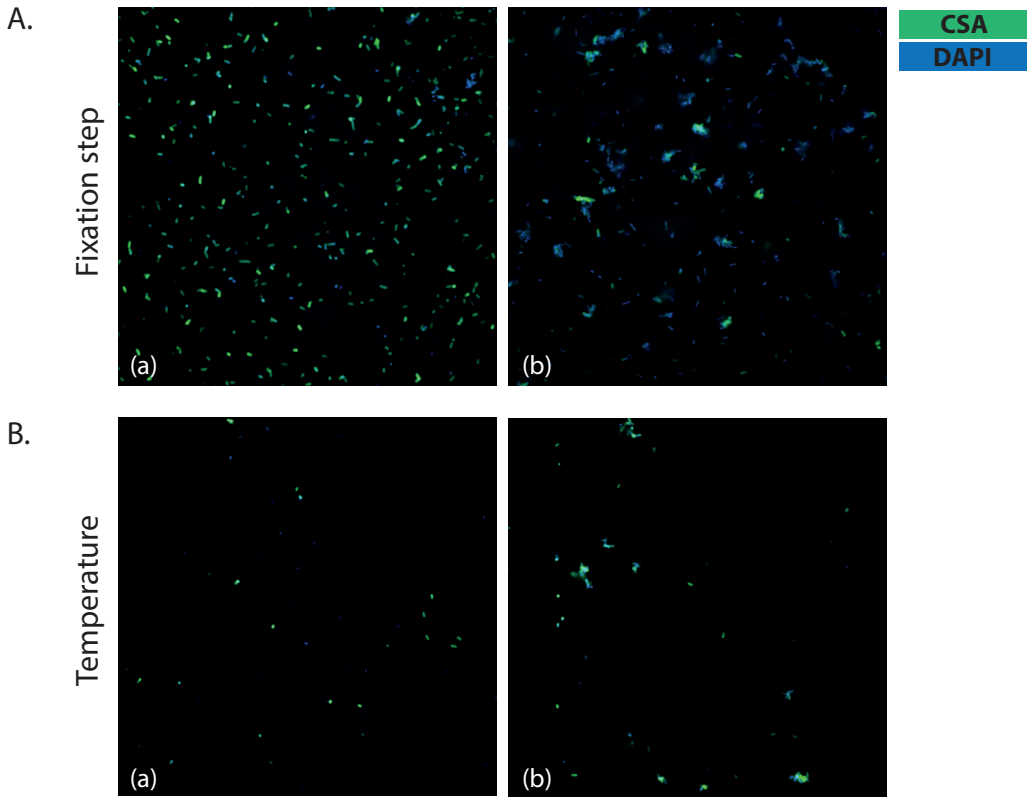

Figure 3.3 Optimization of fixation and temperature conditions for *S*. Typhimurium adhesion. All wells were coated with H:i antiserum prior to the addition of bacteria. **A.** Comparison of bacterial fixation with PFA before (a) or after (b) addition of bacteria to plates. **B.** Comparison of (a) bacteria centrifuged onto plates at room temperature or (b) at 4°C. Bacterial membranes are stained with CSA (green), and nucleic acids are stained with DAPI (blue).

Unsurprisingly, both isolates of *S*. Typhimurium tested adhered well to few coatings, possibly due to their motile nature. However, we found that *S*. Typhimurium could be successfully visualized and analysed after plates were coated with thick rat-tail collagen, Matrigel, or vitronectin (**Figure 3.5 B; Appendix B, Table B.1**). While these coating conditions were initially tested using *S*. Typhimurium SL1344, similar results were validated and confirmed for *S*. Typhimurium D23580 and other invasive *S*. Typhimurium isolates of interest. Based on the significant improvement in adhesion of *S*. Typhimurium with suitable coatings, it was then possible to develop and optimize next stages of the methodology.

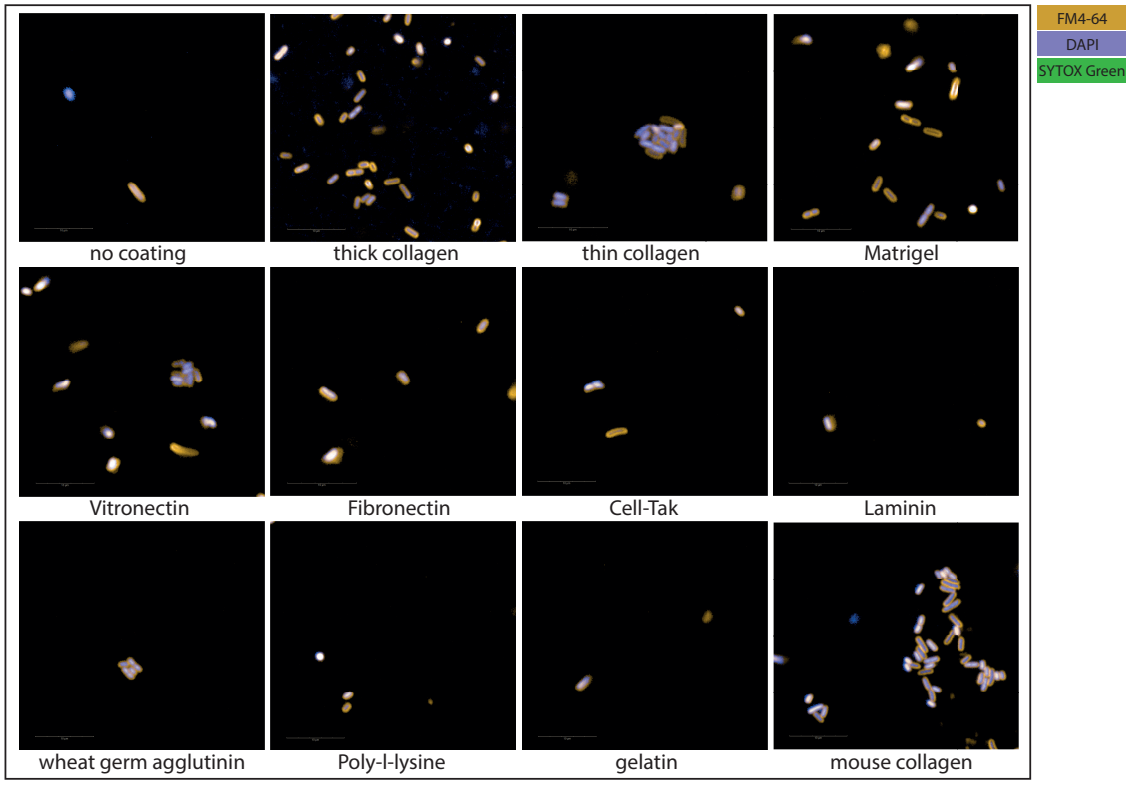

Figure 3.4 Comparison of *S.* Typhimurium SL1344 adhesion on 11 coatings and uncoated wells. Comprehensive optimization of *S.* Typhimurium adhesion to Cell Carrier Ultra wells coated with 11 alternative coatings and uncoated wells. Overnight cultures of *S.* Typhimurium bacteria were grown statically for 2 h in wells and then fixed, stained, and imaged.

3.3 Optimization of staining for *S.* Typhimurium

Following optimization of adhesion conditions, we wanted to evaluate and optimize staining protocols for all bacteria of interest and *S.* Typhimurium in particular. We based our initial fluorescent staining composition upon the work of Nonejuie *et al.*[359]. The stains were FM4-64, a cellular membrane stain; DAPI (4',6-diamidino-2-phenylindole), a membrane-permeable nucleic acid stain; and SYTOX Green, a membrane-impermeable nucleic acid stain. As SYTOX Green is membrane-impermeable, it is used as a readout for non-viable cells with ruptured membranes[415,416]. Upon staining with FM4-64, DAPI, and SYTOX Green, we found that while DAPI and SYTOX Green staining looked similar to those of images published by Nonejuie *et al.*, there was inconsistent surface staining of *S.* Typhimurium with FM4-64 (**Figure 3.6 A**)[359].

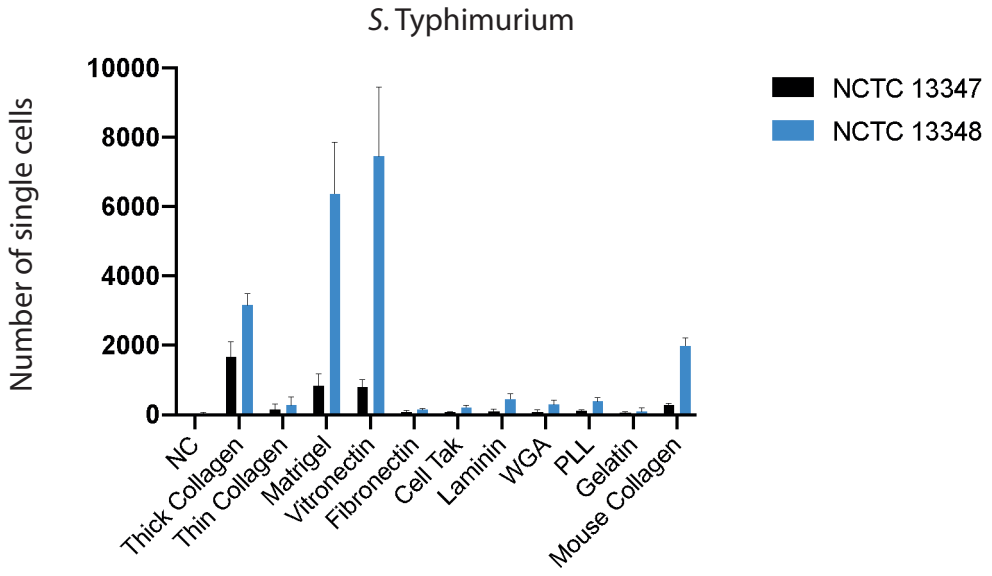

Figure 3.5 Quantification of bacterial single cells adhered to coated plates. Coatings were chosen for each bacterial isolate tested based on higher levels of adherent bacteria for two isolates of *S*. Typhimurium. The number of single cells was calculated using automated analysis by segmenting objects and identifying single cells.

We hypothesized that this may be due to inconsistent adhesion of *Salmonella* to wells or poorer integration of FM4-64 with the *Salmonella* cellular membrane. As a result, we next optimized staining with a FITC-conjugated *Salmonella*-specific antibody that binds the Common Structural Antigens (CSA) of multiple serotypes of *Salmonella* (**Figure 3.6 B**)[417]. As the CSA-FITC stain had the same excitation and emission spectra as SYTOX Green, we attempted to use SYTOX Red to measure dead cells. However, we found it difficult to optimize SYTOX Red concentrations, thus necessitating further stain optimization for *S*. Typhimurium. We subsequently found a CSA antibody conjugated to Alexa-647, which would allow for simultaneous use of SYTOX Green. Not only did this stain combination qualitatively produce the clearest staining of *S*. Typhimurium amongst the variations trialled, it also enabled us to compare directly between *S*. Typhimurium and other bacterial species using similar staining combinations (**Figure 3.6 C**).

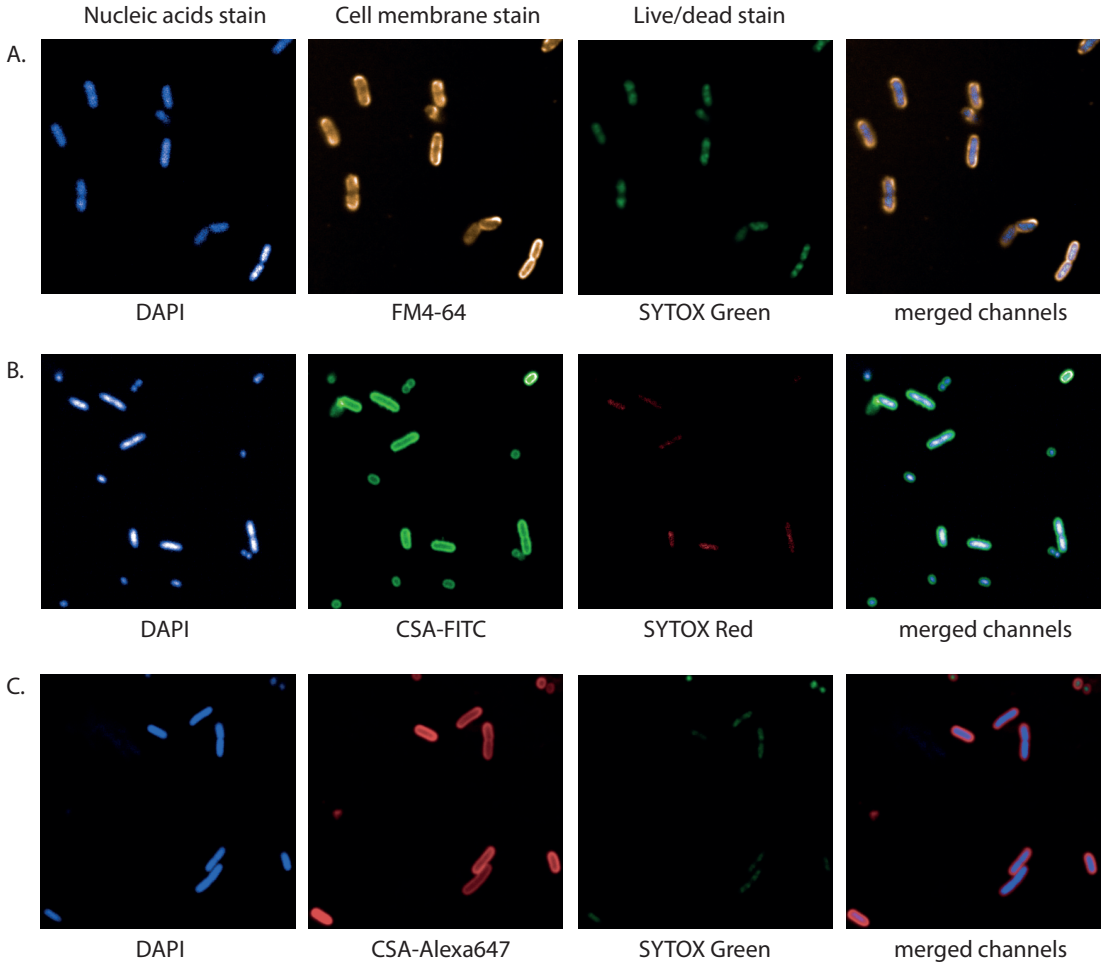

Figure 3.6 Optimization of staining for *S.* Typhimurium. A. Staining of *S.* Typhimurium using DAPI, FM4-64, and SYTOX Green as performed previously by Nonejuie *et al.*, 2013[359]. **B.** *Salmonella*-specific staining using CSA-FITC antibody to visualize outer membrane. **C.** Alternative *Salmonella*-specific staining using CSA-Alexa-647 antibody to visualize outer membrane.

3.4 Development of an *S.* Typhimurium analysis pipeline

Upon optimizing adhesion and staining protocols, we next developed analysis pipelines using the Harmony software by Perkin Elmer. A pipeline was developed specifically to measure less-adherent bacteria including *S.* Typhimurium. The pipeline inputted images taken on the Opera Phenix and then calculated the image data to distinguish objects of interest. Through a series of segmentation and selection steps, objects were refined based on size and other morphological parameters to be characterized as bacteria (**Figure 3.7; Appendix B, Table B.2**).

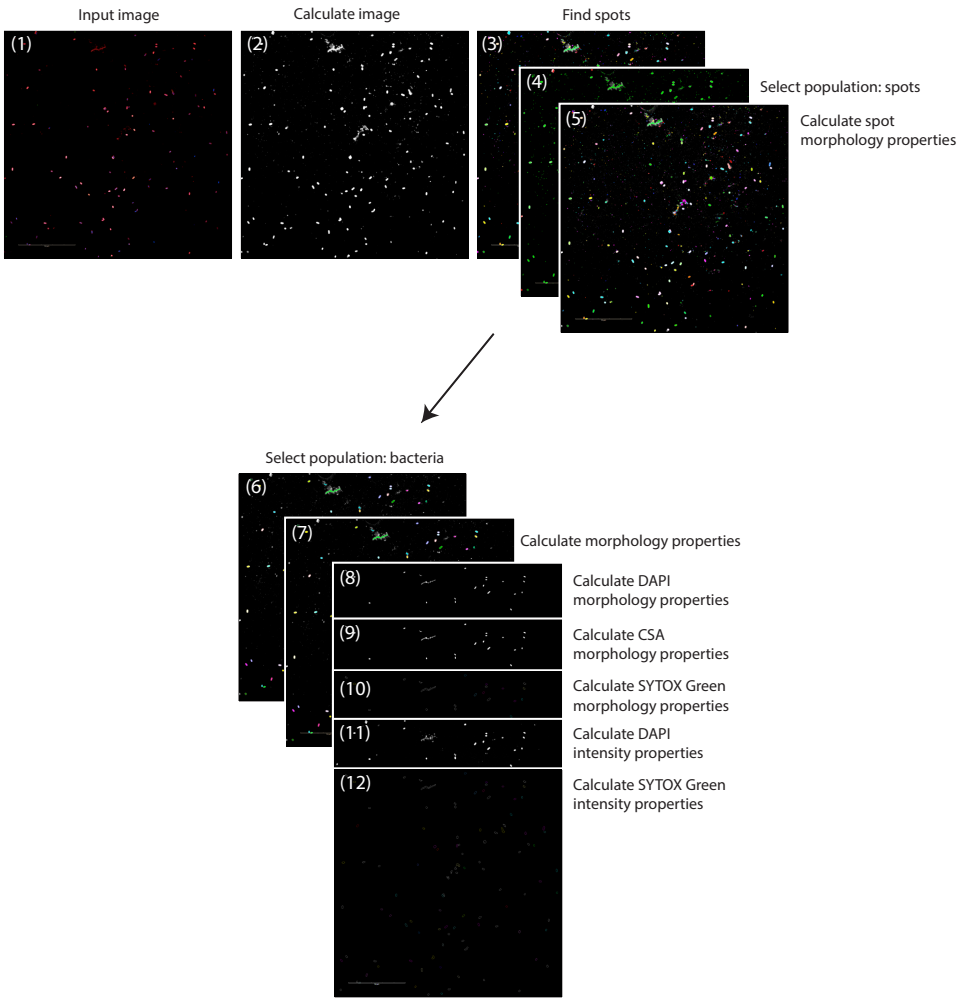

Figure 3.7 Analysis pipeline steps to identify and segment bacterial objects. Objects were calculated and measured from input images of *S.* Typhimurium (1) in a series of 12 steps prior to classification. Morphological and intensity properties were calculated based on overall objects and stains.

Various properties of the determined bacteria were calculated, including the morphological and intensity properties associated with each stain, as well as total morphology properties such as bacterial length and width (**Figure 3.7 (7)**). In addition to calculating more standard measurements, the Perkin Elmer Harmony software can also capture "STAR" morphologies, which calculate thresholds and weights of measurements to more precisely calculate fluorescence distribution, symmetry, and brightness (Perkin Elmer Image Analysis Technical Details). Upon selection of the "bacteria" population and characterization of the individual bacteria, a linear classifier was applied to distinguish between bacterial morphologies. We trained the linear classifier using a machine learning algorithm to identify the bacterial

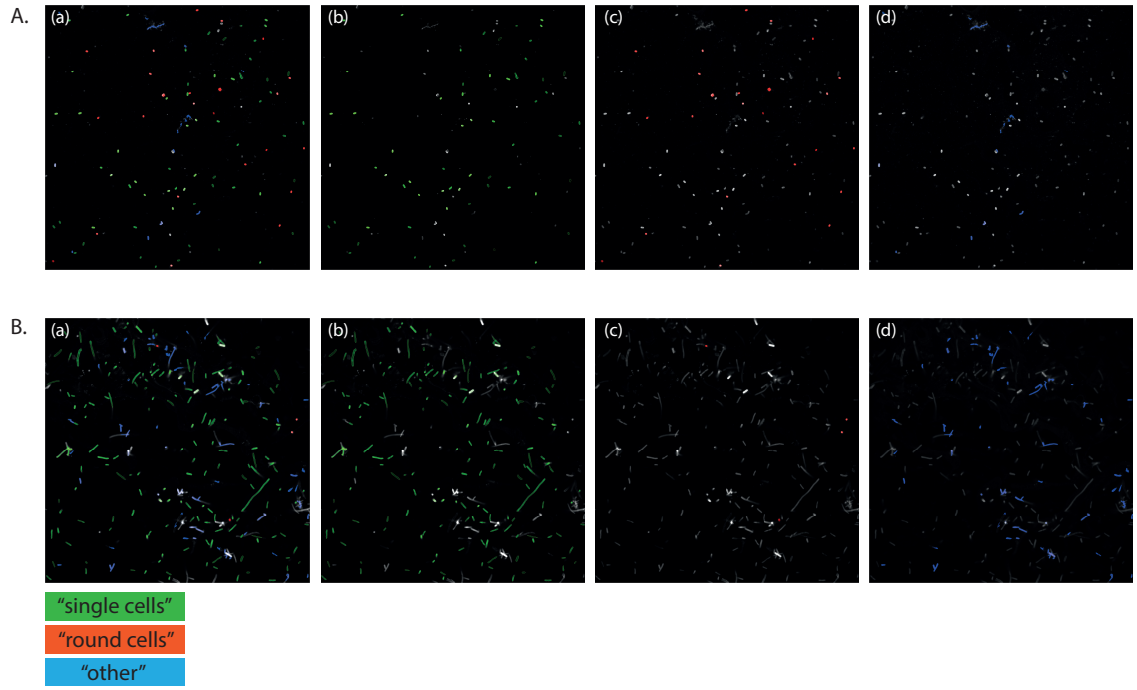

Figure 3.8 Linear classification of bacteria into three categories. A. Example of *S*. Typhimurium bacteria without antimicrobial treatment. **B.** *S*. Typhimurium bacteria under 2x MIC ciprofloxacin exposure. The linear classifier was trained to differentiate between objects in a field: all (a), "single cells" (b), "round cells" (c), and "other" (d) based on chosen morphologies of interest.

population as "single cells", "round cells", or "other". These categories were chosen based on visual scrutiny of the images and our interest in measuring morphological characteristics of single cells (**Figure 3.8**). Importantly, the linear classifier was robust enough to classify bacteria that had undergone morphological changes due to antimicrobial perturbation and still accurately distinguished between "single cells", "round cells", and "other" (**Figure 3.8 B**).

3.5 Imaging of antimicrobial-treated bacteria

We next wanted to test and validate imaging of bacteria perturbed by antimicrobial exposure. To do so, we selected a panel of nine clinically-relevant antimicrobials to *S*. Typhimurium bacteria with 5x MIC concentrations after assessment of antimicrobial susceptibility for each

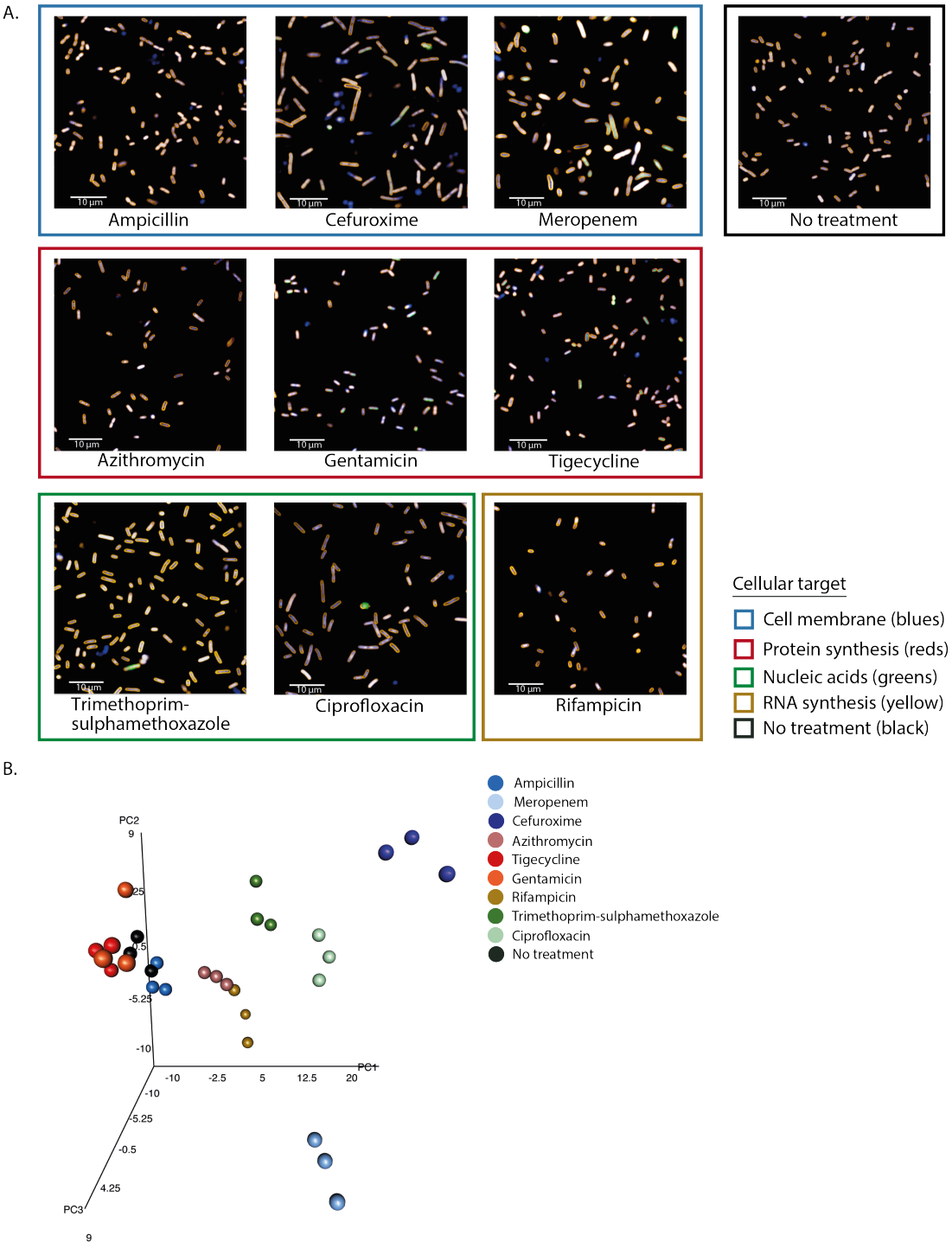

Figure 3.9 Phenotyping on the Opera Phenix of *S.* Typhimurium after 2 h antimicrobial exposure. A. Bacteria were imaged after exposure to 9 different antimicrobials for 2 h using DAPI (blue), FM4-64 (orange), and SYTOX Green (green). **B.** Principal component analysis showing clustering of technical replicates for each antimicrobial and separation between antimicrobial treatments based on morphological parameters.

isolate (**Appendix B, Table B.3**). This study was performed with triplicate wells of each antimicrobial treatment on each plate, and all experiments were done in biological triplicates to assess the consistency of the assay. We found that antimicrobials with different mechanisms of action were linked with different morphological changes to the bacteria (**Figure 3.9 A**). This was also validated by the clustering of the different antimicrobial-treated bacteria in a principal component analysis (**Figure 3.9 B**).

As we were particularly interested in changes to *S*. Typhimurium after ciprofloxacin exposure, we undertook further analysis to assess other bacterial characteristics. Visually, we could identify morphological differences between *S*. Typhimurium single bacteria treated with 0x, 1x, 2x or 4x MIC of ciprofloxacin for 2 h (**Figure 3.10 A**). We then plotted the number of bacteria measured at 2 h in each condition and found that there was considerable variation between bacterial numbers at this given time point (**Figure 3.10 B**). This may have been due to differences in optical densities of the bacterial cultures after 2 h growth. Importantly, there were more than 500 single bacteria per treatment, providing an adequate number of cells to perform further analysis on. We were also interested in performing downstream analysis on only the live bacteria, as distinguished by SYTOX Green fluorescence. This was one of the parameters measured in the automated analysis, and we graphed the density distribution of SYTOX Green mean fluorescence intensity of the total bacterial population at 2 h (**Figure 3.10 C**). We found that while there was not a clean bimodal distribution of fluorescence clearly delineating "live" versus "dead" bacteria, there was the highest density of bacteria with low SYTOX Green fluorescence and a diminishing tail of increasing fluorescence.

To further discriminate between live and dead bacteria, we drew an arbitrary and conservative threshold where the density of bacteria decreased (**Figure 3.10 C**). We called bacteria to the left of this threshold "live" and those to the right "dead" for downstream analysis of the live population. While some live bacteria may have been included in the "dead" bin, we decided that it was better to exclude some "live" bacteria than include "dead" bacteria in further analysis. To guide downstream analysis, we were curious to know what parameters were deemed important for any given treatment condition. To achieve this, we accessed *Z*' (z-prime) statistics for ciprofloxacin-treated versus non-treated *S*. Typhimurium. Interestingly, many of the highest-ranked *Z*' parameters were staining parameters that were not visually discernible; however, they likely influenced clustering of the different antimicrobial treated bacteria in the PC plot (**Figure 3.9; Table 1; Appendix B, Table B.4**).

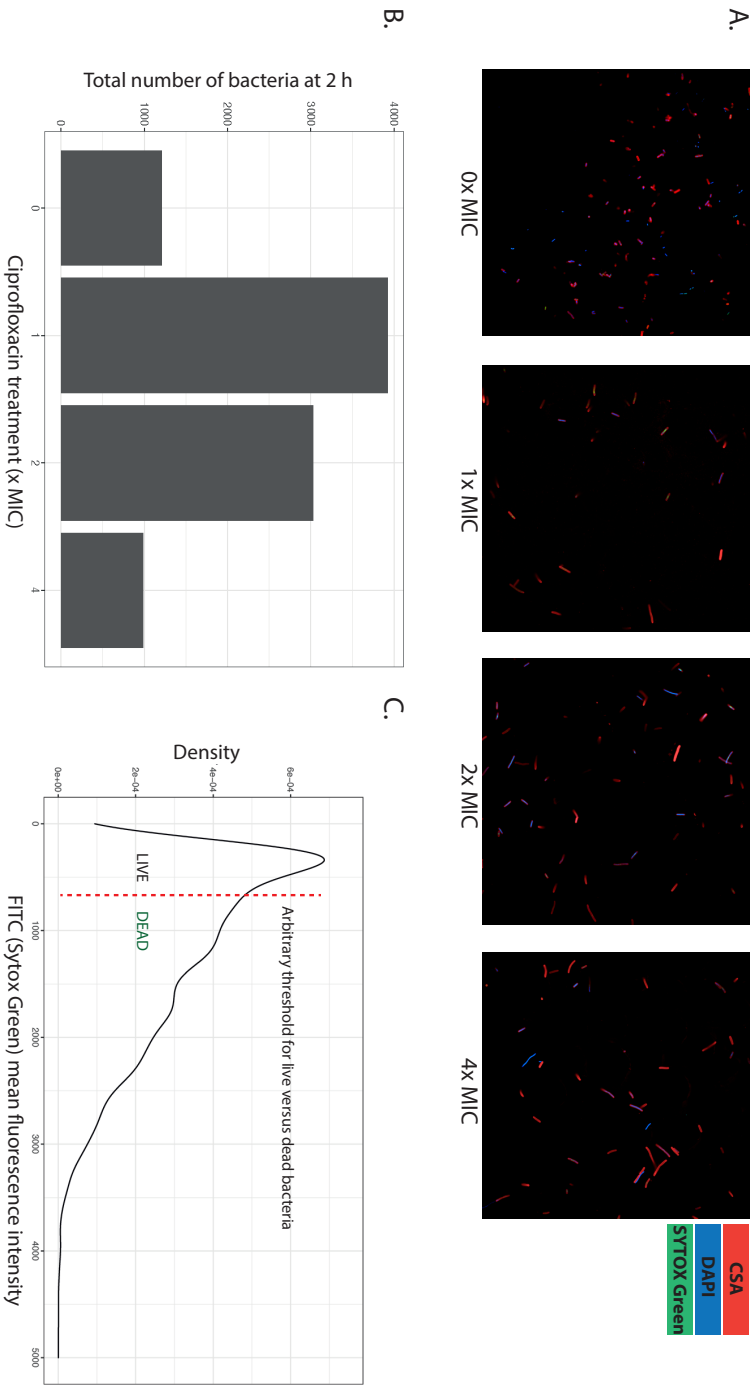

Figure 3.10 Assessment of ciprofloxacin-treated *S.* Typhimurium after Opera Phenix imaging. **A.** Images from *S.* Typhimurium treated with either 0x, 1x, 2x, or 4x MIC of ciprofloxacin for 2 h. **B.** Quantification of total number of analysed bacteria from Perkin Elmer Harmony analysis software. **C.** Analysis of SYTOX Green mean fluorescence intensity at 2 h over all bacteria to measure distribution. An arbitrary cut-off of ∼750 AU was applied to threshold live bacteria.

Table 3.1 *Z'*-statistics for the 20 most important parameters to distinguish between ciprofloxacin-treated (2x MIC) and non-treated *S*. Typhimurium.

Parameter	Z'
CSA Symmetry 14 - StdDev per Well	0.953
CSA Symmetry 04 - StdDev per Well	0.953
CSA Symmetry 15 - Mean per Well	0.938
DAPI Symmetry 15 - Mean per Well	0.935
CSA Symmetry 04 - Mean per Well	0.934
CSA Radial Relative Deviation - Mean per Well	0.933
CSA Symmetry 02 - Mean per Well	0.93
CSA Symmetry 12 - Mean per Well	0.921
CSA Symmetry 14 - Mean per Well	0.918
CSA Threshold Compactness 60% - Mean per Well	0.918
CSA Threshold Compactness 40% - Mean per Well	0.917
CSA Axial Length Ratio - Mean per Well	0.916
CSA Threshold Compactness 30% - Mean per Well	0.913
CSA Radial Mean - Mean per Well	0.9
CSA Threshold Compactness 50% - Mean per Well	0.897
Roundness - Mean per Well	0.896
Spot Roundness - Mean per Well	0.896
DAPI Symmetry 14 - StdDev per Well	0.893
DAPI Threshold Compactness 60% - Mean per Well	0.891
Length [µm] - Mean per Well	0.889

3.6 Discussion

In this study, we developed a methodology to perform HCI and subsequent automated image analysis on individual *S*. Typhimurium bacteria grown in liquid culture using an Opera Phenix high-throughput confocal microscope. We were able to apply this technique to systematically screen large numbers of *S*. Typhimurium exposed to a variety of antimicrobials and could use morphological parameters determined by image analysis to discriminate between antimicrobial treatments.

Despite the clear advantages of HCI to screen bacteria, development of this methodology exposed some of the challenges associated with HCI of individual bacteria. Imaging in 96-well plates enables rapid and efficient screening of bacteria under multiple treatments in parallel, introducing experimental flexibility and ability to collect vast amounts of single-cell data. However, our study illustrated that the acquisition of such information requires extensive

optimization of imaging to have sufficient numbers and quality of bacteria to perform image analysis. We developed our assay based on existing methodologies for lower-throughput imaging, and we found numerous challenges associated with imaging *S*. Typhimurium[359].

The most significant challenge in imaging *S*. Typhimurium was adhesion of bacteria to the plastic wells, which we ascribed to the motility and outer membrane composition of the bacteria. It is anticipated that similar challenges would occur for other motile bacteria, although we did not validate our methodology on alternative motile bacterial species. There was a high degree of variability in adhesion of *S*. Typhimurium to uncoated wells, and overall number of adhered bacteria was low. While there was marginal improvement with *S*. Typhimurium-specific coatings of O4 and H:i antisera, it was interesting that both of those coatings diminished image quality. It may be that the specific binding of the antisera occluded the binding of stain or caused bacterial aggregation, thus worsening the fluorescent signal[418–420]. We found that the most-suitable well coatings for *S*. Typhimurium in terms of image quality and number of adherent cells were compounds often used for stem cell adhesion to plastics.

Upon optimization of coating conditions, it was still necessary to optimize staining conditions for *S*. Typhimurium. Once again, this may have been due to the outer membrane composition of *S*. Typhimurium or that insufficient adhesion of bacteria to wells impacted staining efficacy. In this case, there was a clear advantage to the use of *Salmonella*-specific outer membrane CSA, which yielded brighter and more compact staining of the bacterial membranes. The use of a *Salmonella*-specific stain may also be advantageous in the future when studying interactions of bacteria with host cells. The optimization of SYTOX staining to identify dead cells was important because this allows for more nuanced downstream analysis of live and dead bacterial populations[421,422]. In this study, we did not perform analysis on live versus dead cells; however, the inclusion of the STYOX stain enabled discrimination of antimicrobial mechanisms of action in our principal component analysis of antimicrobial-treated bacteria. Moreover, we were able to plot the density of SYTOX staining across a bacterial population and draw a threshold of SYTOX fluorescence intensity to discriminate between potentially live and dead cells. It is important to recognize that some studies have found incongruity between membrane rupture and cell viability depending on DNA topology and degradation, which may confound interpretation of SYTOX fluorescence intensity[423–425]. Nevertheless, SYTOX intensity may be an important feature in future analyses, particularly when looking at bacterial sub-populations within a well displaying different characteristics.

Adequate imaging of *S*. Typhimurium facilitated screening of bacteria for the development of an automated analysis pipeline that could capture a large number of morphological parameters. In the context of bacteria treated with a panel of antimicrobials, this set of parameters could then be used to perform a principal component analysis to discriminate between bacteria treated with antimicrobials with different mechanisms of action. The value of this methodology is that it can be applied in a multitude of contexts: to predict the mechanisms of action of novel compounds, measure killing efficacy of a panel of drugs, and compare morphological differences between related organisms, among others. The development of high content screening of individual bacteria opens up a multitude of possibilities to explore and characterize the diversity of bacterial phenotypes.

4. Characterization of growth dynamics of *S.* Typhimurium following ciprofloxacin exposure

4.1 Introduction

Genomic and phenotypic analysis of MDR *S.* Typhimurium have identified individual isolates and clades that exhibit evidence of a decrease in ciprofloxacin susceptibility. While there is a growing appreciation for DCS *S.* Typhimurium, there is a lack of overall understanding of the finer dynamics that drive these trends. We know some of the key mutations within genes that encode proteins known to be targeted by fluoroquinolones, such as *gyrA*, but there may be other genes involved in the expression of resistance[426]. Additionally, it remains unclear why ciprofloxacin resistance appears in some genotypes of *S.* Typhimurium but not others.

To better appreciate what is driving the expression of resistance in *Salmonella* in the field, it would be useful to characterize the phenotypic and genotypic aspects of AMR in bacteria in a controlled laboratory setting. Human dosing strategies for ciprofloxacin and other antimicrobials are designed to retain drug concentrations above the MIC of an infecting organism throughout the course of an infection. However, in reality it is likely that a population of bacteria are exposed to varying levels of ciprofloxacin inside and outside the host during and between treatments. While laboratory settings and *in vitro* cultures do not completely mimic field or *in vivo* conditions, they can provide some insight into how *S.* Typhimurium responds to ciprofloxacin exposure over time and may help pinpoint factors that play a role in a more complex environment.

There has been some previous analysis of growth dynamics of *S.* Typhimurium in the presence of ciprofloxacin, and this has revealed the importance of *gyrA* and *parC* mutations as well as the influence of the absolute expression levels of efflux pump genes such as *acrB*, *tolC*, *ramA*, and *soxS*[427,428]. Furthermore, previous work has shown that resistance to the quinolone nalidixic acid can increase the ability of bacteria to survive ciprofloxacin treatment. This phenotype has been linked to so-called persister bacteria[429,362,330,430]. There have been

some studies linking the reduction of ATP pools to this behaviour; however, the mechanisms involved remain unresolved. Additionally, there may be genetic and physiological differences between any mechanisms observed in *Salmonella* and other bacteria[431,432,429,433].

Few previous studies have focused on the comparative analysis of clinical isolates of *Salmonella* that display different susceptibilities to ciprofloxacin. In any such study it would be interesting to perform a comprehensive phenotypic analysis beyond simple growth dynamics and measurement of the MIC. To this end, we chose three clinical isolates of *S.* Typhimurium and a 'laboratory-adapted' reference strain SL1344 to compare such phenotypic behaviours in the presence of ciprofloxacin. The four isolates served as a 'pilot study', have been whole genome sequenced, and have been reported in the literature[370,80,82,57,176]. In addition, some of the isolates have been previously analysed for other phenotypes, including serum resistance, invasion of human cells, and metabolic properties[176,57,80,82,181,434].

Given the difference in MIC and background AMR profiles between the four isolates, we sought to understand how the growth rates of this small but somewhat genetically diverse set of *S.* Typhimurium were affected by increasing concentrations of ciprofloxacin close to and just above the measured MIC. An aim here was to observe whether all the bacteria in the exposed population responded in the same way to the antimicrobial. Additionally, we wanted to visualize changes in morphology associated with ciprofloxacin exposure at and above the MIC. This was in the context of developing methodologies for higher throughput imaging analysis of such bacteria. An aim here was to use novel methodologies to capture morphological data from large numbers of individual bacteria. The use of the Opera Phenix imaging platform facilitated this approach but was still in the early stages of its evaluation despite the optimization discussed in the previous chapter. Lastly, we wanted to identify any potential mutations arising over 24 hours of growth in ciprofloxacin at or above the MIC that may influence growth in such challenging conditions.

We hypothesized that genotypically distinct *S.* Typhimurium isolates might differ in their growth rates upon ciprofloxacin treatment, and that not all bacteria would survive at above-MIC concentrations. We further hypothesized that upon ciprofloxacin exposure, *Salmonella* bacteria could undergo sustained distinct morphological changes that differed prominently between concentrations of ciprofloxacin exposure. Further, any morphological changes might differ (a) within a single isolate's population and (b) between isolates. For bacteria that did survive 24 hours of sustained ciprofloxacin exposure, we hypothesized that there could

be detectable SNPs or other mutations selected in response to the treatment, in addition to mutations in *gyrA*.

4.2 Ciprofloxacin susceptibilities of the *S.* Typhimurium isolates

To explore ciprofloxacin-mediated inhibition and killing of *S.* Typhimurium, four relatively diverse clinical isolates were selected for evaluation based on sequence type, ciprofloxacin susceptibilities, and place of isolation. We selected two *S.* Typhimurium ST313 (D23580 and 5390_4) isolates and one ST34 (VNS20081) isolate, in addition to the ST19 reference strain SL1344 (**Figure 4.1**). To illustrate the phylogenetic diversity of these isolates, we made a phylogenetic tree of the four isolates alongside other *S.* Typhimurium isolates that have been previously studied and sequenced[57,176,82,77,435,81].

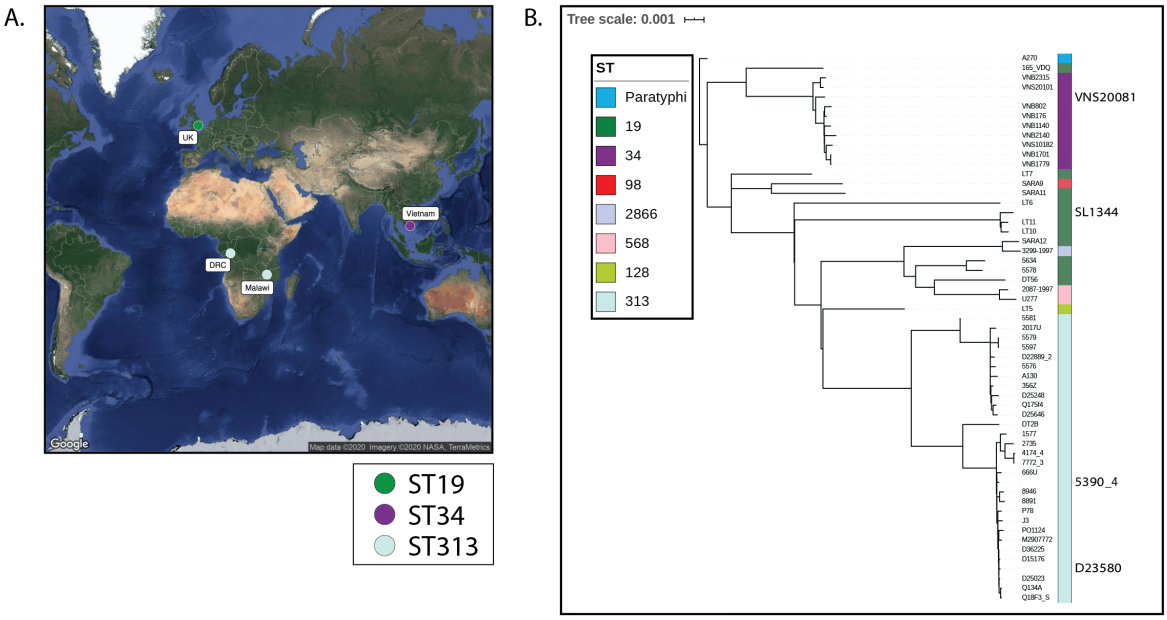

Figure 4.1 Geographic origin and phylogeny of four chosen *S.* Typhimurium isolates in a global context. The four isolates chosen come from distinct geographical locations (**A**) and are dispersed within a global phylogenetic tree of 57 *S.* Typhimurium isolates (**B**). The four chosen isolates are delineated in larger font to the right of the ST column.

The four selected *S.* Typhimurium isolates were subjected to antimicrobial susceptibility testing for ciprofloxacin, and the MICs against ciprofloxacin were determined (using an MIC ETEST) to establish working concentration (**Figure 4.2; Table 4.1**). We chose ETESTs to determine MICs because of their reliability and obvious visual result, and to verify results, we tested each isolate in duplicate. The determined ciprofloxacin MICs were 0.015, 0.03, 0.5, and 1.0 μg/ml for SL1344, D23580, 5390_4, and VNS20081, respectively. Based on CLSI guidelines for *Salmonella*, SL1344 and D23580 would be considered "sensitive," 5390_4 would be considered "intermediate", and VNS20081 would be considered "resistant"[200]. An *in-silico* AMR gene analysis was also performed using ResFinder based on their whole genome DNA sequences to directly compare resistance profiles of the four isolates for a panel of some clinically-important individual and classes of antimicrobials (**Table 4.2**)[384]. Relevant to ciprofloxacin, 5390_4, harbours a plasmid-borne *qnrS* gene but no chromosomal *gyrA* mutation (a rare phenotype), and VNS20081 harbours a chromosomal *gyrA* mutation D87N[268]. In addition, 5390_4 and VNS20081 harbour aac(6')-lb-cr, and VNS20081 also carries *oqxA* and *oqxB*, all of which have been implicated in influencing fluoroquinolone susceptibility[436–438].

Table 4.1 Ciprofloxacin susceptibility of four *S.* Typhimurium isolates.

Isolate	M.I.C.E. ciprofloxacin test result (µg/ml)
SL1344	0.015
VNS20081	1
D23580	0.03
5390_4	0.5

4.3 Phenotypic assessment of ciprofloxacin MIC and growth dynamics

One of the simplest and most informative ways of measuring bacterial growth dynamics in culture is using time kill curves (TKC)[439]. Often, bacteria are grown with agitation in a 96-well plate reader, and this can provide information on changes in the optical density, or turbidity, of the culture, indicating the growth dynamics. When bacteria are removed at pre-determined time points and grown on plates at designated intervals, it is possible to discriminate between viable and non-viable bacteria. This is particularly important in assessing bacteriostatic versus bactericidal concentrations of a given antimicrobial. The

Table 4.2 *In silico* AMR analysis of four *S.* Typhimurium isolates.

	gyrA	Quinolone	Phenicol	Beta-lactam	Tetracycline	Aminoglycoside	Macrolide
SL1344						aac(6')-Iaa, aph(3'')-Ib, aph(6)-Id	
D23580			catA1	blaTEM-1B			
5390_4		qnrS1, aac(6')-Ib-cr		blaSHV-12, blaTEM-1B	tet(B)	aac(3)-IId, aac(6')-Iaa, aac(6')-Ib-cr, aadA1	
VNS20081	D87N	aac(6')-Ib-cr, oqxA, oqxB	catB3, cmlA1, floR	blaCMY-2, blaOXA-1	tet(B)	aac(3)-IV, aac(6')-Iaa, aac(6')-Ib-cr, aadA1, aadA2b, aph(3')-Ia, aph(4)-Ia	mph(A)

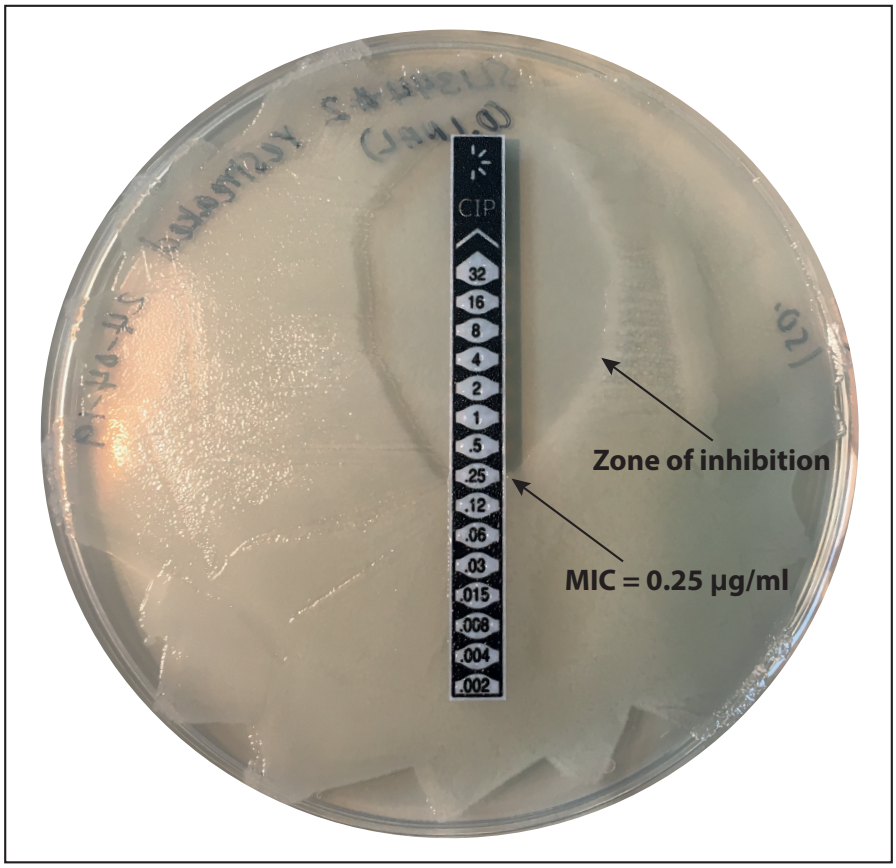

Figure 4.2 Example of a ciprofloxacin MIC ETEST. To perform an MIC ETEST, a bacterial culture is spread evenly on an Isosensitest agar plate, and an ETEST strip is immediately administered to the drying plate. Plates are incubated overnight and the point at which bacterial growth is inhibited is read as the MIC. In this case, the ciprofloxacin MIC was determined to be 0.25 μg/ml.

MIC of an organism is the lowest concentration of drug at which visible growth is inhibited following overnight culture[200,440]. Thus, while there may be live organisms still present in a liquid culture, it is necessary to grow them on solid medium to count viable colony forming units (CFU). Growing and identifying CFU on agar plates enabled us to assess the growth dynamics under ciprofloxacin exposure and detect different growth rates and response to ciprofloxacin between isolates. However, CFUs themselves do not allow us to distinguish between bacteria that remain viable and divide and those that remain viable and do not divide. Hence, although useful, this approach has obvious limitations.

After determining ciprofloxacin MICs of the four isolates, we performed TKC to follow the *S.* Typhimurium growth dynamics in four concentrations (0x, 1x, 2x, 4x) of ciprofloxacin, corresponding to each isolate's MIC (**Figure 4.2**). Interestingly, we found that even at

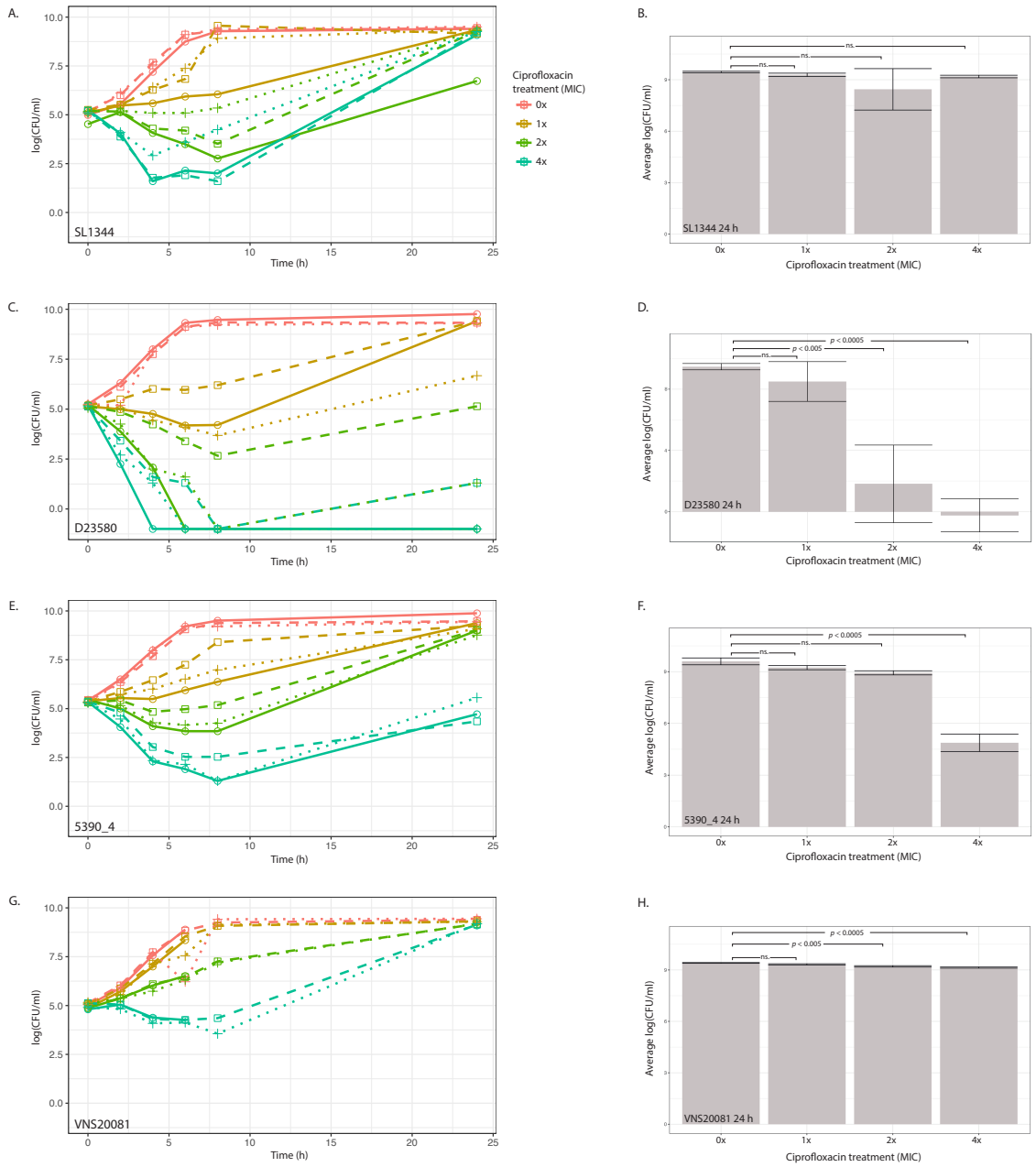

Figure 4.3 Ciprofloxacin 24 h Time Kill Curves of four *S.* Typhimurium isolates. SL1344 (**A**), D23580 (**C**), 5390_4 (**E**), and VNS20081 (**G**) were treated with 4 concentrations of ciprofloxacin: 0x (NT), 1x, 2x, or 4x MIC. A one-way ANOVA was used to compare treatments at 24 h for each isolate (**B**, **D**, **F**, **H**), and Tukey's Honest Significant Difference (HSD) method was used to compare individual treatment means, and mean ± SD was plotted for the 24 h time point. All TKC experiments were performed in triplicate (dashed, dotted, and solid lines).

4x MIC ciprofloxacin exposure, the bacterial population rebounded, which was intriguing given that there was an initial kill phase with bactericidal concentrations of ciprofloxacin. *S.*

Typhimurium D23580 (**Figure 4.3 C**) exhibited some variation in measured killing between replicates, suggesting that there may be 'stochastic' variability in response to 2x and 4x MIC concentrations of ciprofloxacin. The other three isolates generated a more consistent response to ciprofloxacin exposure. At 24 h, *S.* Typhimurium SL1344 showed no significant difference in final CFU between treatments (**Figure 4.3 B**). In contrast, there were significant differences in *S.* Typhimurium D23580 24 h CFU between the 0x, 2x, and 4x treatments (**Figure 4.3 C, D**). There was a significant difference in the 24 h CFU of *S.* Typhimurium 5390_4 between 4x MIC and all other treatments (**Figure 4.3 F**). There were significant differences at in *S.* Typhimurium VNS20081 between the 2x and 0x, 4x and 0x, and 4x and 1x treatments, although all conditions had very high 24 h CFU (**Figure 4.3 H**).

Following this analysis, we wanted to ensure that bacterial growth was not rebounding due to degradation or inactivation of the ciprofloxacin over 24 h. To assess this, TKC for D23580 and 5390_4 were performed over 24 h, and the spent media from the 24 h time point was centrifuged and steri-filtered. The spent media were inoculated with a concentration of 1010^5 bacteria (as for previous TKC) from new overnight cultures, and TKC were performed over the following 24 h. We found that overall trends of bacterial growth in spent media mirrored those of the initial 24 h TKC (**Figure 4.4**). There did appear to be more variation in 5390_4 4x MIC CFU but an impairment of growth was clearly detectable (**Figure 4.4 C, D**). These results suggested that the ciprofloxacin was stable and active up to 48 h and that the ciprofloxacin concentration had not appreciably decreased.

Upon determining that ciprofloxacin degradation/inactivation did not account for the rebound phenotype, we assessed whether the bacteria population had become desensitized to ciprofloxacin using isolates D23580 and 5390_4. This was assessed by performing an initial 24 h TKC followed by inoculation of the 24 h bacterial cultures in fresh medium containing 0x, 1x, 2, or 4x ciprofloxacin MIC. As the actual number of viable bacteria in the inoculum was not known at the time of inoculation, an approximate number of CFU was added based on turbidity of the 24 h cultures (**Figure 4.5**). Regardless of the inoculum, the overall growth dynamics did not mirror those of the initial or ciprofloxacin degradation TKC, suggesting that some of the bacteria in the 're-inoculum' may have become at least transiently desensitized to ciprofloxacin over the initial 24 h. This was more striking in the D23580 re-inoculations than in the 5390_4 re-inoculations, which showed a significant increase in growth when treated with 2x or 4x MIC over the second 24 h period (**Figure 4.5 A, B**). This phenotype may, however, have partly been linked to lower 2x and 4x inoculum

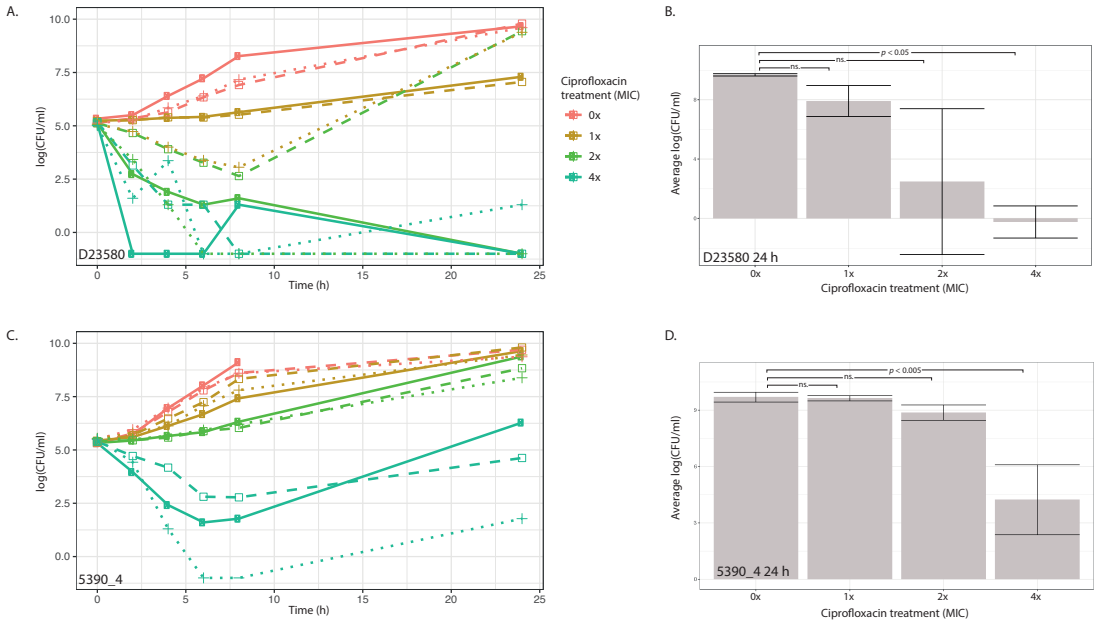

Figure 4.4 TKC measurement of ciprofloxacin sustainability. D23580 (**A**) and 5390_4 (**C**) were inoculated in previously-used and steri-filtered medium containing ciprofloxacin at 0x, 1x, 2x, or 4x MIC and grown for 24 h, with CFU plated at 6 time points. Differences in average log CFU/ml between treatments were calculated at 24 h for D23580 (**B**) and 5390_4 (**D**). Mean ± SD was plotted. A one-way ANOVA was used to compare treatments at 24 h, and Tukey's HSD method was used to compare individual treatment means. All experiments were performed in triplicate (dashed, dotted, and solid lines).

added at the start of the second 24 h period, as shown by the green and blue points plotted above the lines at 0 h (**Figure 4.5 A**). In contrast, the inocula used for re-inoculation in the second 24 h TKC of 5390_4 were more consistent, and there was only a significant difference in growth at 24 h between the 4x and other treatments (**Figure 4.5 C, D**). Based on these findings, we hypothesized that the bacteria were at least transiently adapting within the first 24 h of ciprofloxacin exposure, and we sought to further explore this phenotype, including by confocal microscopy using the Opera Phenix.

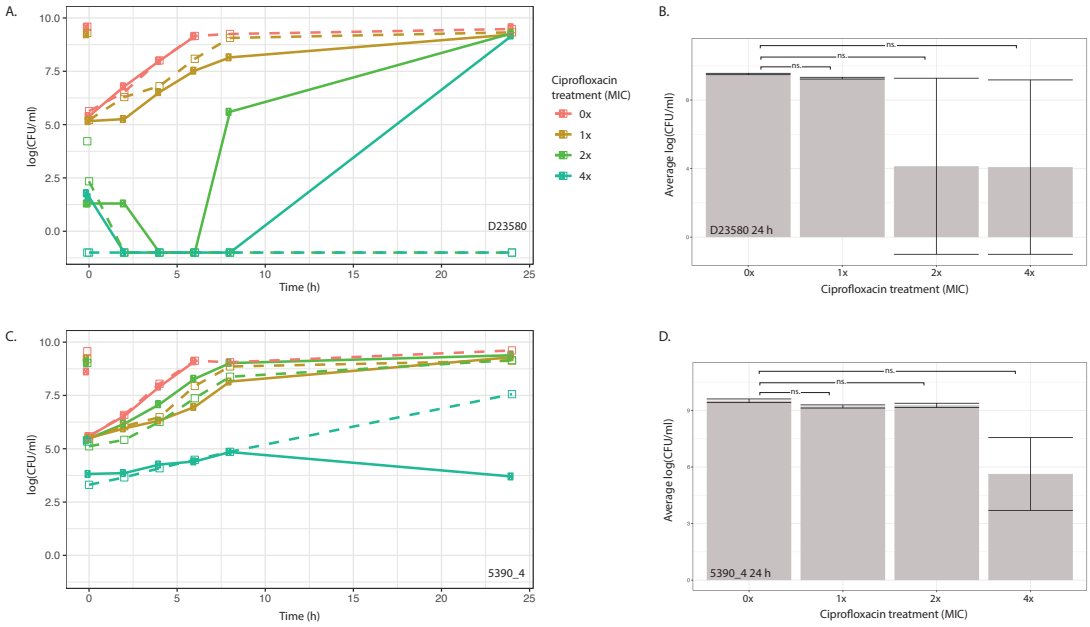

Figure 4.5 Bacteria grown in ciprofloxacin show desensitization over following 24 h. 24 h cultures of D23580 (**A**) and 5390_4 (**C**) were re-inoculated in fresh media containing 0x, 1x, 2x, or 4x MIC ciprofloxacin and grown for 24 h with CFU enumerated at 0, 2, 4, 6, 8, and 24 h. A one-way ANOVA was used to compare treatments at 24 h (**B** and **D** for D23580 and 5390_4, respectively), and Tukey's HSD method was used to compare individual treatment means. All experiments were performed in duplicate (dashed and solid lines).

4.4 Microscopic visualization of isolates exposed to ciprofloxacin

Based on the findings that the four isolates rebounded in the face of ciprofloxacin exposure above their respective MIC, we were curious to determine whether there were any changes in bacterial morphology over the course of 24 h. To assess this, we used the Opera Phenix (Perkin Elmer) high-content microscope to image the bacteria every two hours over 24 h at ciprofloxacin concentrations of 0x, 1x, 2x, and 4x MIC. We chose to focus on susceptible isolate *S.* Typhimurium D23580 and resistant isolate *S.* Typhimurium VNS20081 to capture potential morphological differences between a susceptible and resistant organism. **Figure 4.6** shows *S.* Typhimurium D23580 at six of the 12 time points, illustrating the elongation that has previously been noted in Gram-negative bacteria under ciprofloxacin exposure[359,400]. Interestingly, while some *S.* Typhimurium D23580 bacteria were elongated following ciprofloxacin exposure, not all were, particularly for many 1x MIC treated bacteria

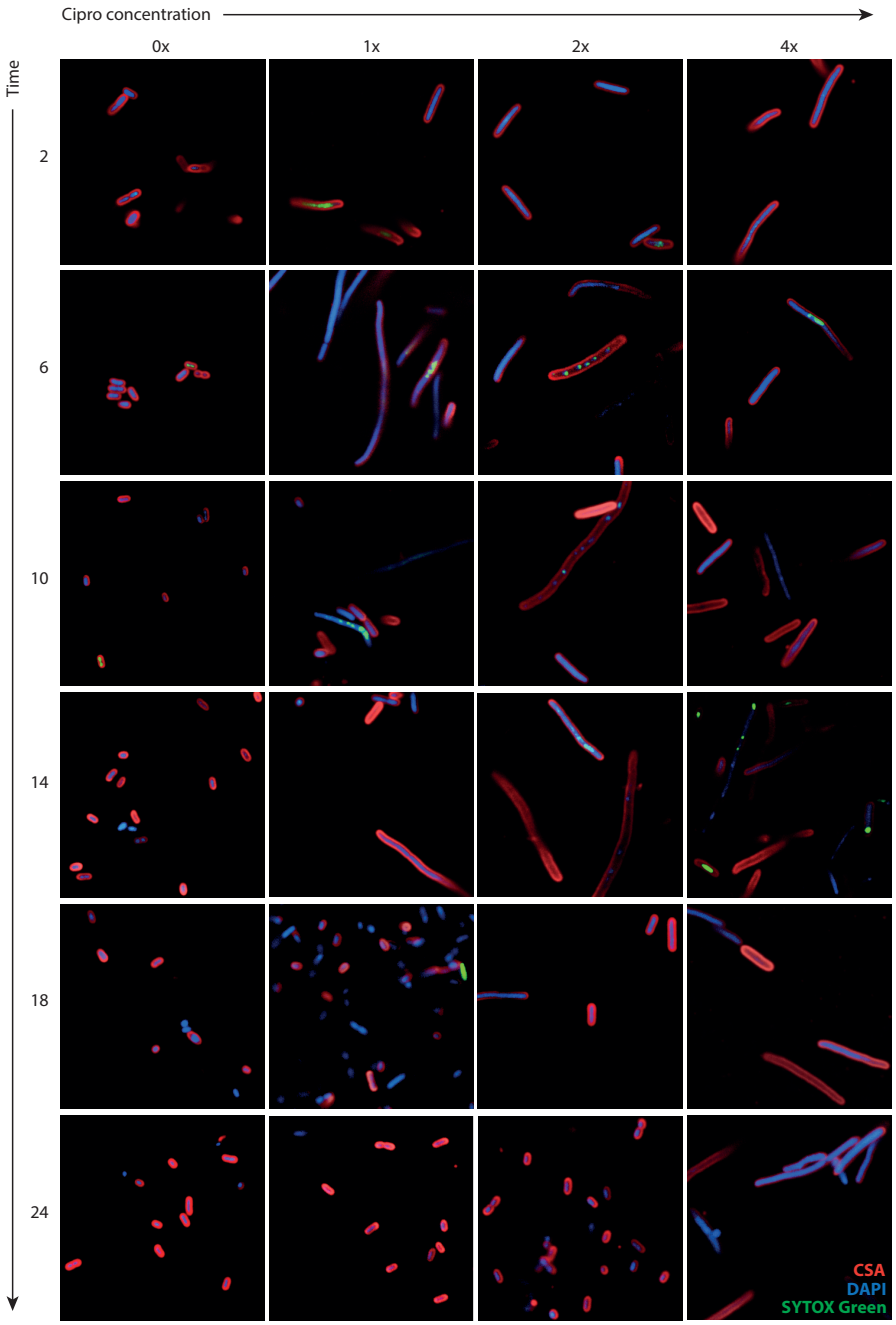

Figure 4.6 Confocal imaging of *S.* Typhimurium D23580 over 24 h of ciprofloxacin exposure. *S.* Typhimurium D23580 was treated with ciprofloxacin at 0x, 1x, 2x, or 4x MIC and imaged at 2 h intervals over 24 h using an Opera Phenix with a 63x objective. Bacteria were stained with CSA-Alexa-647 (bacterial membrane, red), DAPI (nucleic acids, blue), and SYTOX Green (dead cells, green). Six of the 12 time points are shown; images are from one representative experiment (of three).

from 10 h onwards and 2x MIC treated bacteria from 18 h onwards. However, overall, we observed more elongation in *S.* Typhimurium D23580 bacteria treated with ciprofloxacin compared to *S.* Typhimurium D23580 bacteria not treated with ciprofloxacin (**Figure 4.6**). As these images were of bacteria fixed at individual time points rather than being tracked by live imaging over 24 h, it was not possible to determine whether individual bacteria were elongating and subsequently shrinking or whether a subpopulation of bacteria remained as shorter forms. We subsequently sterile-filtered the media from the above experiments

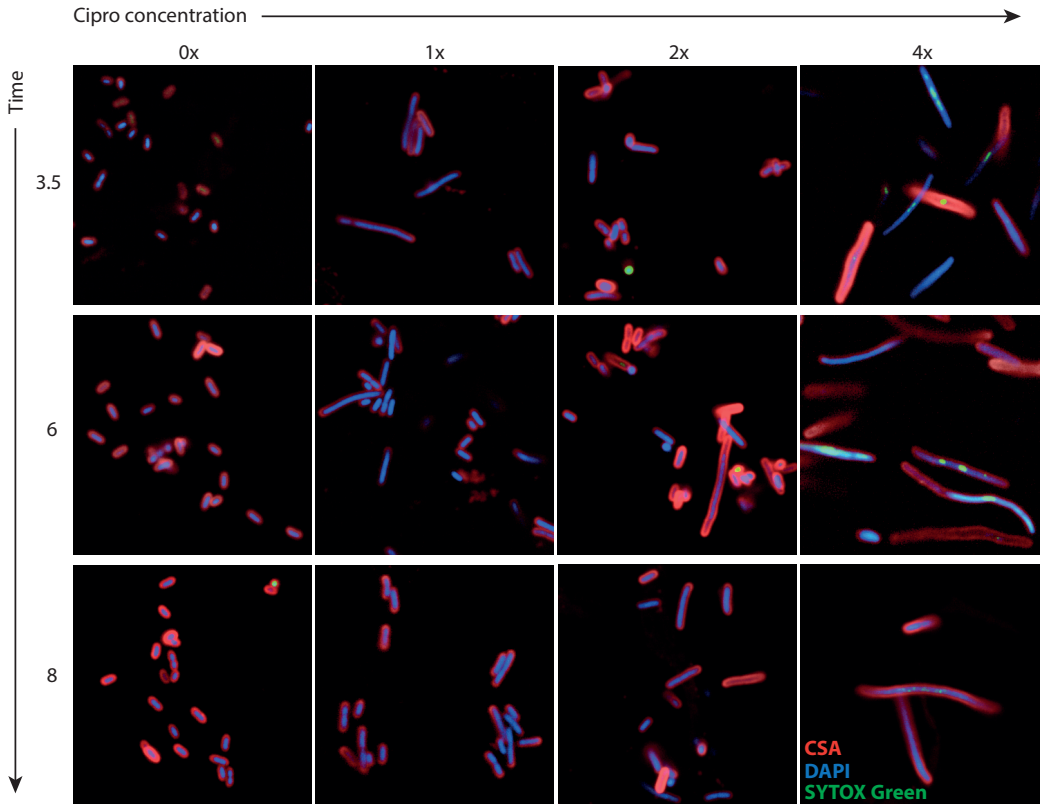

Figure 4.7 Confocal microscopy of ciprofloxacin sustainability after 24 h. *S.* Typhimurium D23580 was inoculated in previously used media containing 0x, 1x, 2x, or 4x MIC ciprofloxacin and imaged at 3.5, 6, and 8 h post-inoculation using an Opera Phenix with a 63x objective. Bacteria were stained with CSA-Alexa-647 (bacterial membrane, red), DAPI (nucleic acids, blue), and SYTOX Green (dead cells, green). Images from one replicate.

and reinoculated this filtered media with *S.* Typhimurium D23580 and imaged growth in these reinoculated samples using the Opera Phenix. Images were captured at 3.5, 6, and 8 h post-inoculation to have enough bacteria for imaging (**Figure 4.7**). *Salmonella* bacteria grown in the spent medium behaved similarly to those grown in fresh medium, concurring

with our observations in the *S.* Typhimurium D23580 TKC using spent medium (**Figure 4.4 A**).

An image analysis pipeline was developed using the Perkin Elmer Harmony software associated with the Opera Phenix system to capture various morphological parameters associated with single *S.* Typhimurium, as previously described in Chapter 3. As a first step, the pipeline used as input the images taken over 24 h of *S.* Typhimurium treated with different concentrations of ciprofloxacin. Initially the images in each well were analysed to determine numbers of bacteria over the 24 h in the four treatment conditions, and across three biological replicates. We found that while there were some outliers at certain time points, there were relatively consistent numbers of *S.* Typhimurium bacteria identified by the software at each imaging time point and across treatments (**Figure 4.8**). The number of *S.* Typhimurium D23580 single bacteria per well across all time points and treatments from three replicates averaged 1173 (sd $\pm$ 1985). The number of *S.* Typhimurium VNS20081 single bacteria per well across all time points and treatments from three replicates averaged 1640 (sd $\pm$ 1913). It was not surprising to see this level of variability across three biological replicates and all time points and treatments.

After determining bacterial numbers across replicates and between time points and treatments, we analysed the change in bacterial length over 24 h (**Figure 4.9**). Consistent with the images (**Figure 4.6**), we determined an initial overall increase in average length of the bacteria treated with ciprofloxacin but then a reduction in average length over time. The higher the ciprofloxacin concentration, the longer it took for the average bacterial length to reduce. Despite the trend that the average length of treated bacteria diminished over time to levels more similar to the non-treated (0x) bacteria, there was a significant difference ($p < 0.05$) in bacterial length between treated and non-treated *S.* Typhimurium D23580 at 24 h, with the exception of 1x and 2x MIC-treated D23580 bacteria. For *S.* Typhimurium VNS20081, there was also a significant difference ($p < 0.05$) in length between all except the 1x and 2x MIC-treated bacteria at 24 h. Given that the most determined variability occurred in the 4x MIC treatment, we further scrutinized this population by comparing differences between the three replicates over 24 h (**Figure 4.9 B, D**). We found that in *S.* Typhimurium D23580, there was significant variance in average length between replicates, especially from 16 h onwards. This mirrored the stochastic behaviour observed in the 24 h TKC (**Figure 4.3 C, D**). In contrast, *S.* Typhimurium VNS20081 4x MIC replicates, while heterogeneous, did not display the same degree of differences at later time points. Based on the growth imaging

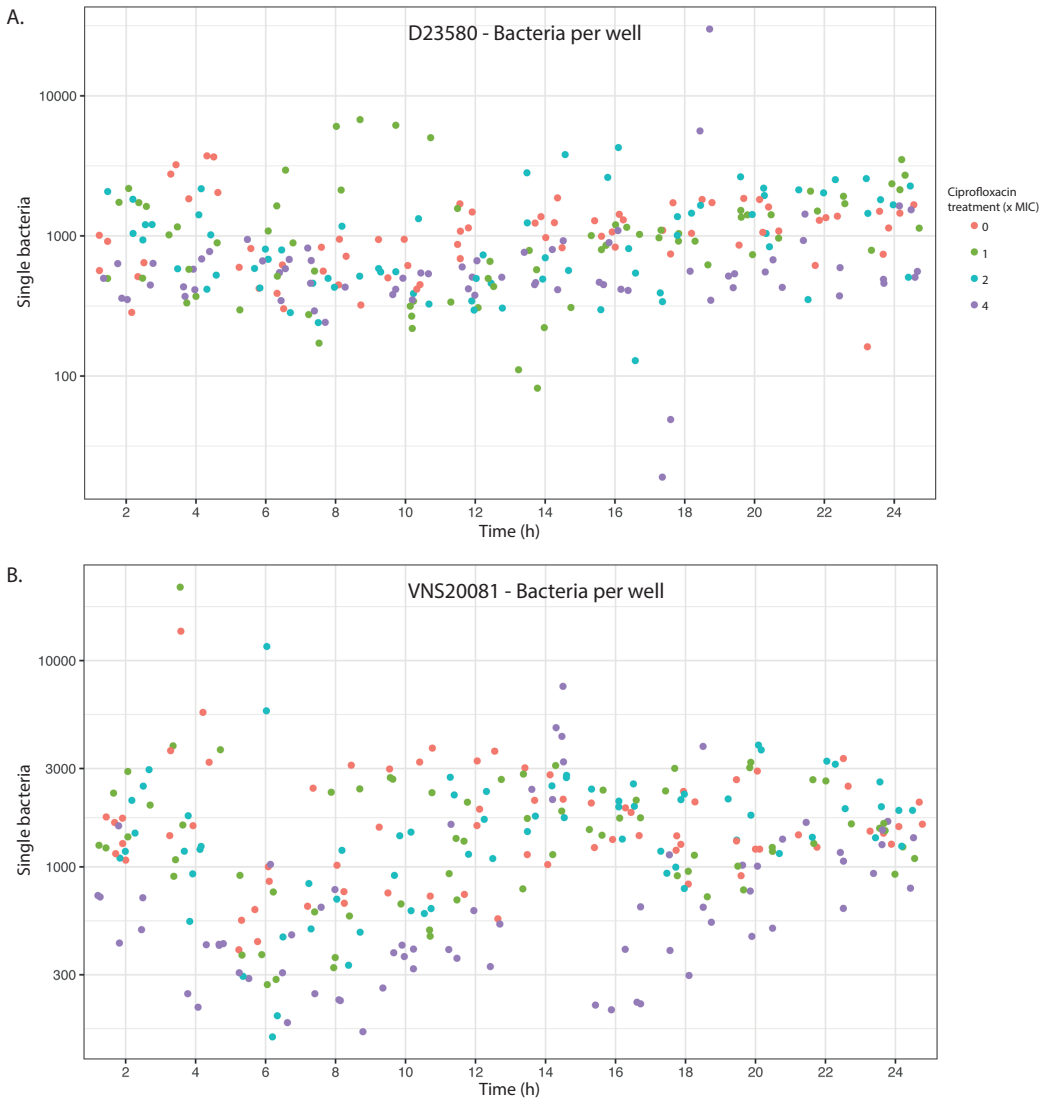

Figure 4.8 Single bacteria per well over 24 h of ciprofloxacin exposure. Numbers of single *S.* Typhimurium D23580 (**A**) and *S.* Typhimurium VNS20081 (**B**) per well over 24 h were plotted for three replicate experiments with bacteria exposed to 0x, 1x, 2x, or 4x ciprofloxacin MIC. Each point represents the number of single bacteria per well (two replicate wells per time point and condition, 6 wells total per time point across three replicates).

analysis, it appeared that the two *S.* Typhimurium isolates investigated were able to adapt to high levels of ciprofloxacin exposure and that there may be resistant subpopulations driving this phenotype. However, the two isolates had slightly differing responses, which may be explained by their genetic backgrounds.

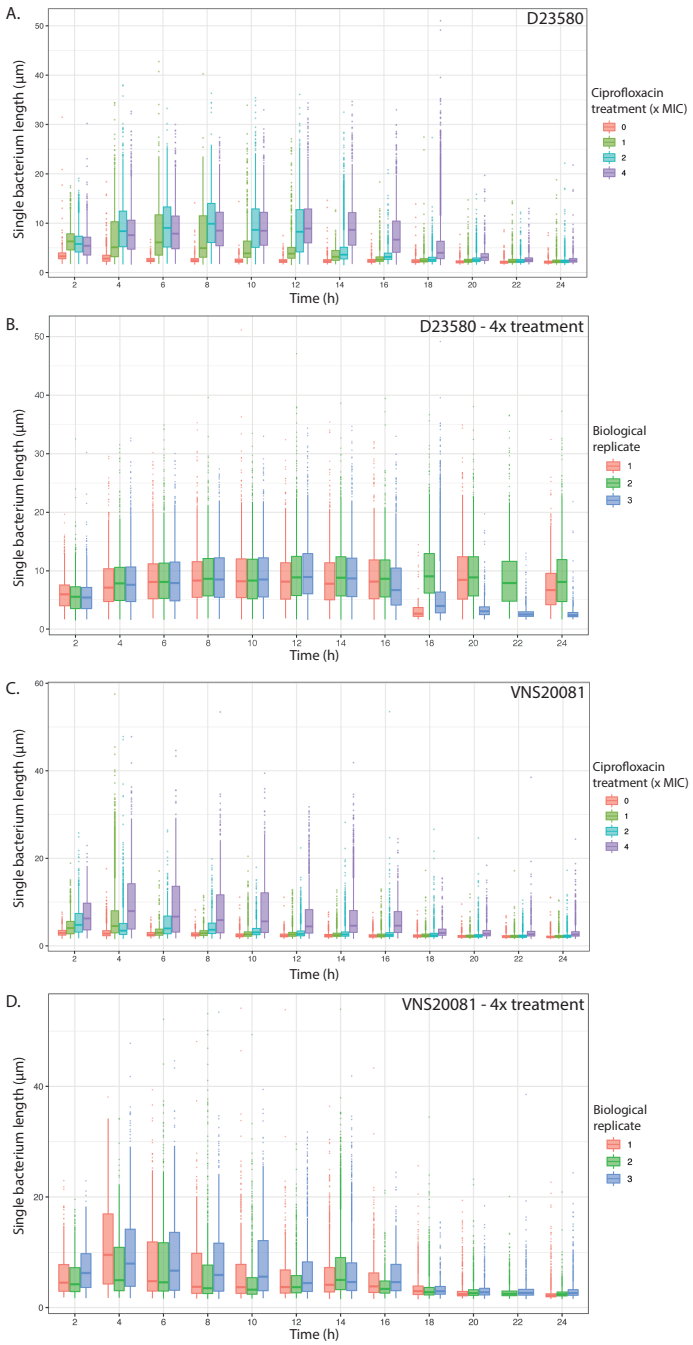

Figure 4.9 *S.* Typhimurium bacterial length over 24 h in total single cell and 4x MIC treated population. *S.* Typhimurium D23580 (**A, B**) and *S.* Typhimurium VNS20081 (**C, D**) were imaged over 24 h and single bacterium data was analysed. Comparison of all four treatments (0x, 1x, 2x, 4x ciprofloxacin MIC) was plotted from one representative experiment (**A, C**), and a comparison of the 4x MIC treatment across 24 h was plotted from the three replicates (**B, D**). A one-way ANOVA was used to compare treatments at 24 h, and Tukey's HSD method was used to compare individual treatment means. All experiments, with the exception of the *S.* Typhimurium D23580 22 h time point, were performed in triplicate.

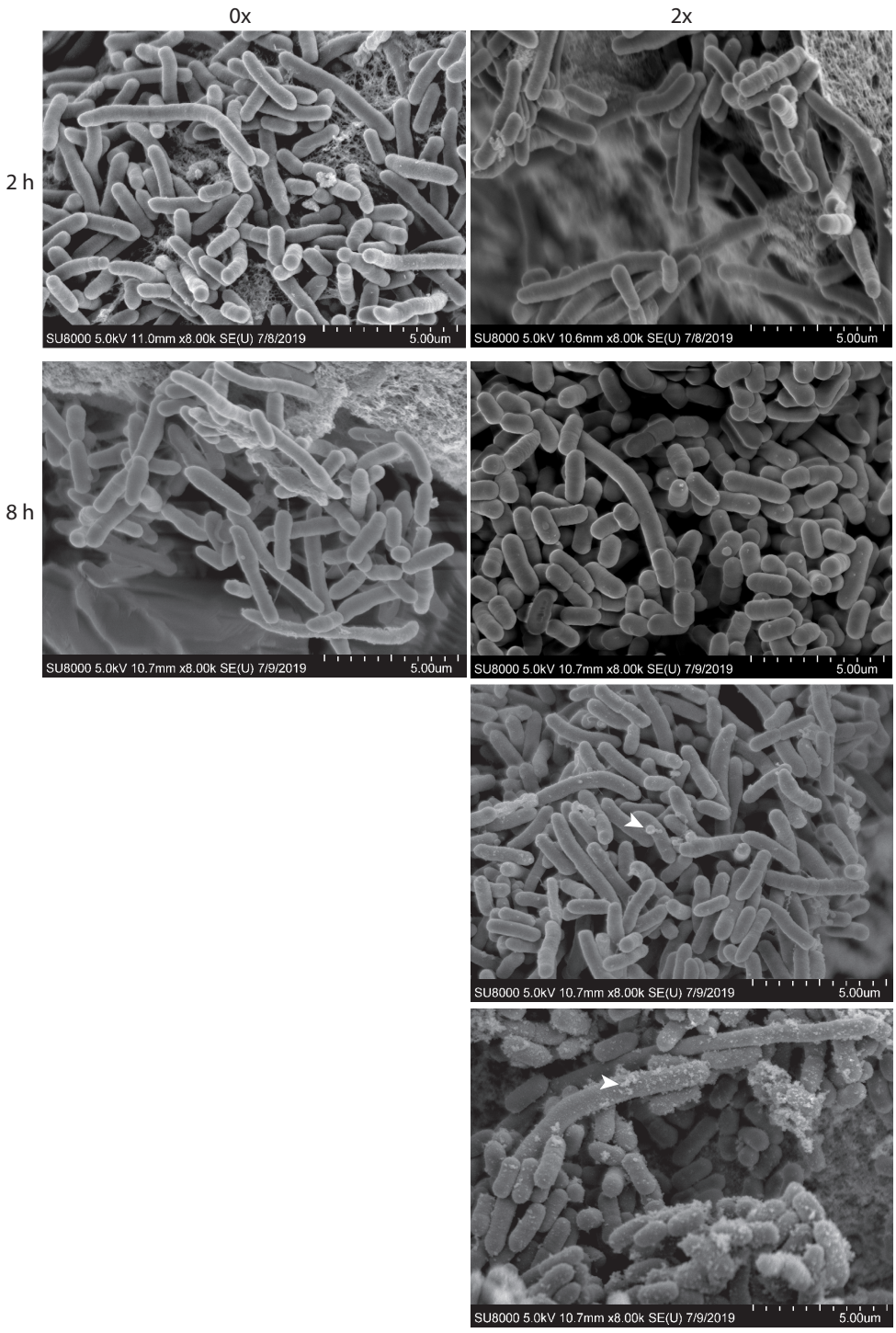

Figure 4.10 Scanning electron microscopy of *S.* Typhimurium D23580 at 2 and 8 h, 0x or 2x ciprofloxacin MIC exposure. SEM was conducted on *S.* Typhimurium D23580 at two time points (2 and 8 h) post-treatment with 0x or 2x ciprofloxacin MIC. White arrows indicate blebbing or shedding from ciprofloxacin-treated bacteria after 8 h.

To explore other options for imaging variation within the bacterial populations, we next performed scanning electron microscopy on *S.* Typhimurium D23580 bacterial colonies at 2 and 8 h post-exposure to 2x ciprofloxacin MIC and compared to non-treated bacteria (**Figure 4.10**). We had previously noted that after growth of *S.* Typhimurium ST313 isolates under biofilm-forming conditions, we could visualise sectored colonies, indicating some sort of population variation in these isolates[176]. Moreover, transcriptomic studies have shown an involvement of outer membrane proteins of the *omp* family in ciprofloxacin resistance[441]. Interestingly, but in concordance with our prior image analysis, we found considerable variability in length of both the ciprofloxacin-treated and non-treated *S.* Typhimurium D23580 bacteria. At 2 h post-treatment, it was difficult to distinguish between the treated and non-treated bacterial populations. However, at 8 h, from the images, there appeared to be multiple phenotypes associated with ciprofloxacin treatment. In the 2x MIC-treated population, there were some *S.* Typhimurium D23580 bacteria with no obvious difference (8 h top panels) from similar non-treated cells, while on some treated bacteria we could visualise small blebs (white arrow), and yet others appeared to be shedding materials from the bacterial cell surface (white arrow). A similar phenotype has been previously documented in other organisms[442–444]. Thus, the SEM analysis indicated that some individual bacteria were undergoing morphological changes after exposure to ciprofloxacin, but there did not appear to be a uniform response.

4.5 Generation of spontaneous *gyrA* mutations in D23580 and SL1344

To further explore the response of *S.* Typhimurium to ciprofloxacin, we generated spontaneous *gyrA* mutants in the ciprofloxacin sensitive isolates SL1344 and D23580. The rationale for doing this was to determine how the acquisition of a SNP in *gyrA* would influence phenotypic responses to ciprofloxacin. Spontaneous *gyrA* mutants were selected by growing *S.* Typhimurium SL1344 and D23580 on agar plates containing increasing concentrations of nalidixic acid, a first-generation fluoroquinolone. It was necessary to first grow *S.* Typhimurium SL1344 and D23580 on nalidixic acid plates because the rate of selection of spontaneous single-step resistant mutants is considerably higher on nalidixic acid than on ciprofloxacin for ciprofloxacin-sensitive bacteria[445]. Any colonies that grew were maintained

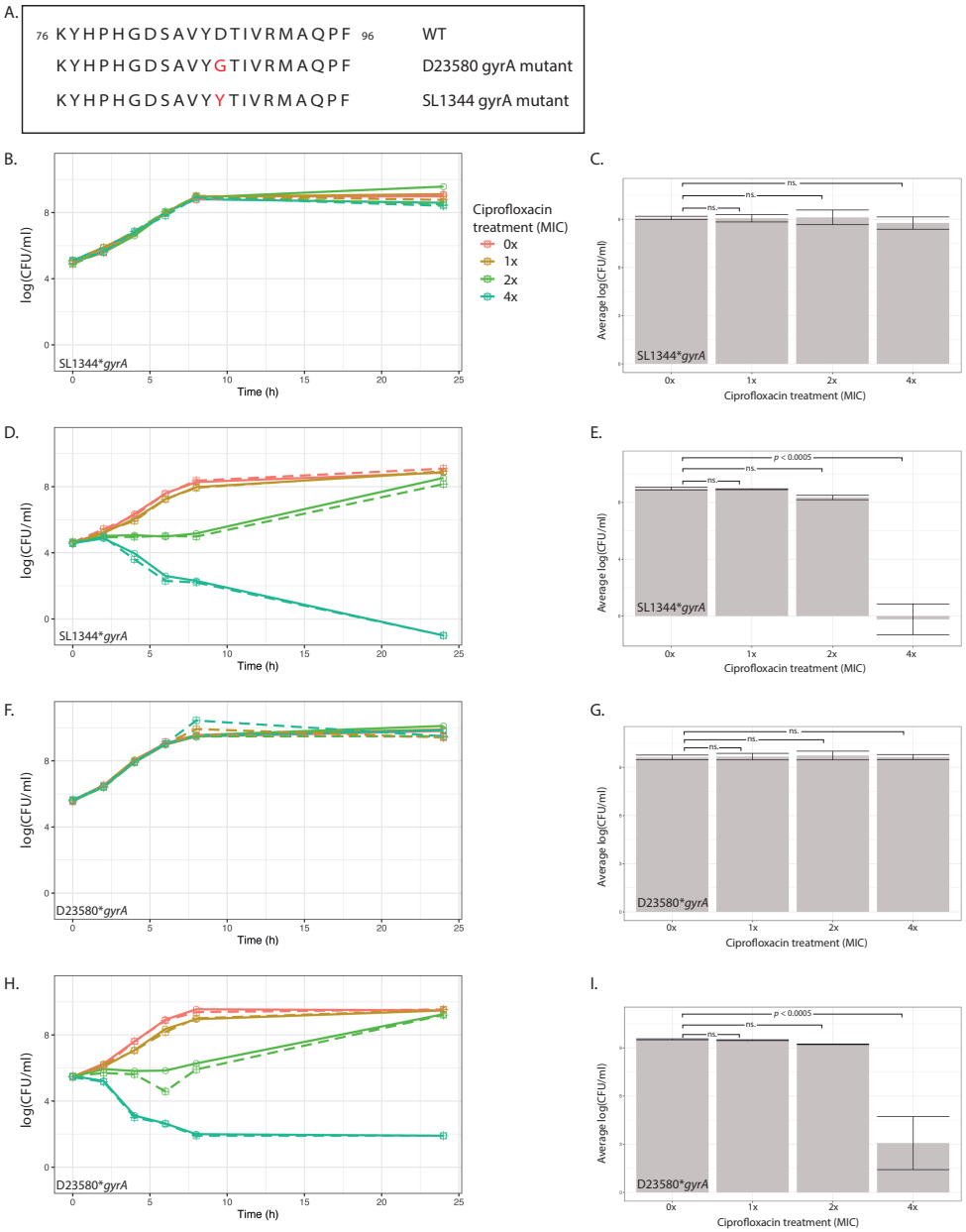

Figure 4.11 Characterization of *S.* Typhimurium SL1344 and D23580 spontaneous *gyrA* mutants. Spontaneous *gyrA* mutations were made in *S.* Typhimurium SL1344 and D23580, and mutations were verified by Sanger sequencing, showing amino acid changes in GyrA at amino acid position 87 (**A**). TKC were performed for SL1344**gyrA* and D23580**gyrA* at the WT concentration (**B, D**, respectively) and new concentration (**C, E**, respectively). A one-way ANOVA was used to compare treatments at 24 h, and Tukey's Honest Significant Difference (HSD) method was used to compare individual treatment means. All experiments were performed in triplicate (dashed, dotted, and solid lines).

over multiple passages on nalidixic acid and then transferred to ciprofloxacin plates and passaged serially. To verify that any selected mutants did contain a SNP within *gyrA*, a portion of *gyrA* was PCR-amplified, and Sanger DNA sequencing was performed.

Sequences of *gyrA* regions determined from different candidate nalidixic acid resistant derivatives were analysed using the Basic Local Alignment Search Tool (BLAST), and this analysis identified an *S.* Typhimurium D23580 spontaneous mutant (D23580**gyrA*) with a non-synonymous mutation at amino acid position 87 changing D to G (D87G)[446]. Additionally, we identified a SL1344**gyrA* derivative, which had a mutation within *gyrA* at position 87, changing D to Y (**Figure 4.11 A**). A brief search in BLAST revealed that these mutations have previously been documented in other *Salmonella* isolates. The MIC of the mutants was assessed, and we found that D23580**gyrA* had an MIC to ciprofloxacin of 0.5 μg/ml, increased from 0.03 μg/ml, and SL1344**gyrA* had a new MIC of 1.0 μg/ml, increased from 0.015 μg/ml. To determine whether these SNPs altered growth dynamics with or without ciprofloxacin treatment, TKC were performed with the *S.* Typhimurium *gyrA* mutants at the wild-type (WT) MIC and new MIC. We found that neither SL1344 nor D23580 treated at WT MIC levels showed differences in growth between the four concentrations of ciprofloxacin exposure ($p > 0.05$) (**Figure 4.11 B and D**, respectively). In contrast, there was a stratified response when the *gyrA* mutant derivatives were exposed to ciprofloxacin levels at and above the new MIC (**Figure 4.11 C and E**). This implied that a mutation in *gyrA* within the quinolone resistance determining region of *S.* Typhimurium has a direct and measurable effect on the MIC, and a significantly higher concentration of ciprofloxacin is required to inhibit growth of the *gyrA* mutant derivatives.

4.6 Investigation of SNPs involved in desensitization to ciprofloxacin

To further understand the changes in bacterial growth over 24 h exposure to ciprofloxacin, we performed whole genome sequencing of *S.* Typhimurium D23580 WT bacteria grown at 0x, 1x, 2x, or 4x ciprofloxacin MIC. Bacteria were collected in three separate ways in three replicates to capture the potential population heterogeneity, and DNA was sequenced (see section 2.4 and **Appendix A**). The three methods of bacterial collection were the 24 h liquid

cultures, single colonies grown on agar plates from the 24 h cultures, and a plate sweep of bacterial spread on agar plates from the 24 h cultures. After whole genome sequencing, we performed a SNP analysis to identify any SNPs arising from ciprofloxacin exposure. SNPs were analysed using bcftools, and the majority base call was set as presence in a minimum of 75% of the reads mapping at a given base. While we appreciate that this was a stringent cut-off and may have been overly strict, this threshold allowed us to examine only dominant SNPs that were found in a clear majority of sequenced reads.

We did not find any SNPs in the non-treated *S.* Typhimurium bacteria, suggesting that spontaneous mutations do not arise when there is no selective pressure. Curiously, there were also no mutations in the bacteria treated at 4x ciprofloxacin MIC. We hypothesized that this may be due to the very low level of growth in the 4x ciprofloxacin MIC-treated cultures across the three replicates. This possibly indicates that 4x ciprofloxacin MIC for *S.* Typhimurium D23580 may be a bacteriostatic concentration of ciprofloxacin that is too low to kill all bacteria but sufficiently high to prevent the formation of viable mutants. In contrast, we observed three SNPs that arose in some of the replicates of the 1x and 2x ciprofloxacin MIC treatments.

Interestingly, there was variation in the occurrence of SNPs between replicates and growth methods. Given the small sample size of three replicates, it was not possible to extrapolate broadly from this experiment how much variation there is within the whole population. However, it was interesting that the SNPs differed between replicates, which suggests that *S.* Typhimurium D23580 bacteria do not have a fixed response to a given concentration of ciprofloxacin, Furthermore, there were some variations between the individual colonies that were selected. This suggests that there might be some degree of genetic heterogeneity within the population that survives ciprofloxacin exposure for 24 h.

There were three SNPs that arose. The first was a SNP in *gyrA*, which we only observed in one replicate of the 2x ciprofloxacin MIC -treated bacteria. Interestingly, upon comparison of the turbidity of the 24 h cultures, we observed that the replicate with a *gyrA* mutation was the only 2x MIC culture that grew to high density on par with the non-treated cultures (**Figure 4.12**). The SNP in *gyrA* conferred an amino acid substitution at position 83 from serine to tyrosine (S83Y), a common GyrA substitution found in *S.* Typhimurium clinical isolates[176,190,447]. In contrast, neither of the low growth 2x MIC treated culture replicates had SNPs in *gyrA*. One replicate, however, did have a SNP in *hydA* (hypF), which partially

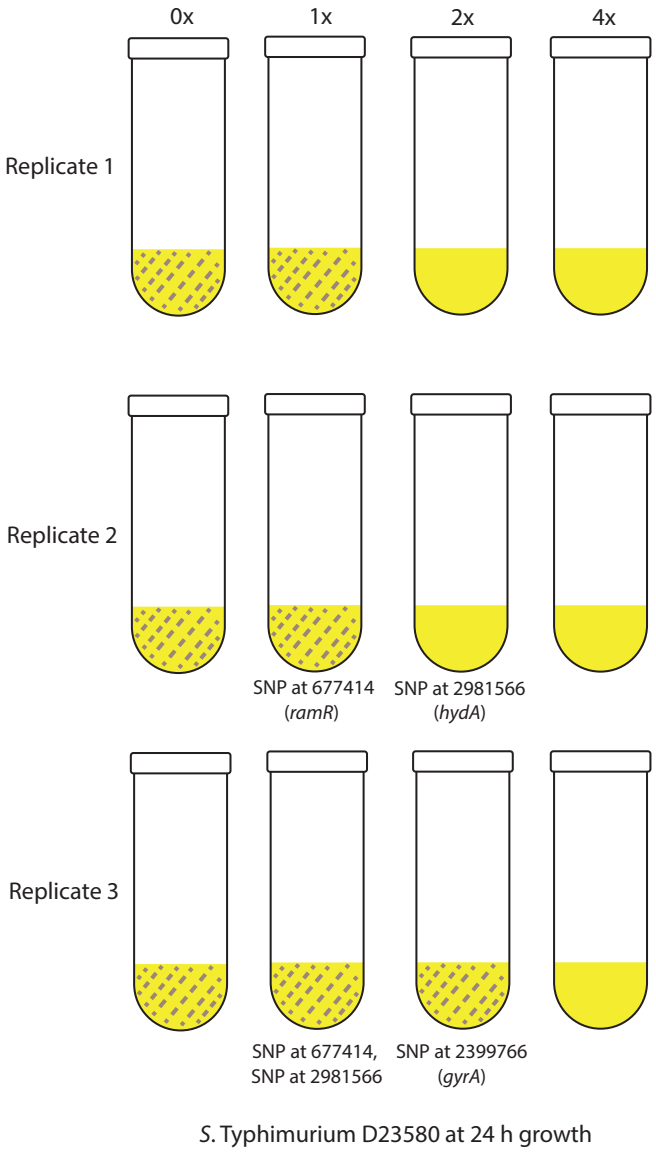

Figure 4.12 SNP analysis of *S.* Typhimurium D23580 bacteria grown for 24 h in culture medium containing ciprofloxacin. *S.* Typhimurium D23580 bacteria were grown for 24 h in 4 different concentrations of ciprofloxacin: 0x, 1x, 2x, or 4x MIC. SNPs only found in the 1x and 2x MIC-treated bacteria. All 1x MIC-treated cultures were noted to be turbid, but only one 2x MIC-treated culture was turbid (Replicate 3) and had a SNP in *gyrA*.

encodes [NiFe]-hydrogenase Hyd-5, an enzyme involved in the process of H_2 oxidation[448]. The subunits comprising Hyd-5 contain a transmembrane domain[449]. Interestingly, this same SNP was observed in one of the 1x ciprofloxacin MIC-treated replicates.

Across the three 1x ciprofloxacin MIC-treated cultures, we observed consistently high turbidity at the end of 24 h growth, suggesting that growth was not impeded by the ciprofloxacin concentration (**Figure 4.12**). Interestingly, the SNPs found differed between the replicates. In the first replicate, there were no SNPs, while in Replicate 2, there was a SNP within *ramR*, a *tetR*-like repressor of *ramA*[450,451]. The inactivation of *ramR* has been shown to confer MDR in *S.* Typhimurium through enhanced activity of the AcrAB efflux pump (Abouzeed, Baucheron, 2008). The same SNP was also found in the third replicate of 1x ciprofloxacin MIC-treated bacteria, although that population also had a SNP in *hydA*. It is possible that the introduction of a SNP in *ramR* sufficiently increases the efflux of ciprofloxacin to help bacterial survival at a 1x MIC dosage without the requirement for changes in *gyrA*. Although this experiment was small, we were surprised by the consistency of the SNPs found between biological replicates, suggesting that these SNPs may play a role in modulating survival during ciprofloxacin exposure. Further analysis of these SNP data to test with altered thresholds for base calling, assessment of SNP heterozygosity within the population, and a greater number of replicates would help clarify these findings.

4.7 Discussion

In this chapter, we explored the phenotypic response of four clinical *S.* Typhimurium isolates to perturbation by ciprofloxacin at and above their MIC *in vitro*. While some degree of phenotypic characterization has been performed previously on ciprofloxacin-treated *S.* Typhimurium, we used a combination of TKC, microscopy, and SNP analysis to provide a more comprehensive analysis of what may be occurring[427–429]. We demonstrated here that while there are measurable differences in the ciprofloxacin response of isolates with different MICs, they all exhibited a similar trend of an initial kill phase followed by recovery despite the continued presence of active ciprofloxacin. Importantly, the degree and consistency of this trend differed between isolates, and it appeared that sensitive isolates may not respond as uniformly to above MIC ciprofloxacin concentrations. This may be because they are very sensitive to the antimicrobial and even small amounts cause major changes in the early behaviour and response of individual bacteria. The presence of ciprofloxacin resistance determinants in *S.* Typhimurium VNS20081 and 5390_4 may contribute to their more uniform response to this antimicrobial. We confirmed that the observed rebounding growth characteristics were not due to the degradation of ciprofloxacin, meaning that the

bacteria are able to not only survive but grow in sustained and consistent concentrations of ciprofloxacin.

A study by Pribis *et al.* evaluated *S.* Typhimurium at sub-inhibitory concentrations of ciprofloxacin and found that small subpopulations of bacteria treated with ciprofloxacin had higher reactive oxygen species (ROS) activity, and the larger subpopulation with higher SOS response contributed to a bet-hedging strategy that increased bacterial survival[331]. This may well be a strategy employed by *S.* Typhimurium as well, and future work may help elucidate the role of ROS and the SOS response in our observed phenotype. Pribis *et al.* also assert that the elongated cells found in ciprofloxacin-treated cultures bud into smaller resistant daughter cells. However, our microscopy and image analysis showed that under any treatment, there is a diversity of bacterial lengths. This suggests that there is an underlying population of shorter bacteria in ciprofloxacin-exposed cultures, and these may be driving the resistant phenotype. Work by Bos *et al.* on *E. coli* has shown that bacteria treated with ciprofloxacin at 0.125x MIC results in asymmetric cell division of filamentous bacteria resulting in the budding off of resistant clones. Interestingly, they did not observe this phenotype at $\geq$ 0.5x ciprofloxacin MIC, which they deemed a concentration of drug that severely impaired chromosomal integrity[433]. While we did not investigate chromosomal viability in our study, we did see surprising resilience of bacteria at $\geq$ 1x MIC concentrations and the development of filamentous and non-filamentous cells between 1x and 4x MIC ciprofloxacin exposure. It would be worthwhile to address chromosomal integrity and the cell fate of filamentous versus non-filamentous organisms in follow up studies.

Finally, our investigation of nonsynonymous SNPs after 24 hours of ciprofloxacin exposure revealed that *gyrA* is not the only gene that may undergo mutation and that there may variation in SNPs depending on chance and the level of ciprofloxacin exposure. Perhaps most importantly, we observed that the same genotypes did not arise over three biological replicates of the same growth conditions, suggesting that the emergence and fixation of these specific SNPs within the population is stochastic. Given the SNPs we observed, it would be worthwhile to repeat a large number of 24 h growth cycles with a range of ciprofloxacin concentrations and specifically assay for these mutations. This would better inform how often these mutations occur and how they relate to bacterial growth.

While we hypothesized that there might be other SNPs in addition to *gyrA* that occurred, it was surprising that there were only two others that occurred, and one of them, *hydA*, has not

previously been observed in the context of ciprofloxacin exposure. It was interesting that the same SNP in *ramR* arose twice, and this was the only drug efflux gene that had a mutation. Gravey *et al.* found that three clinical isolates of *Enterobacter hormaechei* with elevated MICs to ciprofloxacin and other antimicrobials had a 16 bp deletion in *ramR*, with enhanced expression of RamA, AcrA, AcrB, and TolC[452]. We did not search for large deletions within genes of potential interest, but this may be an important further step to probe for additional changes in the genome. Overall, our data suggest that exposure of *S.* Typhimurium to 1x ciprofloxacin MIC may induce SNP changes although not in *gyrA*. In combination with our phenotyping data, it appears that ciprofloxacin exposure at MIC and above-MIC dosages for 24 h effects obvious phenotypic and genotypic changes on *S.* Typhimurium. Further analysis of these genes independently and in concert with other experiments will be critical to understand the full extent of changes wrought on bacteria by ciprofloxacin.

5. Investigation of transcriptional response of *Salmonella* Typhimurium under ciprofloxacin exposure

Data

Data files are located in the folder here: ch5_RNA-seq_data_files.

5.1 Introduction

In the previous chapter, we characterized some of the phenotypic changes that occur when *S.* Typhimurium is exposed to ciprofloxacin over 24 hours. Additionally, we identified a set of nonsynonymous mutations that occur within 24 hours due to exposure. However, there are certainly additional factors at play, which could include a modified transcriptional response to ciprofloxacin soon after exposure. Others have previously shown the importance of the potentially adaptive transcriptional response to antimicrobials, and in particular to ciprofloxacin, in influencing survival. In this chapter, we have explored the transcriptional landscape of *S.* Typhimurium exposed to ciprofloxacin.

As ciprofloxacin and other fluoroquinolones target the DNA replication machinery, there are many widespread downstream effects that could occur. Li *et al.* studied drug-resistant *S.* Typhimurium strains *in vivo* in *Caenorhabditis elegans* and *in vitro*, finding differential transcription patterns between FQR and FQ-susceptible strains, particularly in genes associated with efflux pump expression, stress response, and drug resistance. These data showed some overlap with observations of multidrug efflux in other transcriptomic screens of drug-treated *S.* Typhimurium[366,332,333]. Whitehead *et al.* found that a single exposure of *S.* Typhimurium to working concentrations of a biocide for even a short period can select for multidrug resistant mutants and upregulation of efflux pumps[364]. Interestingly, a study using reverse transcriptase real-time PCR (RT-PCR) did not find any reproducible differences in the expression of the efflux pump genes *acrB*, *tolC*, *acrF*, or *emrB* between

nalidixic acid sensitive and resistant isolates of *S.* Typhimurium and *S.* Enteritidis, and the authors suggest that this observation may implicate other candidate efflux pumps or resistance mechanisms[453]. Hence, an RNA-sequencing strategy may have provided greater insight into the genes and pathways involved. In contrast, Chen *et al.* found higher efflux pump expression in nalidixic acid- and ciprofloxacin-resistant *S.* Typhimurium mutants than in susceptible equivalents, and they further found that the introduction of null deletion mutations into *acrAB*, *acrEF*, or *mdtABC* (a multidrug transporter), amongst others, resulted in greater ciprofloxacin susceptibility[454]. However, some of this work was performed in isolates containing multiple topoisomerase mutations, a somewhat uncommon genotype in human clinical *S.* Typhimurium isolates. Thus, it is difficult to ascertain how relevant the mutations and efflux mechanisms Chen *et al.* found are in human isolates with lower innate levels of resistance. Other work, highlighted previously, has shown the importance of prophages in the induction of the generalized bacterial stress response, and some phages are highly sensitive to exposure to ciprofloxacin[325,337–340].

While some progress has been made to understand the transcriptional profiles of *S.* Typhimurium upon ciprofloxacin exposure, there remains a lack of clarity as to epigenetic and potentially transient factors that may occur. There is also insufficient information on the transcriptional response in recent clinical isolates. In this study, we wanted to compare the response of the four *S.* Typhimurium isolates studied in the previous chapter to identify transcriptional differences and commonalities when treated with 2x MICs of ciprofloxacin. We subsequently characterized the reference ST313 isolate *S.* Typhimurium D23580 following exposure to a number of different insults to explore the specificity and diversity of the transcriptional response under stress. Finally, we investigated the transcriptional differences between populations of elongated and non-elongated D23580 to determine differential gene expression within a fractionated heterogeneous population. We hypothesized that, following treatment with different relative levels of ciprofloxacin, there would be both shared and distinct sets of genes up- and down-regulated between the four isolates. We further hypothesized that D23580 bacteria exposed to different classes of drugs would have distinct transcriptional responses. Finally, we anticipated that morphologically distinct bacterial sub-populations, which we had identified previously, could be physically segregated and that these segregated populations would display distinct transcriptional signatures.

5.2 Comparative transcriptomics of four *S.* Typhimurium isolates

Following the time kill curve findings in the previous chapter, we decided to investigate the transcriptional patterns following ciprofloxacin exposure in order to determine whether these might be influencing the growth dynamics. Thus, we chose two discrete growth time points to evaluate how the bulk bacterial population responded transcriptionally early on and later during 2x MIC ciprofloxacin exposure. The two time points chosen were 2 h and 8 h post-exposure based on the time kill curve dynamics previously determined: 2 h was before significant death had occurred, and 8 h was during the "rebound" phase of growth. The *S.* Typhimurium isolates SL1344 (ST19), D23580 (ST313), 5390_4 (ST313), and VNS20081 (ST34) were grown under standard time kill curve conditions, RNA was isolated and then this was subjected to RNA-sequencing.

There were considerable differences in the transcriptome patterns observed between 2x ciprofloxacin MIC-treated and non-treated bacteria across all isolates (**Figure 5.1**). There were more than 100 significantly relatively upregulated genes at 2 h for all isolates with a $\log_2$ fold change (l2fc) of ≥ 2, a four-fold expression difference from the non-treated (NT) equivalents. In contrast, there was more variation in the number of significantly downregulated genes with an l2fc of $\leq$ -2, ranging from 16 genes for SL1344 to 216 genes for 5390_4. Interestingly, 5390_4 had the most differentially expressed genes with an l2fc of ≥ 2 of the four isolates, differing significantly even from D23580, a closely-related ST313 isolate (**Figure 5.1 B**).

To better understand the transcriptional landscape of each isolate, we visualized the l2fc of genes encoded within the chromosome of each isolate independently (**Figure 5.2**). This revealed patterns in the spatial organization of highly differentially expressed genes. Interestingly, for SL1344, D23580, and 5390_4, much of the first half of the chromosome contained down-regulated genes, although there were some striking differences between SL1344 and the ST313 isolates (**Figure 5.2 A-C**). In particular, the highly upregulated region in D23580 and 5390_4 near the beginning of the chromosome was comprised of primarily genes of prophage BTP1, a prophage unique to ST313 [160,455]. The other two large regions of high upregulation in D23580 and 5390_4 were also ST313 prophage-associated, and thus,

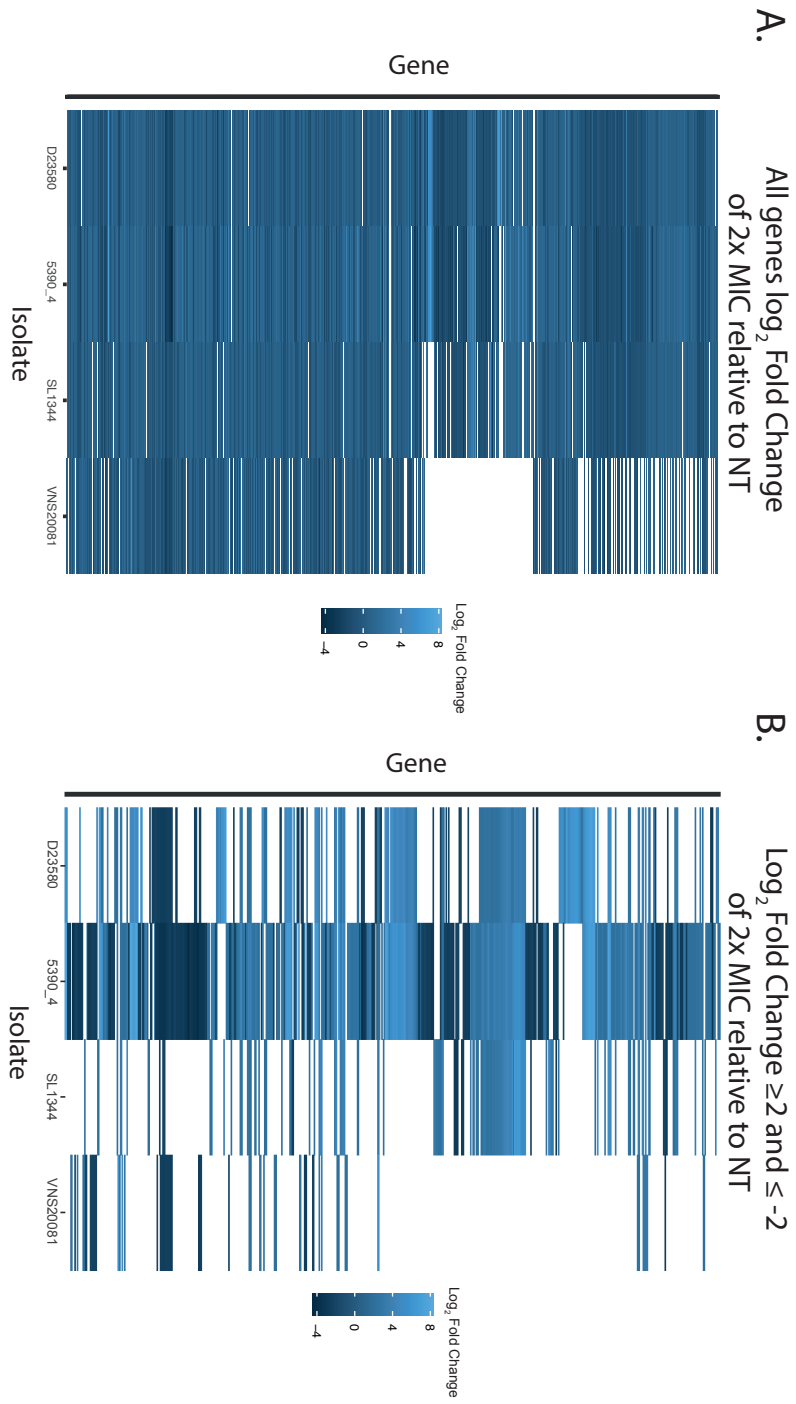

Figure 5.1 Heatmaps of differentially expressed genes upon 2 h of 2x ciprofloxacin MIC exposure. Columns of the x-axis represent the differential expression of each isolate, and each row in the y-axis represents a gene. **A.** All genes ($p < 0.05$) differentially expressed from NT across the four isolates at 2 h post-treatment. **B.** Genes ($p < 0.05$) with a $\log_2$ fold change of ≥ 2 or $\leq$ -2 across the four isolates at 2 h post-treatment. Gaps represent genes with p-value ≥ 0.05 or those without orthologues between the isolates.

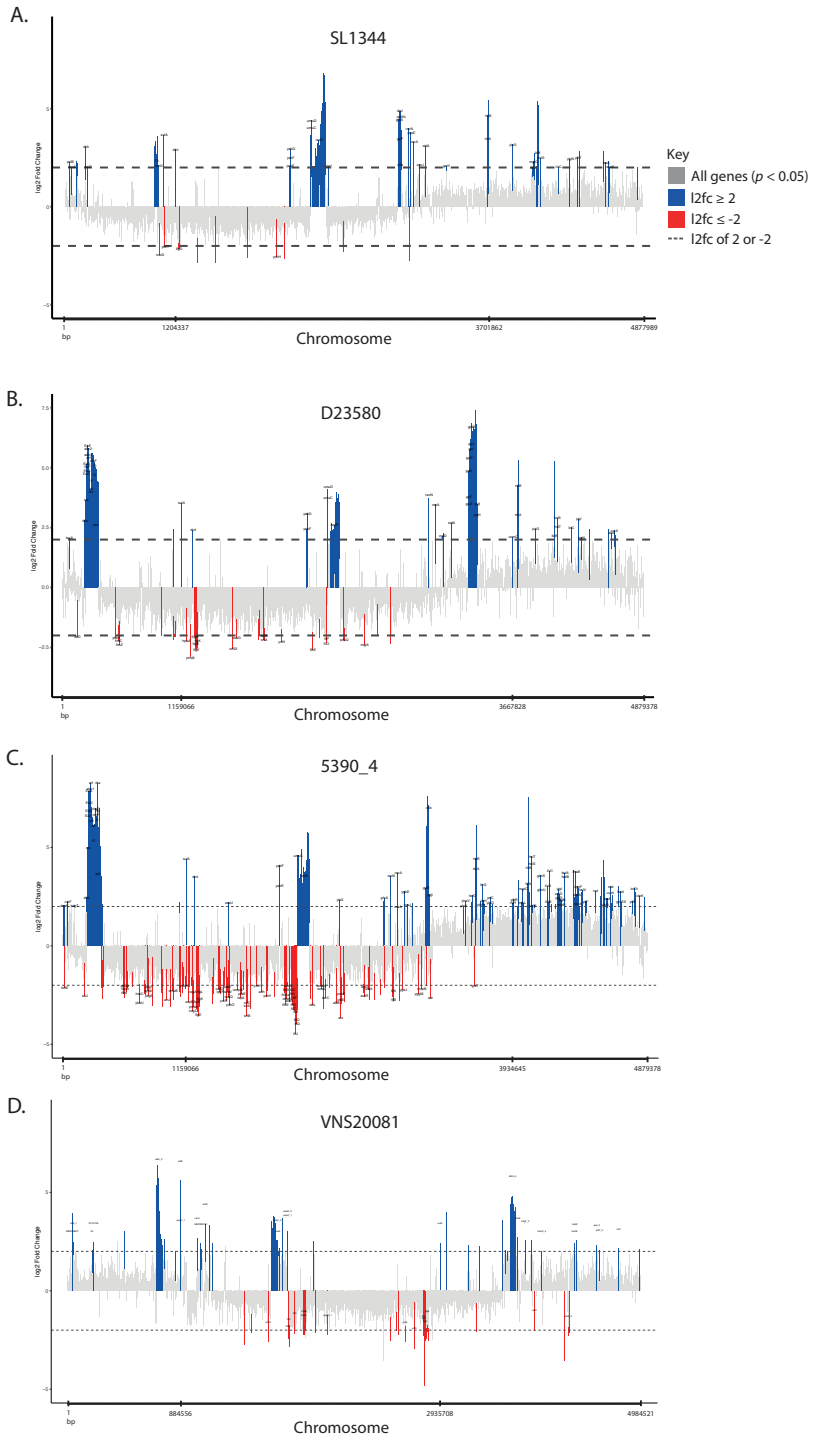

Figure 5.2 Chromosome maps of differentially expressed genes of the four isolates upon 2 h of 2x ciprofloxacin MIC exposure. All chromosomal genes ($p < 0.05$) are represented in grey, genes with an l2fc $\geq$ 2 are coloured in blue, and genes with an l2fc $\leq$ -2 are coloured in red. All known genes with an l2fc $\geq$ 2 or $\leq$ -2 are labelled.

upregulation of these region was lacking in SL1344 and VNS20081 (**Figure 5.2 A, D**). As revealed in the comparative heatmap (**Figure 5.1 B**), 5390_4 had a distinct expression profile compared to the other three isolates, and this was dispersed across much of the chromosome unlike in the other isolates.

We hypothesize that this observation may be influenced by the fact that 5390_4 contains a *qnrS* gene on the plasmid, conferring decreased ciprofloxacin susceptibility by a different mechanism in comparison to VNS20081, which contains a *gyrA* mutation (**Figure 5.2 C, D**). This difference may influence how and which genes respond to ciprofloxacin exposure. The significant difference in shape and differential expression of genes in *S.* Typhimurium VNS20081 may be accounted for by differences in chromosomal organization and its prophage repertoire, which has not been well documented. Further investigation to elucidate genomic differences between ST34 and ST313 would be warranted.

In all four isolates, we observed a large number of "unknown" genes that were highly upregulated. We investigated these further in D23580 using BLAST and Artemis to understand what they were and where they were located[446,456]. Most of the "unknown" genes were small intergenic regions, many of them within prophages BTP1 and BTP3 or upstream of prophage genes. However, there were also some "unknown" regions that spanned or overlapped with known regions of non-coding RNA. While we chose to focus our analyses on known chromosomal genes, it would be useful to explore these "unknown" genes in greater depth to better understand the role they play in potentially modulating prophage and other genes.

We were interested to further explore the differential expression of genes that have previously been implicated in the transcriptional response to ciprofloxacin. To that end, we compiled a list of genes associated with efflux, *rpoS* (an important factor in the SOS response), other genes implicated in the stress response, DNA damage and repair, and transporters[331,457–465]. We anticipated that we might detect more differential expression in regions of the chromosome containing these genes. As above, we mapped the differential expression of genes on the chromosome and highlighted our genes of interest (**Figure 5.3**). Surprisingly, we did not see as many genes with an l2fc $\geq$ 2 or $\leq$ -2 as expected; however, there were several transporters (designated in purple) with an l2fc $\geq$ 1 or $\leq$ -1. Given the role of transporters in drug efflux, we might have expected to see more relative upregulation of these genes, but this was not the case. This could be due to the selection of a 2 h timepoint.

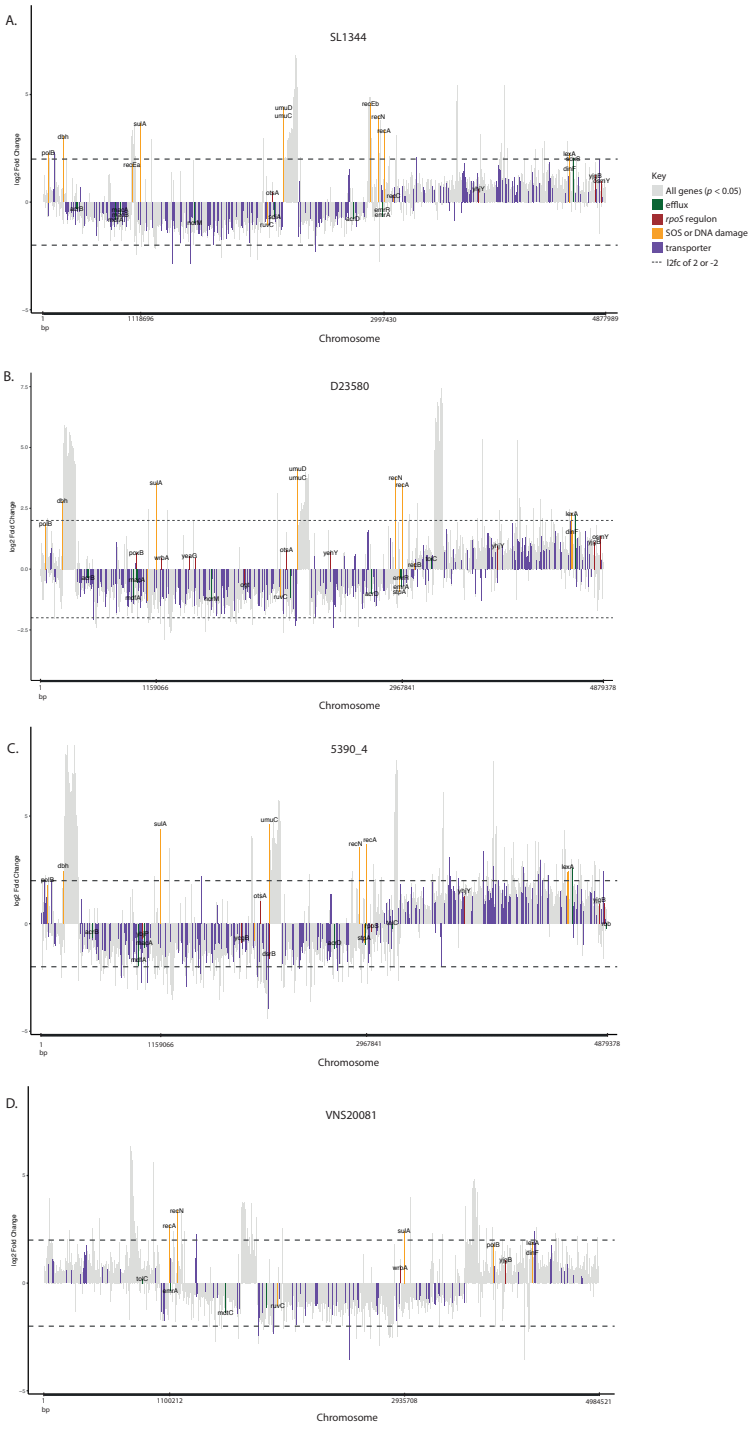

Figure 5.3 Chromosome maps of differentially expressed genes of the four *S.* Typhimurium isolates after 2 h of 2x ciprofloxacin MIC exposure. All chromosomal genes ($p < 0.05$) are represented in grey. Genes are coloured according to their involvement in pathways or functions of interest: efflux (green), *rpoS* (brown), SOS response or DNA damage (yellow), transport (purple).

We observed consistent relative upregulation with l2fc ≥ 2 in the four *S.* Typhimurium isolates under analysis for some key genes involved in the SOS response and DNA damage/repair (designated in yellow), particularly *sulA*, *recA*, *recN*, *umuC*, and *umuD*. This was unsurprising given the well-documented role these genes play in response to DNA damage and stress. For example, *recA*, which was upregulated in the treatment conditions across the four isolates, codes for the RecA protein, which activates the SOS response[466,467]. RecA works in tandem with the LexA protein, the gene (*lexA*), which was also relatively upregulated in all four isolates at 2 h and in all except *S.* Typhimurium VNS20081 at 8 h in our RNA-seq analysis[468]. A study by Thi *et al.* on the role of *recA* in the exposure of *E. coli* to sub-lethal concentrations of antimicrobials found that *recA* mutants are more susceptible to ciprofloxacin and have a much lower MIC as compared to wild-type equivalents[469]. Moreover, they found a requirement for *recA* in inducing a mutagenic phenotype in the presence of antimicrobials, which agrees with our finding that treatment of bacteria with ciprofloxacin would induce a change in *recA* transcription. *sulA* is also part of the SOS regulon and works in concert with *ftsZ* to inhibit cell division and filamentation[469–471]. In addition to these two genes, we found that other genes involved in the SOS pathway, including *recN*, *umuD*, and *umuC* were differentially expressed. *umuD* and *umuC* code for the proteins UmuD and UmuC, respectively, components of the γ-family polymerase DNA Pol V, which are active in DNA repair mechanisms, copying damaged DNA and functioning in the bacterial SOS-mediated pathway of translesion replication[472,473].

Given this function in responding to DNA breaks, potentially caused by ciprofloxacin treatment in our experimental conditions, it is perhaps not surprising that we found that *umuC* and *umuD* were upregulated in all our isolates. A transcriptomic study by Holman *et al.* also found *umuC* upregulated after treatment with the antimicrobials chlortetracycline and florfenicol[474]. The involvement of *umuC* and *umuD* in translesion synthesis makes them candidates for further study, as the mutations introduced through this process may further enhance bacterial survival in the presence of ciprofloxacin.

We subsequently analysed the transcriptional response across the four isolates at 8 h post-treatment with ciprofloxacin (**Figure 5.4**). At 8 h post-treatment, there was considerable upregulation and downregulation of a multitude of genes, and it was difficult to discern which ones were the most important in relation to ciprofloxacin exposure, as there were over 1000 upregulated genes. We once again looked at the chromosomal organization of the differential expression, which revealed widespread relative upregulation, and these did not seem to be

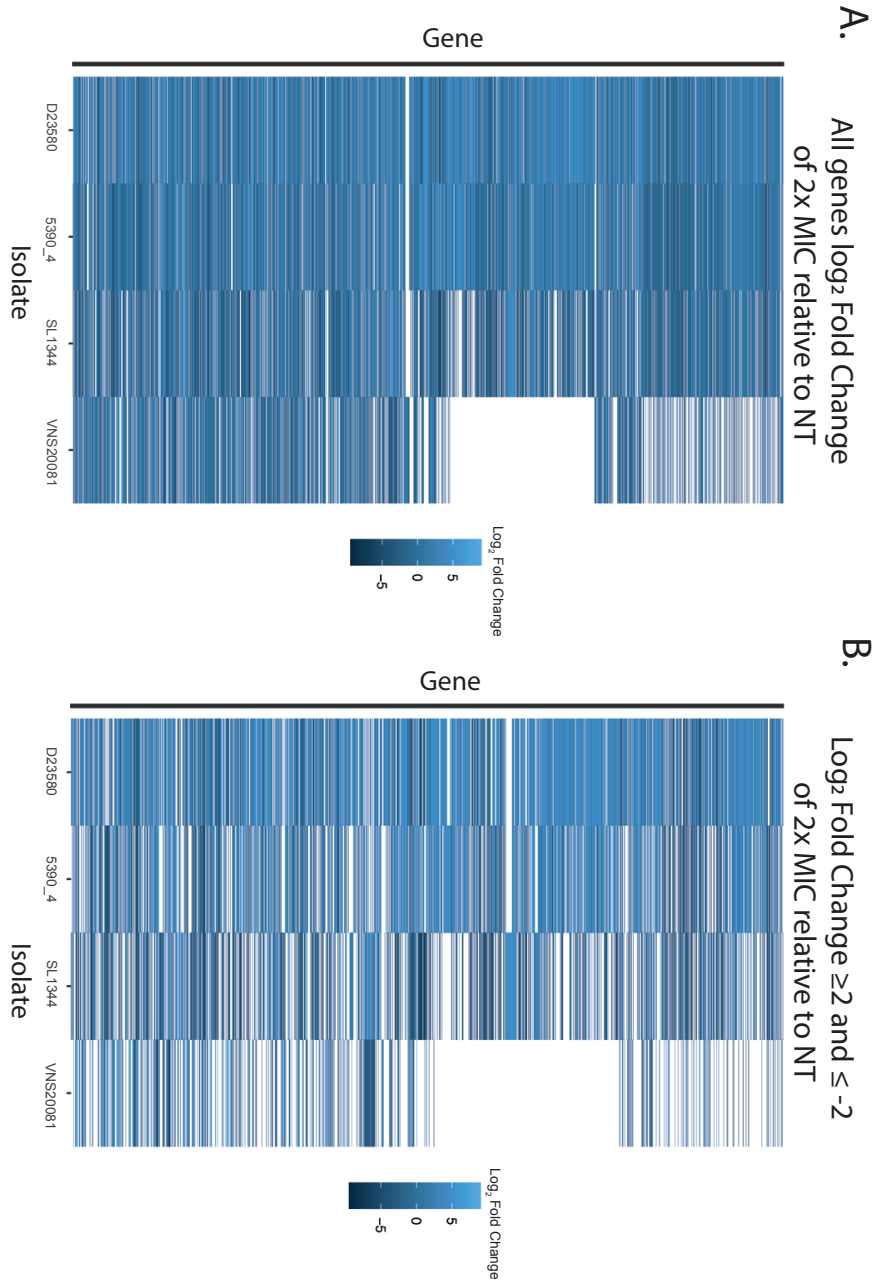

Figure 5.4 Heatmaps of differentially expressed genes upon 8 h of 2x ciprofloxacin MIC exposure. Columns represent the differential expression of each isolate, and each row represents a gene based on an annotated reference genome. **A.** All genes ($p < 0.05$) differentially expressed across the four isolates at 8 h post-treatment. **B.** Genes ($p < 0.05$) with a $\log_2$ fold change of ≥ 2 or $\leq$ -2 across the four isolates at 8 h post-treatment. Gaps represent genes with p-value ≥ 0.05 or not represented within the genome.

as organized into regions of the chromosome, as at 2 h post-treatment (**Figure 5.5**). There did seem to be a greater degree of differential expression in the transporters (denoted in purple), but this may have been due to the general greater degree of differential expression (**Figure 5.5 E-H**). Interestingly, *sulA* was less upregulated at 8 h than at 2 h across the four isolates, suggesting that the strong SOS response occurs earlier post-exposure. Additionally, there appeared to be several *rpoS* genes (denoted in brown) highly downregulated at 8 h that were not noticeable at 2 h, once again suggesting their involvement in the immediate stress response (**Figure 5.5 E-H**). It is possible that a stratified response across sub-populations that have formed by 8 h of ciprofloxacin-exposure may explain the degree of differential expression observed. This would correlate with the observation in the previous chapter of the diversity of bacterial length within a treated population; however, in this study, we focused on the response of the bulk culture.

To investigate whether any of the significantly upregulated genes strongly influenced growth dynamics under ciprofloxacin exposure, we made single-gene knockouts of five genes based on preliminary RNA-seq analysis of the four isolates and performed time kill curves on each of them. These genes were *ybiI*, *sulA*, *malK*, *cadA*, and *ddrA*. However, upon more rigorous analysis of these five genes, it was determined that only *sulA* was significantly differentially upregulated across the four isolates at 2 h, and thus only this was evaluated in greater detail. *S.* Typhimurium D23580Δ*sulA* had a ciprofloxacin MIC nearly identical to D23580 WT, and it did not appear to have altered growth dynamics (**Figure 5.6**). Validation by PCR indicated that D23580Δ*sulA* indeed lacked *sulA*. It is possible that there is some functional redundancy and therefore there was not a visible phenotypic difference between D23580Δ*sulA* and D23580 WT when grown in batch culture[475]. It is also possible that because *sulA* is involved in the bacterial SOS response, mutation of *sulA* might result in enhanced survival of some bacteria in the culture.

5.3 Investigation of specificity of D23580 transcriptional response to ciprofloxacin

Following the transcriptional analysis across four isolates, we wanted to determine whether the response we observed was ciprofloxacin-specific or a generalized response to stress. We

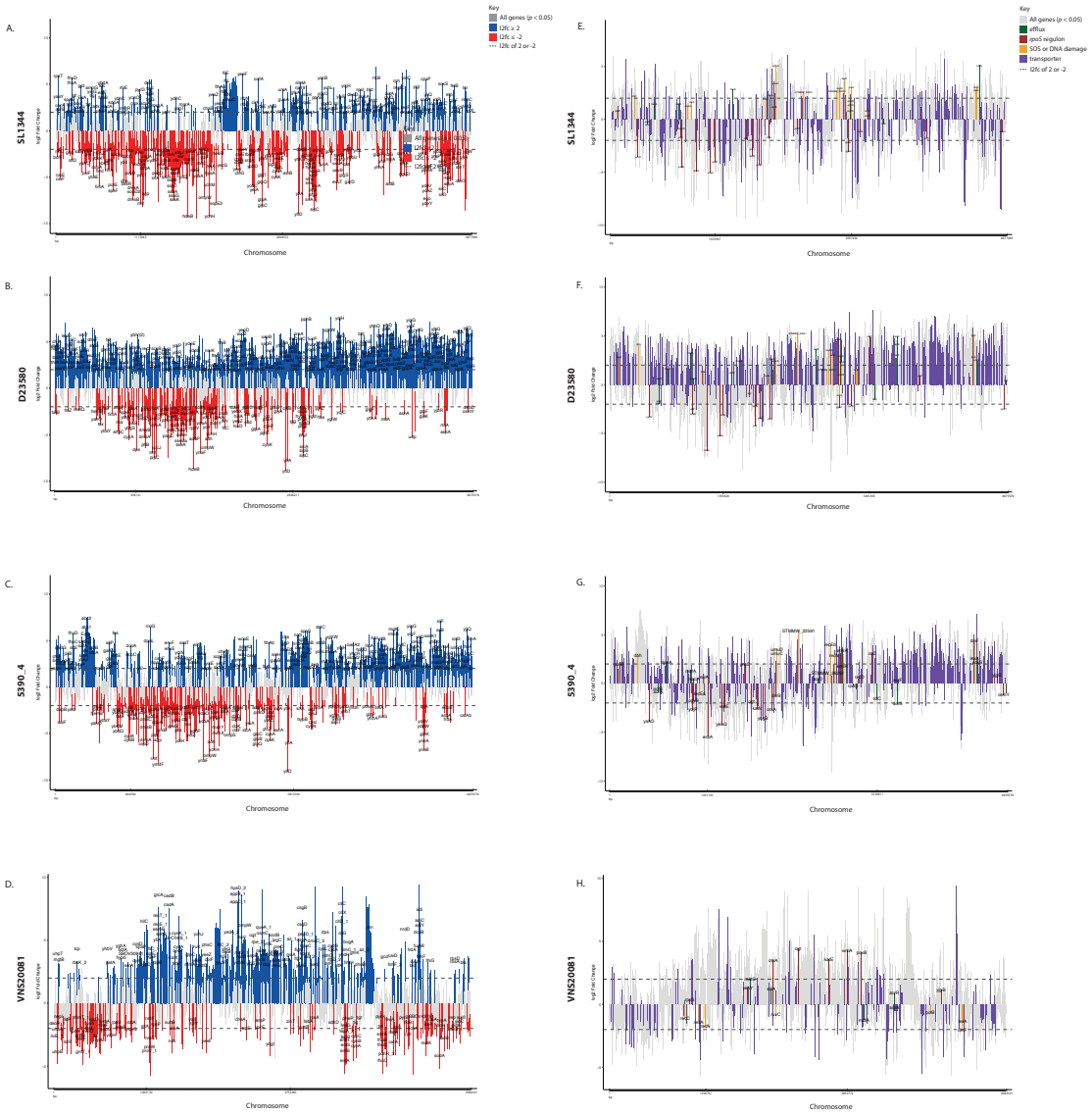

Figure 5.5 Chromosome maps of differentially expressed genes of the four *S.* Typhimurium isolates after 8 h of 2x ciprofloxacin MIC exposure. All chromosomal genes ($p < 0.05$) are represented in grey. **A-D.** Genes with an l2fc ≥ 2 are coloured in blue, and genes with an l2fc $\leq$ -2 are coloured in red. All known genes with an l2fc ≥ 2 or $\leq$ -2 are labelled. **E-H.** Genes are coloured according to their involvement in pathways or functions of interest: efflux (green), *rpoS* (brown), SOS response or DNA damage (yellow), transport (purple).

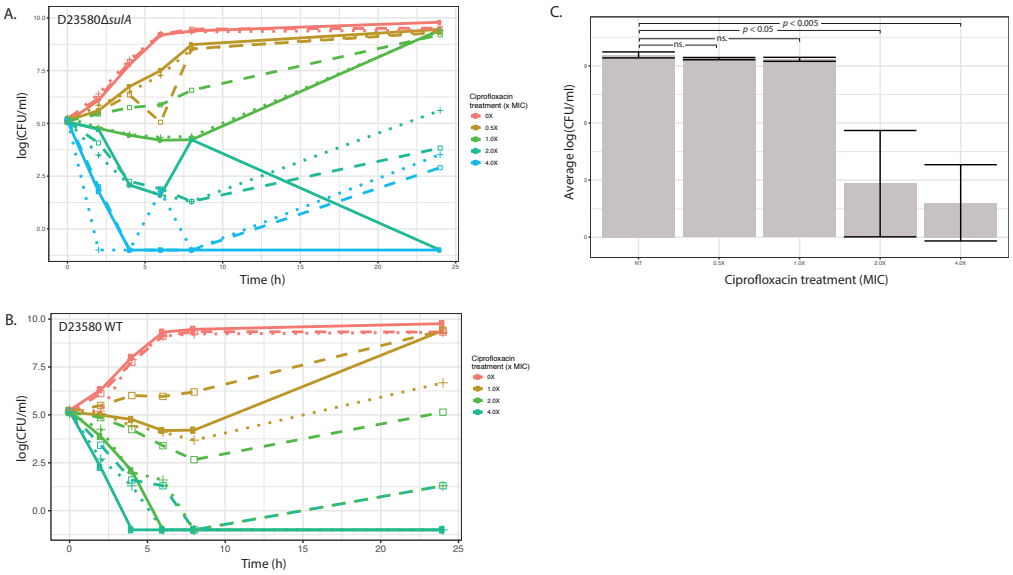

Figure 5.6 Time kill curves of D23580Δ*sulA* and D23580 WT. D23580Δ*sulA* and D23580 were grown over 24 h in different concentrations of ciprofloxacin, and colony forming units (CFU) were determined. **A-B.** Colours represent ciprofloxacin concentration, and lines (solid, dashed, dotted) represent replicate. Experiments were performed in triplicate, and a one-way ANOVA was performed on CFU at 24 h to determine significant differences in growth according to treatment of D23580Δ*sulA* (**C**).

chose four conditions to subject *S.* Typhimurium D23580 to, in addition to no treatment, for two hours. The conditions were: 0.5x ciprofloxacin MIC, 2x ciprofloxacin MIC (0.06 μg/ml), 1 μg/ml Mitomycin C, and 1x azithromycin MIC. The conditions were chosen to distinguish between a sub-inhibitory dosage of ciprofloxacin (0.5x MIC) with a theoretically inhibitory concentration of ciprofloxacin (2x MIC), a DNA damage-inducing drug Mitomycin C, and a macrolide antimicrobial, which has a different mechanism of action to ciprofloxacin. Mitomycin C was chosen as a general inducer of stress with similarities to ciprofloxacin. It is a known potent inhibitor of DNA replication and inducer of double-stranded DNA breaks, and has been shown to upregulate *recA* and other stress associated genes, as well as induce temperate phage[461,476–479].

Upon analysis, we found that there were important differences in differential expression between the treatments (**Figure 5.7**). Interestingly, treatment with 0.5x ciprofloxacin MIC and Mitomycin C appeared more similar to each other than to 2x ciprofloxacin MIC. However, the trends of these three treatments were similar, in contrast to treatment with azithromycin, which had a distinct transcriptional signature.

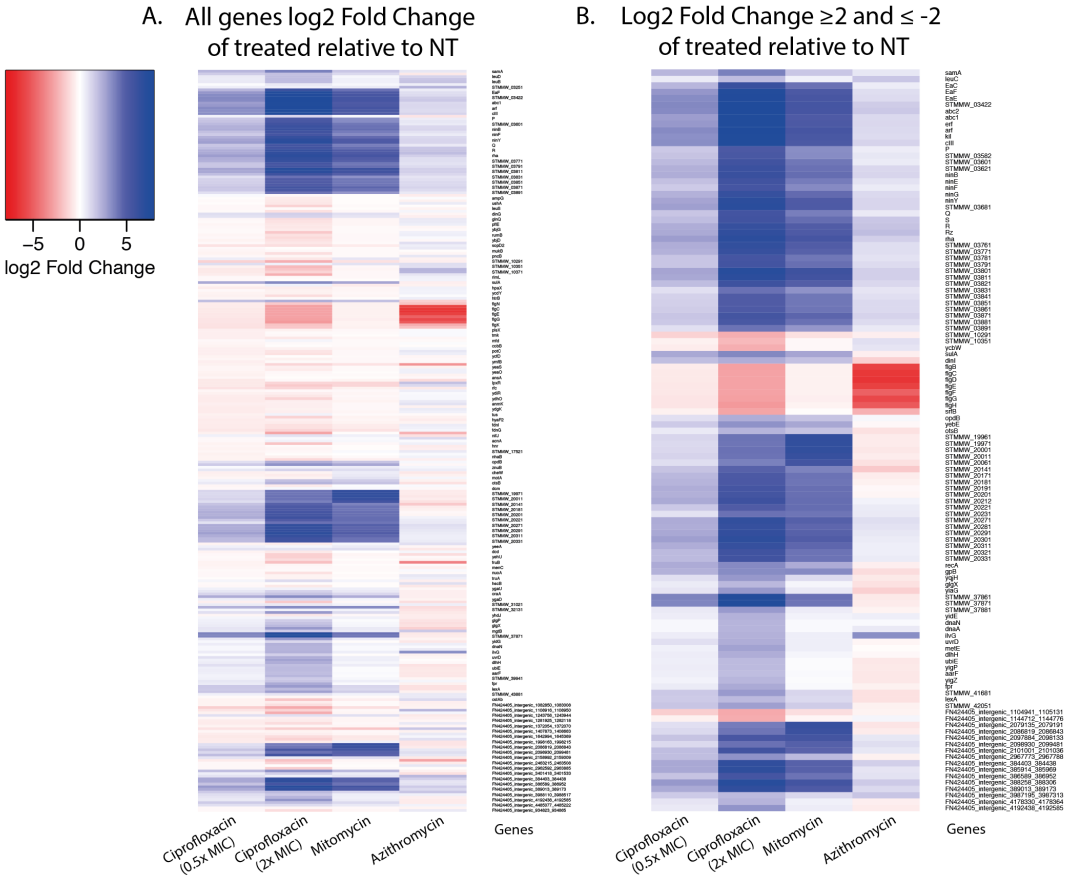

Figure 5.7 Heatmaps of differential expression of *S.* Typhimurium D23580 exposed to four different conditions. Log_2 fold changes of D23580 exposed to ciprofloxacin (0.5x MIC, 2x MIC), Mitomycin C, and azithromycin were plotted relative to non-treated (NT). **A.** All genes with $p < 0.05$. **B.** Genes with $p < 0.05$ and l2fc of ≥ 2 or $\leq$ -2.

To explore the chromosomal distribution of the differential expression, we once again plotted l2fc along the chromosome and highlighted l2fc ≥ 2 or $\leq$ -2 (**Figure 5.8**). It was interesting to observe that the 0.5x ciprofloxacin MIC condition appeared to be a muted version of 2x ciprofloxacin MIC exposure, illustrating that a higher concentration of the same antimicrobial induces a more exaggerated response (**Figure 5.8 A-B**).

Response to Mitomycin C exposure was highly specific, with three highly upregulated regions associated with prophage. In contrast, the rest of the genome had very little differential expression (**Figure 5.8 C**). Finally, the distribution and differential expression of azithromycin-exposed D23580 was profoundly distinct, with very few upregulated genes and more downregulated genes across the genome. Interestingly, several of the downregulated genes are those involved in motility and chemotaxis (**Figure 5.8 D**). Importantly, we did not

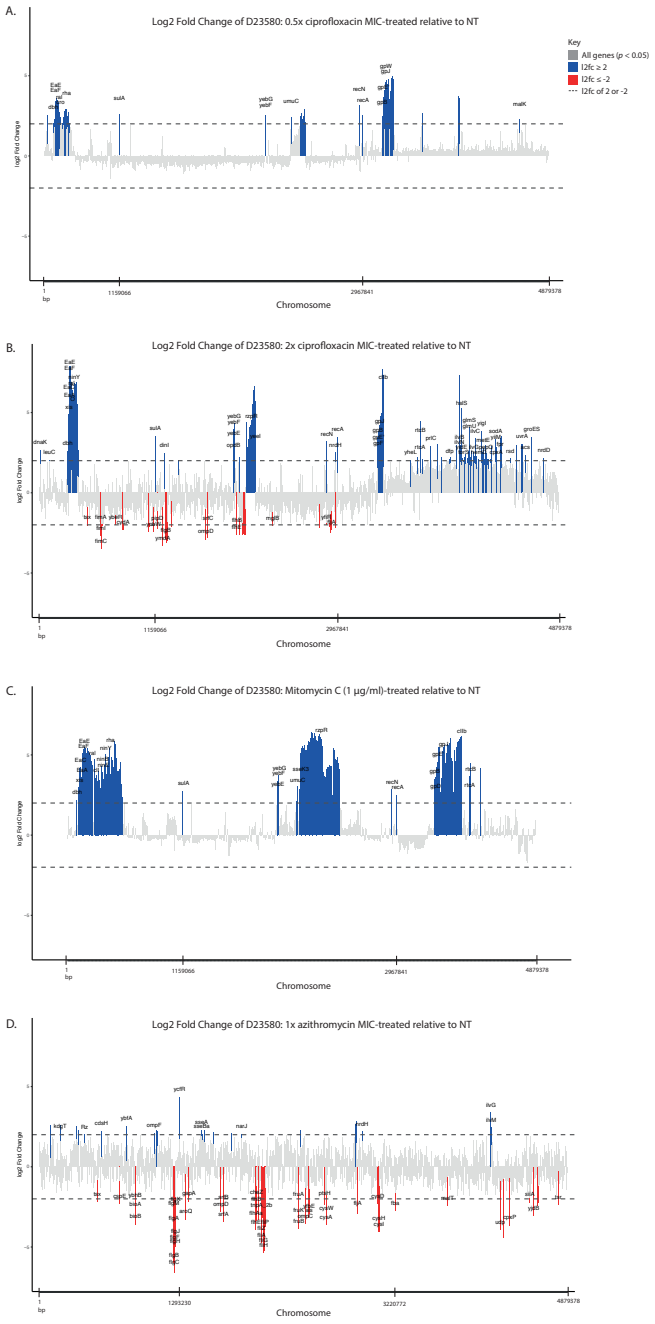

Figure 5.8 Differential expression of *S.* Typhimurium D23580 chromosomal genes in response to four treatments. Log_2 fold changes of chromosomal genes of *S.* Typhimurium D23580 exposed to ciprofloxacin (0.5x MIC, 2x MIC), Mitomycin C, and azithromycin were plotted relative to non-treated (NT). Only genes with $p < 0.05$ are included, and l2fc of ≥ 2 is coloured blue, and l2fc of $\leq$ -2 is coloured red. L2fc of 2 and -2 are demarcated by dashed lines. **A.** Exposure to 0.5x ciprofloxacin MIC. **B.** Exposure to 2x ciprofloxacin MIC. **C.** Exposure to 1 μg/ml Mitomycin C. **D.** Exposure to 1x azithromycin MIC.

observe any upregulation of SOS response or DNA damage-associated genes, confirming that D23580 responds very differently to drugs with distinct mechanisms of action. This study demonstrated that the observed response to ciprofloxacin, while overlapping with the response to Mitomycin C, has a distinct profile to other sources of stress, which may be important in determining how bacteria adapt to and survive during ciprofloxacin exposure.

5.4 Investigation of transcriptional effect of *gyrA* mutation in *S.* Typhimurium D23580

In addition to discerning the specificity of transcriptional response of D23580 to ciprofloxacin, we wanted to understand how an isogenic strain with a *gyrA* mutation would behave. To do so, we used *gyrA* spontaneous mutant D23580**gyrA* that was discussed in the previous chapter. While not resistant to ciprofloxacin, it has an MIC of 0.5 μg/ml, displaying decreased ciprofloxacin susceptibility. We were curious as to the transcriptional differences between a) D23580**gyrA* non-treated and D23580 WT, and b) D23580**gyrA* exposed to the WT 2x ciprofloxacin MIC of 0.06 μg/ml (a sub-inhibitory concentration for D23580**gyrA*). D23580**gyrA* was grown in the presence or absence of ciprofloxacin for 2 h as in previous experiments, and RNA-sequencing was performed. Our first observation was that there was little visible difference between heatmaps of the l2fc of transcription of D23580**gyrA* NT and D23580**gyrA* ciprofloxacin-treated when measured relative to D23580 WT. This indicated that perturbation with ciprofloxacin at nearly 0.1x MIC of the mutant had a negligible effect, and it was difficult to distinguish the treated condition from the non-treated (**Figure 5.9 A**). However, there was a clear difference in transcription between D23580**gyrA* and D23580 WT, with many genes downregulated in D23580**gyrA*.

Interestingly, many of these genes were associated with motility and chemotaxis, including *fljB* and *cheM* (**Figure 5.9 B**). Importantly, one of the few relatively upregulated genes in D23580**gyrA* was *ramA*, a gene known to be involved in ciprofloxacin resistance, mutation rate, and efflux pump production in *S.* Typhimurium[428,458,480]. The upregulation of *ramA* may help explain the lack of difference between treated and non-treated D23580**gyrA*.

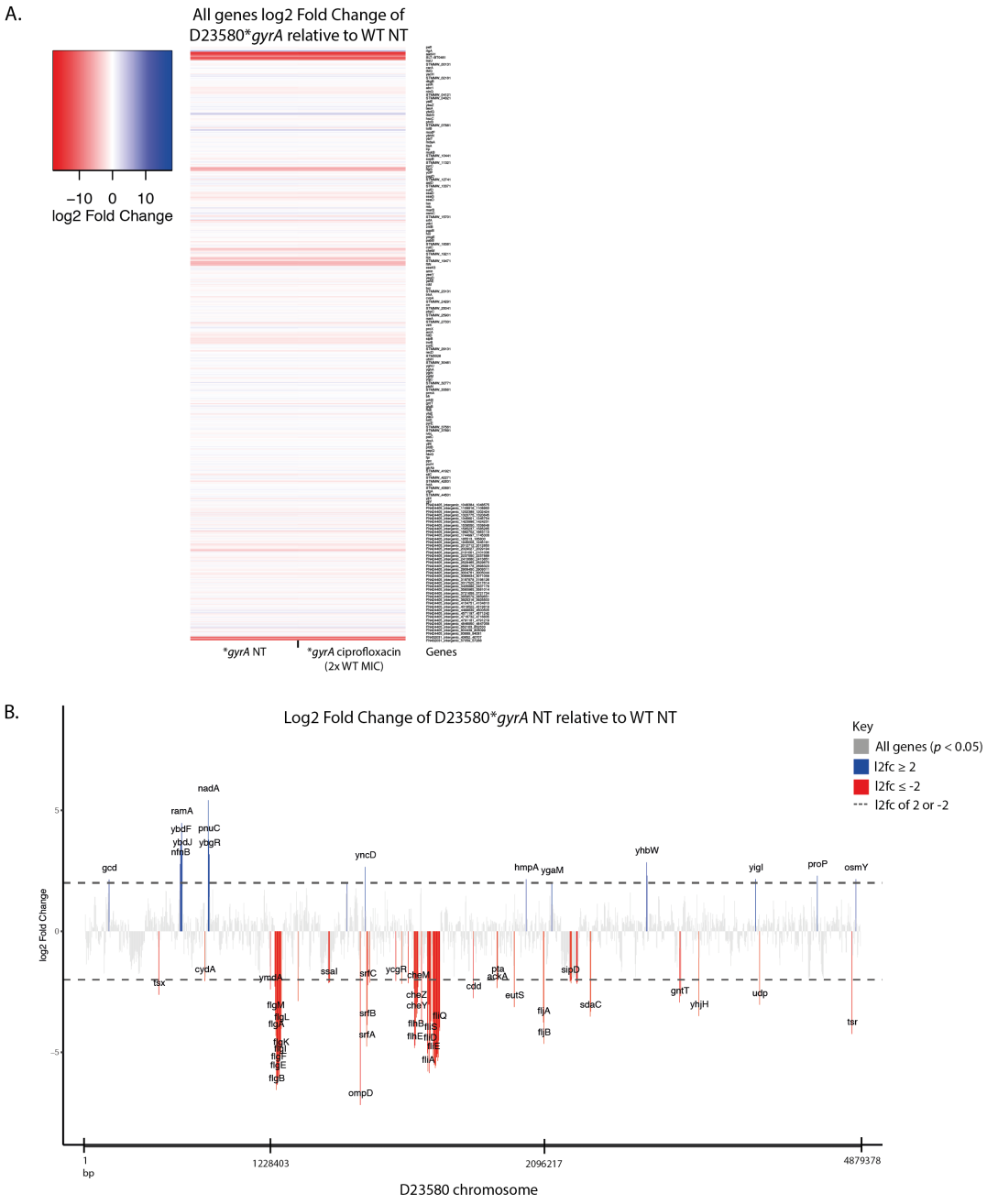

Figure 5.9 Differential expression of D23580gyrA* relative to *S.* Typhimurium D23580 WT after 2 h.** Differential expression of *S.* Typhimurium D23580**gyrA* either not treated or treated with 0.06 μg/ml ciprofloxacin (concentration equivalent to WT 2x ciprofloxacin MIC) relative to D23580 WT. **A.** All genes ($p < 0.05$) differentially expressed between D23580**gyrA* NT and D23580 WT NT (left panel), and ciprofloxacin-treated D23580**gyrA* and D23580 NT (right panel). **B.** Log_2 fold changes of chromosomal genes of D23580**gyrA* NT relative to D23580 WT NT. Only genes with $p <$ 0.05 are included, and l2fc of ≥ 2 is coloured blue, and l2fc of $\leq$ -2 is coloured red. L2fc of 2 and -2 are demarcated by dashed lines.

Next, to fully appreciate the effect of 0.06 μg/ml ciprofloxacin exposure on D23580 WT and on D23580**gyrA*, we investigated all the genes ($p < 0.05$) of treated versus non-treated D23580 WT and D23580**gyrA* (**Figure 5.10**). As observed in **Figure 5.9 A**, there was little difference between treated and non-treated D23580**gyrA*, in stark contrast to ciprofloxacin-treated D23580 WT relative to non-treated WT. As D23580**gyrA* was not exposed to an above- MIC concentration, it is difficult to know whether the lack of differential expression is due to the low ciprofloxacin concentration or the *gyrA* mutation. Future work should compare the transcriptional response of D23580**gyrA* exposed to above-MIC concentrations of ciprofloxacin.

5.5 Transcriptional profile of density-separated D23580 upon ciprofloxacin exposure

Imaging and image analysis in the previous chapter revealed a stratified response of a given bacterial population to ciprofloxacin: there was considerable diversity in bacterial length upon ciprofloxacin exposure. We hypothesized that transcriptional differences might underlie the observed morphological differences. To study this, we used the technique of centrifugation of discontinuous sucrose density gradients to separate out bacteria of different densities. This technique has been used in many contexts, including for the separation of *E. coli* ribosomes, *E. coli* minicells, *Staphylococcus aureus* cell walls, and segregation of other discrete cellular compartments of distinguishable density[354,481–484]. Given our understanding of the transcriptional response of bulk cultures of D23580 following 2 h of ciprofloxacin exposure, we sought to determine the transcriptional response of subpopulations at the same time point. We optimized a set of discrete sucrose concentrations (25%, 50%, 60%, and 70%) and centrifugation conditions to carefully separate bacterial subpopulations.

Centrifugation of treated (2x MIC ciprofloxacin) and non-treated *S.* Typhimurium D23580 revealed a clear difference in separation of bacteria between the two conditions (**Figure 5.12**). In the non-treated tubes, bacteria were primarily found in a diffuse but obvious band within the 50% sucrose (hereafter referred to as "NT"). In contrast, the ciprofloxacin-treated cultures separated into three fractions: one within the 50% sucrose, one within the 60% sucrose, and one at the interface of the 60 and 70% sucrose fractions. To analyse these

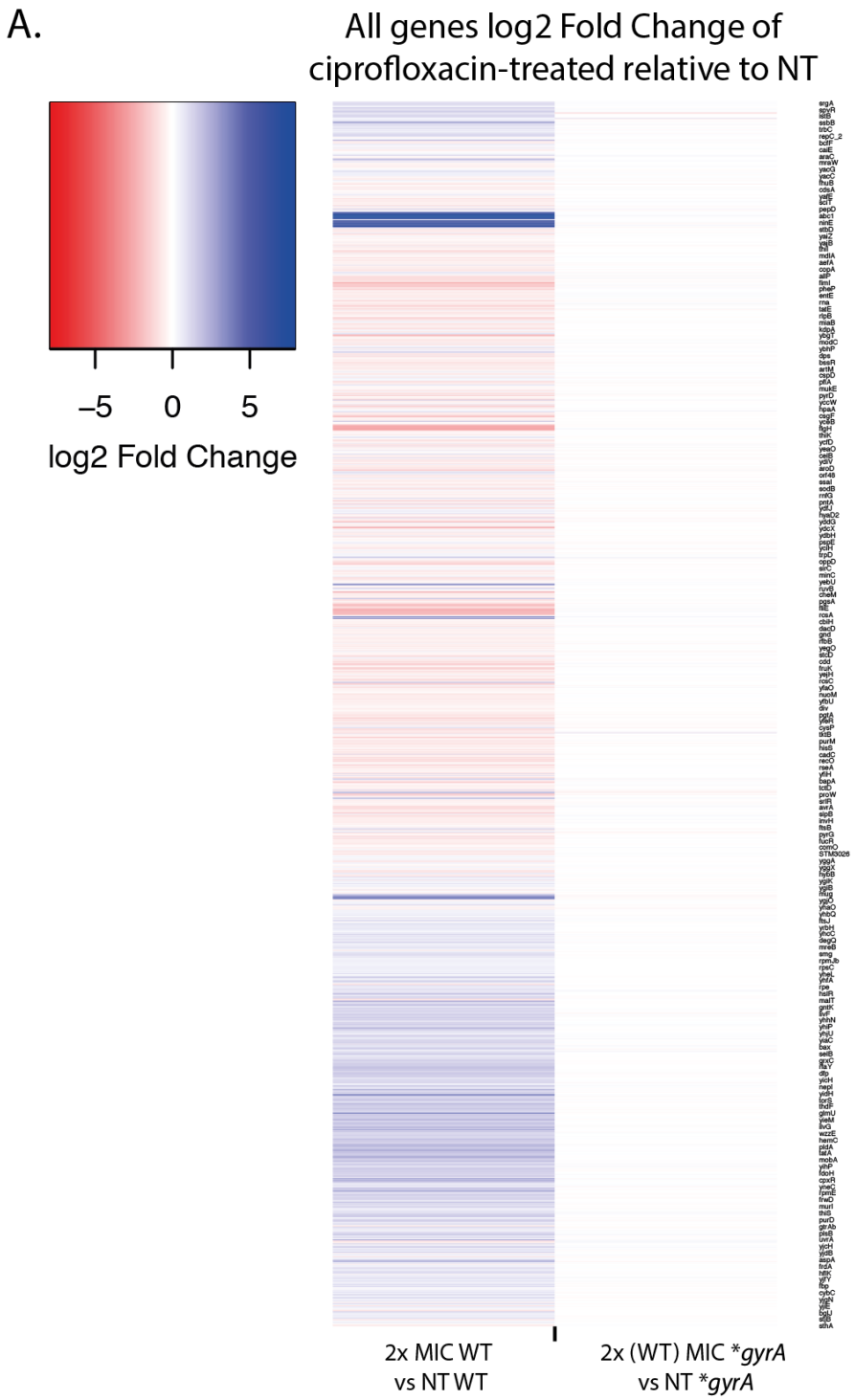

Figure 5.10 Differential expression of *S.* Typhimurium D23580 WT and D23580gyrA* ciprofloxacin-treated relative to NT after 2 h growth.** Differential expression of all genes ($p < 0.05$) in *S.* Typhimurium D23580 WT treated with 2x ciprofloxacin MIC (0.06 μg/ml) relative to D23580 WT NT (left panel) and D23580**gyrA* treated with 0.06 μg/ml ciprofloxacin (concentration equivalent to WT 2x ciprofloxacin MIC) relative to D23580**gyrA* NT (right panel).

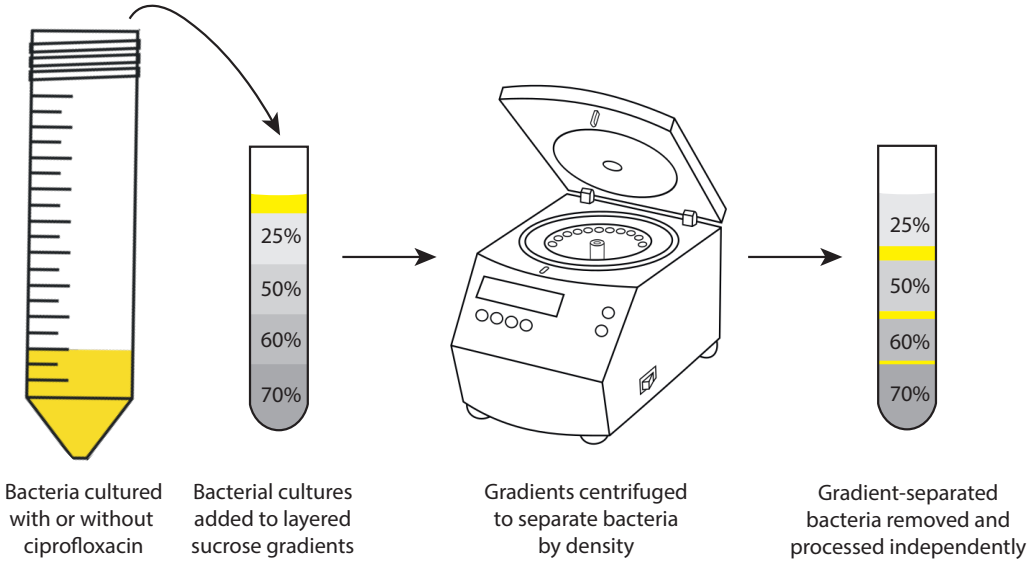

Figure 5.11 Schematic of sucrose density gradient fractionation. Cultures of *S.* Typhimurium D23580 grown in the presence or absence of 2x MIC ciprofloxacin for 2 h were added to the top of layered sucrose gradients. The gradients were centrifuged, and the density-separated bacteria were extracted and processed for RNA-sequencing.

data, we performed two comparisons: that of various fractions relative to NT, and that of the ciprofloxacin fractions relative to the ciprofloxacin-treated 50% gradient.

In comparing ciprofloxacin-treated bacteria in the 50% gradient relative to NT with ciprofloxacin-treated bacteria in the 60% gradient relative to NT, we were surprised by the similarity in patterns of differentially-expressed genes (**Figure 5.13 A (a, b)**). This told us that ciprofloxacin-treated bacteria had broadly the same shape of transcriptional response when compared to NT. However, it is important to note that there was considerable differential expression between the ciprofloxacin-treated and NT, as had been observed in bulk cultures. What was most interesting, however, was the contrast of the ciprofloxacin-treated 60% gradient against the ciprofloxacin-treated 50% gradient (**Figure 5.13 A (c)**). Here, we observed a different response, with less relative upregulation of genes and more downregulation. We also compared the ciprofloxacin-treated 60% gradient and the thin ciprofloxacin-treated 60-70% gradient against the ciprofloxacin-treated 50% gradient (**Figure 5.13 B (c, d)**). There, we observed slightly more relative up and down regulation in the 60-70% fraction, suggesting that those bacteria have undergone a slightly more exacerbated response to ciprofloxacin.

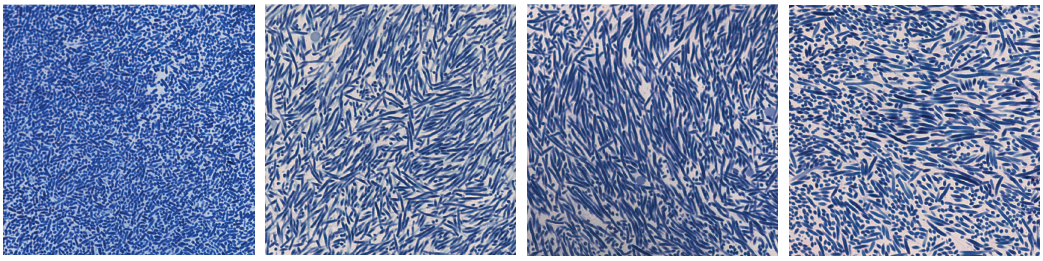

Figure 5.12 Light microscopy of *S.* Typhimurium D23580 separated by density fractionation. NT bacteria were found predominantly within the 50% sucrose fraction. Ciprofloxacin-treated bacteria separated into three distinct fractions: within 50% sucrose, within 60% sucrose, and at the interface between the 60% and 70% gradients. Bacteria were stained using a Gram-staining protocol and imaged on a light microscope at 900-1000x magnification.

We next sought to investigate the location and spatial distribution of some of the genes differentially expressed between the ciprofloxacin-treated 50% gradient relative to the NT, and between the ciprofloxacin-treated 60% gradient relative to the ciprofloxacin-treated 50% gradient. As before, we mapped the chromosomal genes and highlighted genes of interest (**Figure 5.14**). We saw similar patterns as in the bulk treatment in the ciprofloxacin-treated 50% with the NT (**Figure 5.14 A**). However, as observed in the **Figure 5.14**, the landscape was distinct when comparing the ciprofloxacin-treated bacteria of higher density with those of lower density (in 50% gradient). It was striking that *sulA*, a gene that is typically highly upregulated at 2 h post-treatment, including in **Figure 5.14 A**, was downregulated in the ciprofloxacin-treated D23580 in the 60% gradient compared against those in the 50% gradient (**Figure 5.14 D**). Additionally, the *rec* genes were only slightly upregulated, and *umuC* and *umuD* were not discernibly differentially regulated, possibly because they are similarly upregulated in both conditions relative to NT. In contrast, there was strong downregulation of genes within the *Salmonella* Pathogenicity Islands (SPI) 1 and 2 (**Figure 5.14 E**)[485–487]. SPI-1 and SPI-2 are involved in invasion and intracellular replication, respectively, and downregulation of these functions may suggest that the ciprofloxacin-treated higher-density bacteria are incapable of effectively invading host cells and surviving intracellularly. In addition, genes implicated in motility and chemotaxis were downregulated, further suggesting that the ciprofloxacin-treated higher-density bacteria might not be capable of invasion or an intracellular lifestyle (**Figure 5.14 F**).

To clarify the genetic networks involved, we conducted an analysis on the set of downregulated genes with an l2fc $\leq$ -2 on the ciprofloxacin-treated 60% gradient relative to the

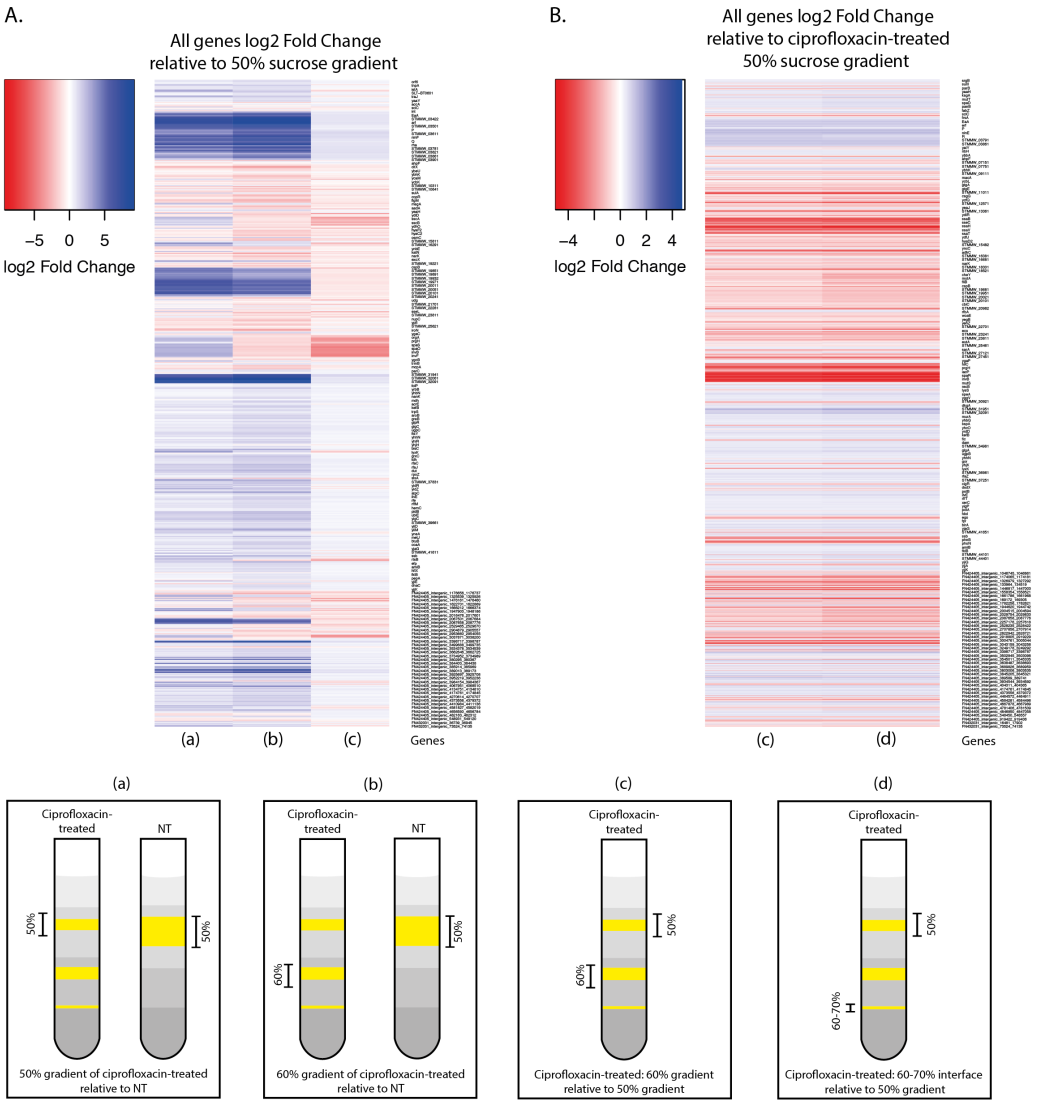

Figure 5.13 Differential expression of *S.* Typhimurium D23580 bacteria separated by sucrose gradients following 2 h growth. A. Differential expression of all genes ($p < 0.05$) of ciprofloxacin-treated *S.* Typhimurium D23580 bacteria in the 50% gradient relative to NT bacteria in the 50% gradient (NT) (a), ciprofloxacin-treated bacteria in the 60% gradient relative to NT bacteria in the 50% gradient (b), and ciprofloxacin-treated bacteria in the 60% gradient relative to ciprofloxacin-treated bacteria in the 50% gradient (c). **B.** Differential expression of all genes ($p < 0.05$) of ciprofloxacin-treated bacteria in the 60% gradient relative to ciprofloxacin-treated bacteria in the 50% gradient (c) and ciprofloxacin-treated bacteria in the 60-70% interface relative to ciprofloxacin-treated bacteria in the 50% gradient (d).

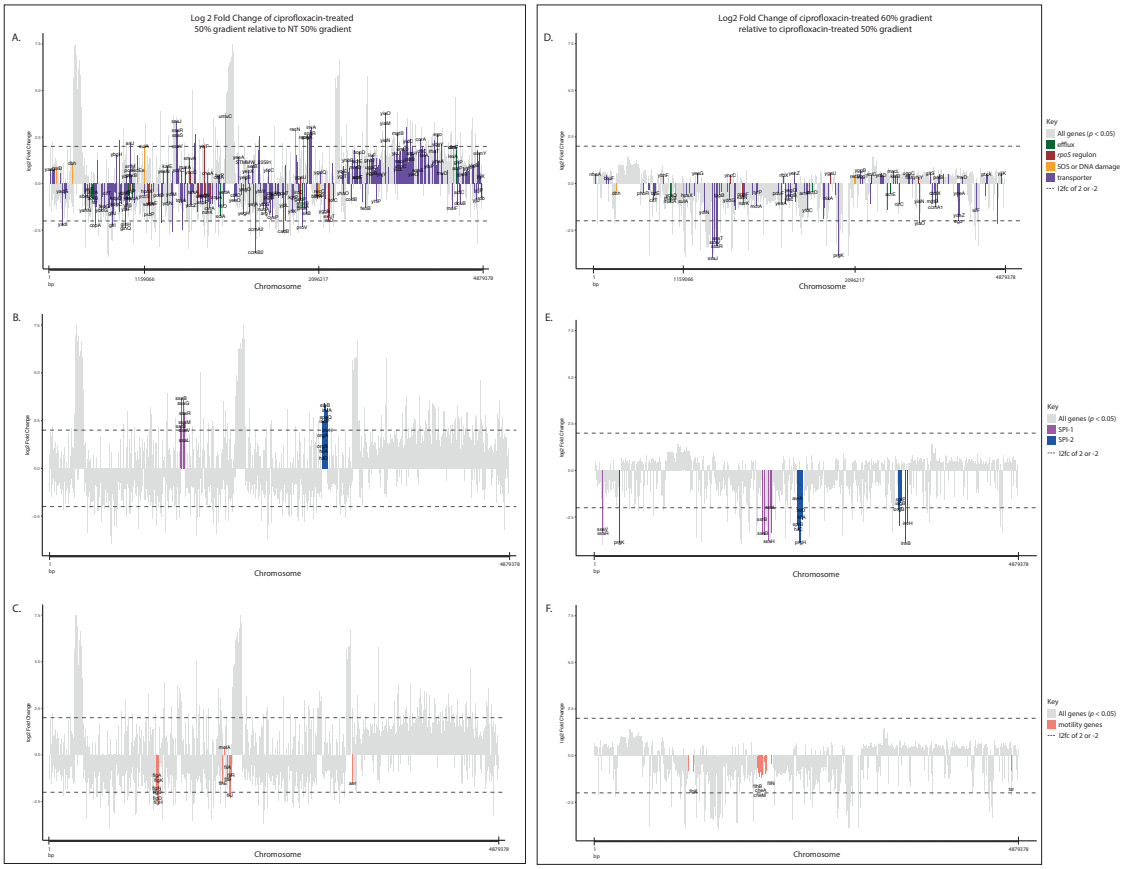

Figure 5.14 Chromosome maps of differentially expressed genes of ciprofloxacin-treated *S.* Typhimurium D23580 in the 50% sucrose gradient relative to NT bacteria in the 50% gradient and ciprofloxacin-treated D23580 in the 60% gradient relative to those in the 50% gradient. All chromosomal genes ($p < 0.05$) are represented in grey. **A-C.** Differentially expressed genes of ciprofloxacin-treated D23580 in the 50% sucrose gradient relative to NT bacteria in the 50% gradient. Each colour represents different functional groups of genes. **D-F.** Differentially expressed genes of ciprofloxacin-treated D23580 in the 60% gradient relative to those in the 50% gradient. Genes are coloured according to their involvement in pathways or functions of interest: efflux (green), *rpoS* (brown), SOS response or DNA damage (yellow), transport (purple), SPI-1 (magenta), SPI-2 (blue), motility (salmon).

ciprofloxacin-treated 50% gradient (**Figure 5.15**). As we had noted by plotting of the genes along the chromosome, the biggest network of genes was comprised of those involved in invasion. In addition, there were three small independent clusters of SPI-1 genes, one of which was centred around SPI-2-encoded transcriptional regulator *ssrB*[486,488]. While there is further analysis to be done to understand the differences between D23580 bacteria of different densities upon ciprofloxacin exposure, our initial analyses have opened some avenues of exploration.

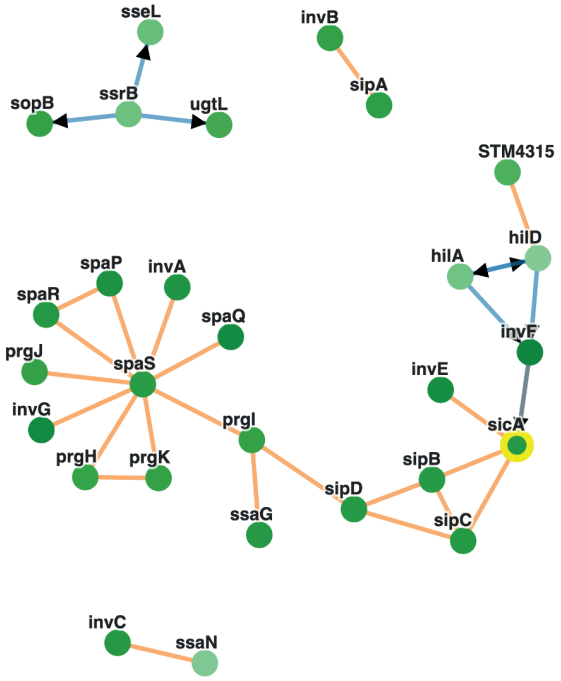

Figure 5.15 Network analysis of genes highly downregulated in ciprofloxacin-treated *S.* Typhimurium D23580 within 60% sucrose gradient relative to 50% sucrose gradient. Genes with an l2fc $\leq$ -2 were subjected to pathway analysis using web tool Phenetic. Genes were clustered according to their location within known *S.* Typhimurium genetic networks.

5.6 Discussion

In this study, we sought to characterize the transcriptional landscape of *S.* Typhimurium after exposure to ciprofloxacin. While the transcriptional study of ciprofloxacin-perturbed *S.* Typhimurium is not novel, our choice of isolates and conditions was unique and revealed some novel insight into *S.* Typhimurium response to ciprofloxacin. Our first analysis comparing four isolates of *S.* Typhimurium exposed to 2x ciprofloxacin MIC demonstrated that the response

to ciprofloxacin is time- and isolate-specific. Future analysis could link the similarities and differences in transcription between the isolates with their genetic background. In particular, the response of ST34 VNS20081 was overlapping but distinct from the other three isolates, and this may be due to the chromosomal architecture and genetic differences. In addition, there were several interesting aspects of the genome that we would like to further analyse in future work. A significant one is the prophage regions of the chromosome, which had amongst the greatest relative upregulation under ciprofloxacin exposure, and it would be worth exploring in greater depth the placement and specific involvement of these genes in response to ciprofloxacin. Additionally, there were several genes annotated as "intergenic regions" within the chromosome that we did not include in our analysis of chromosomal genes. However, a brief analysis of these regions has shown that some of them are non-coding RNAs, some are potentially small RNAs, and others are poorly-annotated genomic regions, many of which are phage-associated. Furthermore, our analyses did not include plasmid genes, which may play a significant role in the adaptation to ciprofloxacin pressure. Such analysis would be important to perform in the future. Lastly, we chose two distinct time points at which to study the four isolates, and it was clear that there were significant differences in the transcriptional response at each time point. This suggests the need for greater investigation of the temporal response to ciprofloxacin, and future work should incorporate additional time points to follow the changes in transcription.

Our subsequent transcriptional analysis of D23580 subjected to a variety of chemical stressors revealed important differences between the response to distinct drugs. An important finding of this analysis was that there was a strong difference in the degree of response between D23580 bacteria treated with a sub-inhibitory (0.5x MIC) and above-MIC (2x MIC) ciprofloxacin dosage. While we have conducted many of our experiments using 2x MIC of ciprofloxacin, many studies in the literature have focused on sub-inhibitory concentrations[331,426,433,469,489]. Given that bacteria are likely exposed to above-MIC concentrations of ciprofloxacin in a clinical context, it is important to evaluate the bacterial response to diverse ciprofloxacin concentrations, and future work should consider this. In addition, our analysis demonstrated that exposure to DNA damage-inducing drug Mitomycin C, while similar in some regards to ciprofloxacin exposure, did have a unique transcriptional signature. Even more importantly, exposure to azithromycin, a drug with a different mechanism of action, triggered a completely distinct transcriptional response. While not unexpected, this was important in recognizing that the transcriptional response of *S.* Typhimurium D23580 to ciprofloxacin appears to be

specific. However, it would be useful to expand the group of chemical perturbations to further elucidate how *S.* Typhimurium responds to each class of antimicrobials.

Alongside this analysis, we were able to demonstrate that a *gyrA* mutant of D23580 has a distinct transcriptional signature to D23580 WT and that perturbation with a sub-inhibitory concentration of ciprofloxacin has almost no effect on it. Further investigation into the factors driving this and response to higher concentrations of ciprofloxacin are warranted. In addition, an isogenic *gyrA* mutant is an important tool for understanding the development of ciprofloxacin resistance, and there are many transcriptomic and other experiments that could be undertaken with this strain.

Lastly, we investigated the transcriptional response of *S.* Typhimurium bacteria that had been density-separated. Given our prior knowledge that a batch culture of ciprofloxacin-exposed D23580 contained bacteria of different lengths (far more so than non-treated bacteria), we wanted to determine transcriptional differences between these populations. Density fractionation proved to be a successful technique to separate the different bacterial populations for sequencing, as has been shown previously, and we, too, were able to glean insight from the different populations[490]. This analysis revealed that there was considerable difference in transcription between higher and lower density bacteria that had been exposed to ciprofloxacin. While others have used fluorescence activated cell sorting and imaging to study the differences between elongated and non-elongated bacteria upon ciprofloxacin-exposure this had not previously been done in *S.* Typhimurium using density fractionation and with above-MIC ciprofloxacin concentrations[331,433]. Importantly, there was strong downregulation of SPI-1 and SPI-2 genes in the higher density ciprofloxacin-treated bacteria, suggesting a decreased ability to invade and replicate within hosts. Future work should pursue the invasion capabilities of bacteria of different densities.

Our initial analyses may be an important step towards understanding how *S.* Typhimurium bacteria are able to cope with and overcome ciprofloxacin exposure. Given the prevalence of ciprofloxacin usage, it is essential to better understand how bacteria are responding to this pressure, and these studies begin to elucidate some of the genes and networks that may be involved.

6. TraDIS analysis of *S.* Typhimurium D23580 during ciprofloxacin exposure and infection of intestinal organoids

Data

Data files are located in the folder here: ch6_TraDIS_data_files.

6.1 Introduction

After exploring the transcriptional landscape of *S.* Typhimurium D23580 upon exposure to ciprofloxacin at 2x MIC, we found that the response changed considerably between two and eight hours of ciprofloxacin exposure. While these data gave us significant insight into the patterns of gene and pathway expression, they provided limited information about the genetic requirements of *S.* Typhimurium D23580 under ciprofloxacin treatment and the ability to survival such stresses and bottlenecks. To address this gap in our understanding, we decided to use transposon directed insertion site sequencing (TraDIS) as a first step in elucidating additional genes that contribute to ciprofloxacin susceptibility and resistance. To get a little closer to an *in vivo* approximation, we also decided to evaluate the fitness landscape of D23580 during interactions with intestinal organoids.

TraDIS is a powerful technique that combines transposon mutagenesis with whole genome sequencing to identify the genes required in a given selective environment. The technique works by exploiting a library of randomly inserted transposons containing a selective antibiotic marker. Discrete sequence tags present at the 5' and 3' ends of the transposon facilitate DNA sequencing of the bacterial genome at the point of integration (**Figure 6.1**). If performed at scale it is possible to achieve a roughly even distribution of transposons scattered across the genome and identify these in single or small numbers of experiments. The insertion of these transposons can interrupt gene function, effectively creating a library of single-gene knockouts. A high-density transposon mutant library is created by pooling

the selected mutants from multiple successful insertion events[491–494]. Importantly, only non-essential genes will contain insertions because bacteria with disruption of an essential gene cannot survive. Thus, sequencing the library before (input library) and after (output library) growth in a specific condition determines the relative frequency of mutations in a particular gene at the beginning and end of a TraDIS assay. This can then be extrapolated to determine the importance of each non-essential gene in contributing to fitness[377,491,494]. Over the past decade, TraDIS has been used to investigate the selective pressures of mouse infection, antimicrobials, and serial passaging of cultures, amongst others[181,426,495–499].

TraDIS differs from RNA-sequencing by clarifying the function of genes at the endpoint of a specific growth condition. Although RNA-sequencing can determine the relative expression of genes and allude to the importance of those genes within a growth condition in real time, it cannot determine whether a set of genes are required for growth. In contrast, TraDIS cannot quantify the relative expression of genes, but it does allow distinguishing of genes required or not required. Furthermore, if the pool of transposon insertions in an organism are substantially dense and random, TraDIS can help identify essential genes[498]. Genes that are determined to cause an increase or decrease in susceptibility to a phenotype can then be individually independently mutated in subsequent experiments to validate the TraDIS screen results.

In the context of antimicrobial exposure, past studies have used TraDIS libraries to explore genetic susceptibility and resistance to various drugs of importance. In particular, there have been several studies to understand exposure to sub-inhibitory concentrations of ciprofloxacin: in *S.* Typhi, *Yersinia pseudotuberculosis*, and *Klebsiella pneumoniae*. Others have investigated the responses of *Acinetobacter baumanii* to colistin and *Pseudomonas aeruginosa* to beta-lactams[426,500,501]. Turner *et al.* recently investigated the response of an *S.* Typhi strain possessing a *gyrA* mutation and decreased ciprofloxacin susceptibility (DCS) to sub-inhibitory concentrations of ciprofloxacin[426]. They grew the *S.* Typhi library in LB with or without $\sim$ 0.2x MIC of ciprofloxacin over a total of an estimated 15 generations. They found several genes associated with enhanced ciprofloxacin susceptibility (fewer mutants in treated than in untreated pool) upon prolonged exposure ($\sim$ 48 h). These included many membrane-associated genes such as *acrA* and *acrB*, involved in the AcrAB-TolC efflux system; regulators of transcription (*phoP*, *tyrR*), antibiotic resistance (*marA*); DNA repair-associated genes such as *hupA*, *recN*, and *uvrD*; genes involved in cell division (*ftsN*, *dedD*); RNA-processing genes including *trpS* and *hfQ*, and others, some of which have unknown

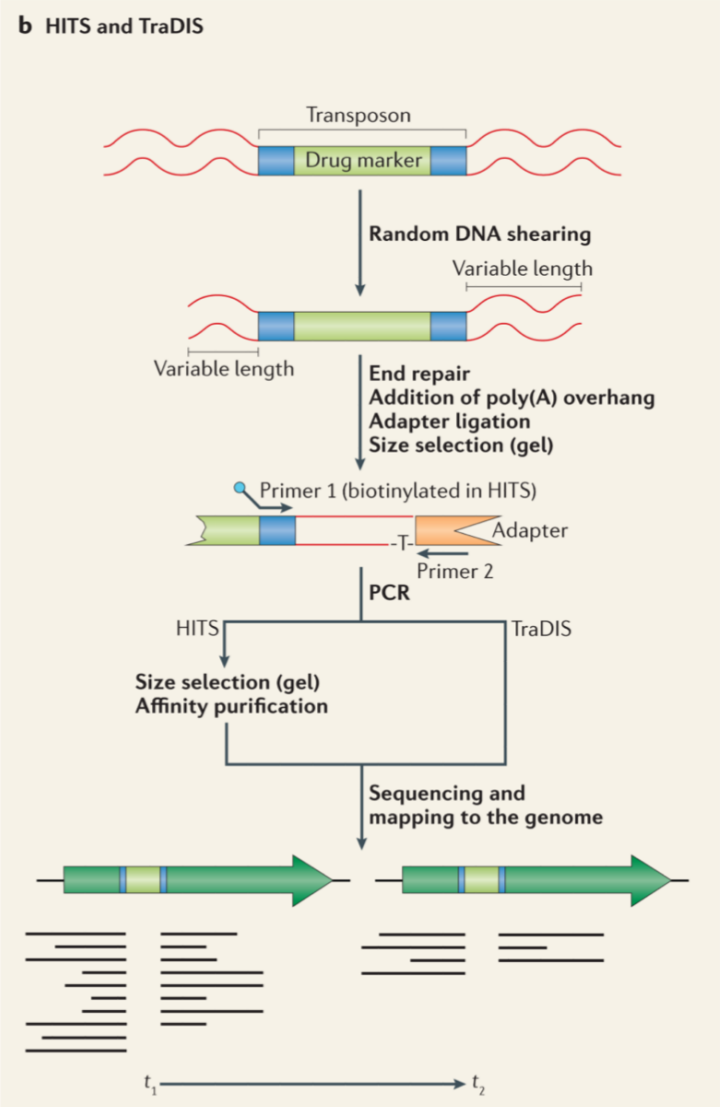

Figure 6.1 Sequencing strategy for TraDIS. Bacterial DNA containing transposon insertions linked to an antibiotic marker is sheared and prepared with an adapter prior to sequencing in short read, single-end sequencing and subsequent mapping and analysis. Adapted from Van Opijnen and Camilli, 2013[494].

function. The underrepresentation of these genes in the ciprofloxacin-treated pool indicates that these genes are required for survival in sub-inhibitory ciprofloxacin environments. In contrast, genes associated with reduced ciprofloxacin susceptibility (greater enrichment of mutants in treated compared to untreated pool) included several carbohydrate metabolism genes (*pfkA*, *tviC*); gene regulators (*slyA*, *emrR*, *envZ*); membrane-associated proteins (*ompF*, *emrD*); redox-associated; nucleoid associated; and others. Interestingly, while there was an enrichment of mutants in the ciprofloxacin-treated pool, the $\log_2$ fold change values above the untreated pool did not go above 3.2. It would be useful to know whether the degree of change increases with a higher dosage of ciprofloxacin to reflect more realistic treatment dosage based on our understanding that *S.* Typhimurium can withstand above-MIC concentrations of ciprofloxacin.

Similarly, Willcocks *et al.* recently used TraDIS on a *Y. pseuodotuberculosis* transposon mutant library of $\sim$ 40,000 unique insertion mutants under sub-inhibitory exposure to ciprofloxacin. Although the specific genes identified in their study differed, they noted a requirement of genes associated with DNA replication and repair (specifically *dksA* and *hda*), SOS response (including *recN*), LPS and outer membrane structure, core biosynthesis, and efflux transporters for tolerance to ciprofloxacin[502]. Conversely, they observed an increase in insertion mutants in *emrA* and *emrB*, which is perhaps surprising, as these genes are involved in multidrug efflux, although Turner *et al.* documented a similar result of more insertions in *emrD*. They hypothesized that the loss of *emrD* may induce an alternative ciprofloxacin exporter[426,502].

Such studies have not yet been conducted using *S.* Typhimurium ST313 D23580, though TraDIS libraries of D23580 have been investigated in other contexts. Canals *et al.* used a D23580 TraDIS library grown in LB, SPI-2-inducing medium, and in murine macrophages to identify genes involved in fitness in these different growth environments. They found that there was a disproportionately low percentage of insertions in the pBT1 plasmid, perhaps signifying an underappreciated role for pBT1 in carriage of essential genes[503]. To understand D23580 fitness in an alternative context, Ondari *et al.* used a D23580 transposon mutant library to study genes required for survival in human serum. They found a requirement for genes associated with LPS and common antigen synthesis, iron transport and binding for survival in serum. In total, they identified 555 genes whose loss increased serum susceptibility and 82 genes whose loss decreased serum susceptibility[181].

While the studies mentioned above have begun to fill gaps in our knowledge of the bacterial response to ciprofloxacin and gene requirements of *S.* Typhimurium ST313 D23580 in specific contexts, there remains an incomplete understanding of how D23580 responds to ciprofloxacin. Our previous work has begun to elucidate some of the phenotypic changes linked to ciprofloxacin exposure, but it has been challenging to link those to the genotype. Therefore, we sought to perform TraDIS on a ciprofloxacin-treated D23580 transposon mutant library. We performed time kill curves at 2x ciprofloxacin MIC using an existing D23580 transposon mutant library and chose three time points (2 h, 10.25 h, and 24 h) at which to sequence the non-treated (NT) and treated libraries to distinguish between genetic requirements during early growth phase, the growth rebound phase, and stationary phase under ciprofloxacin exposure[181]. We hypothesized that at 2 h post-exposure, there would be a strong requirement for genes involved in the SOS response and DNA repair. We further hypothesized that at 10.25 h and 24 h post-exposure, we would see a shift in the genetic requirement to more drug efflux-associated genes, and that there would be significant overlap in genes required at $\sim$ 10 h and 24 h post-exposure. We subsequently performed an independent experiment looking at the gene requirement of D23580 in intestinal organoid infection. Not only did we seek to increase our general knowledge of D23580 behaviour in varied contexts, we were also curious to observe the overlap in genes required in an invasion compared with a drug stress context. Here, we hypothesized that we would see a different spectrum of genes required in organoid invasion compared to ciprofloxacin survival.

6.2 *S.* Typhimurium D23580 transposon mutant library quality control

The D23580 transposon library used in our study was a subset of that used by Ondari *et al.*, and it contained $\sim$ 98,000 unique transposon mutants[181]. Under our growth conditions, the sequence length per unique insertion site (UIS) across the chromosome was $\sim$ 55 meaning that there was an insertion every 55 bp across the genome. Analysis of TraDIS data was conducted using the Bio-TraDIS pipeline. We initially used the default mapping parameters, but upon scrutiny, we found that the percentage of reads matched and reads mapped was lower than expected. We hypothesized that this might be improved by allowing for mismatches when matching the transposon tag. We therefore changed the mapping parameters to allow

for 1 mismatch with the transposon tag, which slightly improved the percentage of reads matched and mapped (**Figure 6.2**). However, in some cases, particularly the treatment conditions, the percentage of reads mapped remained quite low, and this could be a result of SNPs arising due to ciprofloxacin treatment, or imperfect mapping parameters used for the reference genome. Further fine adjustments of mapping parameters may strengthen the data analysis.

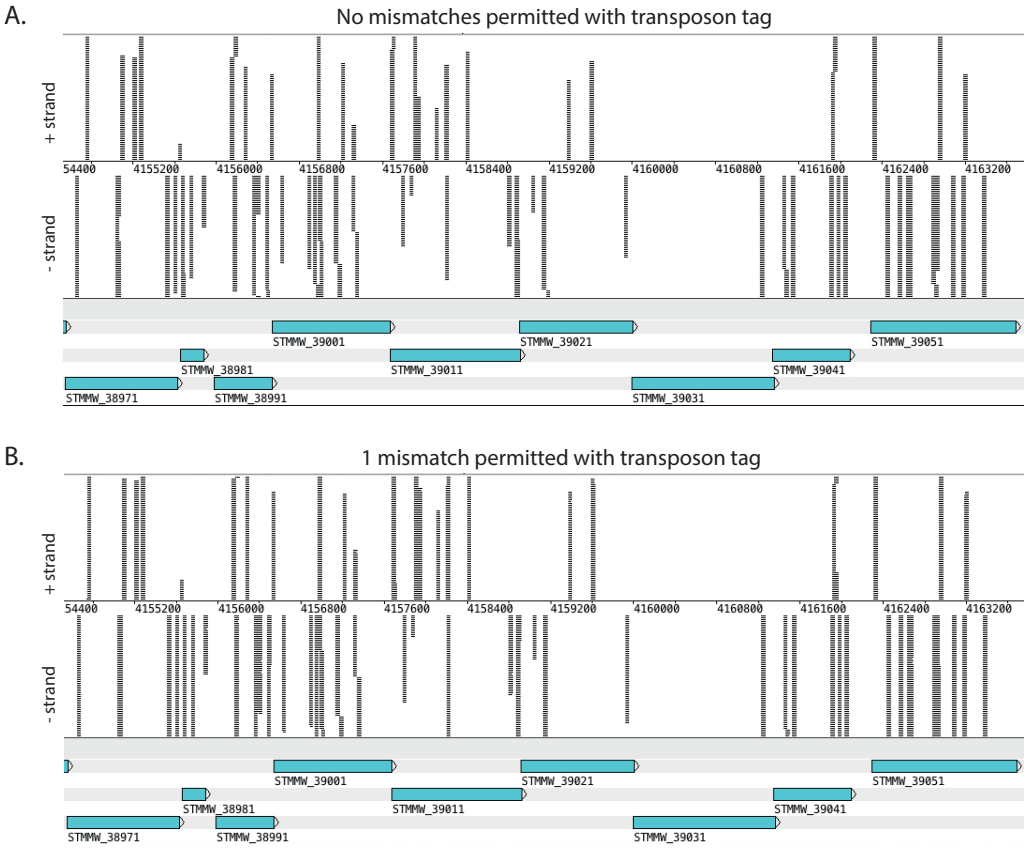

Figure 6.2 Difference in coverage of matched reads of transposon library with known transposon tag depending on the mismatch threshold used. A visual comparison of the BAM coverage plots between the analysis of the data using a mismatch filter of 0 (**A**) or 1 (**B**).

The initial stock library (prior to growth in liquid medium) had ∼92,000 total unique insertion sites in the chromosome. Upon overnight growth in liquid medium, the input library that was used for all experiments, contained ∼82,000 total unique insertion sites—a loss of ∼ 10,000 unique insertion sites. We identified 24 genes that exhibited evidence of some depletion during the overnight growth phase, and the majority of these belonged to genes linked to metabolism, biosynthesis, or redox pathways. There was a small number of genes involved in other pathways: 5 putative or hypothetical genes and one encoding an ABC transporter

domain protein. As these genes were lost during growth in medium, it was not possible to assay for them within the time kill curve or organoid experiments.

The output libraries from the time kill curve assays had upwards of 17,500 total unique insertion sites. While a richer mutant library would have been optimal, we determined that there was sufficient library density to identify genes of interest. Consequently, we identified 612 genes which were under-represented, similar to the 591 deemed essential by Canals *et al.*[503]. Genes were deemed under-represented if they contained 0 or 1 insertions, indicating that mutants containing mutations in those genes were not viable, based on criteria established by Langridge *et al.*[498]. Differences in the exact number of essential genes may be due to sequencing differences, library size, experimental conditions or library quality. We mapped the essential genes to known metabolic pathways in D23580 using BioCyc to determine the baseline pathways of the library prior to perturbation and did not observe any enrichment of particular pathways (**Figure 6.3A**)[504,505]. We also mapped the essential chromosomal genes along the entirety of the genome to see where they were and whether there were any distinct clusters of essential genes (**Figure 6.3B**). We could not observe any particular genomic regions that had unusually high clusters of essential genes. Based on our assessment that the library was sufficiently dense and that the list of essential genes reflected previous understanding of D23580, we were able to progress with an analysis on the D23580 transposon mutant library under ciprofloxacin-perturbation.

6.3 Required genes in *S.* Typhimurium D23580 after exposure to ciprofloxacin

To assess which genes are required for survival under ciprofloxacin exposure, we decided to perform time kill curves with the *S.* Typhimurium D23580 transposon mutant library, choosing three time points at which to harvest bacteria for sequencing. Bacteria were either treated with 2x MIC ciprofloxacin or non-treated (NT) and harvested at 2 h, 10.25 h, and 24 h post-exposure. The choice of these time points was determined based on growth dynamics. In particular, the 10.25 h time point was chosen because this was when the bacterial cultures began to rebound in the ciprofloxacin medium. At each time point, the bacterial cultures were harvested, and genomic DNA was extracted for sequencing (**Figure 6.4**).

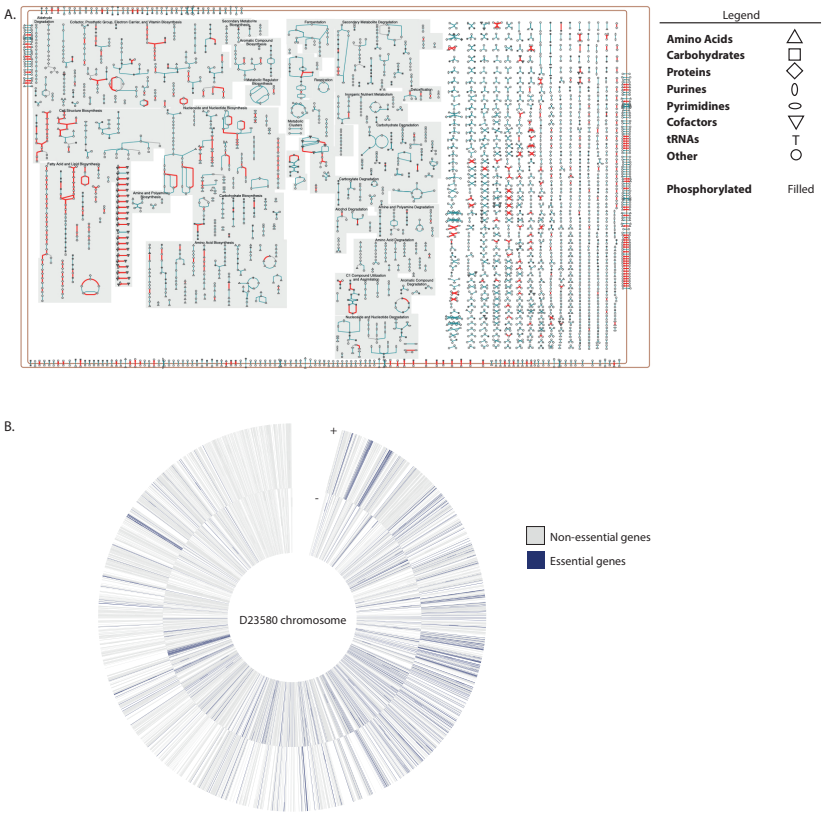

Figure 6.3 Assessment of *S.* Typhimurium D23580 essential genes based on TraDIS. A. Essential genes involved in metabolic pathways mapped on BioCyc cellular map of *S.* Typhimurium D23580. **B.** Chromosomal essential genes (blue) mapped on the *S.* Typhimurium D23580 chromosome. The + strand (outer circle) and – strand (inner circle) are represented separately.

Upon sequencing of the bacteria, analysis was conducted using the Bio-TraDIS software suite, mirroring the analysis protocols of Turner *et al.*[377,426]. Analysis using the Bio-TraDIS toolkit gave us the $\log_2$ fold change (l2fc) differences between treated and non-treated bacteria at each time point, which represents the difference in the number of sequence reads in a given gene. Thus, a negative l2fc in the treated condition (fewer reads relative to the control) indicated that the gene was required for survival in ciprofloxacin, thus contributing to decreased ciprofloxacin susceptibility when functional. Whereas a positive l2fc (higher reads relative to the control) in the treated condition indicated that the gene was not required for survival in the presence of the drug, therefore contributing to increased susceptibility to ciprofloxacin when functional. For analysis, a threshold of > 2.75 was set for the log counts per million (log CPM) to ensure that genes with a low number of reads were not included, and a threshold of $2 \geq$ l2fc ≤ -2 was used to identify only genes that were considerably different between treatment and non-treated[498]. Additionally, a p-value cut-off of < 0.05 and

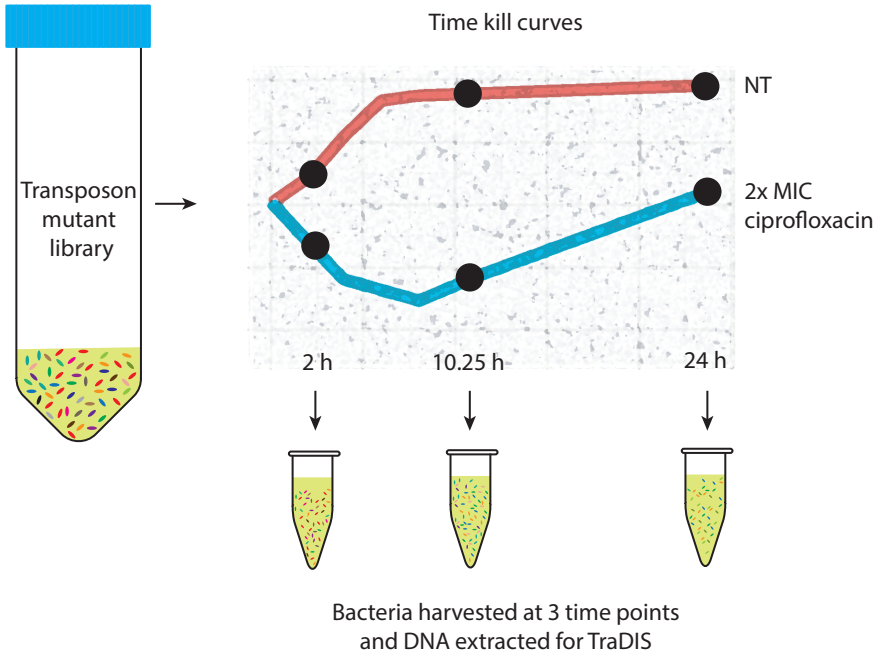

Figure 6.4 Schematic of experiment measuring exposure of *S.* Typhimurium D23580 transposon mutant library to 2x MIC ciprofloxacin. The transposon mutant library was grown overnight and then inoculated in medium containing no ciprofloxacin or 2x MIC ciprofloxacin. Bacteria were grown shaking and harvested at 3 time points for TraDIS.

a *q*-value cut-off (*p*-value adjusted for the false discovery rate) of 0.05 were used to discard genes that had a lower statistical probability of contributing to ciprofloxacin susceptibility.

Using this level of stringency, we were only able to identify one gene (*dksA*) that contributed to decreased ciprofloxacin susceptibility (l2fc $\leq$ -2) at 2 h post-exposure; however, there were 13 genes identified in the 10.25 h pool and 117 in the 24 h pool, two of which (*cbiE* and *ybgJ*) were shared between those two time points (**Figure 6.5 A**). It is possible that there were so few genes identified that contributed to decreased ciprofloxacin susceptibility at 2 h because this was too early post-treatment to result in the loss of many insertion mutants. *dksA* has been implicated in greater resistance of *S.* Typhimurium to nitric oxide and the sensing of oxidative and nitrosative stress[506,507]. As the early SOS response is critically important for bacterial survival against ciprofloxacin, it would make sense that *dksA* might reduce susceptibility to ciprofloxacin. However, at 10.25 h, only the transposon mutants capable of surviving for a longer period in ciprofloxacin medium would remain. Interestingly, there were significantly more genes required for decreased ciprofloxacin susceptibility at 24

h than at either 2 h or 10.25 h. We hypothesized that this may be due to a requirement for more genes to sustain longitudinal survival in ciprofloxacin.

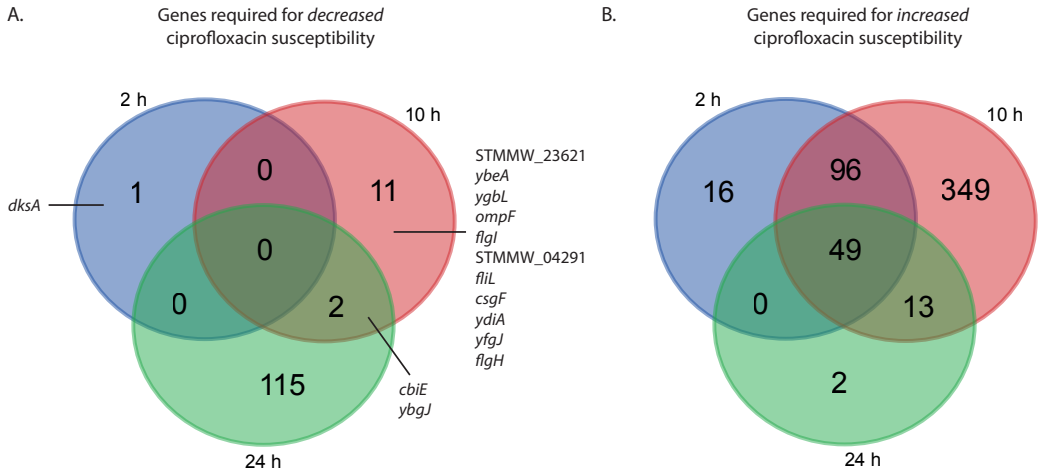

Figure 6.5 Venn diagrams of genes required for increase or decrease of ciprofloxacin susceptibility in *S.* Typhimurium D23580 at 2, 10.25, or 24 h post-exposure. A. The number of genes required for decreased ciprofloxacin susceptibility. **B.** The number of genes required for increased ciprofloxacin susceptibility.

Of the 13 genes identified to decrease ciprofloxacin susceptibility at 10.25 h, several of them were involved in flagellar assembly (*flgH*, *flgI*, *fliL*), several were conserved hypothetical genes (STMMW_04291, *ybeA*, *ybgJ*, *ydiA*, *yfgJ*), and interestingly, *csgF*, a gene encoding a protein for assembly and transport for curli production. Two of these genes (*cbiE* and *ybgJ*) were also found to decrease ciprofloxacin susceptibility at 24 h. In contrast, we observed a different profile when looking at the overlap of genes contributing to increased ciprofloxacin susceptibility at 2, 10.25, and 24 h (**Figure 6.4 B**). There were far more genes that contributed to increased susceptibility, and several (49) of these were shared at all three time points (**Table 6.1**). These genes included *ramR*, a repressor of *ramA*, a gene known to be involved in the AcrAB-TolC efflux system[508]. Given our finding in Chapter 4 that *ramR* may contain mutations after 24 h of 1x MIC ciprofloxacin exposure, it was encouraging to see that its presence contributed to increased ciprofloxacin susceptibility in this TraDIS study.

We split the genes into broad categories based on the function of the proteins they encoded, and we found that the largest group of genes was associated with substrate transport and/or membrane-associated. While only *ramR* was directly involved with efflux, it is possible that the loss of some of these other transport genes inhibits ciprofloxacin entry or enhances its efflux. We were interested to know whether phage genes contributed to increased ciprofloxacin

Table 6.1 Genes associated with increased ciprofloxacin susceptibility in common across time points.

Gene	Function
yieE	Hypothetical protein
yieF	
yieM	
yieN	
yieP	
STMMW_20141	
STMMW_38301	
STMMW_38451	
pstA	Membrane-, LPS-, or transport- associated proteins
pstB	
pstC	
pstS	
phoU	
trkH	
kup (trkD)	
ramR	
yieG	
rbsA	
rbsC	
rfaP (waaP)	
yidY	
yieO (putative)	
rfaG	
acnB	Metabolism
asnA	
rffE	
mtlD	
rfaI (waaI)	
trxA	
rbsR	
STMMW_38441	
gidA	Cell division or replication
gidB	
recF	
STMMW_38311	
atpA	Energy
atpB	
atpD	
atpG	
atpH	
mioC	Phage
R	
S	
Q	
STMMW_20111	
glnC	Others
asnCb	
ppiC	
thF	

susceptibility. We found four prophage-associated genes to be implicated: *R*, *S*, and *Q*, encoding prophage BTP1 lysozyme, holin, and anti-terminator proteins, respectively, and STMMW_20111, a candidate prophage BTP3 holin. We hypothesised that ciprofloxacin may activate regions of phage genomes or even whole prophages, with some phage genes contributing to a more exacerbated response that may diminish survival in some circumstances. However, it is as yet unclear what specific role the four identified phage genes play in that context.

Given that a number of the genes required for increased ciprofloxacin susceptibility in common between the three time points were associated with metabolism, we wanted to know which metabolic pathways were implicated in increased ciprofloxacin susceptibility at each time point. Consequently, we again used BioCyc to map genes encoding proteins with metabolic functions and compared the differences between the time points (**Figure 6.6**). Commensurate with the much larger number of genes with an l2fc $\geq$ 2 in the 10.25 h time point, there were also many more metabolism-associated genes at the 10.25 h time point (**Figure 6.6 B**). However, we could not detect visually any distinct biosynthetic pathways specific to a given time point, suggesting that the biggest differences between the bacterial ciprofloxacin response at these time points are not related to metabolism.

Next, we wanted to explore the genomic landscape of selected mutants at each time point, so we mapped the genes with an l2fc of $\leq$ -2 or $\geq$ 2 to see where they were in the genome (**Figure 6.7**). We were interested to find that at 2 h, the TraDIS landscape looked somewhat similar to the 2 h transcriptional landscape discussed in the previous chapter with the genes in similar regions required for increased ciprofloxacin susceptibility. We wondered whether this was because many of these genes are in prophage regions, and thus whether certain prophage genes (with l2fc $\geq$ 2 over control) could be detrimental to survival early on during ciprofloxacin exposure. There was, however, a clear shift in the pattern at 10.25 h, where there were far more genes required for decreased ciprofloxacin susceptibility. Some of these overlapped with those at 2 h, towards the end of the genome (**Figure 6.7 A-B**). While some of these were also represented at 24 h, there were far fewer genes overall, as previously discussed. At each time point, there were some hypothetical genes, which will require further investigation to determine their roles and importance in the *S.* Typhimurium D23580 response to ciprofloxacin.

Figure 6.6 Metabolic pathways implicated by genes required for *S.* Typhimurium D23580 increased ciprofloxacin susceptibility at 2, 10.25, and 24 h post-exposure. Metabolism-associated genes required for increased ciprofloxacin susceptibility using BioCyc. Arrangement of pathways is intended to mimic the bacterial cellular spatial arrangement. **A.** Genes with l2fc ≥ 2 at 2 h highlighted in red. **B.** Genes with l2fc ≥ 2 at 10.25 h highlighted in purple. **C.** Genes with l2fc ≥ 2 at 24 h highlighted in yellow.

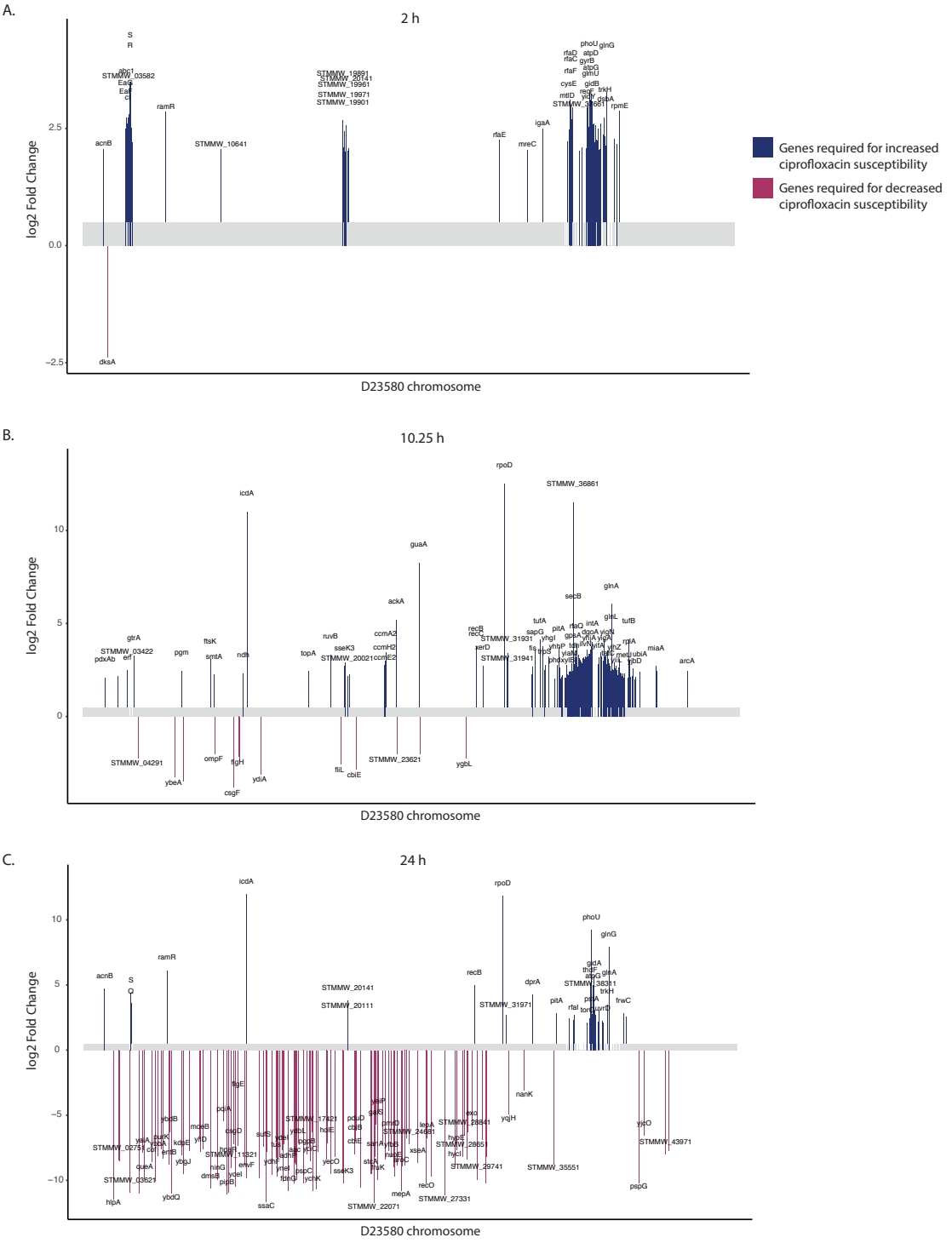

Figure 6.7 Chromosome maps of *S.* Typhimurium D23580 genes implicated in increased and decreased susceptibility to 2x MIC ciprofloxacin using TraDIS. Genes in blue are those with l2fc $\geq$ 2 (increased ciprofloxacin susceptibility), and genes in red are those with l2fc $\leq$ -2 (decreased ciprofloxacin susceptibility). **A.** Genes implicated at 2 h post-treatment. **B.** Genes implicated at 10.25 h post-treatment. **C.** Genes implicated at 24 h post-treatment.

6.4 *S.* Typhimurium D23580 genes required for the invasion of intestinal organoids

We subsequently investigated which *S.* Typhimurium D23580 genes were required for survival and/or invasion of intestinal organoids. This was performed as an exploratory experiment to evaluate the potential of a TraDIS assay in organoids and identify genes involved in organoid infection. To trial this, we microinjected the *S.* Typhimurium D23580 transposon mutant library that had been grown overnight in LB into the lumen of intestinal organoids and left the bacteria injected organoids for 1.5 h. Subsequently, organoids were broken apart, and the intact epithelial cells were treated with gentamicin to kill extracellular bacteria, using a modified gentamicin protection assay[509]. Cells were then lysed, and bacteria were enumerated and harvested after growth on L-agar plates, as previously established by Lees *et al.* (**Figure 6.8**)[378]. Analysis for this experiment was performed as for the ciprofloxacin time kill curve experiments using the Bio-TraDIS software.

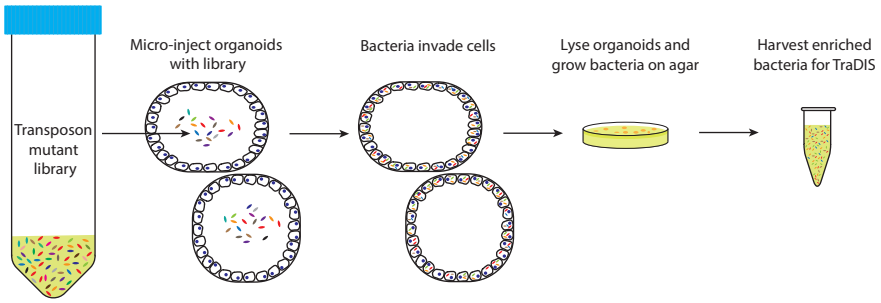

Figure 6.8 Schematic of organoid invasion experiment using *S.* Typhimurium D23580 transposon insertion library. Bacteria from the transposon mutant library were grown overnight in LB and micro-injected into intestinal organoids. Organoids were disrupted and treated with gentamicin to kill extracellular bacteria. Epithelial cells were lysed, and bacteria were plated for enumeration and TraDIS.

Bacteria invading organoids may face considerable bottlenecks before entering the organoid cells. Approximately 10^5 bacteria were injected into the organoid lumen, and 1.5 x 10^3 CFU were recovered post-invasion, a 100-fold loss of bacteria[510]. This was likely due to extracellular killing, including both host factors such as defensins and gentamicin. As the inoculum used for organoid infections is low, this may also prevent a fully representative transposon mutant library from entering the organoid, thus limiting the number of mutants exposed to a given organoid. Thus, a significant bottleneck may be occurring even before bacteria invade the cells. We assessed the number of unique insertion sites in the output

library and compared it to the input library (∼90,000 as discussed above). We found that the number of unique insertion sites had diminished to ∼6000, indicating that there was a significant bottleneck in organoid invasion. As a result of these bottlenecks, we could not confidently determine the genes required for organoid invasion because it is not possible to distinguish between mutants depleted due to extracellular killing, invasion, or absence in the pool. Thus, we could only comment on genes not required for organoid invasion (genes with l2fc ≥ 2 compared to control).

Intriguingly, we identified only two genes across the entire chromosome that were not required for organoid invasion—*srfA* and *ftsY*. Effector protein SrfA has previously been implicated in cytotoxicity to mammalian cells upon secretion into the host cell cytoplasm after infection, and has been noted to cause apoptosis of HeLa cells[511,512]. Lei *et al.* found that the loss of *srfA* results in a lower induction of NF-κB in infected macrophages[512]. While *ftsY* does not appear to have been well-studied in *Salmonella*, studies in *E. coli* have shown protein FtsY to function as a signal recognition particle receptor. It appears to bind to the cellular membrane, but further investigation is warranted to understand its role in organoid invasion[513,514].

6.5 Discussion

In this study, we wanted to explore the genes potentially involved in decreased or increased ciprofloxacin susceptibility at different points post-exposure and the genes required for intestinal organoid invasion. While these were two vastly different conditions, the overarching goal was to develop a deeper understanding of the genetic requirements of *S.* Typhimurium D23580 in two distinct stressful contexts with a focus on gaining insight into the unique response to ciprofloxacin. As exposure to ciprofloxacin and invasion of organoids are two extremely different conditions, it was clear that there were vastly different genes and pathways required for survival under these conditions. Treatment with ciprofloxacin at three distinct time points (2, 10.25, and 24 h) revealed a changing genetic requirement over 24 h, with the most diverse response occurring at 10.25 h post-treatment. To our knowledge, this was the first time TraDIS has been used to study the temporal response of bacteria to ciprofloxacin, which made it difficult to compare directly to other studies. Moreover, we

used ciprofloxacin at 2x MIC, which is far higher than the sub-inhibitory dosages used by others assaying transposon mutant libraries exposed to ciprofloxacin[426,502,515].

However, we could identify some overlapping patterns of genes required for increased ciprofloxacin susceptibility when comparing our data with that of Turner *et al.* Overlapping genes that were implicated in metabolism were *waaI* (*rfaI*), a lipopolysaccharide 1,3-galactosyltransferase and *mtlD*, a mannitol-1-phosphate dehydrogenase, although there were others in parallel pathways[426]. The phosphate transport system regulator *phoU* was also found in common, as was *trkH*, the gene encoding the trk system potassium uptake protein TrkH, and *gidA*, which encodes glucose-inhibited division protein GidA. This was further validated by another study by Turner *et al.* finding that an *E. coli* transposon mutant library treated with fosfomycin implicated phosphate transport systems in differential susceptibility[495]. Importantly, although there was not an exact overlap between our data and that of Turner *et al.* looking at *S.* Typhi, both data sets had genes in similar functional groups, with two of the biggest groups being membrane-associated and metabolism-associated genes[426]. There was also some overlap in the genes we found to have more insertions than expected (genes required for increased ciprofloxacin susceptibility) and those found by Pickard *et al.* in investigating bacteriophage-treated attenuated *S.* Typhi[516]. This suggests that *Salmonella* might actively modulate some membrane and metabolism pathways and functions to better survive in the presence of ciprofloxacin and associated stressors.

One caveat of comparing *S.* Typhimurium D23580 with *S.* Typhi used by Turner *et al.* is that the organisms, while similar, are not identical, nor are the TraDIS libraries and experiments. Thus, we also compared our data to the findings of Ondari *et al.*, who performed TraDIS on the *S.* Typhimurium D23580 transposon mutant library after exposure to human serum[181]. They identified 82 genes with an l2fc ≥ 2, meaning that they contributed to increased serum susceptibility, several of which were associated with the membrane. We compared this set of genes against our set of genes with l2fc ≥ 2 found at all three time points, and we found genes *trkH*, *rbsC*, and *ramR* in common. *trkH* encodes for potassium uptake protein TrkH, and the loss of *trkH* has previously been found to decrease aminoglycoside uptake and enhance its resistance in *Salmonella* Typhimurium and *E. coli*[517–519]. *trkH* has not previously been implicated in ciprofloxacin susceptibility, and the fact that it was found in our TraDIS analysis and in that of Turner *et al.* suggests that it may have an unappreciated role in multidrug resistance. *rbsC* encodes a membrane component of the ribose transporter, and although it has been well-characterized in *E. coli*, it does not appear to have been associated previously

with a change in ciprofloxacin susceptibility[520–522]. It has been found that mutations in ATP-binding cassette transporter proteins can lead to multi-drug resistance, and the same may occur for the ribose transporter[520,523].

Interestingly, *rfaP*, which encodes lipopolysaccharide core biosynthesis protein RfaP, was found in our analysis to contribute to increased ciprofloxacin susceptibility, while it and related gene *rfaH* were found to decrease serum susceptibility in *S.* Typhimurium D23580 by Ondari *et al.* and in *Klebsiella pneumoniae* by Short *et al.*[181,500]. Loss of *rfaP* has previously been implicated in increased susceptibility of *S.* Typhimurium to polymyxin, and thus it is surprising that we found that loss of *rfaP* decreased ciprofloxacin susceptibility in our hands[524,525]. However, modifications in LPS have been known to alter antimicrobial susceptibility, and it may be that this is a case of a differential response to antimicrobial and serum exposure[289,526–528].

We also compared the genes implicated in decreased ciprofloxacin susceptibility found at 10.25 h to the genes found implicated in decreased serum sensitivity by Ondari *et al.*. There was considerable overlap, including with *csgF*, the gene encoding curli production transport and assembly protein CsgF. In addition, the flagellar genes *flgH*, *flgI*, and *fliL* were all implicated in decreased ciprofloxacin susceptibility and decreased serum sensitivity[181]. These similarities suggest that there could be multiple genes and pathways that *S.* Typhimurium D23580 uses to combat various forms of stress. Interestingly, when we compared the genes at 10.25 h implicated in decreased ciprofloxacin susceptibility with those from a study analysing TraDIS of an MDR (including ciprofloxacin) clone of *Klebsiella pneumoniae* exposed to ciprofloxacin, there were no direct overlaps and only one potentially related gene *ydiA* in our analysis that could be similar to *ydiE* found by Jana *et al.*[515]. It may be that there was so little overlap between these studies because the *K. pneumoniae* clone they used was resistant to ciprofloxacin, whereas *S.* Typhimurium D23580 is not. The lack of consistency between our study and others suggests that there is high variability between how individual isolates respond to ciprofloxacin, and the baseline resistance level of an isolate is an important determinant of the response.

In assessing the genes required for organoid invasion, there were no direct comparisons to make with the literature, as this was the first time, to our knowledge, that TraDIS was performed on a transposon mutant library after invasion of organoids. However, the closest comparisons could be made with *in vivo* studies of mice and *in vitro* studies with macrophages.

A study by Canals *et al.* of an *S.* Typhimurium D23580 transposon mutant library in murine macrophages found that 87% of genes were considered required[503]. However, we were not able to determine genes required for organoid invasion due to the significant bottlenecks. One problem with comparing *in vitro* and *in vivo* infection models for TraDIS is that the bottlenecks *in vivo* such as survival in stomach acid and in the face of an immune response are different from those faced *in vitro*. Vohra *et al.* found that loss of SPI-1 and SPI-2 genes conferred loss of fitness in bovine ileum and mesenteric lymph nodes, and there was a total of 1289 genes required for survival in either compartment[499].

While we gleaned some interesting insight into some *S.* Typhimurium D23580 genes required for survival during ciprofloxacin exposure and invasion of intestinal organoids, we recognize that there is considerable work yet to be done. There were some interesting candidate genes implicated in increased ciprofloxacin susceptibility, including several encoding hypothetical proteins, and it would be beneficial to make single gene knock outs of these genes to better understand their individual contribution to ciprofloxacin susceptibility. In addition, it would be valuable to more closely analyse each gene that was implicated in ciprofloxacin susceptibility at each time point to better characterize the differences in the bacterial response at discrete time points. Furthermore, future experiments could use a more sophisticated approach to TraDIS experiments to gain further insight. For example, Hassan *et al.* used cell sorting on a transposon mutant library of *Acinetobacter baumanii* to target investigation of differences in efflux systems between ethidium bromide-treated and non-treated libraries[529]. Such an approach would be feasible for a ciprofloxacin-treated transposon mutant library given the morphological changes that ciprofloxacin-treated bacteria undergo, and this could cast light on genes involved in differential growth and survival. In addition, our study focused solely on ciprofloxacin-treated *S.* Typhimurium D23580, but it would be useful to understand how genes involved in fitness differ between different antimicrobial treatments. To better understand what occurs intracellularly in the context of antimicrobial treatment, it would also be feasible to use a transposon mutant library to look at the interaction of cellular invasion and antimicrobial treatment, which has not previously been investigated.

7. Investigation of genomic and phenotypic characteristics of selected *S.* Typhimurium ST313 isolates with a range of ciprofloxacin susceptibilities

Data

Data files are located here: ch7_genomics_data_files.

7.1 Introduction

The general understanding is that changes in bacterial susceptibility to ciprofloxacin are driven by alterations in the quinolone-resistance determining region (QRDR), primarily by SNPs in *gyrA* and potentially in *gyrB*, *parC*, or *parE*, which may be complemented by plasmid-mediated resistance such as *qnrS*. The role of efflux pumps, including the AcrAB-TolC complex, has also been widely appreciated as a factor in decreasing ciprofloxacin susceptibility[285,233,366,458,292]. However, our studies and work by others have begun to show that there are phenotypic differences between highly related organisms that have not yet been explained by obvious genetic differences[181,176]. It is possible that there are additional genes, regulatory networks and pathways that may be important in the response to external stressors that have not yet been recognized.

In the context of ciprofloxacin, while there have been many analyses of ciprofloxacin susceptibility in *Salmonella* serovars, the primary assessments involve MIC measurements, sequencing for *in silico* AMR analyses, and sometimes efflux pump assays and PCR-based assays to check for specific QRDR genotypes[214,241,530,531]. Additionally, most studies have tried to identify key genes that contribute to resistance, often through a mutagenesis or association approach. However, despite the advances in sequencing technology, assessment of ciprofloxacin susceptibility has not moved beyond the techniques mentioned above. In a

clinical context, this information may be sufficient, but the existence of large sets of isolates that have been whole genome sequenced enables further investigation into additional factors. It is not inconceivable that some other SNP or indel differences may play a subtle role in the differentiation of related isolates with slightly different ciprofloxacin susceptibilities.

In recent years, it has become possible to conduct bacterial genome-wide association studies (GWAS) to investigate variants responsible for a given trait. Microbial GWAS has some complications beyond those of human GWAS given the possibility of recombination events that may introduce new genes, selection for genes due to pressure, and clonal expansion can confound the analysis for a given phenotype. Despite the difficulties associated with bacterial GWAS, it has been successful in cases where there are sufficient samples sequenced, statistical rigor, and a clear phenotype of interest, including for identification of resistance phenotypes[532–534].

Another type of evaluation to investigate genetic differences between a large set of related genomes is by pangenome analysis. A pangenome analysis enables evaluation of the genetic structure of many organisms in parallel, differentiating between genes found in the core and accessory genomes[381,535,536]. While pangenome analysis is frequently used for defining taxonomic borders between related organisms, it can also be useful in probing finer differences between highly related organisms. This methodology has previously been used to analyse *Mycobacterium tuberculosis* genetic signatures involved in antimicrobial resistance, identify drug targets against *Clostridium botulinum*, and predict AMR in *E. coli*, among others[537–539]. Some pangenome analysis tools integrate pangenome association analyses to rapidly look for the presence or absence of genes within a group of organisms of interest, and this enables a rough overview of differences between organisms[540–542]. Combined with analysis of individual SNPs, it may be possible to gain insight into genes and SNPs within genes that differ between bacterial isolates. This approach has now been applied to virulence analysis[161,543].

Surveillance of *S.* Typhimurium ST313 in sub-Saharan Africa has not yet identified evidence for widespread acquisition of decreased ciprofloxacin susceptibility (DCS); however, there have been several isolates within the highly clonal lineage II and sub-lineage II.1 that exhibit significant DCS[176]. Given the extreme relatedness of these isolates, it is not yet clear why most maintain susceptibility to ciprofloxacin while specific clades and some individual isolates develop DCS. In addition, the majority of genomic and experimental analyses

on ST313s has been conducted on reference strain D23580, which does not fully capture the diversity within the lineage. It has previously been shown that the administration of ciprofloxacin drives acquisition of MDR organisms, and further investigation is needed to explain how this occurs[544]. More comprehensive genomic and phenotypic analyses of ST313 isolates could help guide usage of ciprofloxacin and uncover peripheral factors in AMR and response to stress.

Work by Van Puyvelde *et al.* found that in addition to the DCS phenotype displayed within certain regions of the African *S.* Typhimurium ST313 lineage II phylogeny, there is also a unique array of biofilm morphotypes observable under biofilm-forming conditions[176]. Previous studies have investigated the relationship between biofilm formation and evolution of the invasive phenotype[434,545]. In addition, some studies have investigated the relationship between biofilm formation and quinolone susceptibility using *in vitro* measurements of many isolates, finding an inverse relationship between the two[546–548]. In contrast, Shi *et al.* found the co-occurrence of ciprofloxacin resistance and thicker biofilm formation[547]. While we have not previously studied the transcriptional response of ST313 isolates under biofilm-forming conditions, some of the genes upregulated in ciprofloxacin treatment relative to no treatment in our transcriptomic analyses are involved in biofilm formation. Fàbrega *et al.* investigated the interactions between quinolone susceptibility, biofilm production, and efflux, finding that in isogenic strains with higher ciprofloxacin resistance, there was higher expression of AcrB, AcrA, and TolC, components of the AcrAB-TolC efflux complex, and lower biofilm production[548]. However, while these studies have elucidated the inverse relationship between ciprofloxacin susceptibility and biofilm production, there may still be underappreciated links between the response to ciprofloxacin and the formation of biofilms.

In particular, it is important to recognize the potential for differential responses between even closely related individual organisms, and it remains unclear how specific stress conditions such as ciprofloxacin treatment, serum exposure, or biofilm-forming conditions influence bacterial morphology and growth. These differences have implications for the efficacy of therapeutics. Ondari *et al.* showed that highly related isolates of ST313 showed marked differences in serum susceptibility, and in their analysis were unable to find a clear genetic factor underlying these phenotypic differences. Our ongoing work has illustrated differential responses of two ST313 isolates to the same relative dosages of ciprofloxacin. Similarly, Micoli *et al.* have shown the diversity of LPS O-polysaccharide structures across six *S.* Typhimurium strains, and this variation is under investigation within ST313 isolates[549] (Van Puyvelde,

personal communication). Significant differences in O-polysaccharide structures could have a detrimental impact on O-antigen based vaccines. Likewise, the aforementioned diversity in biofilm morphotypes amongst ST313 lineage II.1 isolates illustrates the phenotypic diversity found within a clonal lineage. The genetic basis for these differences is hypothesized to be due to a deletion within the *csgD* promoter, although this has yet to be confirmed (Van Puyvelde, personal communication). Moreover, a body of work on persister bacteria following perturbation have clearly illustrated the heterogeneity that arises within a population, and it is conceivable that similar processes are at play between isolates[328,550,551,362].

While there have now been discrete efforts to explore phenotypic differences between small numbers of ST313 isolates, this has not yet occurred in high-throughput. The ability to combine large sequence analyses with high-throughput phenotypic screening opens up the possibility of linking some of these observations[399]. Given the open questions regarding phenotypic differences between highly related ST313 isolates, the ST313 clade represents an ideal case study and proof-of-concept to investigate the relationship between genetic and phenotypic observations in higher-throughput. By performing targeted screening assays coupled with genomic analyses, it may be possible to find some links between the variation in African *S.* Typhimurium ST313 response to stress that have previously been elusive.

In our study, we aim to identify a set of $\sim$ 100 representative *S.* Typhimurium from sub-Saharan Africa that have a diversity of ciprofloxacin susceptibilities and biofilm morphotypes and perform pangenome and SNP analyses on them. We further aim to perform high-content imaging on a subset of ST313 isolates that have been genotyped but have not previously been phenotyped and perform image analysis to explore ciprofloxacin-associated morphological changes. As high throughput imaging of bacteria is a new approach, we also aim to use these well-characterised *S.* Typhimurium ST313 isolates to further evaluate the potential of the Opera Phenix microscope and its associated software. In this regard we seek to assess whether the pipeline can identify any reproducible novel phenotypes. We then aim to link these morphological changes to the bacterial genomes. By doing so, we aim to show that high content imaging can be used in tandem with genomic analyses to provide biological insight. Lastly, we further aim to phenotype a small subset of these isolates under biofilm-inducing stress conditions to explore granular differences in the biofilm morphotypes between isolates.

We hypothesize that upon genomic analysis of the selected ST313 isolates, we might find SNP differences outside of the QRDR that are roughly correlated with an isolate's susceptibility

to ciprofloxacin. We further hypothesize that there will be clear morphological differences between isolates of different biofilm morphotypes when imaged, and this may overlap with the isolates' ciprofloxacin susceptibility profile. Upon screening a discrete set of ST313 with varying ciprofloxacin susceptibilities, we expect to see differences between isolates independent of ciprofloxacin treatment. We further hypothesize, based on our morphological analyses in Chapter 4, that there will be variation in the degree of response to ciprofloxacin depending on the isolate's MIC: isolates with higher MIC will have less variation across treatment concentrations, whereas susceptible isolates will exhibit greater variation, more cell death, and more distinctive morphological changes.

7.2 Genomic analyses of 108 selected African *S.* Typhimurium isolates

To explore some of the genetic factors beyond mutations in the QRDR that may alter susceptibility to ciprofloxacin, we began by selecting 108 African *S.* Typhimurium isolates to use as a representative subset from a larger set of genomes analysed by Van Puyvelde *et al.* (**Figure 7.1 A**) (Van Puyvelde, personal communication)[176]. Isolates highlighted in purple show the ones chosen for further analysis, and these were selected based on their location within the phylogenetic tree, geographic origin, and any known *gyrA* mutations or *qnrS* presence.

We selected ST19 and ST313 lineage I isolates in addition to ST313 lineage II isolates to potentially investigate ciprofloxacin-associated differences between them. We also tried to sample groups of neighbouring isolates for subsequent pairwise analysis. While attempting to cover diversity within the phylogenetic tree, because we initially wanted to perform phenotypic analysis on all selected isolates, we were limited geographically to where it might be feasible to obtain physical isolates. We then ran a phylogenetic analysis using RAxML on the 108 isolates to map their relatedness on a phylogenetic tree (**Figure 7.1 B**)[379]. On the phylogenetic tree, we identified *gyrA* mutations and *qnrS* presence for isolates determined by *in silico* analysis using ARIBA, and we further included the ciprofloxacin MIC for isolates we were able to obtain and phenotype using ciprofloxacin ETESTs[382].

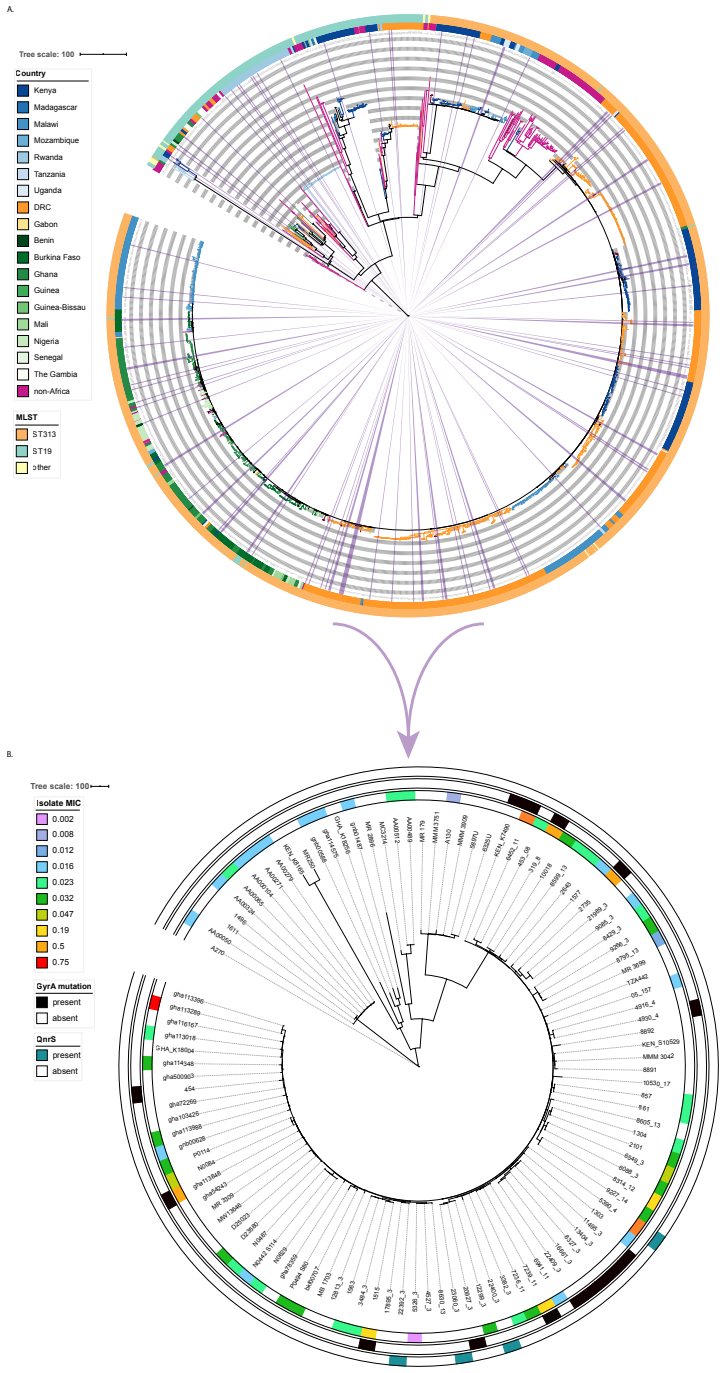

Figure 7.1 Phylogenetic trees of global and 108 selected African *S.* Typhimurium isolates. A. Phylogenetic tree of global collection of *S.* Typhimurium with focus on African isolates with isolates of interest highlighted in purple. The rings denote country of origin (inner) and sequence type (outer). Adapted from Van Puyvelde *et al.*, 2019. **B.** Phylogenetic tree of 108 selected African *S.* Typhimurium isolates. The rings denote ciprofloxacin MIC if measured (inner), presence of a *gyrA* mutation in the QRDR (middle), and presence of *qnrS* (outer).

Interestingly, while there was largely correspondence between a higher ciprofloxacin MIC and a *gyrA* mutation or *qnrS* for the isolates whose MIC were measured, this was not always the case. For instance, isolate 8314_12, which had a ciprofloxacin MIC of 0.19 μg/ml did not have any known or novel *gyrA* mutations nor did it possess a *qnrS* gene. However, we did find that 8314_12 had a *gyrB* mutation resulting in amino acid change S464F, which has been recognized in *Salmonella* and other bacteria as within the QRDR[552,553]. This was even more striking for isolate gha113289, which had an MIC of 0.75 μg/ml, the highest of all the MICs we measured but did not contain any *gyrA* mutations within the QRDR or *qnrS*. The *in silico* analysis of gha113289 could not detect any SNPs in *gyrB*, *parC*, or *parE*, other genes implicated in decreased ciprofloxacin susceptibility. Interestingly, closely-related isolate gha113018 had an MIC of 0.023 (**Figure 7.1 B**). Importantly, we did not observe the inverse scenario of a low detected MIC but presence of *gyrA* mutation or *qnrS*. This suggests that while these two factors do not universally explain a higher ciprofloxacin MIC, our ETEST assessments show that they do raise the MIC when they are present.

Based on this broadly observed correlation between a QRDR mutation and higher MIC, we performed a pangenome analysis of the 108 isolates to identify genes that were present and absent between isolates using pangenome analysis tool Roary[381]. As a pangenome analysis yields a multitude of results that may be difficult to interpret on their own, we followed this with a pangenome-wide association gene scoring using Scoary[542]. To do this, we determined two independent associations we wanted to test. The first was whether there was a genetic association between the classification of an isolate's MIC as "susceptible" or "intermediate" as per CLSI guidelines. Thus, we classified isolates for which we had an MIC as either "susceptible" (0) or "intermediate" (1) and performed an analysis with Scoary. Given that we did not have ciprofloxacin susceptibility phenotypes for many of the isolates, we compared 49 "susceptible" isolates to seven "intermediate" ones, which meant that this analysis was likely underpowered. There were only two genes within the pangenome that approached statistical significance, and these were in hypothetical proteins. Given the small sample size, it is unlikely that it would be possible to identify any statistically significant results, but we looked more closely into these two hypothetical proteins, especially as these genes were present in all the isolates in the "intermediate" group. BLASTP searches were performed on the two hypothetical proteins. We could not find any additional insight into the first hypothetical protein as it was found to be hypothetical or uncharacterized across a multitude of hits and was not found in reference isolate D23580 and therefore lacked a systematic name. It appeared to be located between genes encoding phage tail components. The second

hypothetical protein came up in the BLASTP search as a match for epsilon34_gp40 within *Salmonella* phage epsilon34, and it was located near a gene encoding an antibiotic ABC transporter permease as well as a gene encoding a recombinase characterized as part of the Rad52/22 family double-strand break repair protein. Once again, this gene was not found in reference isolate D23580.

For the second association analysis we compared isolates with and without a *gyrA* mutation and/or *qnrS*. Here, we wanted to know whether there are pangenomic commonalities between isolates with a known DCS determinant that separate them from those without. For this analysis, we compared 88 isolates without any known DCS determinants to 20 isolates with a known resistance determinant. The Scoary analysis identified 10 genes with a p-value of < 0.05. However, upon scrutinizing all of the significant genes from Scoary, there were none exclusive to the isolates carrying a known DCS determinant. This suggests that while there might be some commonalities between these isolates, we could not identify any genes in the pangenome exclusively associated with isolates carrying a known DCS determinant.

Of the genes identified in the Scoary analysis, one of them was the same as the first one found in the prior analysis, encoding a hypothetical protein of unknown function that was not found in reference isolate D23580. Despite the low power of these analyses, this could be interesting as it was the only gene that overlapped between the two association studies. In addition, there was a gene found in the acetyltransferase (GNAT) family; *cat*, a chloramphenicol acetyltransferase; two phage tail fibre components; and *stf*, a DNA-recombinase-like protein. To have greater confidence in specifically associating any of these genes with isolates carrying a known DCS determinant, it would be necessary to run a similar Scoary analysis using a much larger set of isolates.

Following the preliminary pangenome-wide association analyses, we wanted to look at individual SNPs that differ between the selected ST313 isolates to explore whether there are SNP-level differences that may be important in ciprofloxacin susceptibility. To do so, we first established a benchmark using a lineage of ST313 isolates with *gyrA* mutations and known DCS. Here, Van Puyvelde *et al.* found a step-wise increase in ciprofloxacin MIC amongst a highly related set of ST313 lineage II.1 isolates (**Figure 7.2 A**). We analysed the SNPs different between the group of seven isolates with the lowest MIC (light pink) and the group of 5 isolates with the highest MIC (purple). There were nine coding SNPs that differed between the two groups, and of these, six of them were non-synonymous SNPs. These SNPs

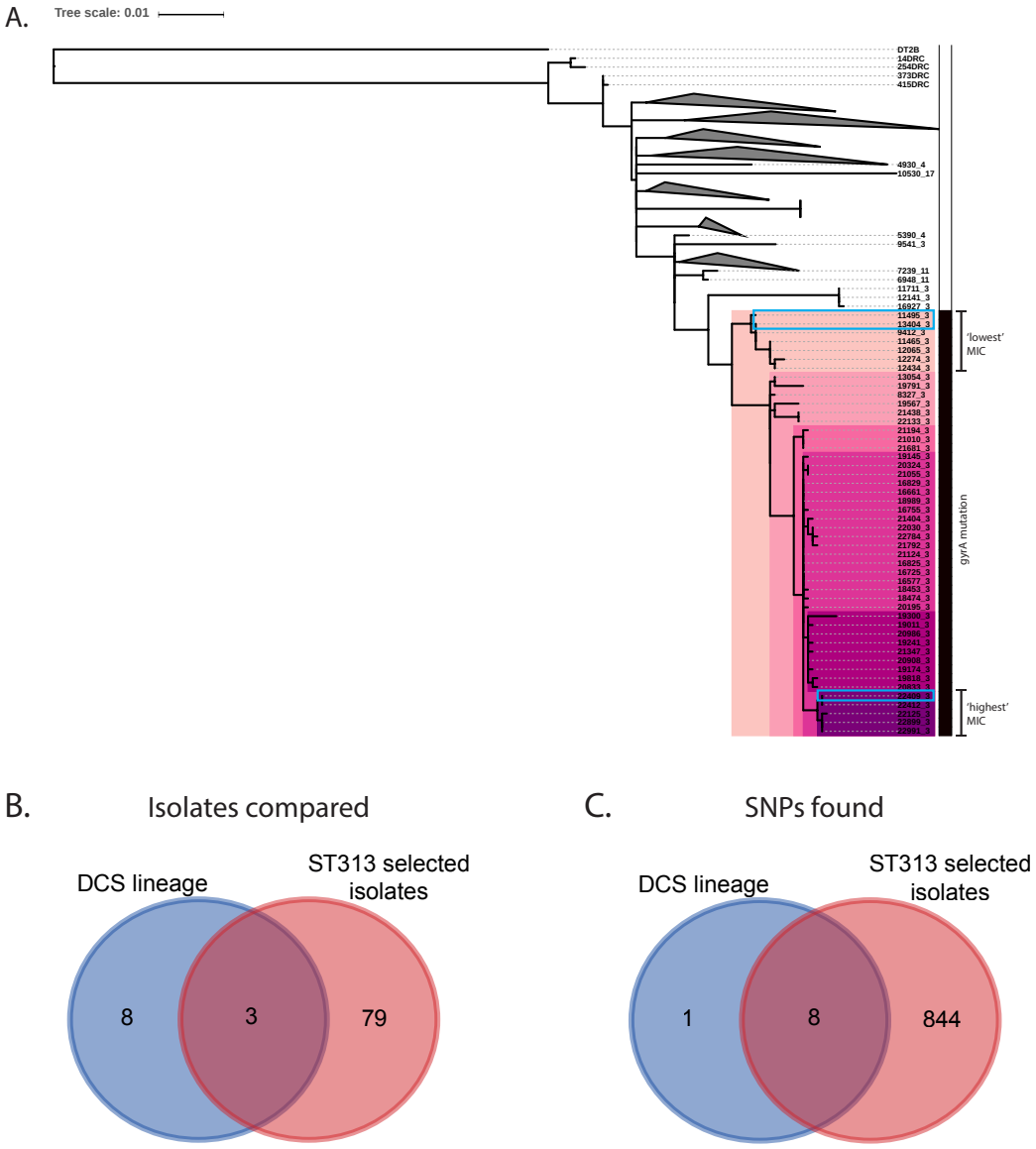

Figure 7.2 Comparison of SNPs in coding regions found in an DCS lineage of ST313 and 82 selected *S.* Typhimurium ST313 isolates. A. A phylogenetic tree of African *S.* Typhimurium ST313 isolates showing a DCS lineage of isolates all carrying a *gyrA* mutation. SNPs were compared between the group of isolates in the lightest pink group ("lowest" MIC) and darkest purple ("highest" MIC). Isolates in blue boxes were those that overlapped within the DCS lineage and 82 ST313 isolate SNP analyses. Adapted from Van Puyvelde *et al.*, personal communication. **B.** Venn diagram showing the overlap in isolates between the two SNP analyses conducted. **C.** Venn diagram showing the overlap in SNPs found between the DCS lineage and 82 ST313 isolate SNP analyses.

were found in genes *speF*, *ybjC*, *yniB*, *orf70*, *eutA*, and *aceB* (**Table 7.1**). Interestingly, three of the six non-synonymous SNPs were in genes encoding membrane-associated proteins.

Table 7.1 Coding SNPs found in highest MIC isolates compared to lower MIC isolates.

Gene	Description	Codon position	Amino acid change	Effect
speF	Ornithine decarboxylase	3	Phe -> Leu	Non-synonymous
ybjC	Putative membrane protein	1	Arg -> Ser	Non-synonymous
yniB	Putative membrane protein	1	Pro -> Thr	Non-synonymous
orf70	Putative pathogenicity island protein	3	Met -> Ile	Non-synonymous
pgtE	Outer membrane protease E	3	Gly -> Gly	Synonymous
eutA	Putative ethanolamine utilization protein EutA	2	Ala -> Val	Non-synonymous
invE	Cell invasion protein	1	Leu -> Leu	Synonymous
aceB	Malate synthase A	2	Val -> Ala	Non-synonymous
yjeT	Putative inner membrane protein YjeT	3	Ala -> Ala	Synonymous

Using this list of coding SNPs as a benchmark, we analysed SNPs found in the 82 ST313 isolates within the selected 108 African *S.* Typhimurium set. Given that the 82 ST313 isolates included lineage I and linage II isolates, there was a total of 852 coding SNPs. To filter these, we first looked for commonalities with the benchmark set from DCS lineage. We had an overlap of three isolates between the DCS set of 12 isolates and our set of 82, one isolate of which was in the 'highest' MIC group (**Figure 7.2 A-B**). Of the nine coding SNPs found in the benchmark set, eight of these were also found in our set of 82 ST313 isolates. The only SNP that was not in our set was one in gene *yjeT*, which encodes a putative inner membrane protein and was a synonymous SNP (**Figure 7.2 C**).

Table 7.2 Drug-associated genes containing SNPs amongst ST313 isolates.

Gene	Function
STMMW_02561	Putative drug efflux protein
mdfA	Multidrug translocase
STMMW_15441	Putative multidrug efflux protein
emrD	Multidrug resistance protein

It was difficult to extrapolate significance from this comparative analysis given the small sample size and the phylogenetic distance between the isolates included in our larger set, so we focused our analysis on functional groups that could be important in ciprofloxacin susceptibility. Interestingly, two of the genes these SNPs were found in encoded putative drug efflux proteins (**Table 7.2**). This suggests that there may be some proteins associated with drug efflux that could play a role in ciprofloxacin susceptibility and would benefit from greater characterization. Furthermore, there were two SNPs in the multidrug translocase *mdfA*, which belongs to the Major Facilitator Superfamily (MFS) transporter family along with *emrAB*. Nishino *et al.* found that deletion of *mdfA* in *S.* Typhimurium 14028s did

not change its susceptibility to nalidixic acid. However, overexpression of *mdfA* in an *S.* Typhimurium *acrB* mutant resulted in resistance to tetracycline, chloramphenicol, norfloxacin, and doxorubicin but an increased susceptibility to nalidixic acid[457]. Debroy *et al.* conducted a network analysis of efflux genes in S. Typhi, finding that there is a close interaction between *mdfA* and *acrA*, as well as with *macB*, which is implicated in an ABC-type efflux pump[554]. They further found that the MFS drug transport system was active against nalidixic acid and norfloxacin. It is as yet unclear what, if any, influence the SNPs in *mdfA* that we observed in ST313 isolates have on ciprofloxacin susceptibility.

emrD has a known association with multidrug efflux. Increased expression of *emrD* has previously been implicated in ciprofloxacin-resistant *S.* Typhimurium[454]. EmrD, like MdfA, belongs to the MFS of transporters, and it has been shown to efflux amphipathic molecules from the cytoplasm[555]. In addition to its role in multidrug resistance across multiple bacterial species including *Vibrio cholerae* and Gram-positive species, it has also been implicated in changes in biofilm formation[556,557]. While some preliminary functional studies have been conducted on EmrD, it is yet to be well-characterized, and the effect of SNPs on its structure and function are unknown. While we could not find any additional information for the two putative drug efflux proteins, we found that there was one ciprofloxacin susceptible isolate bkf00707 with the SNP in STMMW_02561, and there were three isolates—gha113289 gha113396, and D25023—with the SNP in STMMW_15441. Interestingly, both gha113289 and gha113396, which sit next to each other on the phylogenetic tree, had a nucleotide substitution, whereas D25023, which is a more distant relative, had a deletion at the SNP site. gha113289 was the isolate in our collection with the highest measured ciprofloxacin MIC and no known DCS determinants, which was an interesting observation, but we did not have isolates gha113396 or D25023 in our laboratory to investigate whether these also had a high MIC. We looked through all the SNPs in gha113289 to investigate whether there were any unique to this isolate but could only find SNPs that were shared with at least one other isolate. A more thorough analysis of these coding SNPs and also of the non-coding SNPs found within the set of 82 ST313 isolates might reveal greater insight into potential involvement in differential ciprofloxacin susceptibility.

7.3 Small-scale high content imaging screen of ciprofloxacin-exposed *S.* Typhimurium ST313 isolates

Following our exploratory genomic analyses, we wanted to image a subset of *S.* Typhimurium ST313 isolates to identify and measure morphological differences between them upon ciprofloxacin exposure. We chose an arbitrary subset of ST313 from the 108 African *S.* Typhimurium isolates we had analysed based on which isolates were available to us for phenotyping. While it would have been preferable to screen all 108 selected *S.* Typhimurium isolates, we were constrained by isolate availability and therefore chose 24 isolates to image under four different concentrations of ciprofloxacin (**Figure 7.3**).

The ciprofloxacin susceptibility of these isolates ranged from 0.016 to 0.75 μg/ml, 19 of which were ciprofloxacin susceptible and five of which had an "intermediate" susceptibility classification. We chose concentrations that correlate to MICs within the CLSI classifications for "susceptible", "intermediate", and "resistant" *S. enterica*. *S. enterica* are considered "susceptible" if they have a ciprofloxacin MIC of 0.06 μg/ml, and so we chose 0.06 μg/ml ciprofloxacin as our "sensitive" concentration of ciprofloxacin. *S. enterica* are considered to have "intermediate" susceptibility if they have an MIC between 0.12 and 0.5 μg/ml, and we chose our "intermediate" treatment condition to be 0.25 μg/ml ciprofloxacin. Finally, an MIC of ≥ 1 is considered resistant, so we used 1 μg/ml ciprofloxacin as our "resistant" treatment condition (**Figure 7.3 B**)[200].

After growing overnight cultures of the 24 *S.* Typhimurium isolates, we added them to wells containing 0, 0.06, 0.25, or 1 μg/ml ciprofloxacin and incubated them for 2 h. These were then imaged on the Opera Phenix high content microscopy followed by automated image analysis using our Harmony pipeline, as described in Chapter 3. We were then able to look for morphological differences between the isolates. We first assessed the number of bacteria that were analysed per well by the pipeline across the three biological replicates, splitting the bacteria by ciprofloxacin treatment (**Figure 7.4**).

Firstly, we found that replicates were largely consistent with one another, with the exception of isolates 453_08 and gha113848. Given the exploratory nature of our analysis, we decided to retain all of the replicates in our analysis, but in a larger-scale screen, it might be preferable

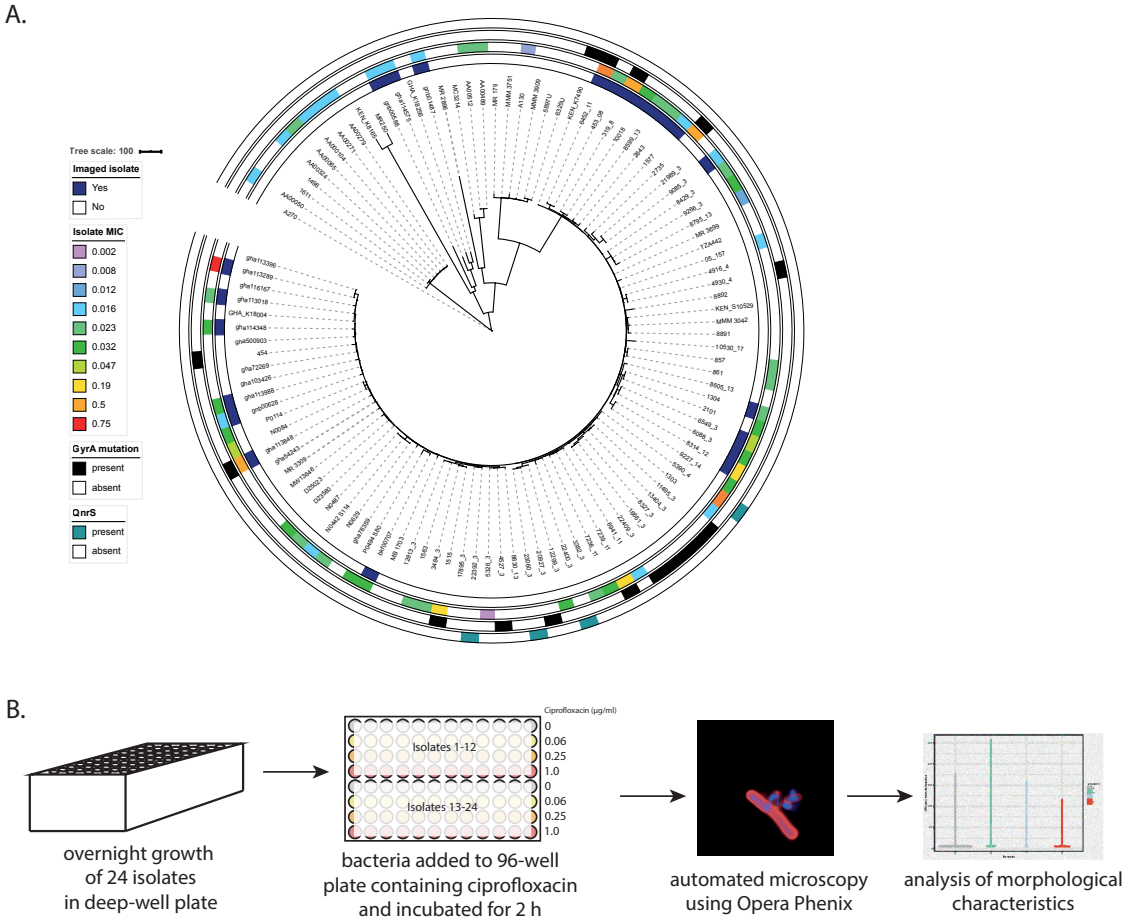

Figure 7.3 Choice of 24 *S.* Typhimurium ST313 isolates and workflow for high-content imaging. **A.** The 24 *S.* Typhimurium ST313 isolates that were chosen for phenotyping were denoted in dark blue (innermost ring) on the phylogenetic tree of the 108 African *S.* Typhimurium isolates. The ciprofloxacin MICs (second ring), *gyrA* mutations (third ring), and *qnrS* presence of the isolates were also marked. The set of 24 isolates for phenotyping had a range of ciprofloxacin MICs between 0.016 and 0.75 μg/ml. **B.** The workflow for high-content screening and analysis of the 24 *S.* Typhimurium ST313 isolates. Isolates were grown overnight in a deep-well plate, sub-cultured in the presence of ciprofloxacin for 2 h, imaged on the Opera Phenix, analysed using Perkin Elmer analysis software Harmony, and the measured morphological parameters were assessed.

to discard the outlier replicates or even all isolates with outliers. While the number of bacteria captured for analysis averaged 1000-5000 for most isolates, there were two isolates 6088_3 and 8314_12, which had between fewer than 1000 analysed bacteria per well. The two isolates are located adjacent to each other on the phylogenetic tree, suggesting that there could be a genetic basis to this difference from the other isolates (**Figure 7.3 A**). However, another highly related isolate 6549_3 also imaged did not have low bacterial counts. We could not discern clear differences between the number of bacteria analysed between the four

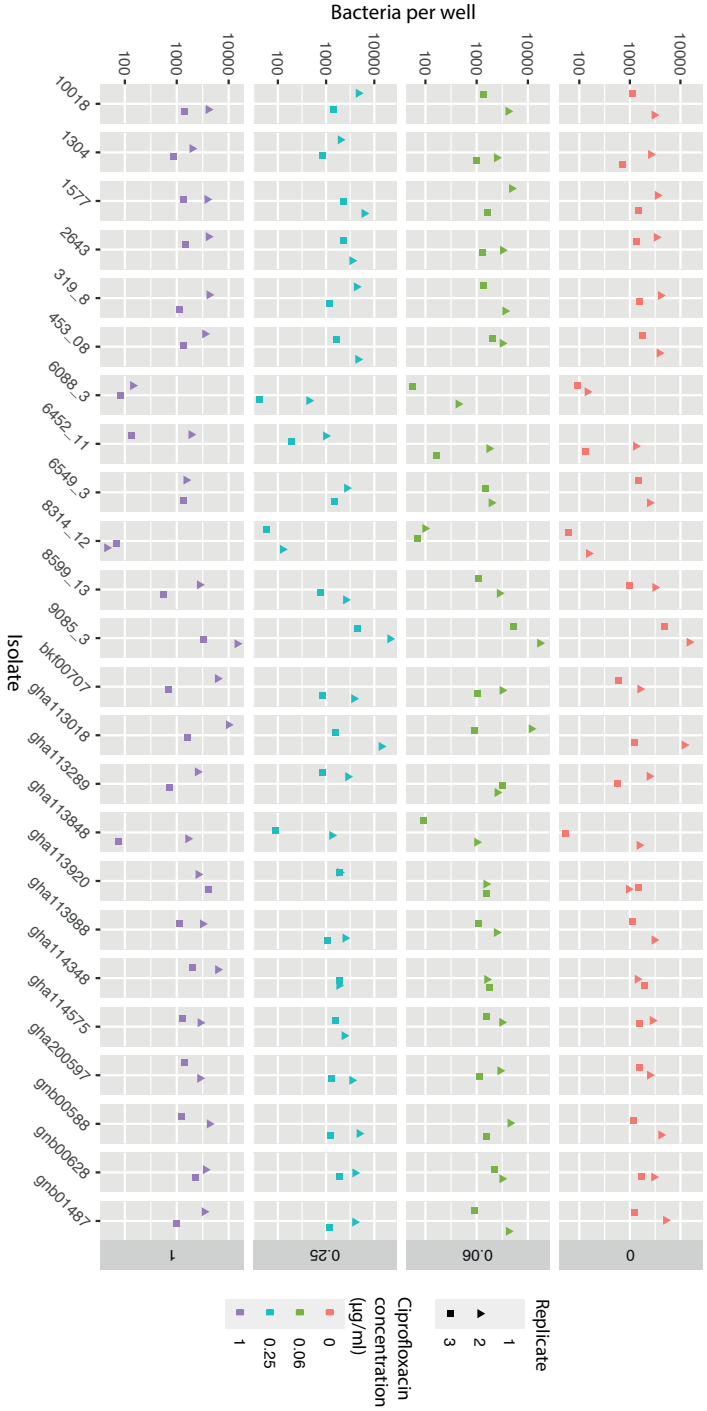

Figure 7.4 Number of analysed *S.* Typhimurium ST313 bacteria analysed per well across three replicates. The number of analysed bacteria for each isolate was determined using the Perkin Elmer Harmony software, and the number of bacteria from three biological replicates was divided by ciprofloxacin treatment to compare differences in bacterial numbers between treatments. Biological replicates are denoted by shape, and ciprofloxacin concentration added is denoted by colour.

ciprofloxacin treatments, and this may be because this level of analysis did not differentiate between live and dead cells.

We subsequently looked at the distribution of SYTOX Green fluorescence intensity, a parameter captured in the automated analysis pipeline. As described in Chapter 3, FITC-conjugated stain SYTOX Green was used in an attempt to differentiate between live and dead cells as SYTOX Green should only enter permeabilized cells. One caveat of this analysis is that the chosen time point of 2 h may not have been long enough for the membranes of dead or dying cells to rupture, and thus, we may have undercounted dead or dying cells. We initially looked at the SYTOX Green mean fluorescence intensity for each treatment independently by isolate, but there were no significant differences in the density distribution by treatment, so we consequently compared the SYTOX Green mean fluorescence intensity of each isolate, independent of the ciprofloxacin treatment (**Figure 7.5**).

There appeared to be some differences in the density distribution of SYTOX Green mean fluorescence intensity across the 24 isolates. We used a threshold of 1000 on the x-axis to differentiate between live cells (< 1000) and dead (> 1000), as described in Chapter 3. Looking at the density of bacteria within these two bins, it appeared that some isolates including 453_08, 6088_3, 8314_12, gha113848, and gnb00628 had a higher density of dead cells. For these isolates specifically, it may have been beneficial to scrutinize the density of SYTOX Green mean fluorescence intensity by ciprofloxacin treatment to see whether the proportion of dead cells was treatment-dependent. We referred back to the phylogenetic organization of these isolates to determine whether there was a pattern to this phenotype, but these five isolates were distributed across the phylogenetic tree (**Figure 7.3 A**).

We then wanted to look at additional parameters that might help us distinguish between isolates, with regards to their ciprofloxacin MICs. We chose three parameters that we have previously determined from *Z*'-statistics as being useful in organisms treated with ciprofloxacin: bacterial length-to-width ratio, DAPI radial relative deviation, and CSA threshold compactness 60%. Analysis of the bacterial length-to-width ratio across all isolates divided by treatment showed that there was little difference in the median length-to-width ratio between treatments for a given isolate (**Figure 7.6 A**).

However, we were surprised by the considerable variation observed between isolates. It was also interesting that there was not a clear pattern of greater variability in bacterial length

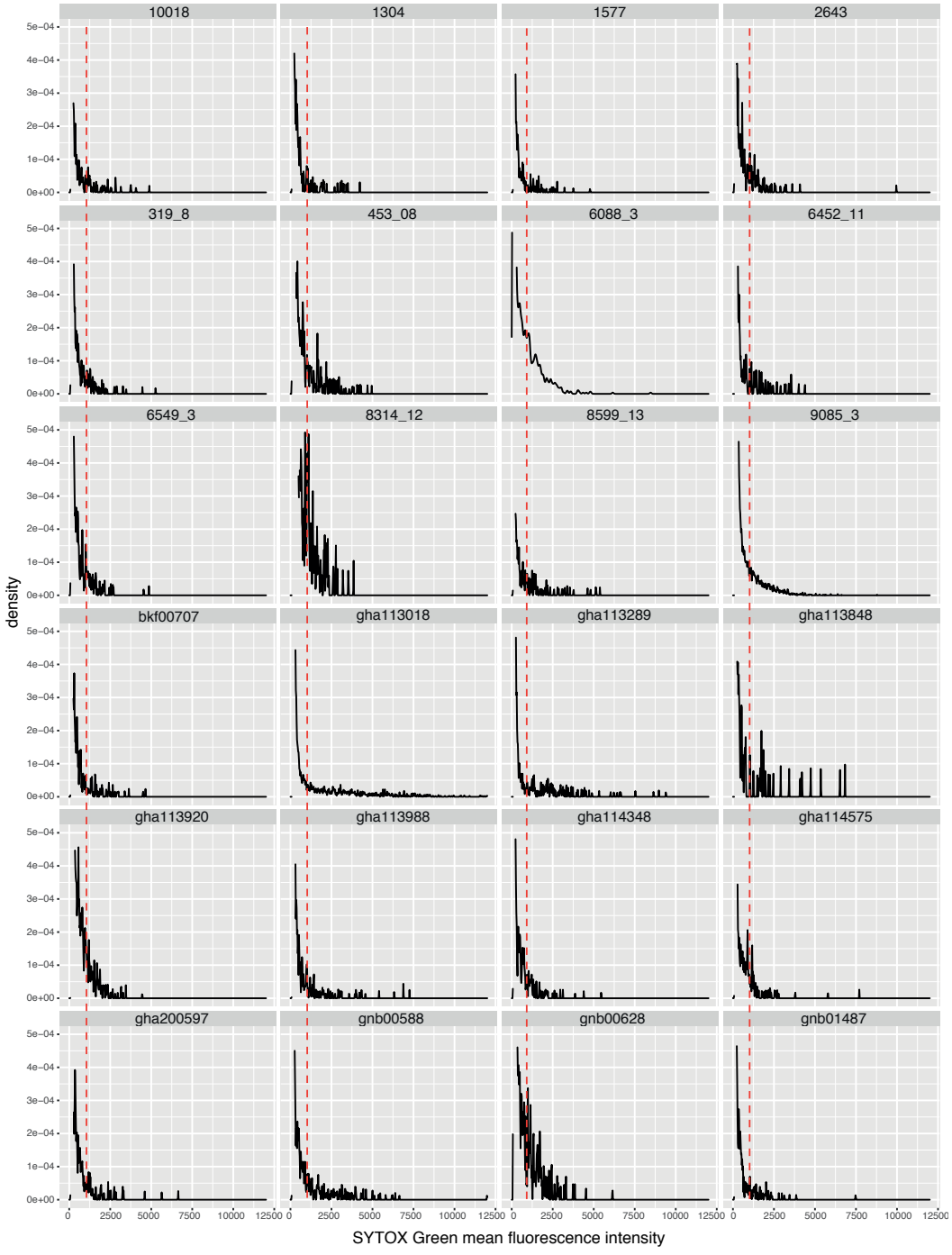

Figure 7.5 SYTOX Green mean fluorescence intensity for each of the 24 *S.* Typhimurium ST313 isolates. The SYTOX Green mean fluorescence intensity was calculated for each analysed object, and the distribution of the fluorescence intensity was plotted for each isolate. A threshold of 1000 fluorescence units was applied to demarcate live versus dead cells, using SYTOX Green fluorescence intensity as a proxy for cell viability. Differences in the density distribution were compared between isolates.

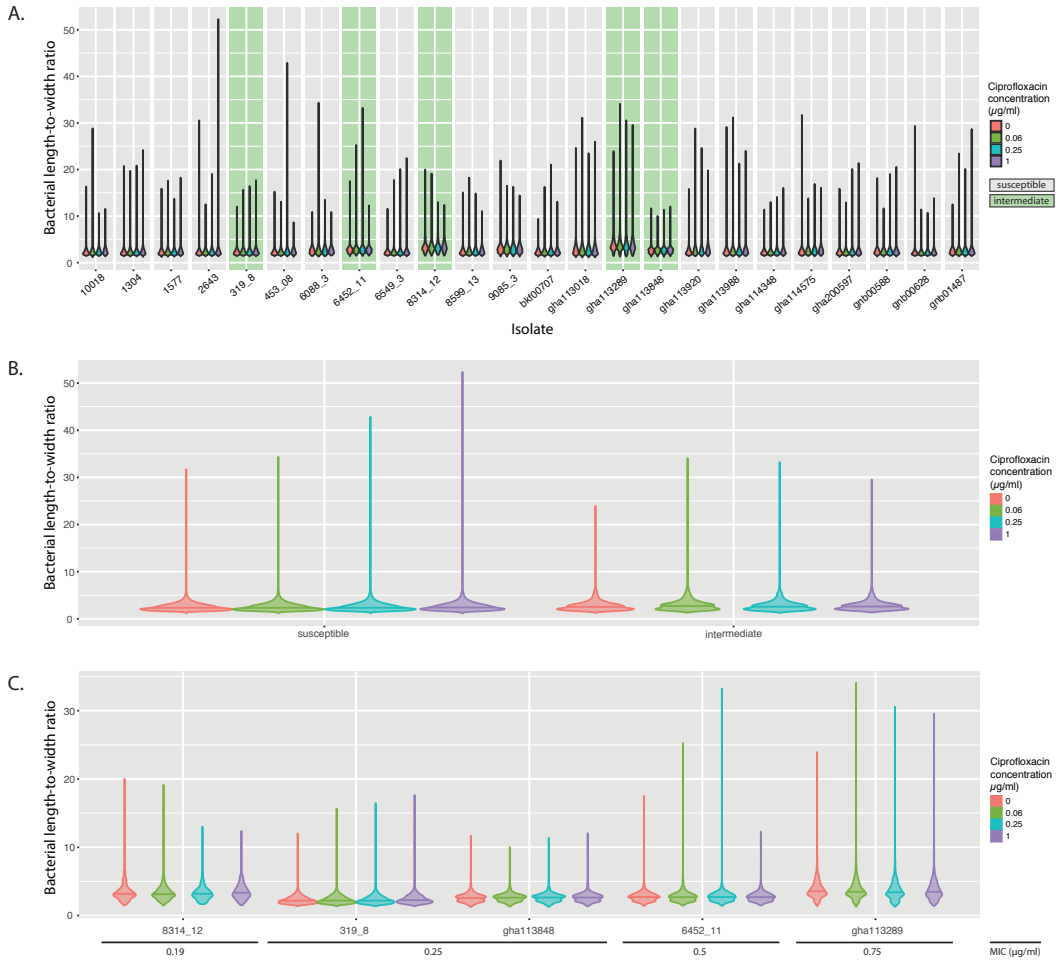

Figure 7.6 Measurement of the length-to-width ratio across isolates and ciprofloxacin treatments of 24 imaged *S.* Typhimurium ST313 isolates. A. The length-to-width ratio per analysed bacterium was compared for all isolates dependent on treatment. **B.** The isolates were divided into two groups depending on ciprofloxacin susceptibility ("susceptible" versus "intermediate"), and the bacterial length-to-width ratio was compared between groups for each ciprofloxacin treatment. **C.** The length-to-width ratio of "intermediate" susceptibility isolates were independently compared to one another, in ascending order of ciprofloxacin MIC (left-to-right) by ciprofloxacin treatment. Colours represent ciprofloxacin treatment, and all data are of three biological replicates.

with increased treatment. While isolate 2643 roughly displayed this behaviour of greatest variability in bacteria treated with 1 μg/ml ciprofloxacin, isolate gha114575 displayed the opposite phenotype. Isolates on the green panels were those with an "intermediate" ciprofloxacin MIC, but we could not detect any clearly distinguishable pattern that set these isolates apart from the susceptible ones.

To probe further into the association between ciprofloxacin susceptibility and the bacterial length-to-width ratio, we separated out the "susceptible" from "intermediate" MIC isolates (**Figure 7.6 B**). Here, while the median length-to-width ratio was similar between the two groups, we did see an increase of the greatest length-to-width ratio as the treatment increased for the "susceptible" isolates. This pattern was not detectable within the "intermediate" group. We noticed that the "intermediate" isolates had irregularly shaped violin plots, and we wondered whether this was due to the large differences in ciprofloxacin MIC between the five isolates. The MICs ranged from 0.19 to 0.75 μg/ml, a much larger difference than the range of the "susceptible" isolates, which was 0.016 to 0.047 μg/ml. Thus, we separated out the "intermediate" isolates to look at the length-to-width ratio independently for each (**Figure 7.6 C**).

Once again, we could not see strong patterns between treatments for a given isolate, but there were clear differences in the response between isolates. We were surprised by the distribution of length-to-width ratios found in gha113289, the isolate with the highest MIC, given that bacterial elongation suggests greater perturbation of the bacteria by ciprofloxacin. In contrast, isolate gha113848, a closely-related organism, which has an MIC of 0.25 μg/ml showed the least variation in the length-to-width ratio for any given treatment. It is possible that the known *gyrA* mutation in gha113848 accounts for its muted response, whereas because gha113289 does not have a *gyrA* mutation, it is not able to modulate its response to ciprofloxacin in the same way.

We next applied the same approach as above to look at the DAPI radial relative deviation and CSA threshold compactness 60% between the isolates, two fluorescence distribution parameters measured by the Perkin Elmer Harmony software (**Figures 7.7, 7.8**). The DAPI radial relative deviation is a measurement of the radial diffuseness of DAPI fluorescence within the cell. The CSA threshold compactness is a measurement of how concentrated the brightest 60% of pixels from the CSA membrane stain within an analysed object are. We hypothesized that elongated bacteria might have more diffuse DAPI across their length, but given the minimal changes in bacterial length between treatments, we were not able to distinguish any clear patterns in the DAPI radial relative deviation within or between isolates (**Figure 7.7 A**). We also could not detect any clear patterns in the CSA threshold compactness across isolates or treatments (**Figure 7.8 A**).

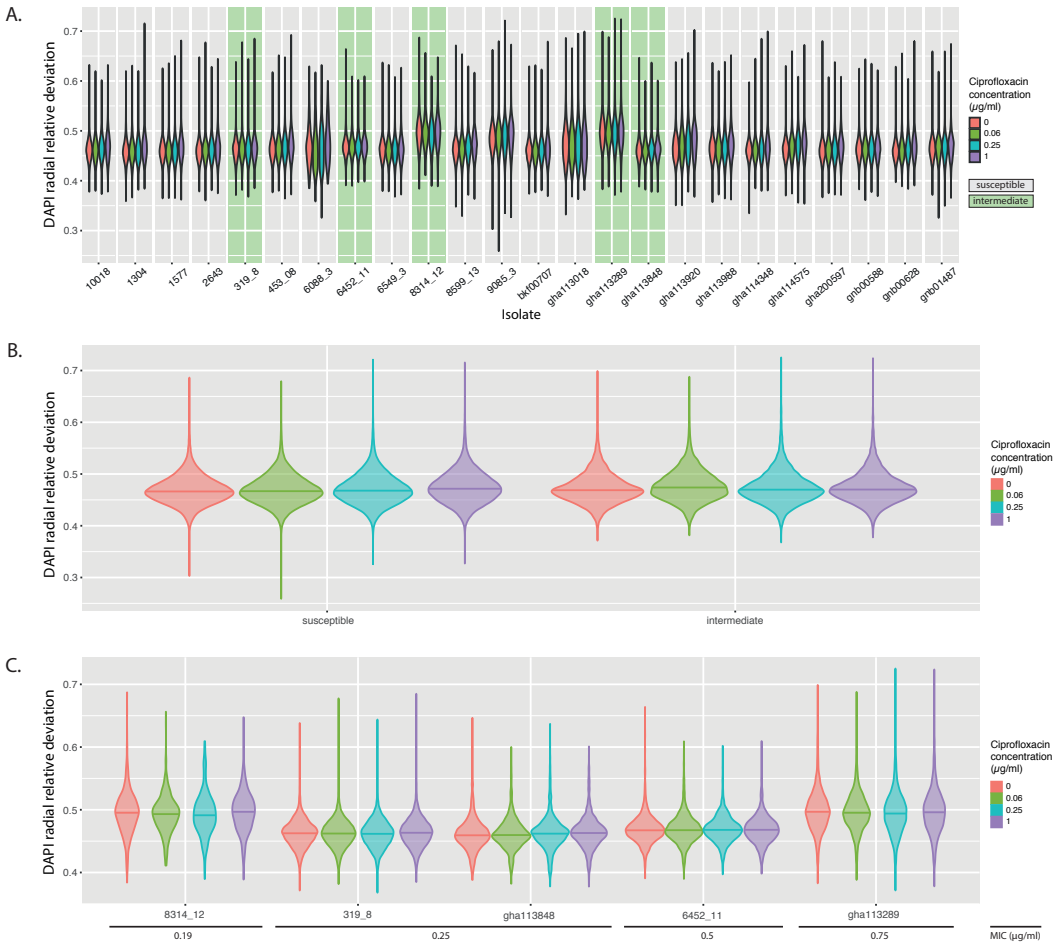

Figure 7.7 Measurement of the DAPI radial relative deviation across isolates and ciprofloxacin treatments of 24 imaged *S.* Typhimurium ST313 isolates. A. The DAPI radial relative deviation per analysed bacterium was compared for all isolates dependent on treatment. **B.** The isolates were divided into two groups depending on ciprofloxacin susceptibility ("susceptible" versus "intermediate"), and the bacterial DAPI radial relative deviation was compared between groups for each ciprofloxacin treatment. **C.** The DAPI radial relative deviation of "intermediate" susceptibility isolates were independently compared to one another, in ascending order of ciprofloxacin MIC (left-to-right) by ciprofloxacin treatment. Colours represent ciprofloxacin treatment, and all data are of three biological replicates.

We once again separated out the "susceptible" and "intermediate" isolates for the DAPI and CSA measurements, which showed even less difference than when comparing the bacterial length-to-width ratios, suggesting that these parameters were not independently useful in distinguishing between susceptibility levels. We once again saw differences between the "intermediate" ciprofloxacin MIC isolates when looking at them independently; however, we still could not detect any clear stepwise or differential patterns depending on MIC or treatment, respectively (**Figures 7.7 C, 7.8 C**). As we could not distinguish between isolates

Figure 7.8 Measurement of the CSA threshold compactness 60% across isolates and ciprofloxacin treatments of 24 imaged *S.* Typhimurium ST313 isolates. A. The CSA threshold compactness 60% per analysed bacterium was compared for all isolates dependent on treatment. **B.** The isolates were divided into two groups depending on ciprofloxacin susceptibility ("susceptible" versus "intermediate"), and the bacterial CSA threshold compactness 60% was compared between groups for each ciprofloxacin treatment. **C.** CSA threshold compactness 60% of "intermediate" susceptibility isolates were independently compared to one another, in ascending order of ciprofloxacin MIC (left-to-right) by ciprofloxacin treatment. Colours represent ciprofloxacin treatment, and all data are of three biological replicates.

by looking at independent parameters, we decided to perform a principal component analysis to explore how they clustered together.

To do this, we included all the morphological parameters and first analysed all 24 isolates, independently looking at the isolates treated with 0 μg/ml (no) and 1 μg/ml ciprofloxacin (**Figure 7.9**). It was immediately distinguishable that the bulk of the isolates clustered relatively closely together but that there were a few isolates that separated out. There

were seven of these "outliers" in the 0 μg/ml ciprofloxacin treatment and eight in the 1 μg/ml treatment. Interestingly, it was the same set of isolates that were "outliers" in both treatments, although they did not cluster in the same way (**Figures 7.9 A, 7.9 B**). These isolates were: gha113848, 6452_11, 9085_3, 8314_12, gha113289, gha113920, 6033_3, and 2643. Intriguingly, while this set included four of the five isolates with "intermediate" susceptibility, it did not include isolate 319_8 (blue). We referred back to its position within the phylogenetic tree, and we observed that it is most closely related to isolate 10018 (blue), with which it clustered relatively closely. However, it is also closely related to isolate 6452_11 (red), which did not reside in the main cluster of isolates. Given that both 319_8 and 6452_11 had *gyrA* mutations, we checked our earlier *in silico* AMR analysis to see whether they might have different *gyrA* mutations that could explain their differential response to ciprofloxacin. Indeed, we found that isolate 319_8 has amino acid substitution D87Y, while 6452_11 has amino acid substitution D87N.

Weigel *et al.* found that in fluoroquinolone-resistant isolates of eight *Enterobacteriaceae* species, the GyrA amino acid substitution impacted the ciprofloxacin MIC; however, it is difficult to extrapolate how well that correlates with DCS *S.* Typhimurium, which they did not test[558]. Baker *et al.* similarly found differences in ciprofloxacin susceptibility in isogenic derivatives of *S.* Typhi strain BRD948 depending on the *gyrA* mutation, although they did not include a D87Y substitution[217]. Another anomaly was isolate 6088_3 (dark green), which was susceptible to ciprofloxacin and did not cluster with any other isolates under 0 μg/ml ciprofloxacin, but appeared to be less distant when treated with 1 μg/ml ciprofloxacin (**Figure 7.9**).

To delve further into the differences between the "intermediate" MIC isolates, we then performed a separate principal component analysis on these five for each ciprofloxacin treatment (**Figure 7.10**). Here, we were interested to find that the clustering of the isolates after 0 μg/ml ciprofloxacin (no treatment) was distinct from the clustering following the other treatments (**Figure 7.10 A**).

In particular, isolates gha113848 (gold) and 6452_11 (red) were spatially separated without treatment, but following treatment, they clustered more closely together. However, we could not explain this by their MIC or *gyrA* mutation, both of which were different. They also did not cluster phylogenetically, but a deeper SNP analysis may provide greater insight. Interestingly, isolates 8314_12 with a *gyrB* mutation and gha113289 with unknown DCS

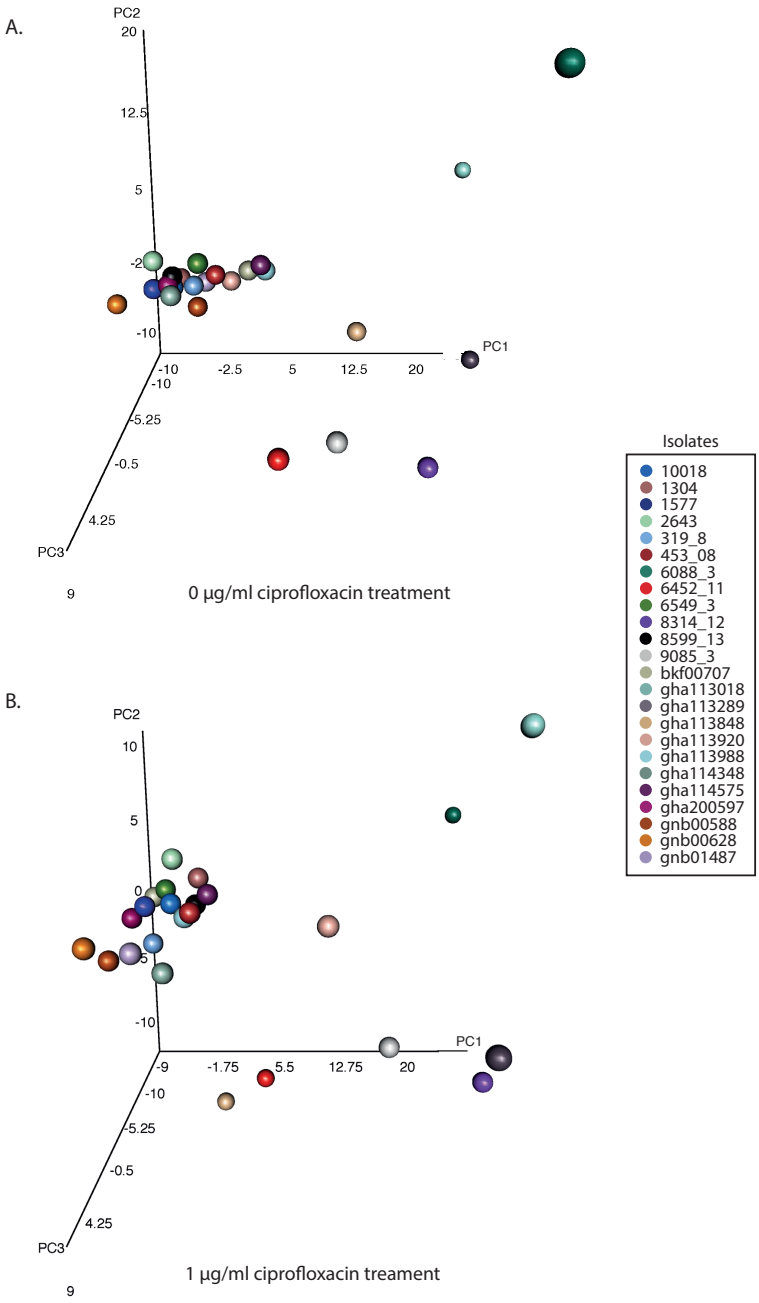

Figure 7.9 Principal component analysis of morphological parameters of 24 *S.* Typhimurium ST313 isolates following 0 or 1 μg/ml ciprofloxacin treatment. **A.** Separation of the 24 *S.* Typhimurium ST313 isolates imaged across the first three principal components following principal component analysis of morphological parameters analysed from growth for 2 h without ciprofloxacin treatment. **B.** Separation of the 24 *S.* Typhimurium ST313 isolates imaged across the first three principal components following principal component analysis of morphological parameters analysed from growth for 2 h in 1 μg/ml ciprofloxacin. Analysis was performed on combined three biological replicates, and each isolate was depicted in a different colour.

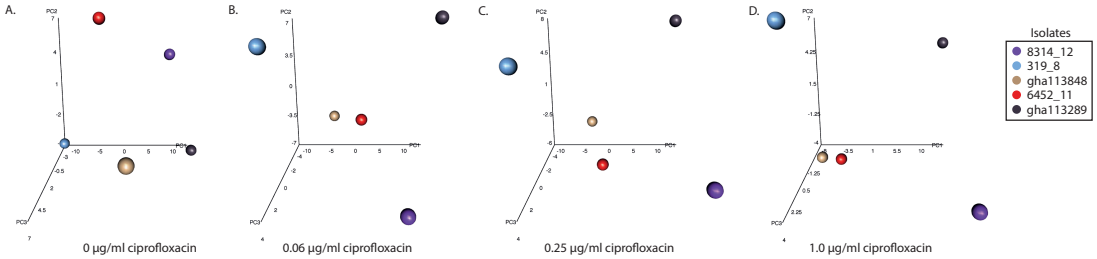

Figure 7.10 Principal component analysis of morphological parameters of 5 *S.* Typhimurium ST313 isolates with "intermediate" ciprofloxacin susceptibility following four different ciprofloxacin treatments. A. Principal component plot of the 5 *S.* Typhimurium ST313 "intermediate" isolates after growth for 2 h without ciprofloxacin treatment. **B.** Principal component plot of the 5 *S.* Typhimurium ST313 "intermediate" isolates after growth for 2 h in 0.06 μg/ml ciprofloxacin. **C.** Principal component plot of the 5 *S.* Typhimurium ST313 "intermediate" isolates after growth for 2 h in 0.25 μg/ml ciprofloxacin. **D.** Principal component plot of the 5 *S.* Typhimurium ST313 "intermediate" isolates after growth for 2 h in 1.0 μg/ml ciprofloxacin. Analysis was performed on combined three biological replicates, the first three principal components were plotted, and each isolate was depicted in a different colour.

mechanisms clustered distinctly from all the other isolates and each other. This may imply that the unknown mechanism of DCS in gha113289 is unique from the known ones found in the other isolates and results in distinct morphological changes to the bacteria. Identification of SNPs found uniquely in gha113289 compared against the other "intermediate" susceptibility isolates could help narrow down a potential DCS mechanism, for instance the putative drug efflux protein discussed earlier.

While the image analysis and subsequent principal component analyses did not identify any genetic mechanisms involved in ciprofloxacin susceptibility, they exposed some finer differences between the organisms that would not otherwise be obvious from genomic analysis and MIC testing.

7.4 Assessment of two distinct biofilm morphotypes in *S.* Typhimurium ST313 lineages.

Our final analysis in this line of study looked at the biofilm morphotypes of a set of 10 *S.* Typhimurium ST313 isolates. Previous work by Van Puyvelde *et al.* has shown the distinct biofilm morphotypes of isolates found on specific branches of ST313 lineage II and

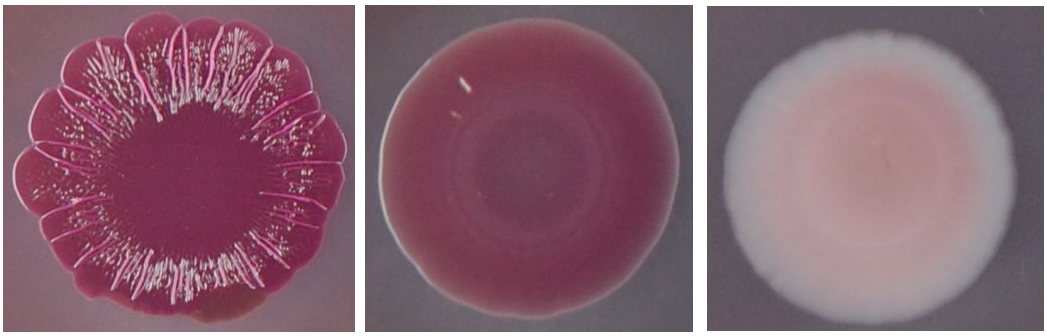

Figure 7.11 Colony morphotypes of *S.* Typhimurium bacteria grown under biofilm-forming conditions across ST19, ST313 lineage II, and ST313 lineage II.1. *S.* Typhimurium ST19 isolates grown under biofilm-forming conditions develop a distinct colony morphology known as "red, dry, and rough". *S.* Typhimurium lineage II isolates grown under the same conditions display red and smooth colony morphology, while ST313 lineage II.1 isolates display white and smooth colony morphology. Adapted from Van Puyvelde *et al.*, 2019[176].

connected the distinct biofilm morphotype to a 1-nucleotide gap in the poly-A stretch of the promoter of *csg*, the amyloid curli master regulator (**Figure 7.11**)[176,434].

We wanted to investigate these bacterial morphologies in greater depth using scanning electron microscopy (SEM) following biofilm growth conditions to determine whether there were discernible differences between isolates within colonies based on our pre-existing knowledge of the genetic factor and consequent biofilm morphology (**Figure 7.12**). Using ST313 lineage II reference isolate D23580 as a baseline, we compared nine isolates found in four different blocks across the phylogenetic tree. The isolates were chosen for their biofilm morphotypes of either red or white, both of which are found with ST313 lineage II isolates and distinct from the characteristic ST19 "red, dry, and rough" (RDAR) morphotype of ST19 isolates (**Figure 7.11**)[434].

The phylogenetic clusters were further chosen because of the observation of similar phylogenetic sub-structure within ST313 lineage II, which may imply some deeper similarities between these branches (**Figure 7.12 B**). We were able to compare five white colonies against five red colonies for SEM. We first looked for gross differences between the red (red box) and white (white box) morphotype isolates. It appeared that the red colonies were more likely to have a coat-like structure around them and seemed to be smaller and rounder, while the white

biofilm morphotype isolates appeared to be slightly more elongated and had more fimbriae. However, these distinctions were not uniform as isolate 6549_3 (red, 10 on the phylogenetic tree) showed bacterial length more similar to the white morphotypes and also appeared to have considerable fimbriae. Interestingly, isolate 8429_3 (white, 8 on the phylogenetic tree) lacks the *csgD* promoter gap, although we could not immediately link this information to the isolate's bacterial morphology.

We then scrutinized the SEM images by phylogenetic cluster to determine whether we could detect differences between clusters. It was difficult to pull out systematic differences between the isolates, especially given that there was considerable heterogeneity within a given bacterial isolate's image. To the untrained eye, isolate 6549_3 (red, 10 on the phylogenetic tree) looked most distinct from the rest, given that all the bacteria in the field were oriented in the same direction and did not display the wrinkled or shedding phenotype that many of the others had. Isolate 10433_3 (white, 6 on the phylogenetic tree) also looked distinct in that it did not have any surface decorations. We hypothesized that the substance being produced or shed could be amyloid curli, the primary component of *Salmonella* biofilms[434]. However, this remains to be confirmed, and we have requested specific anti-curli antibodies from collaborators.

We attempted to correlate biofilm morphotype to ciprofloxacin MIC, given the known correlations between these two factors. We found that all the red biofilm morphotype isolates with measured MICs were between 0.002 and 0.016 μg/ml (18 tested). In contrast, the white biofilm morphotype colonies had an MIC of 0.023 μg/ml (6 tested). This was a marginal difference in ciprofloxacin MICs, although we were intrigued by the consistently lower MICs of the red biofilm morphotype isolates. Given the small sample size in the overlap of isolates tested for biofilm morphotype and ciprofloxacin MIC, it was difficult to extrapolate real meaning from this information, and it would be worthwhile assessing the biofilm phenotype and ciprofloxacin MIC in a larger set of ST313 isolates. While we did not conduct pairwise SNP analyses of the isolates within each phylogenetic branch, it is possible that doing so could yield greater insight into how the genetic differences between these isolates are impacting biofilm formation. Conversely, a SNP analysis may help elucidate which morphological characteristics are more relevant in the context of biofilm formation. SEM imaging of the 10 isolates gave us a closer look at the morphological differences between the biofilm morphotypes contained within distinct phylogenetic clusters, but there is more work to be done to distil what these morphological characteristics mean.

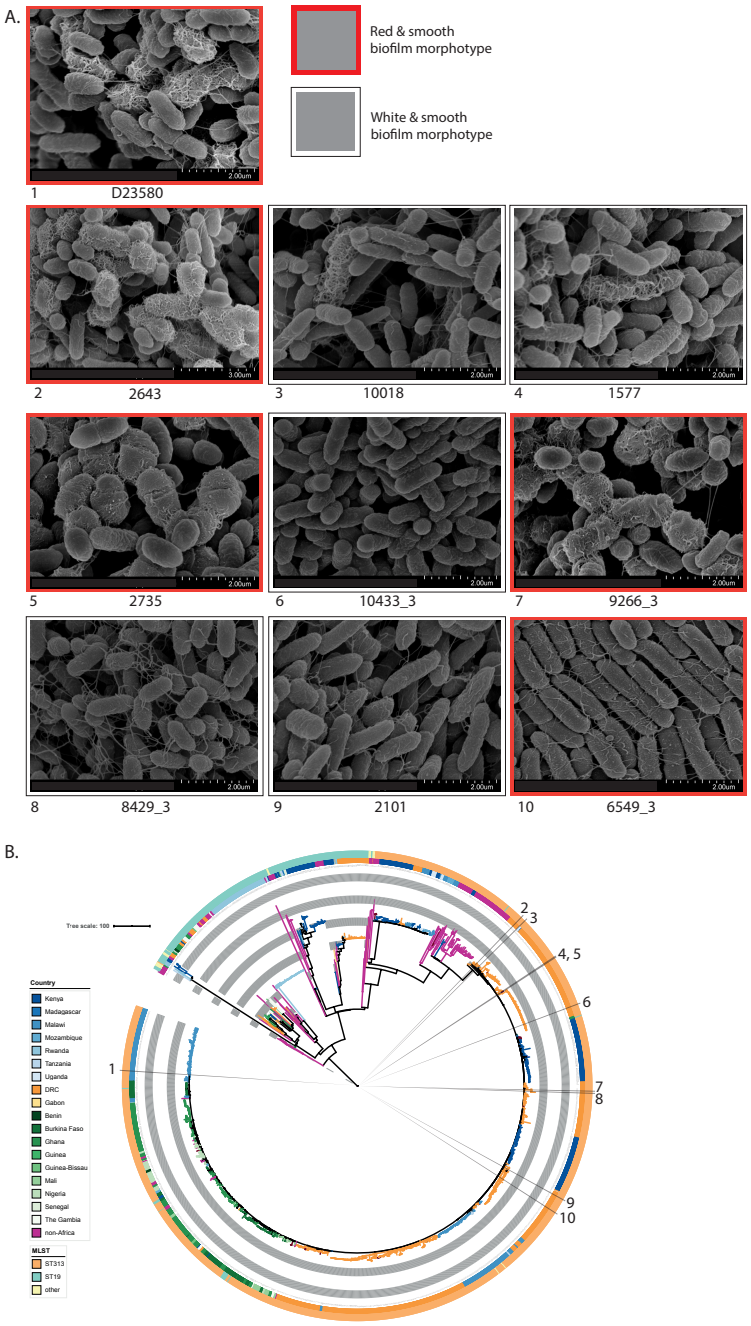

Figure 7.12 Scanning electron microscopy and phylogeny of selected *S.* Typhimurium ST313 lineage II and lineage II.1 isolates grown under biofilm-forming conditions. A. Scanning electron microscopy images were taken of 5 *S.* Typhimurium ST313 lineage II ("red and smooth" colony morphotype) and 5 lineage II.1 ("white and smooth" colony morphotype) isolates grown in biofilm-inducing conditions. Background box colour indicates whether the isolate has a red or white biofilm morphotype, and the number next to each isolate corresponds to location on the phylogenetic tree of African *S.* Typhimurium. **B.** Phylogenetic tree of *S.* Typhimurium with chosen isolates for SEM under biofilm-forming conditions highlighted in grey. Adapted from Van Puyvelde *et al.*, 2019[176].

7.5 Discussion

In this study, we attempted to gain greater insight into *S.* Typhimurium ST313 biology and bacterial response to stress by identifying links between genotype and phenotype. We began by choosing a representative set of 108 diverse African *S.* Typhimurium isolates to focus genomic and phenotypic analysis. On these isolates, we performed pangenomic and SNP-level analyses to identify potential genes and SNPs that may be implicated in ciprofloxacin susceptibility. The combination of phenotypic MIC data and SNP sequence data enabled us to focus on the differences in MIC that could be explained by the genetic basis of an isolate. While we were able to find some promising candidate SNPs and genes, particularly relating to drug efflux and hypothetical proteins, a larger set of phenotyped isolates would have given our pangenomic analyses greater power to discern differences between isolates with different ciprofloxacin MICs. Esaiassen *et al.* studied pathogenicity in the *Bifidobacterium* pangenome by measuring the MICs of a small set of 15 clinical isolates and then performing pangenomic analysis on these isolates and sequences from genomically-determined non-invasive and invasive isolates publicly available in GenBank. This enabled them to phenotype a small sample of isolates but compare these to a larger set of existing *Bifidobacterium* sequences[559]. However, their analysis did not find any pathogenicity traits associated with invasive isolates, similar to our lack of any specific genes linked to ciprofloxacin susceptibility or known DCS determinants. This suggests that a pangenomic analysis would benefit from a greater number of samples tied to more robust phenotypic data. For instance, Katiyar *et al.* performed a pangenomic analysis of phenotyped clinical isolates of *S.* Typhi, and they were able to find genes in the core genome linked to metabolism and in the accessory genome linked to AMR and pathogenesis[560]. In our analysis, it was essential to have phenotypic (MIC) data where possible because this allowed us to correlate mechanisms of DCS with the MIC. Performing pangenomic analysis in the absence of phenotypic data could be a rapid and powerful way of determining AMR in a large set of sequenced bacterial isolates, as shown by Moradigaravand *et al.*; however, this type of analysis paired with phenotypic information could provide greater insight into AMR differences between related organisms[561].

Combining SNP-based analyses with pangenomic analysis could yield yet more information on the relatedness between organisms and genetic factors contributing to a phenotype because it is possible to look for changes within genes in addition to their presence or absence. In our exploratory study of 82 *S.* Typhimurium ST313 isolates, it was feasible to compare the

limited number of SNPs because the organisms are highly related, which meant that we could more easily look for differences that might be associated with ciprofloxacin MICs. A study of *E. faecalis* and *E. faecium* showed that SNP-based analysis could differentiate between human-specific and human-associated isolates. Also, combining *in silico* and phenotypic antimicrobial resistance profiling was able to more precisely pinpoint genetic diversity in the organisms[562]. Similarly, Fashae *et al.* used a combined approach of MIC phenotyping and SNP-based analysis to distinguish between *Salmonella* species obtained from cattle and humans[563]. Our analysis of SNPs within genes of different functional groups gave us some insight into which pathways and cellular compartments were different between our 82 isolates of interest. However, it was still difficult to determine which SNPs and genes might be most relevant to investigate in greater detail to discover meaningful phenotypic differences.

An exploratory approach to studying genotype-phenotype interactions is to perform high-content phenotyping of organisms and then extract genes or SNPs from the genomic data that correspond to the phenotype. In recent years, high-content phenotyping has become more feasible, although this has not yet been used widely in screening bacteria for AMR profiles. We were interested in using such an approach to differentiate between a set of isolates treated with different levels of ciprofloxacin, and our imaging yielded multiple interesting findings. First, it appeared that 2 h treatment with ciprofloxacin might not be long enough to easily distinguish between dosages for a given isolate; second, there was considerable variability between isolates when looking at individual morphological parameters; and third, combined analysis of all morphological parameters may be able to help distinguish between isolates of differing ciprofloxacin susceptibility and phylogenetic relatedness. Shi *et al.* developed a method for rapid high-throughput imaging and analysis of bacterial collections using single-cell microscopy, which could be used for screening bacterial mutant libraries or cells grown in a variety of conditions[564]. Conceivably, the analysed output of their screen could be integrated with genomic data for the screened isolates to inform the link between genotype and phenotype. However, their screening platform did not integrate automated analysis of morphological features, which would be useful in extracting information about the imaged bacteria. Others have similarly developed high-throughput phenotyping protocols and methodologies, but these have not yet been applied in the context of large-scale phenotype-genotype studies[565–567]. While Grosheva *et al.* recently used high-throughput screening to demonstrate the impact of microbial factors on intestinal barrier function and integrity, their study did not image at single-cell bacterial resolution to distinguish bacterial morphologies

that could influence barrier function[568]. A similar screening approach but looking at infection dynamics of a group of ST313 isolates and identifying morphological differences between them could be an important next step in understanding differences between ST313 isolates and relevance in infection.

Importantly, our high-content imaging and analysis illustrated the utility of image analysis in distinguishing differences between bacterial isolates that were not readily apparent. This was particularly true in trying to differentiate between the 10 ST313 isolates grown under biofilm-forming conditions because we could not objectively analyse minute morphological differences between isolates by eye. It would be beneficial to follow up our initial morphological studies of the biofilm morphotypes by high-content imaging analysis of bacteria grown in biofilm-forming conditions. It is possible that we would then be able to detect differences between the isolates on discrete branches of ST313 lineage II that display the white biofilm morphotype. Furthermore, despite evidence suggesting a link between reduced biofilm formation and ciprofloxacin resistance, we could not detect any strong correlation in our small set of isolates. Once again, high-content imaging of the interesting biofilm morphotypes under ciprofloxacin treatment might produce previously unexplored morphological insights that could connect the two.

Overall, in this study, we investigated a set of African *S.* Typhimurium isolates with the objective of interrogating their genomes and morphological properties for greater insight into differences in ciprofloxacin susceptibility and biofilm formation. We used a combined approach of phylogenetics and high-content imaging to search for differences and similarities across isolates. Although we did not immediately find any obvious genes or SNPs implicated in ciprofloxacin susceptibility, we did learn that the type of QRDR mutation may play a significant role in the bacterial response to ciprofloxacin, and that there may be some putative drug efflux proteins that could be implicated in ciprofloxacin susceptibility. We further found that a high-content imaging approach to screen large numbers of bacteria is not only feasible for this type of analysis but may add considerable insight to our understanding of highly related organisms under antimicrobial or other pressures. In addition, we found that the agnostic approach of automated image analysis may be significantly better at recognizing important morphological differences between bacteria than we can by eye. Given the reduction in cost and feasibility of whole genome sequencing as well as the ease and robustness of high-content imaging and analysis, it could be beneficial in the future to more

systematically integrate genomic and morphological analyses for understanding antimicrobial resistance patterns, infection dynamics, and other bacterial characteristics.

8. Developing and implementing a SARS-CoV-2 testing workflow in a CL2 research laboratory for screening and viral sequencing

8.1 Introduction

Coronavirus disease (COVID-19) is a novel disease caused by severe acute respiratory syndrome coronavirus 2 (SARS-CoV-2), which emerged as a serious public health threat in Wuhan, China in December 2019[593,594,567]. SARS-CoV-2 is a highly-transmissible positive-sense, single-stranded RNA coronavirus, which causes a range of symptoms, from a mild fever to severe pneumonia requiring intervention[596]. In addition, SARS-CoV-2 appears to be readily spread by asymptomatic carriers[597]. Due to its transmissibility, SARS-CoV-2 rapidly spread beyond China, and the World Health Organization declared a pandemic on March 11, 2020, at which point there were 118,319 cases and 4292 deaths globally[598]. In the UK, while there was not yet a high burden of COVID-19 cases, the number was increasing, and by March 23rd, when the UK instituted a country-wide lockdown, there were over 300,000 cases globally and 5687 confirmed cases and 281 deaths in the UK[599].

A common diagnostic test for SARS-CoV-2 is real-time reverse-transcriptase polymerase chain reaction (RT-PCR) from a nasopharyngeal swab, which detects viral particles in the sample[600,601]. An alternative to RT-PCR-based assays for hospital-admitted patients is chest x-rays, which have a greater sensitivity but are not feasible for early detection or screening purposes[602]. The principle of an RT-PCR assay is conversion of RNA to DNA using the enzyme reverse transcriptase and subsequent amplification of the DNA. The virus is detected by including SARS-CoV-2 specific primers linked to a fluorescent probe, and the detection is assayed in real time by quantifying the amount of fluorescence from the specific probe[603]. At the outset of the pandemic, SARS-CoV-2 was designated a containment level 3 (CL3) organism in the UK by Public Health England (PHE) based on the lack of treatment and the potential for adverse outcomes from infection[604]. Potential positive samples had to be

handled within a CL3 facility until fully inactivated. Therefore, there was a bottleneck in testing capabilities due to the limitations in CL3 facilities nationwide and the time required to inactivate samples. This had a deleterious effect on the number of samples that could be safely processed, thus limiting the ability to detect and treat COVID-19 patients.

In particular, at the outset of the UK lockdown, limited testing posed a challenge to early detection amongst the healthcare worker (HCW) population, which was vulnerable due to high risk of exposure and elongated contact with COVID-19 patients[593,605–607]. Additionally, due to public health guidance, there was likely a large proportion of healthcare workers self-isolating, thus reducing the number of staff available within hospitals[608–610]. Furthermore, it was desirable to conduct SARS-CoV-2 surveillance within hospitals to mitigate the risk of hospitals becoming outbreak epicentres. However, given the low testing capacity and increasing patient volume in the UK in late March and early April, it was not feasible for hospitals to test HCW in addition to patients. As a result, one possible solution was the utilization of research laboratories proximate to hospitals to increase testing capacity. This could be carried out with strict safety protocols in place and adherence to PHE-approved testing procedures.

Thus, our CL2 laboratory on the Biomedical Campus of the University of Cambridge, proximate to the Cambridge University Hospitals (CUH), began assisting CUH by screening HCW for SARS-CoV-2 from early April 2020. This involved the modification and optimization of existing non-kit viral inactivation protocols to quickly and easily work with patient samples at CL2, bypassing the time-consuming and rate-limiting CL3 inactivation steps[611]. In addition to optimizing and validating CL2 sample extraction procedures using home-made reagents, we liaised extensively with the regional PHE personnel within Addenbrooke's Hospital to ensure standardization of our protocols and results with theirs. We worked closely with clinicians within Addenbrooke's hospital to create a streamlined workflow to obtain samples from HCW, process them and run the diagnostic RT-PCR, and report results directly to the clinicians. We were able to train a designated workforce within our laboratory to run each step of the pipeline and ensure timely result reporting. Finally, we were able to transfer the extract RNA samples from our workflow to other groups within the hospital to enable rapid whole genome viral sequencing. As a result of screening nearly 10,000 HCW over a three-month period, we were able to detect small clusters of infected HCW on hospital wards and found that asymptomatic carriage may play a significant role in COVID-19 transmission within hospital settings.

While this period from late March through early July was highly disruptive to my PhD, it was an opportunity to be involved in the local COVID-19 response and use my expertise and training to contribute to COVID-19 epidemiology, diagnostic testing, and sample workflows. Specifically, a core group of lab members tested pre-existing PHE RT-PCR assays to recapitulate results in our laboratory. We tested a number of RT-PCR master mix reagents to optimize test sensitivity, specificity, and costs using a pre-existing set of known positive SARS-CoV-2 samples. I was one of the leads on this work. We then established and optimized a standardized set of protocols to manage incoming swabs from HCW, including determining appropriate handover procedures to maximize our sample throughput and minimize our turnaround times. Five lab members were trained on hospital sample management software to directly register samples received in the lab and update test results. One of the greatest complexities was maintaining effective communication with the clinical team and associated research nurses to anticipate and manage sample numbers with quick turnover.

8.2 A blueprint for the implementation of a validated approach for the detection of SARS-CoV-2 in clinical samples in academic facilities.

In this study, we established and implemented a set of procedures to perform diagnostic testing for SARS-CoV-2 in a CL2 laboratory. We validated and optimized the RT-PCR protocol used in the Cambridge University Hospitals diagnostic lab, developed a sample workflow from the hospital to our lab, and created a comprehensive system of space and personnel to manage each step of the sample processing and SARS-CoV-2 testing[612]. A pdf version of the paper can be found here.

8.3 Screening of healthcare workers for SARS-CoV-2 highlights the role of asymptomatic carriage in COVID-19 transmission.

For this study, we performed SARS-CoV-2 testing using the protocols and workflows discussed in section 8.2. The HCW swab results we reported to CUH clinicians were combined with collated information from HCW about their symptoms to determine the rate of symptomatic and asymptomatic infections amongst a subset of the hospital staff. The extracted viral RNA from SARS-CoV-2 positive cases were additionally used for viral genome sequencing[613]. A pdf version of the paper can be found here.

8.4 Effective control of SARS-CoV-2 transmission between healthcare workers during a period of diminished community prevalence of COVID-19.

The work in this study followed on from that discussed in section 8.3, in which we continued testing symptomatic and asymptomatic HCW for SARS-CoV-2. The period captured in this study was from April 25th to May 24th, 2020, during which 3388 swabs were obtained from HCW. We used our pre-established protocols and workflows to extract RNA and perform RT-PCR on these samples, finding 34 positive tests, a 1.0% positivity rate across asymptomatic and symptomatic testing initiatives. From our testing, we were able to detect a small ward-based outbreak of cases, enabling a rapid response from the hospital for additional screening and cleaning measures[614]. A pdf version of the paper can be found here.

8.5 Rapid implementation of SARS-CoV-2 sequencing to investigate cases of health-care associated COVID-19: a prospective genomic surveillance study.

This study was a genomic analysis of SARS-CoV-2 cases in hospital settings within CUH and East of England. Viral sequencing was conducted using nanopore sequencing on samples from hospital patients and healthcare workers. Our involvement in this study was the RNA extraction and SARS-CoV-2 testing of HCW samples. Any positive RNA samples were transferred for nanopore sequencing[615]. A pdf version of the paper can be found here.

8.6 Secondary pneumonia in critically ill ventilated patients with COVID-19.

As part of our SARS-CoV-2 RT-PCR diagnostic testing, we also assisted CUH by providing early results for patients receiving mechanical ventilation in the intensive care unit (ICU) based on RNA samples extracted in a CL3 laboratory. During a period of high volumes of SARS-CoV-2 testing within the hospital, we were able to rapidly run RT-PCR tests and report results. Any positive samples were subsequently assayed for secondary pathogen signatures using a TaqMan multi-pathogen array card. By doing this, it was possible to assess associations between COVID-19 positivity and ventilator-associated pneumonia (VAP). While this was a small study with a few patients, it was possible to determine that there was a higher rate of VAP within the COVID-19 positive patients[616]. A pdf version of the paper can be found here.

9. Future directions

In the body of work presented, we explored the response of *S*. Typhimurium to ciprofloxacin, optimised assays for high-content imaging of bacteria, and probed for genomic and phenotypic characteristics in *S*. Typhimurium ST313. While these studies produced some interesting observations, there are many additional avenues of exploration that would strengthen our understanding of *S*. Typhimurium and the bacterial response to ciprofloxacin and other stressors.

9.1 Further development of genotype-phenotype investigations

In Chapter 3, we developed methodologies for high-content imaging (HCI) of bacteria using the Opera Phenix imaging platform. While we have implemented a fairly robust imaging setup, there are many improvements and advances that could be made to our methods. Firstly, given the resolution of single-bacterium imaging on the Opera Phenix, it would be useful to study bacterial subcellular properties. One strategy for doing so would be to develop bespoke reporter bacterial stains, such as with novel combinations of LPS and O-antigen to study biofilm formation[569]. Additionally, isolates expressing GFP of specific reporters might be useful. In addition, the detection of flagella could also be important, possibly even to determine how well a given isolate might adhere to imaging plates[570]. Another way to better study bacterial subcellular properties would be to improve the analysis pipelines in the Perkin Elmer Harmony software. In our existing pipelines, we did not segment bacteria after classifying them as single cells, but it may be possible to delineate membrane thickness, localization of nucleic acids, and other properties, with more fine-tuning. Doing so might give us some insight into how bacterial subcellular morphologies change with perturbation or vary between organisms[571]. Finally, the next step in understanding bacterial population heterogeneity and temporal changes is to implement live-cell imaging using the Opera Phenix. An added complexity of doing this on bacteria alone is their motility, and live cell imaging of *Salmonella* has largely been done in the context of host cells[572]. Single-cell live bacteria imaging has been achieved on low-throughput confocal microscopes, and Varadarajan *et al.* describe a time-lapse microscopy protocol for *E. coli* using agarose gel pads, and a similar

protocol could be adapted for *Salmonella*[573]. Plochowietz *et al.* used a similar agarose gel pad method for imaging tRNA diffusion within live *E. coli*, illustrating the utility of single cell imaging for not only tracking individual bacteria over time but also visualising subcellular changes[574].

We used our existing fixed-cell imaging method in Chapter 4 to study the temporal response of *S*. Typhimurium to ciprofloxacin, and while we were able to observe changes in bacterial length over time in response to ciprofloxacin, there is far more to be investigated. One important assessment would be determining the most influential parameters influencing bacterial morphological changes and how those vary between treatments. Additionally, we were able to measure the distribution of bacterial length over time, but we did not distinguish subpopulations within each field. Given our findings regarding the different transcriptional responses of denser and less-dense bacteria upon ciprofloxacin exposure, it would be important to determine the heterogeneity of morphology in the population. Many hypotheses exist about the nature of bacterial heterogeneity in response to stress, and it remains unclear whether a given bacterial population is homogeneous prior to perturbation and diversifies its response or is initially heterogeneous and that subpopulations respond or expand differentially[575].

Sánchez-Romero and Casadesús demonstrated the role of differentially expressed efflux pumps and porins in a subpopulation of *S*. Typhimurium grown in nalidixic acid, revealing the importance of studying these[576]. It is not yet known whether these subpopulations can be morphologically distinguished at the single cell level, which could be investigated using single cell imaging and differentiating the bacterial populations through image analysis. Ideally, this would be performed using live cell imaging, which could additionally inform us about the relative growth and viability of individual cells. Sánchez-Romero and Casadesús used flow cytometry to differentiate between subpopulations, and it may be possible to use fluorescence activated cell sorting to separate these for whole genome and RNA-sequencing to determine mutational and adaptive resistance[576]. It has previously been demonstrated that bacterial efflux may increase due to gene duplications of *acrAB*, and measuring genetic and epigenetic changes in a subpopulation of ciprofloxacin-treated bacteria may help pinpoint which processes are responsible[577,578].

Furthermore, we did not link the phenotypes we observed regarding temporal growth to the genetic background of the bacteria measured. We observed that there were differences between

the two *S*. Typhimurium isolates measured—ST313 D23580 and ST34 VNS20081—but we did not perform a direct comparison of these two. Here, it would be informative to look at SNP differences between the two isolates and determine whether there are any that could explain the morphological changes we observed. It may also be relevant to compare the transcriptional response of subpopulations of the two bacterial isolates to understand the heterogeneity of response to ciprofloxacin across isolates.

In Chapter 7, we similarly used the Opera Phenix to screen a diverse set of 24 S. Typhimurium ST313 isolates in the presence of ciprofloxacin. There, we did attempt to connect the morphological differences between the isolates to their genetic backgrounds, although there is far more to be studied. To further develop this approach, it would be useful to screen a larger set of isolates. Doing so would tell us whether the variation we observed between isolates holds true across the phylogenetic tree of ST313. Van Puyvelde *et al.* have observed repeated phylogenetic substructures within *S*. Typhimurium ST313 lineage II, and it would be useful to understand how these phylogenetically distinct groups cluster morphologically, and whether there is convergent evolution towards a common phenotype (Van Puyvelde, personal communication)[176]. Moreover, MacKenzie *et al.* have recently studied biofilm formation in invasive nontyphoidal *Salmonella* from Africa, finding parallel reduction in biofilm formation between isolates of *S*. Enteritidis and *S*. Typhimurium due to SNPs in the biofilm production master regulator *csgD* or its promoter[434]. They were able to show the phenotype of *csgD* impairment and extrapolate to historic isolates of S. Typhimurium ST313. Given our access to more recent ST313 isolates, some of which also show decreased ciprofloxacin susceptibility (DCS), it would be useful to phenotype a larger set of isolates for their biofilm morphology, follow this by screening of isolates with diverse biofilm morphologies, and look for SNPs shared or divergent between these isolates.

9.2 Effects of ciprofloxacin on *Salmonella* invasion of host cells

With the exception of our pilot study of a *S*. Typhimurium D23580 TraDIS library infection of intestinal organoids, all of our studies were conducted on bacterial cultures. While this was an important first step, we recognize the necessity of studying the response of bacteria

to ciprofloxacin in the context of host cells. While bacteria may encounter antimicrobials in the environment prior to entering a host, the greatest exposure to antimicrobials would be during an infected person or animal that gets treated with antimicrobials. However, the concentration of drug that bacteria are exposed to depends on the drug pharmacokinetics and pharmacodynamics, and interaction of the host immune system. Sakoulas *et al.* demonstrated that clinical isolates *S. enterica* serotype Newport pre-treated overnight with 0.25x MIC of ciprofloxacin showed no difference compared to non-treated bacteria in neutrophil killing assays. However, they found that bacterial survival was significantly reduced if pre-treated with 1x MIC ciprofloxacin and then 0.25x MIC of immune factor cathelicidin LL-37, suggesting a synergistic role for ciprofloxacin and LL-37 in enhanced neutrophil killing of *Salmonella* species causing meningitis[404]. It would be beneficial to perform similar studies using gut-relevant immune cells, such as macrophages, to understand the effect of ciprofloxacin on *Salmonella* invasion and replication. Given our prior assessment of bacterial subpopulations that form under ciprofloxacin treatment, it could be relevant to treat *S*. Typhimurium with ciprofloxacin for two hours, similar to many of our previous assays, and then measure invasion and intracellular replication. Moreover, imaging of the infected cells could help elucidate whether bacterial morphology (elongated versus non-elongated bacteria) influences infection potential.

In addition to studying the dynamics of macrophage infections after *Salmonella* pre-treatment with ciprofloxacin, it would also be useful to investigate the effect of *Salmonella* infection on cells that have been incubated in medium containing ciprofloxacin. Anuforom *et al.* showed that *S*. Typhimurium SL1344 had reduced invasion of J774 murine macrophages when the macrophages were treated with ciprofloxacin, but there was greater adhesion to cells[365]. A study by Tarazona *et al.* demonstrated that *Brucella militensis* infecting canine macrophages exposed to ciprofloxacin had fluoroquinolone MICs ten times higher than bacteria grown in non-exposed macrophages. However, despite the acquisition of GyrA mutations in the ciprofloxacin-exposed set, the mutants did not infect new macrophages at a higher rate than the wild-type bacteria[579]. Barcia-Macay found that intracellular exposure of *Staphylococcus aureus* to ciprofloxacin was bacteriostatic even at the human C_{max} (total drug concentration), in contrast to much higher levels of bacterial killing extracellularly[580]. In contrast, Rajagopalan-Levasseur *et al.* found a 10-fold reduction in intracellular *Legionella pneumophila* bacteria that were grown in macrophages in ciprofloxacin-containing medium compared to those in non-treated medium[581]. This indicates the important role of host cells in modulating drug exposure to bacteria inside of cells and thus the need for further

investigation of how host cells influence drug availability and bacterial intracellular survival. Furthermore, antimicrobials including ciprofloxacin have been noted to have a direct effect on macrophages, including by influencing macrophage gene expression. For instance, Marquez *et al.* demonstrated that treatment of macrophages with ciprofloxacin upregulates the Mrp4 transporter, which may be involved in ciprofloxacin efflux[582,583]. Sanchez *et al.* showed that pre-treatment of gland polymorphonuclear neutrophils, macrophages, and blood monocytes with tumour necrosis factor and then exposure to ciprofloxacin increased killing of intracellular *S. aureus*. However, this synergistic effect only occurred for antimicrobials that can independently target intracellular *S. aureus*[584]. Interestingly, Anuforom found that the combination of ciprofloxacin-treatment and SL1344 infection increased IL-1β and TNF-α expression far more than ciprofloxacin- or bacterial-exposure alone[365]. Infecting *S*. Typhimurium in the presence of ciprofloxacin-exposed macrophages for the purpose of measuring intracellular invasion and replication efficiency, macrophage gene expression, and morphological characteristics of drug-exposed macrophages and bacteria would be a useful set of experiments to further understand bacteria-macrophage-drug interactions. It would be particularly interesting to compare this for isolates with different invasion potentials and antimicrobial susceptibilities to determine what and how large a role macrophages play in limiting infection by invasive and drug-resistant organisms.

9.3 Interaction of *S*. Typhimurium with additional antimicrobials

Finally, we recognize that ciprofloxacin, and fluoroquinolones more broadly, represent only one class of antimicrobials effective against susceptible invasive *Salmonella* infections. While we chose to focus on ciprofloxacin for our studies, it would be worthwhile also exploring the dynamics of *S*. Typhimurium growth in the presence of other antimicrobials and in conjunction with cells. Most pressingly, it would be informative to conduct similar studies on the interaction of bacteria and macrophages with azithromycin, which has gained favour as a widespread prophylactic and reducer of childhood mortality[585–587]. Azithromycin acts on bacteria by inhibiting protein synthesis and is known to readily enter cells, making it an effective antimicrobial for treating intracellular infections[588]. Azithromycin has been recognized to have immunomodulatory effects, including stimulating the downregulation of

CD80 and CD86 as well as suppression of IL-6, IL-10, and TNF-α in LPS-treated dendritic cells and CD4+ cells[589]. In addition, it has been shown to alter the effect of transcription factor NFκB and modulate mucin production, expression of macrophage surface receptors, and autophagy[588]. Given the widespread effects azithromycin has on cells and that it has a mechanism of action on bacteria distinct from fluoroquinolones, it would be useful to study in greater depth. This is particularly true given that our transcriptional studies of S. Typhimurium D23580 treated with azithromycin revealed a distinct set of differentially expressed genes from bacteria treated with ciprofloxacin. This suggests that any transcriptomics or imaging of macrophages treated with azithromycin would behave and look distinct to those treated with ciprofloxacin. A study of co-cultured macrophages and fibroblasts with *Pseudomonas aeruginosa* showed that azithromycin dampens the inflammatory response, and a separate study of cystic fibrosis mice found that azithromycin treatment reduced expression of inflammatory cytokines IL-1β, CCl-2, and TNF-α[590,591]. Given its strong immunomodulatory role and efficacy at bacterial killing, it would be relevant and important to further investigate the effects of azithromycin, particularly in the context of invasive *S*. Typhimurium for which there are limited treatment options in some regions.

As antimicrobial resistance grows, it becomes increasingly important to fully understand the effects of antimicrobial treatment on bacteria and cells. By doing so, it may be possible to discover cases in which certain antimicrobials will not be effective and may lead to greater resistance. Our work has begun to show the widespread effect of ciprofloxacin treatment on *S*. Typhimurium bacteria, and future work will seek to build upon this foundation to better explain bacteria-drug interactions and influence appropriate drug usage.

References

1. Institute for Health Metrics and Evaluation. Global Burden of Disease Study 2017. *The Lancet*, 2017(Gbd):1–7, 2017.

2. Jim O'Neill. Tackling Drug-resistant Infections Globally : Final Report and Recommendations. Technical Report May, 2016.

3. Christopher Troeger, Brigette F Blacker, Ibrahim A Khalil, Puja C Rao, Shujin Cao, Stephanie R M Zimsen, Samuel B Albertson, Jeffery D Stanaway, Aniruddha Deshpande, Zegeye Abebe, Nelson Alvis-Guzman, Azmeraw T Amare, Solomon W Asgedom, Zelalem Alamrew Anteneh, Carl Abelardo T Antonio, Olatunde Aremu, Ephrem Tsegay Asfaw, Tesfay Mehari Atey, Suleman Atique, Euripide Frinel G Arthur Avokpaho, Ashish Awasthi, Henok Tadesse Ayele, Aleksandra Barac, Mauricio L Barreto, Quique Bassat, Saba Abraham Belay, Isabela M Bensenor, Zulfiqar A Bhutta, Ali Bijani, Hailemichael Bizuneh, Carlos A Castañeda-Orjuela, Abel Fekadu Dadi, Lalit Dandona, Rakhi Dandona, Huyen Phuc Do, Manisha Dubey, Eleonora Dubljanin, Dumessa Edessa, Aman Yesuf Endries, Babak Eshrati, Tamer Farag, Garumma Tolu Feyissa, Kyle J Foreman, Mohammad H Forouzanfar, Nancy Fullman, Peter W Gething, Melkamu Dedefo Gishu, William W Godwin, Harish Chander Gugnani, Rahul Gupta, Gessessew Bugssa Hailu, Hamid Yimam Hassen, Desalegn Tsegaw Hibstu, Olayinka S Ilesanmi, Jost B Jonas, Amaha Kahsay, Gagandeep Kang, Amir Kasaeian, Yousef Saleh Khader, Ibrahim A Khalil, Ejaz Ahmad Khan, Muhammad Ali Khan, Young-Ho Khang, Niranjan Kissoon, Sonali Kochhar, Karen L Kotloff, Ai Koyanagi, G Anil Kumar, Hassan Magdy Abd El Razek, Reza Malekzadeh, Deborah Carvalho Malta, Suresh Mehata, Walter Mendoza, Desalegn Tadese Mengistu, Bereket Gebremichael Menota, Haftay Berhane Mezgebe, Fitsum Weldegebreal Mlashu, Srinivas Murthy, Gurudatta A Naik, Cuong Tat Nguyen, Trang Huyen Nguyen, Dina Nur Anggraini Ningrum, Felix Akpojene Ogbo, Andrew Toyin Olagunju, Deepak Paudel, James A Platts-Mills, Mostafa Qorbani, Anwar Rafay, Rajesh Kumar Rai, Saleem M Rana, Chhabi Lal Ranabhat, Davide Rasella, Sarah E Ray, Cesar Reis, Andre M N Renzaho, Mohammad Sadegh Rezai, George Mugambage Ruhago, Saeid Safiri, Joshua A Salomon, Juan Ramon Sanabria, Benn Sartorius, Monika Sawhney, Sadaf G Sepanlou, Mika Shigematsu, Mekonnen Sisay, Ranjani Somayaji, Chandrashekhar T Sreeramareddy, Bryan L Sykes, Getachew Redae Taffere, Roman Topor-Madry, Bach Xuan Tran, Kald Beshir Tuem, Kingsley Nnanna Ukwaja, Stein Emil Vollset, Judd L Walson, Marcia R Weaver, Kidu Gidey Weldegwergs, Andrea Werdecker, Abdulhalik Workicho, Muluken Yenesew, Biruck Desalegn Yirsaw, Naohiro Yonemoto, Maysaa El Sayed

Zaki, Theo Vos, Stephen S Lim, Mohsen Naghavi, Christopher J L Murray, Ali H Mokdad, Simon I Hay, and Robert C Reiner Jr. Estimates of the global, regional, and national morbidity, mortality, and aetiologies of diarrhoea in 195 countries: a systematic analysis for the Global Burden of Disease Study 2016. *The Lancet Infectious Diseases*, 18(11):1211–1228, nov 2018.

4. ShannonÂ E. Majowicz, Jennie Musto, Elaine Scallan, FrederickÂ J. Angulo, Martyn Kirk, SarahÂ J. O'Brien, TimothyÂ F. Jones, Aamir Fazil, and RobertÂ M. Hoekstra. The Global Burden of Nontyphoidal Salmonella Gastroenteritis . *Clinical Infectious Diseases*, 50(6):882–889, 2010.

5. World Health Organization. Preventing diarrhoea through better water, sanitation and hygiene. *World Health Organization*, pages 1–48, 2014.

6. Pierre Wattiau, Cécile Boland, and Sophie Bertrand. Methodologies for Salmonella enterica subsp. Enterica Subtyping: Gold Standards and Alternatives. *Applied and Environmental Microbiology*, 77(22):7877–7885, 2011.

7. Ruiting Lan, Peter R. Reeves, and Sophie Octavia. Population structure, origins and evolution of major Salmonella enterica clones. *Infection, Genetics and Evolution*, 9(5):996–1005, 2009.

8. F. W. Brenner, R. G. Villar, F. J. Angulo, R. Tauxe, and B. Swaminathan. Salmonella nomenclature, 2000.

9. Giovanni M. Giammanco, Sarina Pignato, Caterina Mammina, Francine Grimont, Patrick A.D. Grimont, Antonino Nastasi, and Giuseppe Giammanco. Persistent endemicity of salmonella bongori 48:z35:- In southern Italy: Molecular characterization of human, animal, and environmental isolates. *Journal of Clinical Microbiology*, 40(9):3502–3505, 2002.

10. R. K. Selander, P. Beltran, N. H. Smith, R. Helmuth, F. A. Rubin, D. J. Kopecko, K. Ferris, B. D. Tall, A. Cravioto, and J. M. Musser. Evolutionary genetic relationships of clones of Salmonella serovars that cause human typhoid and other enteric fevers. *Infection and Immunity*, 58(7):2262–2275, 1990.

11. Manuela Raffatellu, Daniela Chessa, R Paul Wilson, Richard Dusold, Salvatore Rubino, and Andreas J Bäumler. The Vi capsular antigen of Salmonella enterica serotype Typhi reduces Toll-like receptor-dependent interleukin-8 expression in the intestinal mucosa. *Infection and immunity*, 73(6):3367–3374, jun 2005.

12. Xiaomei Hu, Zhijin Chen, Kun Xiong, Jing Wang, Xiancai Rao, and Yanguang Cong. Vi capsular polysaccharide: Synthesis, virulence, and application. *Critical Reviews in Microbiology*, 43(4):440–452, 2017.

13. Le Tang, Chun Xiao Wang, Song Ling Zhu, Yang Li, Xia Deng, Randal N. Johnston, Gui Rong Liu, and Shu Lin Liu. Genetic boundaries to delineate the typhoid agent and other Salmonella serotypes into distinct natural lineages. *Genomics*, 102(4):331–337, 2013.

14. Mark Achtman, John Wain, François Xavier Weill, Satheesh Nair, Zhemin Zhou, Vartul Sangal, Mary G. Krauland, James L. Hale, Heather Harbottle, Alexandra Uesbeck, Gordon Dougan, Lee H. Harrison, and Sylvain Brisse. Multilocus sequence typing as a replacement for serotyping in Salmonella enterica. *PLoS Pathogens*, 8(6), 2012.

15. Jessica E. Cooper and Edward J. Feil. Multilocus sequence typing - What is resolved? *Trends in Microbiology*, 12(8):373–377, 2004.

16. Carl Gustaf Hellerqvist, Bengt Lindberg, Sigfrid Svensson, Tord Holme, and Alf A Lindberg. Structural studies on the O-specific side-chains of the cell-wall lipopolysaccharide from Salmonella typhimurium 395 ms. *Carbohydrate Research*, 8(1):43–55, 1968.

17. H J Jörbeck, S B Svenson, and A A Lindberg. Immunochemistry of Salmonella O-antigens: specificity of rabbit antibodies against the O-antigen 4 determinant elicited by whole bacteria and O-antigen 4 specific saccharide-protein conjugates. *Journal of immunology (Baltimore, Md. : 1950)*, 123(3):1376–1381, sep 1979.

18. J. M. Slauch, M. J. Mahan, P. Michetti, M. R. Neutra, and J. J. Mekalanos. Acetylation (O-factor 5) affects the structural and immunological properties of Salmonella typhimurium lipopolysaccharide O antigen. *Infection and Immunity*, 63(2):437–441, 1995.

19. John Wain, Rene S. Hendriksen, Matthew L. Mikoleit, Karen H. Keddy, and R. Leon Ochiai. Typhoid fever. In *Lancet*, volume 385, pages 1136–1145, mar 2015.

20. Claire S Waddington, Thomas C Darton, and Andrew J Pollard. The challenge of enteric fever. *The Journal of infection*, 68 Suppl 1:S38–50, jan 2014.

21. Asma Azmatullah, Farah Naz Qamar, Durrane Thaver, Anita KM Zaidi, and Zulfiqar A. Bhutta. Systematic review of the global epidemiology, clinical and laboratory profile of enteric fever. *Journal of Global Health*, 5(2), 2015.

22. Stephen P Luby, Samir Saha, and Jason R Andrews. Towards sustainable public health surveillance for enteric fever. *Vaccine*, 33 Suppl 3:C3–7, jun 2015.

23. Michael McClelland, Kenneth E Sanderson, Sandra W Clifton, Phil Latreille, Steffen Porwollik, Aniko Sabo, Rekha Meyer, Tamberlyn Bieri, Phil Ozersky, Michael Mclellan, C Richard Harkins, Chunyan Wang, Christine Nguyen, Amy Berghoff, Glendoria Elliott, Sara Kohlberg, Cindy Strong, Feiyu Du, Jason Carter, Colin Kremizki, Dan Layman, Shawn Leonard, Hui Sun, Lucinda Fulton, William Nash, Tracie Miner, Patrick Minx, Kim Delehaunty, Catrina Fronick, Vincent Magrini, Michael Nhan, Wesley Warren, Liliana Florea, John Spieth, and Richard K Wilson. Comparison of genome degradation in Paratyphi A and Typhi , human-restricted serovars of Salmonella enterica that cause typhoid. *Nature Genetics*, 36(12):1268–1274, 2004.

24. Stephen Baker and Gordon Dougan. The Genome of Salmonella enterica Serovar Typhi. *Clinical Infectious Diseases*, pages 29–33, 2007.

25. James J Gilchrist and Calman A MacLennan. Invasive Nontyphoidal Salmonella Disease in Africa. *EcoSal Plus*, 8(2), jan 2019.

26. Elaine Scallan, Robert M Hoekstra, Frederick J Angulo, Robert V Tauxe, Marc-alain Widdowson, Sharon L Roy, Jeffery L Jones, and Patricia M Griffi. Foodborne Illness Acquired in the United States â Major Pathogens. *Emerging Infectious Diseases*, 17(1):7–15, 2011.

27. Jeffrey D. Stanaway, Robert C. Reiner, Brigette F. Blacker, Ellen M. Goldberg, Ibrahim A. Khalil, Christopher E. Troeger, Jason R. Andrews, Zulfiqar A. Bhutta, John A. Crump, Justin Im, Florian Marks, Eric Mintz, Se Eun Park, Anita K.M. Zaidi, Zegeye Abebe, Ayenew Negesse Abejie, Isaac Akinkunmi Adedeji, Beriwan Abdulqadir Ali, Azmeraw T. Amare, Hagos Tasew Atalay, Euripide F.G.A. Avokpaho, Umar Bacha, Aleksandra Barac, Neeraj Bedi, Adugnaw Berhane, Annie J. Browne, Jesus L. Chirinos, Abdulaal Chitheer, Christiane Dolecek, Maysaa El Sayed Zaki, Babak Eshrati, Kyle J. Foreman, Abdella Gemechu, Rahul Gupta, Gessessew Bugssa Hailu, Andualem Henok, Desalegn Tsegaw Hibstu, Chi Linh Hoang, Olayinka Stephen Ilesanmi, Veena J. Iyer, Amaha Kahsay, Amir Kasaeian, Tesfaye Dessale Kassa, Ejaz Ahmad Khan, Young Ho Khang, Hassan Magdy Abd El Razek, Mulugeta Melku, Desalegn Tadese Mengistu, Karzan Abdulmuhsin Mohammad, Shafiu Mohammed, Ali H. Mokdad, Jean B. Nachega, Aliya Naheed, Cuong Tat Nguyen, Huong Lan Thi Nguyen, Long Hoang Nguyen, Nam Ba Nguyen, Trang Huyen Nguyen, Yirga Legesse Nirayo, Tikki Pangestu, George C. Patton, Mostafa Qorbani, Rajesh Kumar Rai, Saleem M. Rana, Chhabi Lal Ranabhat, Kedir Teji Roba, Nicholas L.S. Roberts, Salvatore Rubino, Saeid Safiri, Benn Sartorius, Monika Sawhney, Mekonnen Sisay Shiferaw, David L. Smith, Bryan L. Sykes, Bach Xuan Tran, Tung Thanh Tran, Kingsley Nnanna Ukwaja, Giang Thu Vu, Linh Gia Vu, Fitsum Weldegebreal, Melaku Kindie Yenit, Christopher J.L. Murray, and Simon I. Hay. The global burden of typhoid and paratyphoid fevers: a systematic analysis for the Global Burden of Disease Study 2017. *The Lancet Infectious Diseases*, 19(4):369–381, 2019.

28. Stephen Baker, Joachim Hombach, and Florian Marks. What Have We Learned From the Typhoid Fever Surveillance in Africa Program?, mar 2016.

29. Gordon Dougan. Typhoid in Africa and vaccine deployment. *The Lancet. Global health*, 5(3):e236–e237, mar 2017.

30. Olumide Ajibola, Mari B Mshelia, Bashar H Gulumbe, and Anthonius A Eze. Typhoid Fever Diagnosis in Endemic Countries: A Clog in the Wheel of Progress? *Medicina (Kaunas, Lithuania)*, 54(2), apr 2018.

31. Samuel Kariuki. Typhoid fever in sub-Saharan Africa: challenges of diagnosis and management of infections. *Journal of infection in developing countries*, 2(6):443–447, dec 2008.

32. Lalith Wijedoru, Sue Mallett, and Christopher M Parry. Rapid diagnostic tests for typhoid and paratyphoid (enteric) fever. *The Cochrane database of systematic reviews*, 5(5):CD008892, may 2017.

33. Jeffrey D. Stanaway, Andrea Parisi, Kaushik Sarkar, Brigette F. Blacker, Robert C. Reiner, Simon I. Hay, Molly R. Nixon, Christiane Dolecek, Spencer L. James, Ali H. Mokdad, Getaneh Abebe, Elham Ahmadian, Fares Alahdab, Birhan Tamene T. Alemnew, Vahid Alipour, Fatemeh Allah Bakeshei, Megbaru Debalkie Animut, Fereshteh

Ansari, Jalal Arabloo, Ephrem Tsegay Asfaw, Mojtaba Bagherzadeh, Quique Bassat, Yaschilal Muche Muche Belayneh, Félix Carvalho, Ahmad Daryani, Feleke Mekonnen Demeke, Asmamaw Bizuneh Bizuneh Demis, Manisha Dubey, Eyasu Ejeta Duken, Susanna J. Dunachie, Aziz Eftekhari, Eduarda Fernandes, Reza Fouladi Fard, Getnet Azeze Gedefaw, Birhanu Geta, Katherine B. Gibney, Amir Hasanzadeh, Chi Linh Hoang, Amir Kasaeian, Amir Khater, Zelalem Teklemariam Kidanemariam, Ayenew Molla Lakew, Reza Malekzadeh, Addisu Melese, Desalegn Tadese Mengistu, Tomislav Mestrovic, Bartosz Miazgowski, Karzan Abdulmuhsin Mohammad, Mahdi Mohammadian, Abdollah Mohammadian-Hafshejani, Cuong Tat Nguyen, Long Hoang Nguyen, Son Hoang Nguyen, Yirga Legesse Nirayo, Andrew T. Olagunju, Tinuke O. Olagunju, Hadi Pourjafar, Mostafa Qorbani, Mohammad Rabiee, Navid Rabiee, Anwar Rafay, Aziz Rezapour, Abdallah M. Samy, Sadaf G. Sepanlou, Masood Ali Shaikh, Mehdi Sharif, Mika Shigematsu, Belay Tessema, Bach Xuan Tran, Irfan Ullah, Ebrahim M. Yimer, Zoubida Zaidi, Christopher J.L. Murray, and John A. Crump. The global burden of non-typhoidal salmonella invasive disease: a systematic analysis for the Global Burden of Disease Study 2017. *The Lancet Infectious Diseases*, 19(12):1312–1324, 2019.

34. Trong T. Ao, Nicholas A. Feasey, Melita A. Gordon, Karen H. Keddy, Frederick J. Angulo, and John A. Crump. Global burden of invasive nontyphoidal salmonella disease, 2010. *Emerging Infectious Diseases*, 21(6):941–949, 2015.

35. A. P. Maskey, J. N. Day, P. Q. Tuan, G. E. Thwaites, J. I. Campbell, M. Zimmerman, J. J. Farrar, and B. Basnyat. Salmonella enterica Serovar Paratyphi A and S. enterica Serovar Typhi Cause Indistinguishable Clinical Syndromes in Kathmandu, Nepal. *Clinical Infectious Diseases*, 2006.

36. John A. Crump, Maria Sjölund-Karlsson, Melita A. Gordon, and Christopher M. Parry. Epidemiology, clinical presentation, laboratory diagnosis, antimicrobial resistance, and antimicrobial management of invasive Salmonella infections. *Clinical Microbiology Reviews*, 28(4):901–937, 2015.

37. Gordon Dougan and Stephen Baker. Salmonella enterica Serovar Typhi and the Pathogenesis of Typhoid Fever . *Annual Review of Microbiology*, 68(1):317–336, 2014.

38. Nguyen T Nhung, Nguyen V Cuong, Guy Thwaites, and Juan Carrique-Mas. Antimicrobial Usage and Antimicrobial Resistance in Animal Production in Southeast Asia: A Review. *Antibiotics (Basel, Switzerland)*, 5(4), nov 2016.

39. R. Leon Ochiai, Xuanyi Wang, Lorenz Von Seidlein, Jin Yang, Zulfiqar A. Bhutta, Sojit K. Bhattacharya, Magdarina Agtini, Jacqueline L. Deen, John Wain, Deok Ryun Kim, Mohammad Ali, Camilo J. Acosta, Luis Jodar, and John D. Clemens. Salmonella paratyphi A rates, Asia. *Emerging Infectious Diseases*, 11(11):1764–1766, 2005.

40. Sadia Shakoor, James A Platts-Mills, and Rumina Hasan. Antibiotic-Resistant Enteric Infections. *Infectious disease clinics of North America*, 33(4):1105–1123, dec 2019.

41. Isabel Frost, Thomas P Van Boeckel, João Pires, Jessica Craig, and Ramanan Laxminarayan. Global geographic trends in antimicrobial resistance: the role of international travel. *Journal of travel medicine*, 26(8), dec 2019.

42. Malick M Gibani, Carl Britto, and Andrew J Pollard. Typhoid and paratyphoid fever: a call to action. *Current opinion in infectious diseases*, 31(5):440–448, oct 2018.

43. Kathryn E. Holt, Nicholas R. Thomson, John Wain, Gemma C. Langridge, Rumina Hasan, Zulfiqar A. Bhutta, Michael A. Quail, Halina Norbertczak, Danielle Walker, Mark Simmonds, Brian White, Nathalie Bason, Karen Mungall, Gordon Dougan, and Julian Parkhill. Pseudogene accumulation in the evolutionary histories of Salmonella enterica serovars Paratyphi A and Typhi. *BMC Genomics*, 2009.

44. J Parkhill, G Dougan, K D James, N R Thomson, D Pickard, J Wain, C Churcher, K L Mungall, S D Bentley, M T Holden, M Sebaihia, S Baker, D Basham, K Brooks, T Chillingworth, P Connerton, A Cronin, P Davis, R M Davies, L Dowd, N White, J Farrar, T Feltwell, N Hamlin, A Haque, T T Hien, S Holroyd, K Jagels, A Krogh, T S Larsen, S Leather, S Moule, P O'Gaora, C Parry, M Quail, K Rutherford, M Simmonds, J Skelton, K Stevens, S Whitehead, and B G Barrell. Complete genome sequence of a multiple drug resistant Salmonella enterica serovar Typhi CT18. *Nature*, 413(6858):848–852, oct 2001.

45. Christopher M Parry, Tran Tinh Hien, Gordon Dougan, Nicholas J White, and Jeremy J Farrar. YPHOID fever is a systemic infection with the bacterium. *The New England Journal of Medicine*, 347(22):1770–1782, 2002.

46. Malick M Gibani, Elizabeth Jones, Amber Barton, Celina Jin, Juliette Meek, Susana Camara, Ushma Galal, Eva Heinz, Yael Rosenberg-Hasson, Gerlinde Obermoser, Claire Jones, Danielle Campbell, Charlotte Black, Helena Thomaides-Brears, Christopher Darlow, Christina Dold, Laura Silva-Reyes, Luke Blackwell, Maria Lara-Tejero, Xuyao Jiao, Gabrielle Stack, Christoph J Blohmke, Jennifer Hill, Brian Angus, Gordon Dougan, Jorge Galán, and Andrew J Pollard. Investigation of the role of typhoid toxin in acute typhoid fever in a human challenge model. *Nature medicine*, 25(7):1082–1088, jul 2019.

47. Hazel C Dobinson, Malick M Gibani, Claire Jones, Helena B Thomaides-Brears, Merryn Voysey, Thomas C Darton, Claire S Waddington, Danielle Campbell, Iain Milligan, Liqing Zhou, Sonu Shrestha, Simon A Kerridge, Anna Peters, Zoe Stevens, Audino Podda, Laura B Martin, Flavia D'Alessio, Duy Pham Thanh, Buddha Basnyat, Stephen Baker, Brian Angus, Myron M Levine, Christoph J Blohmke, and Andrew J Pollard. Evaluation of the Clinical and Microbiological Response to Salmonella Paratyphi A Infection in the First Paratyphoid Human Challenge Model. *Clinical infectious diseases : an official publication of the Infectious Diseases Society of America*, 64(8):1066–1073, apr 2017.

48. Stephanie Fresnay, Monica A McArthur, Laurence S Magder, Thomas C Darton, Claire Jones, Claire S Waddington, Christoph J Blohmke, Brian Angus, Myron M Levine, Andrew J Pollard, and Marcelo B Sztein. Importance of Salmonella Typhi-Responsive CD8+ T Cell Immunity in a Human Typhoid Fever Challenge Model. *Frontiers in immunology*, 8:208, 2017.

49. Yan Zhang, Arthur Brady, Cheron Jones, Yang Song, Thomas C Darton, Claire Jones, Christoph J Blohmke, Andrew J Pollard, Laurence S Magder, Alessio Fasano, Marcelo B Sztein, and Claire M Fraser. Compositional and Functional Differences in

the Human Gut Microbiome Correlate with Clinical Outcome following Infection with Wild-Type Salmonella enterica Serovar Typhi. *mBio*, 9(3), may 2018.

50. Thomas C Darton, Claire Jones, Christoph J Blohmke, Claire S Waddington, Liqing Zhou, Anna Peters, Kathryn Haworth, Rebecca Sie, Christopher A Green, Catherine A Jeppesen, Maria Moore, Ben A V Thompson, Tessa John, A Kingsley, Ly-mee Yu, Merryn Voysey, Zoe Hindle, Stephen Lockhart, B Sztein, Gordon Dougan, Brian Angus, Myron M Levine, and Andrew J Pollard. Using a Human Challenge Model of Infection to Measure Vaccine Efficacy : A Randomised , Controlled Trial Comparing the Typhoid Vaccines M01ZH09 with Placebo and Ty21a. *PLoS Neglected Tropical Diseases*, 09:1–27, 2016.

51. Sharon M Tennant, Calman A Maclennan, Raphael Simon, Laura B Martin, and M Imran Khan. Nontyphoidal salmonella disease : Current status of vaccine research and development. *Vaccine*, 34(26):2907–2910, 2016.

52. Christopher R Braden. Salmonella enterica serotype Enteritidis and eggs: a national epidemic in the United States. *Clinical infectious diseases : an official publication of the Infectious Diseases Society of America*, 43(4):512–517, aug 2006.

53. Luciana B M Kottwitz, Joice Aparecida Leão, Alberto Back, Dalia dos P Rodrigues, Marciane Magnani, and Tereza C R M de Oliveira. Commercially laid eggs vs. discarded hatching eggs: contamination by Salmonella spp. *Brazilian journal of microbiology : [publication of the Brazilian Society for Microbiology]*, 44(2):367–370, 2013.

54. Lapo Mughini-Gras, Joost Smid, Remko Enserink, Eelco Franz, Leo Schouls, Max Heck, and Wilfrid van Pelt. Tracing the sources of human salmonellosis: a multi-model comparison of phenotyping and genotyping methods. *Infection, genetics and evolution : journal of molecular epidemiology and evolutionary genetics in infectious diseases*, 28:251–260, dec 2014.

55. CDC. What are Salmonella? (June):46–47, 2016.

56. DucÂ J. Vugia, Michael Samuel, MonicaÂ M. Farley, Ruthanne Marcus, Beletshachew Shiferaw, Sue Shallow, Kirk Smith, and FrederickÂ J. Angulo. Invasive Salmonella Infections in the United States, FoodNet, 1996â1999: Incidence, Serotype Distribution, and Outcome . *Clinical Infectious Diseases*, 38(s3):S149–S156, 2004.

57. Alison E. Mather, Tu Le Thi Phuong, Yunfeng Gao, Simon Clare, Subhankar Mukhopadhyay, David A. Goulding, Nhu Tran Do Hoang, Ha Thanh Tuyen, Nguyen Phu Huong Lan, Corinne N. Thompson, Nguyen Hoang Thu Trang, Juan Carrique-Mas, Ngo Tri Tue, James I. Campbell, Maia A. Rabaa, Duy Pham Thanh, Katherine Harcourt, Ngo Thi Hoa, Nguyen Vinh Trung, Constance Schultsz, Gabriel G. Perron, John E. Coia, Derek J. Brown, Chinyere Okoro, Julian Parkhill, Nicholas R. Thomson, Nguyen Van Vinh Chau, Guy E. Thwaites, Duncan J. Maskell, Gordon Dougan, Linda J. Kenney, and Stephen Baker. New variant of multidrug-resistant Salmonella enterica serovar typhimurium associated with invasive disease in immunocompromised patients in Vietnam. *mBio*, 9(5):1–11, 2018.

58. Nicholas A. Feasey, Gordon Dougan, Robert A. Kingsley, Robert S. Heyderman, and Melita A. Gordon. Invasive non-typhoidal salmonella disease: An emerging and neglected tropical disease in Africa. *The Lancet*, 379(9835):2489–2499, 2012.

59. Stephen M. Graham, Amanda L. Walsh, Elizabeth M. Molyneux, Amos J. Phiri, and Malcolm E. Molyneux. Clinical presentation of non-typhoidal Salmonella bacteraemia in Malawian children. *Transactions of the Royal Society of Tropical Medicine and Hygiene*, 94(3):310–314, 2000.

60. Karen H. Keddy, Arvinda Sooka, Alfred Musekiwa, Anthony M. Smith, Husna Ismail, Nomsa P. Tau, Penny Crowther-Gibson, Frederick J. Angulo, and Keith P. Klugman. Clinical and microbiological features of salmonella meningitis in a South African Population, 2003-2013. *Clinical Infectious Diseases*, 61(Suppl 4):S272–S282, 2015.

61. Se Eun Park, Gi Deok Pak, Peter Aaby, Yaw Adu-Sarkodie, Mohammad Ali, Abraham Aseffa, Holly M. Biggs, Morten Bjerregaard-Andersen, Robert F. Breiman, John A. Crump, Ligia Maria Cruz Espinoza, Muna Ahmed Eltayeb, Nagla Gasmelseed, Julian T. Hertz, Justin Im, Anna Jaeger, Leon Parfait Kabore, Vera Von Kalckreuth, Karen H. Keddy, Frank Konings, Ralf Krumkamp, Calman A. MacLennan, Christian G. Meyer, Joel M. Montgomery, Aissatou Ahmet Niang, Chelsea Nichols, Beatrice Olack, Ursula Panzner, Jin Kyung Park, Henintsoa Rabezanahary, Raphaël Rakotozandrindrainy, Emmanuel Sampo, Nimako Sarpong, Heidi Schütt-Gerowitt, Arvinda Sooka, Abdramane Bassiahi Soura, Amy Gassama Sow, Adama Tall, Mekonnen Teferi, Biruk Yeshitela, Jürgen May, Thomas F. Wierzba, John D. Clemens, Stephen Baker, and Florian Marks. The Relationship between Invasive Nontyphoidal Salmonella Disease, Other Bacterial Bloodstream Infections, and Malaria in Sub-Saharan Africa. *Clinical Infectious Diseases*, 62(March):s23–s31, 2016.

62. Milagritos D Tapia, Sharon M Tennant, Kristin Bornstein, Uma Onwuchekwa, Boubou Tamboura, Almoustapha Maiga, Mamadou B Sylla, Seydou Sissoko, Nana Kourouma, Aliou Toure, Dramane Malle, Sofie Livio, Samba O Sow, and Myron M Levine. Invasive Nontyphoidal Salmonella Infections Among Children in Mali, 2002-2014: Microbiological and Epidemiologic Features Guide Vaccine Development. *Clinical infectious diseases : an official publication of the Infectious Diseases Society of America*, 61 Suppl 4(Suppl 4):S332–8, nov 2015.

63. Sophie Norton, Essi Huhtinen, Stephen Conaty, Kirsty Hope, Brett Campbell, Marianne Tegel, Rowena Boyd, and Beth Cullen. A large point-source outbreak of Salmonella Typhimurium linked to chicken, pork and salad rolls from a Vietnamese bakery in Sydney. *Western Pacific surveillance and response journal : WPSAR*, 3(2):16–23, apr 2012.

64. Laurent Guillier, Corinne Danan, Hélène Bergis, Marie-Laure Delignette-Muller, Sophie Granier, Sylvie Rudelle, Annie Beaufort, and Anne Brisabois. Use of quantitative microbial risk assessment when investigating foodborne illness outbreaks: the example of a monophasic Salmonella Typhimurium 4,5,12:i:- outbreak implicating beef burgers. *International journal of food microbiology*, 166(3):471–478, sep 2013.

65. P Antunes, J Mourão, J Campos, and L Peixe. Salmonellosis: the role of poultry meat. *Clinical microbiology and infection : the official publication of the European Society of Clinical Microbiology and Infectious Diseases*, 22(2):110–121, feb 2016.

66. Kathryn Bernard and Gary P Wormser. Biodefense Principles and Pathogens Edited By M. S. Bronze and R. A. Greenfield Norfolk, United Kingdom: Horizon Bioscience, 2005. 838 pp. $380.00 (hardcover). *Clinical Infectious Diseases*, 42(5):735, mar 2006.

67. J Ryan Kenneth and C. George Ray. *Sherris Medical Microbiology (4th ed.). McGraw Hill.* 2004.

68. Annette Nygaard Jensen, Anders Dalsgaard, Anders Stockmarr, Eva Møller Nielsen, and Dorte Lau Baggesen. Survival and transmission of Salmonella enterica serovar typhimurium in an outdoor organic pig farming environment. *Applied and Environmental Microbiology*, 72(3):1833–1842, 2006.

69. Susan W.M. Hendriksen, Karin Orsel, Jaap A. Wagenaar, Angelika Miko, and Engeline Van Duijkeren. Animal-to-human transmission of Salmonella Typhimurium DT104A variant. *Emerging Infectious Diseases*, 10(12):2225–2227, 2004.

70. Alison E Mather, Timothy G Vaughan, and Nigel P French. Molecular Approaches to Understanding Transmission and Source Attribution in Nontyphoidal Salmonella and Their Application in Africa. *Clinical infectious diseases : an official publication of the Infectious Diseases Society of America*, 61 Suppl 4:S259–65, nov 2015.

71. Samuel Kariuki, Gunturu Revathi, Francis Gakuya, Victor Yamo, Jane Muyodi, and C. Anthony Hart. Lack of clonal relationship between non-typhi Salmonella strain types from humans and those isolated from animals living in close contact. *FEMS Immunology and Medical Microbiology*, 33(3):165–171, 2002.

72. Samuel Kariuki, Gunturu Revathi, Nyambura Kariuki, John Kiiru, Joyce Mwituria, Jane Muyodi, Jane W. Githinji, Dorothy Kagendo, Agnes Munyalo, and C. Anthony Hart. Invasive multidrug-resistant non-typhoidal Salmonella infections in Africa: Zoonotic or anthroponotic transmission? *Journal of Medical Microbiology*, 55(5):585–591, 2006.

73. Annelies S Post, Seydou Nakanabo Diallo, Issa Guiraud, Palpouguini Lompo, Marc Christian Tahita, Jessica Maltha, Sandra Van Puyvelde, Wesley Mattheus, Benedikt Ley, Kamala Thriemer, Eli Rouamba, Karim Derra, Stijn Deborggraeve, Halidou Tinto, and Jan Jacobs. Supporting evidence for a human reservoir of invasive non-Typhoidal Salmonella from household samples in Burkina Faso. *PLoS neglected tropical diseases*, 13(10):e0007782–e0007782, oct 2019.

74. Mary E Wikswo, Anita Kambhampati, Kayoko Shioda, Kelly A Walsh, Anna Bowen, and Aron J Hall. Outbreaks of Acute Gastroenteritis Transmitted by Person-to-Person Contact, Environmental Contamination, and Unknown Modes of Transmission–United States, 2009-2013. *Morbidity and mortality weekly report. Surveillance summaries (Washington, D.C. : 2002)*, 64(12):1–16, dec 2015.

75. Martina Oneko, Simon Kariuki, Vincent Muturi-Kioi, Kephas Otieno, Vincent O. Otieno, John M. Williamson, Jason Folster, Michele B. Parsons, Laurence Slutsker, Barbara E. Mahon, and Mary J. Hamel. Emergence of community-acquired, multidrug-resistant invasive nontyphoidal salmonella disease in Rural Western Kenya, 2009-2013. *Clinical Infectious Diseases*, 61(Suppl 4):S310–S316, 2015.

76. Robert A Kingsley, Sally Kay, Thomas Connor, Lars Barquist, Leanne Sait, Kathryn E Holt, Karthi Sivaraman, Thomas Wileman, David Goulding, Simon Clare, Christine Hale, Aswin Seshasayee, Simon Harris, Nicholas R Thomson, Paul Gardner, Wolfgang Rabsch, Paul Wigley, Tom Humphrey, Julian Parkhill, and Gordon Dougan. Genome and transcriptome adaptation accompanying emergence of the definitive type 2 host-restricted Salmonella enterica serovar Typhimurium pathovar. *mBio*, 4(5):e00565, aug 2013.

77. Liljana Petrovska, Alison E. Mather, Manal Abuoun, Priscilla Branchu, Simon R. Harris, Thomas Connor, K. L. Hopkins, A. Underwood, Antonia A. Lettini, Andrew Page, Mary Bagnall, John Wain, Julian Parkhill, Gordon Dougan, Robert Davies, and Robert A. Kingsley. Microevolution of monophasic Salmonella typhimurium during epidemic, United Kingdom, 2005â2010. *Emerging Infectious Diseases*, 22(4):617–624, 2016.

78. Catherine E. Yoshida, Peter Kruczkiewicz, Chad R. Laing, Erika J. Lingohr, Victor P.J. Gannon, John H.E. Nash, and Eduardo N. Taboada. The salmonella in silico typing resource (SISTR): An open web-accessible tool for rapidly typing and subtyping draft salmonella genome assemblies. *PLoS ONE*, 11(1):1–17, 2016.

79. P Beltran, S A Plock, N H Smith, T S Whittam, D C Old, and R K Selander. Reference collection of strains of the Salmonella typhimurium complex from natural populations. *Journal of general microbiology*, 137(3):601–606, mar 1991.

80. Robert A Kingsley, Chisomo L Msefula, Nicholas R Thomson, Robert A Kingsley, Chisomo L Msefula, Nicholas R Thomson, Samuel Kariuki, Kathryn E Holt, Melita A Gordon, David Harris, Louise Clarke, Sally Whitehead, Vartul Sangal, Kevin Marsh, Mark Achtman, Malcolm E Molyneux, Martin Cormican, Julian Parkhill, Calman A Maclennan, Robert S Heyderman, and Gordon Dougan. Epidemic multiple drug resistant Salmonella Typhimurium causing invasive disease in sub-Saharan Africa have a distinct genotype Epidemic multiple drug resistant Salmonella Typhimurium causing invasive disease in sub-Saharan Africa have a distinct genotype. pages 2279–2287, 2009.

81. T W Pennycott, A Park, and H A Mather. Isolation of different serovars of Salmonella enterica from wild birds in Great Britain between 1995 and 2003. *The Veterinary record*, 158(24):817–820, jun 2006.

82. Chinyere K. Okoro, Robert A. Kingsley, Thomas R. Connor, Simon R. Harris, Christopher M. Parry, Manar N. Al-Mashhadani, Samuel Kariuki, Chisomo L. Msefula, Melita A. Gordon, Elizabeth De Pinna, John Wain, Robert S. Heyderman, Stephen Obaro, Pedro L. Alonso, Inacio Mandomando, Calman A. MacLennan, Milagritos D. Tapia, Myron M. Levine, Sharon M. Tennant, Julian Parkhill, and Gordon Dougan. Intracontinental spread of human invasive Salmonella Typhimurium pathovariants in sub-Saharan Africa. *Nature Genetics*, 44(11):1215–1221, 2012.

83. Priyanka Jain, Sudhanthiramani Sudhanthirakodi, Goutam Chowdhury, Sangeeta Joshi, Shalini Anandan, Ujjwayni Ray, Asish Mukhopadhyay, and Shanta Dutta. Antimicrobial resistance, plasmid, virulence, multilocus sequence typing and pulsed-field gel electrophoresis profiles of Salmonella enterica serovar Typhimurium clinical and environmental isolates from India. *PLoS ONE*, 13(12):1–16, 2018.

84. Philip M. Ashton, Siân V. Owen, Lukeki Kaindama, Will P.M. Rowe, Chris R. Lane, Lesley Larkin, Satheesh Nair, Claire Jenkins, Elizabeth M. de Pinna, Nicholas A. Feasey, Jay C.D. Hinton, and Timothy J. Dallman. Public health surveillance in the UK revolutionises our understanding of the invasive Salmonella Typhimurium epidemic in Africa. *Genome Medicine*, 9(1), 2017.

85. Pedro Henrique N. Panzenhagen, Narayan C. Paul, Carlos A. Conte, Renata G. Costa, Dália P. Rodrigues, and Devendra H. Shah. Genetically distinct lineages of Salmonella Typhimurium ST313 and ST19 are present in Brazil. *International Journal of Medical Microbiology*, 308(2):306–316, 2018.

86. S S Long, C G Prober, and M Fischer. *Principles and Practice of Pediatric Infectious Diseases E-Book*. Elsevier Health Sciences, 2017.

87. Centers for Disease Control and Prevention. Antibiotic resistance threats in the United States. pages 1–113, 2019.

88. Melita A. Gordon, Hastings T. Banda, Macpherson Gondwe, Stephen B. Gordon, Martin J. Boeree, Amanda L. Walsh, John E. Corkill, C. Anthony Hart, Charles F. Gilks, and Malcolm E. Molyneux. Non-typhoidal salmonella bacteraemia among HIV-infected Malawian adults: High mortality and frequent recrudescence. *Aids*, 16(12):1633–1641, 2002.

89. Sandra Y. Wotzka, Bidong D. Nguyen, and Wolf Dietrich Hardt. Salmonella Typhimurium Diarrhea Reveals Basic Principles of Enteropathogen Infection and Disease-Promoted DNA Exchange. *Cell Host and Microbe*, 21(4):443–454, 2017.

90. J W Foster and H K Hall. Inducible pH homeostasis and the acid tolerance response of Salmonella typhimurium. *Journal of bacteriology*, 173(16):5129–5135, aug 1991.

91. K Y Leung and B B Finlay. Intracellular replication is essential for the virulence of Salmonella typhimurium. *Proceedings of the National Academy of Sciences of the United States of America*, 88(24):11470–11474, dec 1991.

92. B B Finlay, S Ruschkowski, and S Dedhar. Cytoskeletal rearrangements accompanying salmonella entry into epithelial cells. *Journal of cell science*, 99 (Pt 2):283–296, jun 1991.

93. C L Francis, M N Starnbach, and S Falkow. Morphological and cytoskeletal changes in epithelial cells occur immediately upon interaction with Salmonella typhimurium grown under low-oxygen conditions. *Molecular microbiology*, 6(21):3077–3087, nov 1992.

94. C L Francis, T A Ryan, B D Jones, S J Smith, and S Falkow. Ruffles induced by Salmonella and other stimuli direct macropinocytosis of bacteria. *Nature*, 364(6438):639–642, aug 1993.

95. B B Finlay and S Falkow. Virulence factors associated with Salmonella species. *Microbiological sciences*, 5(11):324–328, nov 1988.

96. H Ochman and E A Groisman. Distribution of pathogenicity islands in Salmonella spp. *Infection and immunity*, 64(12):5410–5412, dec 1996.

97. Sandra L. Marcus, John H. Brumell, Cheryl G. Pfeifer, and B. Brett Finlay. Salmonella pathogenicity islands: Big virulence in small packages. *Microbes and Infection*, 2(2):145–156, 2000.

98. V Kuhle and M Hensel. Cellular microbiology of intracellular Salmonella enterica: functions of the type III secretion system encoded by Salmonella pathogenicity island 2. *Cellular and molecular life sciences : CMLS*, 61(22):2812–2826, nov 2004.

99. F Garcia-del Portillo and B B Finlay. The varied lifestyles of intracellular pathogens within eukaryotic vacuolar compartments. *Trends in microbiology*, 3(10):373–380, oct 1995.

100. F Garcia-del Portillo and B B Finlay. Targeting of Salmonella typhimurium to vesicles containing lysosomal membrane glycoproteins bypasses compartments with mannose 6-phosphate receptors. *The Journal of cell biology*, 129(1):81–97, apr 1995.

101. M Rathman, L P Barker, and S Falkow. The unique trafficking pattern of Salmonella typhimurium-containing phagosomes in murine macrophages is independent of the mechanism of bacterial entry. *Infection and immunity*, 65(4):1475–1485, apr 1997.

102. Susan L Fink and Brad T Cookson. Pyroptosis and host cell death responses during Salmonella infection. *Cellular microbiology*, 9(11):2562–2570, nov 2007.

103. R M Tsolis, L G Adams, T A Ficht, and A J Bäumler. Contribution of Salmonella typhimurium virulence factors to diarrheal disease in calves. *Infection and immunity*, 67(9):4879–4885, sep 1999.

104. B D Jones, N Ghori, and S Falkow. Salmonella typhimurium initiates murine infection by penetrating and destroying the specialized epithelial M cells of the Peyer's patches. *The Journal of experimental medicine*, 180(1):15–23, jul 1994.

105. Isabel Martinez-Argudo and Mark A. Jepson. Salmonella translocates across an in vitro M cell model independently of SPI-1 and SPI-2. *Microbiology*, 154(12):3887–3894, 2008.

106. Andres Vazquez-Torres, Jessica Jones-Carson, Andreas J. Bäumler, Stanley Falkow, Raphael Valdivia, William Brown, Mysan Le, Ruth Berggren, W. Tony Parks, and Ferric C. Fang. Extraintestinal dissemination CD18-expressing phagocytes. *Nature*, 401(October):623–626, 1999.

107. M Rescigno, M Urbano, B Valzasina, M Francolini, G Rotta, R Bonasio, F Granucci, J P Kraehenbuhl, and P Ricciardi-Castagnoli. Dendritic cells express tight junction proteins and penetrate gut epithelial monolayers to sample bacteria. *Nature immunology*, 2(4):361–367, apr 2001.

108. Donald G Guiney and Marc Lesnick. Targeting of the actin cytoskeleton during infection by Salmonella strains. *Clinical immunology (Orlando, Fla.)*, 114(3):248–255, mar 2005.

109. D Zhou, M S Mooseker, and J E Galán. An invasion-associated Salmonella protein modulates the actin-bundling activity of plastin. *Proceedings of the National Academy of Sciences of the United States of America*, 96(18):10176–10181, aug 1999.

110. M Hensel, J E Shea, S R Waterman, R Mundy, T Nikolaus, G Banks, A Vazquez-Torres, C Gleeson, F C Fang, and D W Holden. Genes encoding putative effector proteins of the type III secretion system of Salmonella pathogenicity island 2 are required for bacterial virulence and proliferation in macrophages. *Molecular microbiology*, 30(1):163–174, oct 1998.

111. J R Klein and B D Jones. Salmonella pathogenicity island 2-encoded proteins SseC and SseD are essential for virulence and are substrates of the type III secretion system. *Infection and immunity*, 69(2):737–743, feb 2001.

112. Anamaria M.P. dos Santos, Rafaela G. Ferrari, and Carlos A. Conte-Junior. Virulence Factors in Salmonella Typhimurium: The Sagacity of a Bacterium. *Current Microbiology*, 76(6):762–773, 2019.

113. Madeleine A Wemyss and Jaclyn S Pearson. Host Cell Death Responses to Non-typhoidal Salmonella Infection. *Frontiers in immunology*, 10:1758, 2019.

114. Hanna K de Jong, Chris M Parry, Tom van der Poll, and W Joost Wiersinga. Host-pathogen interaction in invasive Salmonellosis. *PLoS pathogens*, 8(10):e1002933, 2012.

115. Sebastian E Winter, Parameth Thiennimitr, Maria G Winter, Brian P. Butler, Douglas L Huseby, Robert W. Crawford, Joseph M Russell, Charles L Bevins, L Garry Adams, Renée M. Tsolis, John R Roth, and Andreas J. Bäumler. Gut inflammation provides a respiratory electron acceptor for Salmonella. *Nature*, 467(7314):426–429, sep 2011.

116. Hiba Ibrahim, Basim Askar, Scott Hulme, Peter Neilson, and Paul Barrow. Differential Immune Phenotypes in Human Monocytes Induced by Non-Host-Adapted Salmonella enterica Serovar Choleraesuis and Host-Adapted S. Typhimurium. *Infection and Immunity*, 86(10):1–12, 2018.

117. Annika Hausmann and Wolf-Dietrich Hardt. The Interplay between Salmonella enterica Serovar Typhimurium and the Intestinal Mucosa during Oral Infection. *Microbiology spectrum*, 7(2), mar 2019.

118. Anna Fàbrega and Jordi Vila. Salmonella enterica serovar Typhimurium skills to succeed in the host: Virulence and regulation. *Clinical Microbiology Reviews*, 26(2):308–341, 2013.

119. Andrea H. Haselbeck, Ursula Panzner, Justin Im, Stephen Baker, Christian G. Meyer, and Florian Marks. Current perspectives on invasive nontyphoidal Salmonella disease, 2017.

120. James J Gilchrist, Calman A Maclennan, and Adrian V S Hill. Genetic susceptibility to invasive Salmonella disease. *Nature Publishing Group*, 15(7):452–463, 2015.

121. Dadi Falay, Laura Maria Francisca Kuijpers, Marie France Phoba, Hilde De Boeck, Octavie Lunguya, Emmanuel Vakaniaki, Sophie Bertrand, Wesley Mattheus, Pieter Jan Ceyssens, Raymond Vanhoof, Hugo Devlieger, Chris Van Geet, Erik Verheyen, Dauly Ngbonda, and Jan Jacobs. Microbiological, clinical and molecular findings of non-typhoidal Salmonella bloodstream infections associated with malaria, Oriental Province, Democratic Republic of the Congo. *BMC Infectious Diseases*, 16(1), 2016.

122. P L Petit and J K van Ginneken. Analysis of hospital records in four African countries, 1975-1990, with emphasis on infectious diseases. *The Journal of tropical medicine and hygiene*, 98(4):217–227, aug 1995.

123. Jennifer Bryce, Cynthia Boschi-Pinto, Kenji Shibuya, and Robert E. Black. WHO estimates of the causes of death in children. *Lancet*, 365(9465):1147–1152, 2005.

124. Lennox K. Archibald and L. Barth Reller. Clinical microbiology in developing countries. *Emerging Infectious Diseases*, 7(2):302–305, 2001.

125. C. A. Petti, C. R. Polage, T. C. Quinn, A. R. Ronald, and M. A. Sande. Laboratory Medicine in Africa: A Barrier to Effective Health Care. *Clinical Infectious Diseases*, 42(3):377–382, 2006.

126. John A. Crump, Habib O. Ramadhani, Anne B. Morrissey, Levina J. Msuya, Lan Yan Yang, Shein Chung Chow, Susan C. Morpeth, Hugh Reyburn, Boniface N. Njau, Andrea V. Shaw, Helmut C. Diefenthal, John A. Bartlett, John F. Shao, Werner Schimana, Coleen K. Cunningham, and Grace D. Kinabo. Invasive bacterial and fungal infections among hospitalized HIV-infected and HIV-uninfected children and infants in northern Tanzania. *Tropical Medicine and International Health*, 16(7):830–837, 2011.

127. Ifeanyi Valentine Uche, Calman A. MacLennan, and Allan Saul. A Systematic Review of the Incidence, Risk Factors and Case Fatality Rates of Invasive Nontyphoidal Salmonella (iNTS) Disease in Africa (1966 to 2014). *PLoS Neglected Tropical Diseases*, 11(1), 2017.

128. Florian Marks, Vera von Kalckreuth, Peter Aaby, Yaw Adu-Sarkodie, Muna Ahmed El Tayeb, Mohammad Ali, Abraham Aseffa, Stephen Baker, Holly M. Biggs, Morten Bjerregaard-Andersen, Robert F. Breiman, James I. Campbell, Leonard Cosmas, John A. Crump, Ligia Maria Cruz Espinoza, Jessica Fung Deerin, Denise Myriam Dekker, Barry S. Fields, Nagla Gasmelseed, Julian T. Hertz, Nguyen Van Minh Hoang, Justin Im, Anna Jaeger, Hyon Jin Jeon, Leon Parfait Kabore, Karen H. Keddy, Frank Konings, Ralf Krumkamp, Benedikt Ley, Sandra Valborg Løfberg, Jürgen May, Christian G. Meyer, Eric D. Mintz, Joel M. Montgomery, Aissatou Ahmet Niang, Chelsea Nichols, Beatrice Olack, Gi Deok Pak, Ursula Panzner, Jin Kyung Park, Se Eun Park, Henintsoa Rabezanahary, Raphaël Rakotozandrindrainy, Tiana Mirana Raminosoa, Tsiriniaina Jean Luco Razafindrabe, Emmanuel Sampo, Heidi Schütt-Gerowitt, Amy Gassama Sow, Nimako Sarpong, Hye Jin Seo, Arvinda Sooka, Abdramane Bassiahi Soura, Adama Tall, Mekonnen Teferi, Kamala Thriemer, Michelle R. Warren, Biruk Yeshitela, John D. Clemens, and Thomas F. Wierzba. Incidence of invasive salmonella disease in sub-Saharan Africa: a multicentre population-based surveillance study. *The Lancet Global Health*, 5(3):e310–e323, 2017.

129. Andrew J. Brent, Joe O. Oundo, Isaiah Mwangi, Lucy Ochola, Brett Lowe, and James A. Berkley. Salmonella bacteremia in Kenyan children. *Pediatric Infectious Disease Journal*, 25(3):230–236, 2006.

130. Ruchita Balasubramanian, Justin Im, Jung Seok Lee, Hyon Jin Jeon, Ondari D. Mogeni, Jerome H. Kim, Raphaël Rakotozandrindrainy, Stephen Baker, and Florian Marks. The global burden and epidemiology of invasive non-typhoidal Salmonella infections. *Human Vaccines and Immunotherapeutics*, 15(6), 2019.

131. Nguyen Phu Huong Lan, Tu Le Thi Phuong, Hien Nguyen Huu, Le Thuy, Alison E. Mather, Se Eun Park, Florian Marks, Guy E. Thwaites, Nguyen Van Vinh Chau, Corinne N. Thompson, and Stephen Baker. Invasive Non-typhoidal Salmonella Infections in Asia: Clinical Observations, Disease Outcome and Dominant Serovars from an Infectious Disease Hospital in Vietnam. *PLoS Neglected Tropical Diseases*, 10(8):1–13, 2016.

132. Sudipta Patra, Yasha Mukim, Muralidhar Varma, Chiranjay Mukhopadhyay, and Vandana Kalwaje Eshwara. Invasive nontyphoidal Salmonella disease in southern India: A 5-year experience from a tertiary care hospital. *Turkish Journal of Medical Sciences*, 48(5):1030–1035, 2018.

133. Edna Catering Rodríguez, Paula Díaz-Guevara, Jaime Moreno, Adriana Bautista, Lucy Montaño, María Elena Realpe, Anabella della Gaspera, and Magdalena Wiesner. Laboratory surveillance of Salmonella enterica from human clinical cases in Colombia 2005â2011. *Enfermedades infecciosas y microbiologia clinica (English ed.)*, 35(7):417–425, 2017.

134. Remco P H Peters, Ed E Zijlstra, Maarten J Schijffelen, Amanda L Walsh, George Joaki, John J Kumwenda, James G Kublin, Malcolm E Molyneux, and David K Lewis. A prospective study of bloodstream infections as cause of fever in Malawi: clinical predictors and implications for management. *Tropical medicine & international health : TM & IH*, 9(8):928–934, aug 2004.

135. Esther Muthumbi, Susan C. Morpeth, Michael Ooko, Alfred Mwanzu, Salim Mwarumba, Neema Mturi, Anthony O. Etyang, James A. Berkley, Thomas N. Williams, Samuel Kariuki, and J. Anthony G. Scott. Invasive salmonellosis in Kilifi, Kenya. *Clinical Infectious Diseases*, 61(Suppl 4):S290–S301, 2015.

136. Inácio Mandomando, Quique Bassat, Betuel Sigaúque, Sérgio Massora, Llorenç Quintó, Sozinho Ácacio, Tacilta Nhampossa, Delfino Vubil, Marcelino Garrine, Eusébio Macete, Pedro Aide, Charfudin Sacoor, Silvia Herrera-León, Joaquim Ruiz, Sharon M. Tennant, Clara Menéndez, and Pedro L. Alonso. Invasive salmonella infections among children from Rural Mozambique, 2001-2014. *Clinical Infectious Diseases*, 61(Suppl 4):S339–S345, 2015.

137. Godwin Enwere, Ekow Biney, Yinbun Cheung, Syed M.A. Zaman, Brown Okoko, Claire Oluwalana, Adeola Vaughan, Brian Greenwood, Richard Adegbola, and Felicity T. Cutts. Epidemiologic and clinical characteristics of community-acquired invasive bacterial infections in children aged 2-29 months in The Gambia. *Pediatric Infectious Disease Journal*, 25(8):700–705, 2006.

138. E. M. Molyneux, L. A. Mankhambo, Phiri Ajib, S. M. Graham, H. Forsyth, Phiri Amos, A. L. Walsh, L. K. Wilson, and M. E. Molyneux. The outcome of non-typhoidal salmonella meningitis in Malawian children, 1997-2006. *Annals of Tropical Paediatrics*, 2009.

139. E. M. Molyneux, A. L. Walsh, H. Forsyth, M. Tembo, J. Mwenechanya, K. Kayira, L. Bwanaisa, A. Njobvu, S. Rogerson, and G. Malenga. Dexamethasone treatment in childhood bacterial meningitis in Malawi: A randomised controlled trial. *Lancet*, 2002.

140. Nicholas A. Feasey, Amy K. Cain, Chisomo L. Msefula, Derek Pickard, Maaike Alaerts, Martin Aslett, Dean B. Everett, Theresa J. Allain, Gordon Dougan, Melita A. Gordon, Robert S. Heyderman, and Robert A. Kingsley. Drug resistance in salmonella enteric ser. Typhimurium bloodstream infection, Malawi. *Emerging Infectious Diseases*, 20(11):1957–1959, 2014.

141. Evelin Schwarzer, Franco Turrini, Daniela Ulliers, Giuliana Giribaldi, Hagai Ginsburg, and Paolo Arese. Impairment of macrophage functions after ingestion of plasmodium falciparum-infected erythrocytes or isolated malarial pigment. *Journal of Experimental Medicine*, 176(4):1033–1041, 1992.

142. Nancy K. Nyakoe, Ronald P. Taylor, Joseph N. Makumi, and John N. Waitumbi. Complement consumption in children with Plasmodium falciparum malaria. *Malaria Journal*, 8(1), 2009.

143. Esther N. Gondwe, Malcolm E. Molyneux, Margaret Goodall, Stephen M. Graham, Pietro Mastroeni, Mark T. Drayson, and Calman A. MacLennan. Importance of antibody and complement for oxidative burst and killing of invasive nontyphoidal Salmonella by blood cells in Africans. *Proceedings of the National Academy of Sciences of the United States of America*, 107(7):3070–3075, 2010.

144. Kristen L. Lokken, Jason P. Mooney, Brian P. Butler, Mariana N. Xavier, Jennifer Y. Chau, Nicola Schaltenberg, Ramie H. Begum, Werner Müller, Shirley Luckhart, and Renée M. Tsolis. Malaria Parasite Infection Compromises Control of Concurrent Systemic Non-typhoidal Salmonella Infection via IL-10-Mediated Alteration of Myeloid Cell Function. *PLoS Pathogens*, 2014.

145. J. P. Mooney, B. P. Butler, K. L. Lokken, M. N. Xavier, J. Y. Chau, N. Schaltenberg, S. Dandekar, M. D. George, R. L. Santos, S. Luckhart, and R. M. Tsolis. The mucosal inflammatory response to non-typhoidal Salmonella in the intestine is blunted by IL-10 during concurrent malaria parasite infection. *Mucosal Immunology*, 2014.

146. Christof Geldmacher, Alexandra Schuetz, Njabulo Ngwenyama, JosephÂ P. Casazza, Erica Sanga, Elmar Saathoff, Catharina Boehme, Steffen Geis, Leonard Maboko, Mahavir Singh, Fred Minja, Andreas Meyerhans, RichardÂ A. Koup, and Michael Hoelscher. Early Depletion of Mycobacterium tuberculosis âSpecific T Helper 1 Cell Responses after HIVâ1 Infection . *The Journal of Infectious Diseases*, 2008.

147. Satya Dandekar, Michael D George, and Andreas J Bäumler. Th17 cells, HIV and the gut mucosal barrier. *Current opinion in HIV and AIDS*, 5(2):173–178, mar 2010.

148. Manuela Raffatellu, Renato L. Santos, David E. Verhoeven, Michael D. George, R. Paul Wilson, Sebastian E. Winter, Ivan Godinez, Sumathi Sankaran, Tatiane A. Paixao, Melita A. Gordon, Jay K. Kolls, Satya Dandekar, and Andreas J. Bäumler. Simian immunodeficiency virus-induced mucosal interleukin-17 deficiency promotes Salmonella dissemination from the gut. *Nature Medicine*, 2008.

149. D R Brewster, M J Manary, I S Menzies, and R L Henry. Intestinal permeability in kwashiorkor. *Archives of Disease in Childhood*, pages 236–241, 1997.

150. Maren Johanne Heilskov Rytter, Lilian Kolte, André Briend, Henrik Friis, and Vibeke Brix Christensen. The immune system in children with malnutrition - A systematic review, 2014.

151. Kurt Schopfer and Steven D. Douglas. Neutrophil function in children with kwashiorkor. *The Journal of Laboratory and Clinical Medicine*, 1976.

152. T Rikimaru, K Taniguchi, J E Yartey, D O Kennedy, and F K Nkrumah. Humoral and cell-mediated immunity in malnourished children in Ghana. *European Journal of Clinical Nutrition*, pages 344–350, 1998.

153. Minelva R. Nanton, Sing Sing Way, Mark J. Shlomchik, and Stephen J. Mcsorley. Cutting Edge: B Cells Are Essential for Protective Immunity against Salmonella Independent of Antibody Secretion. *The Journal of Immunology*, 2012.

154. Thomas N Williams, Sophie Uyoga, Alex Macharia, Carolyne Ndila, Charlotte F Mcauley, Daniel H Opi, Salim Mwarumba, Julie Makani, Albert Komba, Moses N Ndiritu, Shahnaaz K Sharif, Kevin Marsh, James A Berkley, and J Anthony G Scott. Bacteraemia in Kenyan children with sickle-cell anaemia : a retrospective cohort and case â control study. *The Lancet*, 374(9698):1364–1370, 2009.

155. Richard B. Johnston, Simon L. Newman, and Alan G. Struth. An Abnormality of the Alternate Pathway of Complement Activation in Sickle-Cell Disease. *New England Journal of Medicine*, 1973.

156. Denise Dekker, Ralf Krumkamp, Daniel Eibach, Nimako Sarpong, Kennedy Gyau Boahen, Michael Frimpong, Elina Fechtner, Sven Poppert, Ralf Matthias Hagen, Norbert Georg Schwarz, Yaw Adu-Sarkodie, Ellis Owusu-Dabo, Justin Im, Florian Marks, Hagen Frickmann, and Jürgen May. Characterization of Salmonella enterica from invasive bloodstream infections and water sources in rural Ghana. *BMC Infectious Diseases*, 18(1), 2018.

157. Chinyere K Okoro, Lars Barquist, Thomas R Connor, Simon R Harris, Simon Clare, Mark P Stevens, Mark J Arends, Christine Hale, Leanne Kane, Derek J Pickard, Jennifer Hill, Katherine Harcourt, Julian Parkhill, Gordon Dougan, and Robert A Kingsley. Signatures of adaptation in human invasive Salmonella Typhimurium ST313 populations from sub-Saharan Africa. *PLoS neglected tropical diseases*, 9(3):e0003611, mar 2015.

158. Sarah E Carden, Gregory T Walker, Jared Honeycutt, Kyler Lugo, Trung Pham, Amanda Jacobson, Donna Bouley, Juliana Idoyaga, Renee M Tsolis, and Denise Monack. Pseudogenization of the Secreted Effector Gene sseI Confers Rapid Systemic Dissemination of S. Typhimurium ST313 within Migratory Dendritic Cells. *Cell host & microbe*, 21(2):182–194, feb 2017.

159. Sarah Carden, Chinyere Okoro, Gordon Dougan, and Denise Monack. Non-typhoidal Salmonella Typhimurium ST313 isolates that cause bacteremia in humans stimulate less inflammasome activation than ST19 isolates associated with gastroenteritis. *Pathogens and disease*, 73(4), 2015.

160. Erica Kintz, Mark R. Davies, Disa L. Hammarlöf, Rocío Canals, Jay C.D. Hinton, and Marjan W. van der Woude. A BTP1 prophage gene present in invasive non-typhoidal Salmonella determines composition and length of the O-antigen of the lipopolysaccharide. *Molecular Microbiology*, 96(2):263–275, 2015.

161. Disa L. Hammarlöf, Carsten Kröger, Siân V. Owen, Rocío Canals, Lizeth Lacharme-Lora, Nicolas Wenner, Anna E. Schager, Timothy J. Wells, Ian R. Henderson, Paul Wigley, Karsten Hokamp, Nicholas A. Feasey, Melita A. Gordon, and Jay C.D. Hinton. Role of a single noncoding nucleotide in the evolution of an epidemic African clade of Salmonella. *Proceedings of the National Academy of Sciences of the United States of America*, 115(11), 2018.

162. K. L. Gillen and K. T. Hughes. Negative regulatory loci coupling flagellin synthesis to flagellar assembly in Salmonella typhimurium. *Journal of Bacteriology*, 173(7):2301–2310, 1991.

163. Phillip D Aldridge, Cheng Wu, Joshua Gnerer, Joyce E Karlinsey, Kelly T Hughes, and Matthew S Sachs. Regulatory protein that inhibits both synthesis and use of the target protein controls flagellar phase variation in Salmonella enterica. *Proceedings of the National Academy of Sciences*, 103(30), 2006.

164. Sani Ousmane, Miwako Kobayashi, Issaka Seidou, Bassira Issaka, Sable Sharpley, Jennifer L Farrar, Cynthia G Whitney, and Mahamoudou Ouattara. Characterization of pneumococcal meningitis before and after introduction of 13-valent pneumococcal conjugate vaccine in Niger, 2010-2018. *Vaccine*, 38(23):3922–3929, may 2020.

165. Heidi M Soeters, Dinanibè Kambiré, Guetawendé Sawadogo, Rasmata Ouédraogo-Traoré, Brice Bicaba, Isaïe Medah, Lassana Sangaré, Abdoul-Salam Ouédraogo, Soumeya Ouangraoua, Issaka Yaméogo, Malika Congo-Ouédraogo, Absatou Ky Ba, Flavien Aké, Velusamy Srinivasan, Ryan T Novak, Lesley McGee, Cynthia G Whitney, and Chris Van Beneden. Impact of 13-Valent Pneumococcal Conjugate Vaccine on Pneumococcal Meningitis, Burkina Faso, 2016-2017. *The Journal of infectious diseases*, 220(220 Suppl 4):S253–S262, oct 2019.

166. Bianca Paglietti, Giovanni Falchi, Peter Mason, Owen Chitsatso, Satheesh Nair, Lovemore Gwanzura, Sergio Uzzau, Piero Cappuccinelli, John Wain, and Salvatore Rubino. Diversity among human non-typhoidal salmonellae isolates from Zimbabwe. *Transactions of the Royal Society of Tropical Medicine and Hygiene*, 107(8):487–492, 2013.

167. Troy D Moon, Monika Johnson, Monique A Foster, Wilson P Silva, Manuel Buene, Emilio Valverde, Luís Morais, John V Williams, Sten H Vermund, and Paula E Brentlinger. Identification of Invasive Salmonella Enterica Serovar Typhimurium ST313 in Ambulatory HIV-Infected Adults in Mozambique. *Journal of global infectious diseases*, 7(4):139–142, 2015.

168. Benedikt Ley, Simon Le Hello, Octavie Lunguya, Veerle Lejon, Jean-Jacques Muyembe, François-Xavier Weill, and Jan Jacobs. Invasive Salmonella enterica serotype typhimurium infections, Democratic Republic of the Congo, 2007-2011. *Emerging infectious diseases*, 20(4):701–704, apr 2014.

169. Adam Akullian, Joel M. Montgomery, Grace John-Stewart, Samuel I. Miller, Hillary S. Hayden, Matthew C. Radey, Kyle R. Hager, Jennifer R. Verani, John Benjamin Ochieng, Jane Juma, Jim Katieno, Barry Fields, Godfrey Bigogo, Allan Audi, and Judd Walson. Multi-drug resistant non-typhoidal Salmonella associated with invasive disease in western Kenya. *PLoS Neglected Tropical Diseases*, 12(1), 2018.

170. Nicholas A. Feasey, James Hadfield, Karen H. Keddy, Timothy J. Dallman, Jan Jacobs, Xiangyu Deng, Paul Wigley, Lars Barquist Barquist, Gemma C. Langridge, Theresa Feltwell, Simon R. Harris, Alison E. Mather, Maria Fookes, Martin Aslett, Chisomo Msefula, Samuel Kariuki, Calman A. Maclennan, Robert S. Onsare, François Xavier Weill, Simon Le Hello, Anthony M. Smith, Michael McClelland, Prerak Desai, Christopher M. Parry, John Cheesbrough, Neil French, Josefina Campos, Jose A. Chabalgoity, Laura Betancor, Katie L. Hopkins, Satheesh Nair, Tom J. Humphrey, Octavie Lunguya, Tristan A. Cogan, Milagritos D. Tapia, Samba O. Sow, Sharon M. Tennant, Kristin Bornstein, Myron M. Levine, Lizeth Lacharme-Lora, Dean B. Everett, Robert A. Kingsley, Julian Parkhill, Robert S. Heyderman, Gordon Dougan, Melita A. Gordon, and Nicholas R. Thomson. Distinct Salmonella Enteritidis lineages associated with enterocolitis in high-income settings and invasive disease in low-income settings. *Nature Genetics*, 48(10):1211–1217, 2016.

171. Nicholas A Feasey, Dean Everett, E Brian Faragher, Arantxa Roca-feltrer, Arthur Kang, Brigitte Denis, Marko Kerac, Elizabeth Molyneux, Malcolm Molyneux, Andreas Jahn, Melita A Gordon, and Robert S Heyderman. Modelling the Contributions of Malaria , HIV , Malnutrition and Rainfall to the Decline in Paediatric Invasive Non-typhoidal Salmonella Disease in Malawi. *PLoS Neglected Tropical Diseases*, 9(7):1–12, 2015.

172. Ondari D. Mogeni, Ligia María Cruz Espinoza, Justin Im, Ursula Panzner, Trevor Toy, Gi Deok Pak, Andrea Haselbeck, Enusa Ramani, Heidi Schütt-Gerowitt, Jan Jacobs, Octavie Lunguya Metila, Oluwafemi J. Adewusi, Iruka N. Okeke, Veronica I. Ogunleye, Ellis Owusu-Dabo, Raphaël Rakotozandrindrainy, Abdramane Bassiahi Soura, Mekonnen Teferi, Keriann Conway Roy, William MacWright, Robert F. Breiman, Jerome H. Kim, Vittal Mogasale, Stephen Baker, Se Eun Park, and Florian Marks. The Monitoring and Evaluation of a Multicountry Surveillance Study, the Severe Typhoid Fever in Africa Program. *Clinical Infectious Diseases*, 69(Suppl 6):S510–S518, 2019.

173. C F Gilks, R J Brindle, L S Otieno, P M Simani, R S Newnham, S M Bhatt, G N Lule, G B Okelo, W M Watkins, and P G Waiyaki. Life-threatening bacteraemia in HIV-1 seropositive adults admitted to hospital in Nairobi, Kenya. *Lancet (London, England)*, 336(8714):545–549, sep 1990.

174. Samuel Kariuki, Gunturu Revathi, Nyambura Kariuki, John Kiiru, Joyce Mwituria, and Charles A. Hart. Characterisation of community acquired non-typhoidal Salmonella from bacteraemia and diarrhoeal infections in children admitted to hospital in Nairobi, Kenya. *BMC Microbiology*, 6:1–10, 2006.

175. Melita A Gordon, Stephen M Graham, Amanda L Walsh, Lorna Wilson, Amos Phiri, Elizabeth Molyneux, Eduard E Zijlstra, Robert S Heyderman, C Anthony Hart, and Malcolm E Molyneux. Epidemics of invasive Salmonella enterica serovar enteritidis and S. enterica Serovar typhimurium infection associated with multidrug resistance among

adults and children in Malawi. *Clinical infectious diseases : an official publication of the Infectious Diseases Society of America*, 46(7):963–969, apr 2008.

176. Sandra Van Puyvelde, Derek Pickard, Koen Vandelannoote, Eva Heinz, Barbara Barbé, Tessa de Block, Simon Clare, Eve L. Coomber, Katherine Harcourt, Sushmita Sridhar, Emily A. Lees, Nicole E. Wheeler, Elizabeth J. Klemm, Laura Kuijpers, Lisette Mbuyi Kalonji, Marie France Phoba, Dadi Falay, Dauly Ngbonda, Octavie Lunguya, Jan Jacobs, Gordon Dougan, and Stijn Deborggraeve. An African Salmonella Typhimurium ST313 sublineage with extensive drug-resistance and signatures of host adaptation. *Nature Communications*, 10(1):1–12, 2019.

177. Priscilla Branchu, Matt Bawn, and Robert A. Kingsley. Genome variation and molecular epidemiology of Salmonella enterica serovar Typhimurium pathovariants. *Infection and Immunity*, 86(8):1–17, 2018.

178. Carsten Kröger, Shane C. Dillon, Andrew D.S. Cameron, Kai Papenfort, Sathesh K. Sivasankaran, Karsten Hokamp, Yanjie Chao, Alexandra Sittka, Magali Hébrard, Kristian Händler, Aoife Colgan, Pimlapas Leekitcharoenphon, Gemma C. Langridge, Amanda J. Lohan, Brendan Loftus, Sacha Lucchini, David W. Ussery, Charles J. Dorman, Nicholas R. Thomson, Jörg Vogel, and Jay C.D. Hinton. The transcriptional landscape and small RNAs of Salmonella enterica serovar Typhimurium. *Proceedings of the National Academy of Sciences of the United States of America*, 109(20):1277–1286, 2012.

179. Rocío Canals, Disa L. Hammarlöf, Carsten Kröger, Siân V. Owen, Wai Yee Fong, Lizeth Lacharme-Lora, Xiaojun Zhu, Nicolas Wenner, Sarah E. Carden, Jared Honeycutt, Denise M. Monack, Robert A. Kingsley, Philip Brownridge, Roy R. Chaudhuri, Will P.M. Rowe, Alexander V. Predeus, Karsten Hokamp, Melita A. Gordon, and Jay C.D. Hinton. *Adding function to the genome of African Salmonella Typhimurium ST313 strain D23580*, volume 17. 2019.

180. Jiseon Yang, Jennifer Barrila, Kenneth L Roland, Jacquelyn Kilbourne, C Mark Ott, Rebecca J Forsyth, and Cheryl A Nickerson. Characterization of the Invasive, Multidrug Resistant Non-typhoidal Salmonella Strain D23580 in a Murine Model of Infection. *PLoS neglected tropical diseases*, 9(6):e0003839, jun 2015.

181. Edna M. Ondari, Elizabeth J. Klemm, Chisomo L. Msefula, Moataz Abd El Ghany, Jennifer N. Heath, Derek J. Pickard, Lars Barquist, Gordon Dougan, Robert A. Kingsley, and Calman A. Maclennan. Rapid transcriptional responses to serum exposure are associated with sensitivity and resistance to antibody-mediated complement killing in invasive salmonella typhimurium st313 [version 1; peer review: 2 approved]. *Wellcome Open Research*, 4:1–17, 2019.

182. Larissa A. Singletary, Joyce E. Karlinsey, Stephen J. Libby, Jason P. Mooney, Kristen L. Lokken, Renée M. Tsolis, Mariana X. Byndloss, Lauren A. Hirao, Christopher A. Gaulke, Robert W. Crawford, Satya Dandekar, Robert A. Kingsley, Chisomo L. Msefula, Robert S. Heyderman, and Ferric C. Fang. Loss of multicellular behavior in epidemic African nontyphoidal Salmonella enterica serovar Typhimurium ST313 strain D23580. *mBio*, 7(2), 2016.

183. Girish Ramachandran, Komi Aheto, Mark E. Shirtliff, and Sharon M. Tennant. Poor biofilm-forming ability and long-term survival of invasive Salmonella Typhimurium ST313. *Pathogens and disease*, 74(5), 2016.

184. Girish Ramachandran, Darren J Perkins, Patrick J Schmidlein, Mohan E Tulapurkar, and Sharon M Tennant. Invasive Salmonella Typhimurium ST313 with naturally attenuated flagellin elicits reduced inflammation and replicates within macrophages. *PLoS neglected tropical diseases*, 9(1):e3394, jan 2015.

185. Ana Herrero-Fresno, Irene Cartas Espinel, Malene Roed Spiegelhauer, Priscila Regina Guerra, Karsten Wiber Andersen, and John Elmerdahl Olsen. The Homolog of the Gene bstA of the BTP1 Phage from Salmonella enterica Serovar Typhimurium ST313 Is an Antivirulence Gene in Salmonella enterica Serovar Dublin. *Infection and immunity*, 86(1), jan 2018.

186. Girish Ramachandran, Aruna Panda, Ellen E Higginson, Eugene Ateh, Michael M Lipsky, Sunil Sen, Courtney A Matson, Jasnehta Permala-Booth, Louis J DeTolla, and Sharon M Tennant. Virulence of invasive Salmonella Typhimurium ST313 in animal models of infection. *PLoS neglected tropical diseases*, 11(8):e0005697, aug 2017.

187. Evelina Tacconelli, Elena Carrara, Alessia Savoldi, Stephan Harbarth, Marc Mendelson, Dominique L. Monnet, Céline Pulcini, Gunnar Kahlmeter, Jan Kluytmans, Yehuda Carmeli, Marc Ouellette, Kevin Outterson, Jean Patel, Marco Cavaleri, Edward M. Cox, Chris R. Houchens, M. Lindsay Grayson, Paul Hansen, Nalini Singh, Ursula Theuretzbacher, and Nicola Magrini. Discovery, research, and development of new antibiotics: The WHO priority list of antibiotic-resistant bacteria and tuberculosis. *The Lancet Infectious Diseases*, 3099(17):1–10, 2017.

188. Vanessa K. Wong, Stephen Baker, Derek J. Pickard, Julian Parkhill, Andrew J. Page, Nicholas A. Feasey, Robert A. Kingsley, Nicholas R. Thomson, Jacqueline A. Keane, François Xavier Weill, David J. Edwards, Jane Hawkey, Simon R. Harris, Alison E. Mather, Amy K. Cain, James Hadfield, Peter J. Hart, Nga Tran Vu Thieu, Elizabeth J. Klemm, Dafni A. Glinos, Robert F. Breiman, Conall H. Watson, Samuel Kariuki, Melita A. Gordon, Robert S. Heyderman, Chinyere Okoro, Jan Jacobs, Octavie Lunguya, W. John Edmunds, Chisomo Msefula, Jose A. Chabalgoity, Mike Kama, Kylie Jenkins, Shanta Dutta, Florian Marks, Josefina Campos, Corinne Thompson, Stephen Obaro, Calman A. Maclennan, Christiane Dolecek, Karen H. Keddy, Anthony M. Smith, Christopher M. Parry, Abhilasha Karkey, E. Kim Mulholland, James I. Campbell, Sabina Dongol, Buddha Basnyat, Muriel Dufour, Don Bandaranayake, Take Toleafoa Naseri, Shalini Pravin Singh, Mochammad Hatta, Paul Newton, Robert S. Onsare, Lupeoletalalei Isaia, David Dance, Viengmon Davong, Guy Thwaites, Lalith Wijedoru, John A. Crump, Elizabeth De Pinna, Satheesh Nair, Eric J. Nilles, Duy Pham Thanh, Paul Turner, Sona Soeng, Mary Valcanis, Joan Powling, Karolina Dimovski, Geoff Hogg, Jeremy Farrar, Kathryn E. Holt, and Gordon Dougan. Phylogeographical analysis of the dominant multidrug-resistant H58 clade of Salmonella Typhi identifies inter-and intracontinental transmission events. *Nature Genetics*, 47(6):632–639, 2015.

189. Duy Pham Thanh, Abhilasha Karkey, Sabina Dongol, Nhan Ho Thi, Corinne N Thompson, Maia A Rabaa, Amit Arjyal, Kathryn E Holt, Vanessa Wong, Nga Tran Vu Thieu, Phat Voong Vinh, Tuyen Ha Thanh, Ashish Pradhan, Saroj Kumar Shrestha,

Damoder Gajurel, Derek Pickard, Christopher M Parry, Gordon Dougan, Marcel Wolbers, Christiane Dolecek, Guy E Thwaites, Buddha Basnyat, and Stephen Baker. A novel ciprofloxacin-resistant subclade of H58 Salmonella Typhi is associated with fluoroquinolone treatment failure. *eLife*, 5:e14003, mar 2016.

190. Vanessa K Wong, Kathryn E Holt, Chinyere Okoro, Stephen Baker, Derek J Pickard, Florian Marks, Andrew J Page, Grace Olanipekun, Huda Munir, Roxanne Alter, Paul D Fey, Nicholas A Feasey, Francois-Xavier Weill, Simon Le Hello, Peter J Hart, Samuel Kariuki, Robert F Breiman, Melita A Gordon, Robert S Heyderman, Jan Jacobs, Octavie Lunguya, Chisomo Msefula, Calman A MacLennan, Karen H Keddy, Anthony M Smith, Robert S Onsare, Elizabeth De Pinna, Satheesh Nair, Ben Amos, Gordon Dougan, and Stephen Obaro. Molecular Surveillance Identifies Multiple Transmissions of Typhoid in West Africa. *PLoS neglected tropical diseases*, 10(9):e0004781, sep 2016.

191. Elizabeth J. Klemm, Sadia Shakoor, Andrew J. Page, Farah Naz Qamar, Kim Judge, Dania K. Saeed, Vanessa K. Wong, Timothy J. Dallman, Satheesh Nair, Stephen Baker, Ghazala Shaheen, Shahida Qureshi, Mohammad Tahir Yousafzai, Muhammad Khalid Saleem, Zahra Hasan, Gordon Dougan, and Rumina Hasan. Emergence of an extensively drug-resistant Salmonella enterica serovar typhi clone harboring a promiscuous plasmid encoding resistance to fluoroquinolones and third-generation cephalosporins. *mBio*, 9(1):1–10, 2018.

192. Marie-France Phoba, Barbara Barbé, Octavie Lunguya, Lysette Masendu, Deo Lulengwa, Gordon Dougan, Vanessa K Wong, Sophie Bertrand, Pieter-Jan Ceyssens, Jan Jacobs, Sandra Van Puyvelde, and Stijn Deborggraeve. Salmonella enterica serovar Typhi Producing CTX-M-15 Extended Spectrum β-Lactamase in the Democratic Republic of the Congo. *Clinical infectious diseases : an official publication of the Infectious Diseases Society of America*, 65(7):1229–1231, oct 2017.

193. Se Eun Park, Duy Thanh Pham, Christine Boinett, Vanessa K Wong, Gi Deok Pak, Ursula Panzner, Ligia Maria Cruz Espinoza, Vera von Kalckreuth, Justin Im, Heidi Schütt-Gerowitt, John A Crump, Robert F Breiman, Yaw Adu-Sarkodie, Ellis Owusu-Dabo, Raphaël Rakotozandrindrainy, Abdramane Bassiahi Soura, Abraham Aseffa, Nagla Gasmelseed, Karen H Keddy, Jürgen May, Amy Gassama Sow, Peter Aaby, Holly M Biggs, Julian T Hertz, Joel M Montgomery, Leonard Cosmas, Beatrice Olack, Barry Fields, Nimako Sarpong, Tsiriniaina Jean Luco Razafindrabe, Tiana Mirana Raminosoa, Leon Parfait Kabore, Emmanuel Sampo, Mekonnen Teferi, Biruk Yeshitela, Muna Ahmed El Tayeb, Arvinda Sooka, Christian G Meyer, Ralf Krumkamp, Denise Myriam Dekker, Anna Jaeger, Sven Poppert, Adama Tall, Aissatou Niang, Morten Bjerregaard-Andersen, Sandra Valborg Løfberg, Hye Jin Seo, Hyon Jin Jeon, Jessica Fung Deerin, Jinkyung Park, Frank Konings, Mohammad Ali, John D Clemens, Peter Hughes, Juliet Nsimire Sendagala, Tobias Vudriko, Robert Downing, Usman N Ikumapayi, Grant A Mackenzie, Stephen Obaro, Silvia Argimon, David M Aanensen, Andrew Page, Jacqueline A Keane, Sebastian Duchene, Zoe Dyson, Kathryn E Holt, Gordon Dougan, Florian Marks, and Stephen Baker. The phylogeography and incidence of multi-drug resistant typhoid fever in sub-Saharan Africa. *Nature communications*, 9(1):5094, nov 2018.

194. Jillian S Gauld, Franziska Olgemoeller, Rose Nkhata, Chao Li, Angeziwa Chirambo, Tracy Morse, Melita A Gordon, Jonathan M Read, Robert S Heyderman, Neil Kennedy,

Peter J Diggle, and Nicholas A Feasey. Domestic River Water Use and Risk of Typhoid Fever: Results From a Case-control Study in Blantyre, Malawi. *Clinical infectious diseases : an official publication of the Infectious Diseases Society of America*, 70(7):1278–1284, mar 2020.

195. J H Jorgensen and M J Ferraro. Antimicrobial susceptibility testing: general principles and contemporary practices. *Clinical infectious diseases : an official publication of the Infectious Diseases Society of America*, 26(4):973–980, apr 1998.

196. Sigrid Mayrhofer, Konrad J. Domig, Christiane Mair, Ulrike Zitz, Geert Huys, and Wolfgang Kneifel. Comparison of broth microdilution, Etest, and agar disk diffusion methods for antimicrobial susceptibility testing of Lactobacillus acidophilus group members. *Applied and Environmental Microbiology*, 74(12):3745–3748, 2008.

197. GL Woods and JA Washington. Antibacterial susceptibility tests: dilution and disk diffusion methods. In *Manual of clinical microbiology. 6th ed.*, pages 1327–41. American Society for Microbiology, 6 edition, 1995.

198. A W Bauer, W M Kirby, J C Sherris, and M Turck. Antibiotic susceptibility testing by a standardized single disk method. *American journal of clinical pathology*, 45(4):493–496, apr 1966.

199. Anand Manoharan, Rekha Pai, V. Shankar, Kurien Thomas, and M. K. Lalitha. Comparison of disc diffusion & E test methods with agar dilution for antimicrobial susceptibility testing of Haemophilus influenzae. *Indian Journal of Medical Research*, 117(FEB.):81–87, 2003.

200. Melvin P Weinstein, Brandi Limbago, and Jean B Patel. *28th Edition M100 Performance Standards for Antimicrobial Susceptibility Testing*. 2018.

201. Romney M. Humphries, April N. Abbott, and Janet A. Hindler. Understanding and addressing CLSI breakpoint revisions: A primer for clinical laboratories. *Journal of Clinical Microbiology*, 57(6):1–15, 2019.

202. T. P. Cusack, E. A. Ashley, C. L. Ling, S. Rattanavong, T. Roberts, P. Turner, T. Wangrangsimakul, and D. A.B. Dance. Impact of CLSI and EUCAST breakpoint discrepancies on reporting of antimicrobial susceptibility and AMR surveillance. *Clinical Microbiology and Infection*, 25(7):910–911, 2019.

203. Nesrin Ghanem-Zoubi, Danny Zorbavel, Johad Khoury, Yuval Geffen, Majd Qasum, Svetlana Predescu, and Mical Paul. The association between treatment appropriateness according to EUCAST and CLSI breakpoints and mortality among patients with candidemia: a retrospective observational study. *European Journal of Clinical Microbiology and Infectious Diseases*, 37(12):2397–2404, 2018.

204. Katherine E. Fleming-Dutra, Adam L. Hersh, Daniel J. Shapiro, Monina Bartoces, Eva A. Enns, Thomas M. File, Jonathan A. Finkelstein, Jeffrey S. Gerber, David Y. Hyun, Jeffrey A. Linder, Ruth Lynfield, David J. Margolis, Larissa S. May, Daniel Merenstein, Joshua P. Metlay, Jason G. Newland, Jay F. Piccirillo, Rebecca M. Roberts, Guillermo V. Sanchez, Katie J. Suda, Ann Thomas, Teri Moser Woo, Rachel M. Zetts, and Lauri A. Hicks. Prevalence of inappropriate antibiotic prescriptions among

us ambulatory care visits, 2010-2011. *JAMA - Journal of the American Medical Association*, 315(17):1864–1873, 2016.

205. Kimberly C. Claeys, Teri L. Hopkins, Ana D. Vega, and Emily L. Heil. Fluoroquinolone Restriction as an Effective Antimicrobial Stewardship Intervention. *Current Infectious Disease Reports*, 20(5):12–15, 2018.

206. H. Goossens, M. Ferech, S. Coenen, and P. Stephens. Comparison of Outpatient Systemic Antibacterial Use in 2004 in the United States and 27 European Countries. *Clinical Infectious Diseases*, 44(8):1091–1095, 2007.

207. Vu Thuy Duong, Ha Thanh Tuyen, Pham Van Minh, James I. Campbell, Hoang Le Phuc, Tran Do Hoang Nhu, Le Thi Phuong Tu, Tran Thi Hong Chau, Le Thi Quynh Nhi, Nguyen Thanh Hung, Nguyen Minh Ngoc, Nguyen Thi Thanh Huong, Lu Lan Vi, Corinne N. Thompson, Guy E. Thwaites, Ruklanthi De Alwis, and Stephen Baker. No Clinical benefit of empirical antimicrobial therapy for pediatric diarrhea in a high-usage, high-resistance setting. *Clinical Infectious Diseases*, 66(4):504–511, 2018.

208. Li Yang Hsu, Thean Yen Tan, Vincent H. Tam, Andrea Kwa, Dale Andrew Fisher, Tse Hsien Koh, Prabha Krishnan, Yoke Fong Chiew, Roland Jureen, and Nancy Tee. Surveillance and correlation of antibiotic prescription and resistance of gram-negative bacteria in Singaporean hospitals. *Antimicrobial Agents and Chemotherapy*, 54(3):1173–1178, 2010.

209. Danielle J. Ingle, Myron M. Levine, Karen L. Kotloff, Kathryn E. Holt, and Roy M. Robins-Browne. Dynamics of antimicrobial resistance in intestinal Escherichia coli from children in community settings in South Asia and sub-Saharan Africa. *Nature Microbiology*, 3(9):1063–1073, 2018.

210. Zuhura I. Kimera, Stephen E. Mshana, Mark M. Rweyemamu, Leonard E.G. Mboera, and Mecky I.N. Matee. Antimicrobial use and resistance in food-producing animals and the environment: an African perspective. *Antimicrobial resistance and infection control*, 9(1):37, 2020.

211. John A. Crump, Katrina Kretsinger, Kathryn Gay, R. Michael Hoekstra, Due J. Vugia, Sharon Hurd, Susan D. Segler, Melanie Megginson, L. Jeffrey Luedeman, Beletshachew Shiferaw, Samir S. Hanna, Kevin W. Joyce, Eric D. Mintz, and Frederick J. Angulo. Clinical response and outcome of infection with Salmonella enterica serotype typhi with decreased susceptibility to fluoroquinolones: A United States FoodNet multicenter retrospective cohort study. *Antimicrobial Agents and Chemotherapy*, 52(4):1278–1284, apr 2008.

212. Samuel Kariuki, Melita A Gordon, Nicholas Feasey, Christopher M Parry, Wellcome Trust, Genome Campus, United Kingdom, Global Health, Liverpool Wellcome, Trust Clinical, Keppel Street, Keppel Street, and Global Health. Salmonella disease. 33(0 3), 2016.

213. Kathryn E. Holt, Christiane Dolecek, Tran Thuy Chau, Pham Thanh Duy, Tran Thi Phi La, Nguyen van Minh Hoang, Tran Vu Thieu Nga, James I. Campbell, Bui Huu Manh, Nguyen van Vinh Chau, Tran Tinh Hien, Jeremy Farrar, Gordon Dougan, and Stephen Baker. Temporal fluctuation of multidrug resistant Salmonella typhi haplotypes in the

mekong river delta region of Vietnam. *PLoS Neglected Tropical Diseases*, 5(1):1–10, 2011.

214. R. J. Hassing, W. H.F. Goessens, D. J. Mevius, W. Van Pelt, J. W. Mouton, A. Verbon, and P. J. Van Genderen. Decreased ciprofloxacin susceptibility in Salmonella Typhi and Paratyphi infections in ill-returned travellers: The impact on clinical outcome and future treatment options. *European Journal of Clinical Microbiology and Infectious Diseases*, 32(10):1295–1301, 2013.

215. Samir Koirala, Buddha Basnyat, Amit Arjyal, Olita Shilpakar, Kabina Shrestha, Rishav Shrestha, Upendra Man Shrestha, Krishna Agrawal, Kanika Deshpande Koirala, Sudeep Dhoj Thapa, Abhilasha Karkey, Sabina Dongol, Abhishek Giri, Mila Shakya, Kamal Raj Pathak, James Campbell, Stephen Baker, Jeremy Farrar, Marcel Wolbers, and Christiane Dolecek. Gatifloxacin Versus Ofloxacin for the Treatment of Uncomplicated Enteric Fever in Nepal: An Open-Label, Randomized, Controlled Trial. *PLoS Neglected Tropical Diseases*, 7(10), 2013.

216. Amit Arjyal, Buddha Basnyat, Ho Thi Nhan, Samir Koirala, Abhishek Giri, Niva Joshi, Mila Shakya, Kamal Raj Pathak, Saruna Pathak Mahat, Shanti Pradhan Prajapati, Nabin Adhikari, Rajkumar Thapa, Laura Merson, Damodar Gajurel, Kamal Lamsal, Dinesh Lamsal, Bharat Kumar Yadav, Ganesh Shah, Poojan Shrestha, Sabina Dongol, Abhilasha Karkey, Corinne N Thompson, Nga Tran Vu Thieu, Duy Pham Thanh, Stephen Baker, Guy E Thwaites, Marcel Wolbers, and Christiane Dolecek. Gatifloxacin versus ceftriaxone for uncomplicated enteric fever in Nepal: an open-label, two-centre, randomised controlled trial. *The Lancet. Infectious diseases*, 16(5):535–545, may 2016.

217. Stephen Baker, Pham Thanh Duy, Tran Vu Thieu Nga, Tran Thi Ngoc Dung, Voong Vinh Phat, Tran Thuy Chau, A Keith Turner, Jeremy Farrar, and Maciej F Boni. Fitness benefits in fluoroquinolone-resistant Salmonella Typhi in the absence of antimicrobial pressure. *eLife*, 2:1–17, 2013.

218. Abi Manesh, Veeraraghavan Balaji, Devanga Ragupathi Naveen Kumar, and Priscilla Rupali. A case of clinical and microbiological failure of azithromycin therapy in Salmonella enterica serotype Typhi despite low azithromycin MIC. *International Journal of Infectious Diseases*, 54:62–63, 2017.

219. Winnie C. Mutai, Anne W.T. Muigai, Peter Waiyaki, and Samuel Kariuki. Multidrug resistant Salmonella enterica serovar Typhi isolates with reduced susceptibility to ciprofloxacin in Kenya. *BMC Microbiology*, 18(1):4–8, 2018.

220. Bieke Tack, Marie France Phoba, Sandra Van Puyvelde, Lisette M. Kalonji, Liselotte Hardy, Barbara Barbé, Marianne A.B. Van Der Sande, Elise Monsieurs, Stijn Deborggraeve, Octavie Lunguya, and Jan Jacobs. Salmonella typhi from blood cultures in the democratic republic of the congo: A 10-year surveillance. *Clinical Infectious Diseases*, 68(Suppl 2):S130–S137, 2019.

221. Anu Kantele, Sari H. Pakkanen, Riitta Karttunen, and Jussi M. Kantele. Head-to-Head Comparison of Humoral Immune Responses to Vi Capsular Polysaccharide and Salmonella Typhi Ty21a Typhoid Vaccines-A Randomized Trial. *PLoS ONE*, 8(4):6–8, 2013.

222. Rachael Milligan, Mical Paul, Marty Richardson, and Ami Neuberger. Vaccines for preventing typhoid fever. *Cochrane Database of Systematic Reviews*, 2018(5), 2018.

223. Myron M. Levine, Robert E. Black, Catterine Ferreccio, and Rene Germanier. Large-Scale Field Trial of Ty21a Live Oral Typhoid Vaccine in Enteric-Coated Capsule Formulation. *The Lancet*, 329(8541):1049–1052, 1987.

224. Keith P. Klugman, Hendrik J. Koornhof, John B. Robbins, and Nancy N. Le Cam. Immunogenicity, efficacy and serological correlate of protection of Salmonella typhi Vi capsular polysaccharide vaccine three years after immunization. *Vaccine*, 14(5):435–438, 1996.

225. Karen H. Keddy, Keith P. Klugman, C. Frank Hansford, Christine Blondeau, and Nancy N. Bouveret Le Cam. Persistence of antibodies to the Salmonella typhi Vi capsular polysaccharide vaccine in South African school children ten years after immunization. *Vaccine*, 17(2):110–113, 1999.

226. Merryn Voysey and Andrew J. Pollard. Seroefficacy of VI polysaccharideâtetanus toxoid typhoid conjugate vaccine (typbar TCV). *Clinical Infectious Diseases*, 67(1):18–24, 2018.

227. Adwoa D Bentsi-Enchill and Joachim Hombach. Revised Global Typhoid Vaccination Policy. *Clinical infectious diseases : an official publication of the Infectious Diseases Society of America*, 68(Suppl 1):S31–S33, feb 2019.

228. World Health Organization. Typhoid vaccines: WHO position paper, March 2018 - Recommendations. *Vaccine*, 37(2):214–216, jan 2019.

229. Farah Naz Qamar, Mohammad Tahir Yousafzai, Asif Khaliq, Sultan Karim, Hina Memon, Amber Junejo, Inayat Baig, Najeeb Rahman, Shafqat Bhurgry, Hina Afroz, and Uzma Sami. Adverse events following immunization with typhoid conjugate vaccine in an outbreak setting in Hyderabad, Pakistan. *Vaccine*, 38(19):3518–3523, apr 2020.

230. Kashmira Date, Rahul Shimpi, Stephen Luby, Ramaswami N, Pradeep Haldar, Arun Katkar, Kathleen Wannemuehler, Vittal Mogasale, Sarah Pallas, Dayoung Song, Abhishek Kunwar, Anagha Loharikar, Vijay Yewale, Danish Ahmed, Lily Horng, Elisabeth Wilhelm, Sunil Bahl, Pauline Harvey, Shanta Dutta, and Pankaj Bhatnagar. Decision Making and Implementation of the First Public Sector Introduction of Typhoid Conjugate Vaccine-Navi Mumbai, India, 2018. *Clinical infectious diseases : an official publication of the Infectious Diseases Society of America*, 71(Supplement_2):S172–S178, jul 2020.

231. Megan E Carey and A Duncan Steele. The Severe Typhoid Fever in Africa Program Highlights the Need for Broad Deployment of Typhoid Conjugate Vaccines. *Clinical infectious diseases : an official publication of the Infectious Diseases Society of America*, 69(Suppl 6):S413–S416, oct 2019.

232. Laura B. Martin, Raphael Simon, Calman A. MacLennan, Sharon M. Tennant, Sushant Sahastrabuddhe, and M. Imran Khan. Status of paratyphoid fever vaccine research and development. *Vaccine*, 34(26):2900–2902, 2016.

233. Anubha Pathak, Deepak Kumar, Prasanna Kumar V., Aman Kamboj, Jaishree Sharma, Maansi Shukla, Ajay Kumar Upadhyay, Nagappa Karabasanavar, Purushottam Kaushik, and Suresh P. Singh. Mutations in DNA gyrase and topoisomerase genes linked to fluoroquinolone resistance in Salmonella Typhimurium of animal origin in India. *Journal of Global Antimicrobial Resistance*, 15:268–270, 2018.

234. Monique Ribeiro Tiba Casas, Carlos Henrique Camargo, Flávia Barrosa Soares, Wanderley Dias da Silveira, and Sueli Aparecida Fernandes. Presence of plasmid-mediated quinolone resistance determinants and mutations in gyrase and topoisomerase in Salmonella enterica isolates with resistance and reduced susceptibility to ciprofloxacin. *Diagnostic Microbiology and Infectious Disease*, 85(1):85–89, 2016.

235. Qifa Song, Danyang Zhang, Hong Gao, and Junhua Wu. Salmonella Species' Persistence and Their High Level of Antimicrobial Resistance in Flooded Man-Made Rivers in China. *Microbial drug resistance (Larchmont, N.Y.)*, 24(9):1404–1411, nov 2018.

236. Tu Le Thi Phuong, Sayaphet Rattanavong, Manivanh Vongsouvath, Viengmon Davong, Nguyen Phu Huong Lan, James I Campbell, Thomas C Darton, Guy E Thwaites, Paul N Newton, David A B Dance, and Stephen Baker. Non-typhoidal Salmonella serovars associated with invasive and non-invasive disease in the Lao People's Democratic Republic. *Transactions of The Royal Society of Tropical Medicine and Hygiene*, (January):418–424, 2018.

237. Vanessa K. Wong, Derek J. Pickard, Lars Barquist, Karthikeyan Sivaraman, Andrew J. Page, Peter J. Hart, Mark J. Arends, Kathryn E. Holt, Leanne Kane, Lynda F. Mottram, Louise Ellison, Ruben Bautista, Chris J. McGee, Sally J. Kay, Thomas M. Wileman, Linda J. Kenney, Calman A. MacLennan, Robert A. Kingsley, and Gordon Dougan. Characterization of the yehUT two-component regulatory system of Salmonella enterica serovar Typhi and Typhimurium. *PLoS ONE*, 8(12):1–14, 2013.

238. Jiufeng Sun, Bixia Ke, Yanhui Huang, Dongmei He, Xiaocui Li, Zhaoming Liang, and Changwen Ke. The molecular epidemiological characteristics and genetic diversity of Salmonella Typhimurium in Guangdong, China, 2007-2011. *PLoS ONE*, 9(11):2007–2011, 2014.

239. A. A. Orogade and R. M. Akuse. Changing patterns in sensitivity of causative organisms of septicaemia in children: the need for quinolones. *African journal of medicine and medical sciences*, 33(1):69–72, 2004.

240. Samuel Kariuki and Robert S. Onsare. Epidemiology and genomics of invasive non-typhoidal salmonella infections in Kenya. *Clinical Infectious Diseases*, 61(Suppl 4):S317–S324, 2015.

241. Daniel Eibach, Hassan M Al-emran, Myriam Dekker, Ralf Krumkamp, Yaw Adu-sarkodie, Ligia Maria, Cruz Espinoza, Christa Ehmen, Kennedy Boahen, Peter Heisig, Justin Im, Anna Jaeger, Vera Von Kalckreuth, Gi Deok Pak, Ursula Panzner, Se Eun Park, Alexander Reinhardt, Nimako Sarpong, Heidi Schütt-gerowitt, Thomas F Wierzba, Florian Marks, and Jürgen May. The Emergence of Reduced Ciprofl oxacin Susceptibility in Salmonella enterica Causing Bloodstream Infections in Rural Ghana. 62(March), 2018.

242. Calman A. MacLennan, Laura B. Martin, and Francesca Micoli. Vaccines against invasive Salmonella disease: Current status and future directions. *Human Vaccines and Immunotherapeutics*, 10(6):1478–1493, 2014.

243. Raphael Simon, Jin Y. Wang, Mary A. Boyd, Mohan E. Tulapurkar, Girish Ramachandran, Sharon M. Tennant, Marcela Pasetti, James E. Galen, and Myron M. Levine. Sustained Protection in Mice Immunized with Fractional Doses of Salmonella Enteritidis Core and O Polysaccharide-Flagellin Glycoconjugates. *PLoS ONE*, 8(5):8–11, 2013.

244. Sharon M. Tennant, Jin Yuan Wang, James E. Galen, Raphael Simon, Marcela F. Pasetti, Orit G. Gat, and Myron M. Levine. Engineering and preclinical evaluation of attenuated nontyphoidal salmonella strains serving as live oral vaccines and as reagent strains. *Infection and Immunity*, 79(10):4175–4185, 2011.

245. Francesca Micoli, Simona Rondini, Renzo Alfini, Luisa Lanzilao, Francesca Necchi, Aurel Negrea, Omar Rossi, Cornelia Brandt, Simon Clare, Pietro Mastroeni, Rino Rappuoli, Allan Saul, and Calman A. MacLennan. Comparative immunogenicity and efficacy of equivalent outer membrane vesicle and glycoconjugate vaccines against nontyphoidal Salmonella. *Proceedings of the National Academy of Sciences of the United States of America*, 115(41):10428–10433, 2018.

246. Christiane Gerke, Anna Maria Colucci, Carlo Giannelli, Silvia Sanzone, Claudia Giorgina Vitali, Luigi Sollai, Omar Rossi, Laura B. Martin, Jochen Auerbach, Vito Di Cioccio, and Allan Saul. Production of a Shigella sonnei vaccine based on generalized modules for membrane antigens (GMMA), 1790GAHB. *PLoS ONE*, 10(8):1–22, 2015.

247. Anna E. Schager, C. Coral Dominguez-Medina, Francesca Necchi, Francesca Micoli, Yun Shan Goh, Margaret Goodall, Adriana Flores-Langarica, Saeeda Bobat, Charlotte N.L. Cook, Melissa Arcuri, Arianna Marini, Lloyd D.W. King, Faye C. Morris, Graham Anderson, Kai Michael Toellner, Ian R. Henderson, Constantino López-Macías, Calman A. MacLennan, and Adam F. Cunningham. IgG responses to porins and lipopolysaccharide within an outer membrane-based vaccine against nontyphoidal Salmonella develop at discordant rates. *mBio*, 9(2):1–15, 2018.

248. Peter Ball. Quinolone generations: natural history or natural selection? *Journal of Antimicrobial Chemotherapy*, 46(suppl_3):17–24, 2000.

249. Peter Ball, Lionell Mandell, Yoshihito Niki, and Glenn Tillotson. Comparative tolerability of the newer fluoroquinolone antibacterials. *Drug Safety*, 21(5):407–421, 1999.

250. D N Fish. Fluoroquinolone adverse effects and drug interactions. *Pharmacotherapy*, 21(10 Pt 2):253S–272S, oct 2001.

251. Laura Baranello, David Levens, Ashutosh Gupta, and Fedor Kouzine. The importance of being supercoiled : How DNA mechanics regulate dynamic processes â. *Biochimica et Biophysica Acta*, 1819(7):632–638, 2012.

252. Liam S. Redgrave, Sam B. Sutton, Mark A. Webber, and Laura J.V. V Piddock. Fluoroquinolone resistance : Mechanisms, impact on bacteria, and role in evolutionary success. *Trends in Microbiology*, 22(8):438–445, 2014.

253. Katie J. Aldred, Robert J. Kerns, and Neil Osheroff. Mechanism of quinolone action and resistance. *Biochemistry*, 53(10):1565–1574, 2014.

254. Martin Gellert, Kiyoshi Mizuuchi, Mary H O 'dea, and Howard A Nasht. DNA gyrase: An enzyme that introduces superhelical turns into DNA (Escherichia coli/ATP-dependent reaction/superhelix density). 73(11):3872–3876, 1976.

255. João H. Morais Cabral, Andrew P. Jackson, Clare V. Smith, Nita Shikotra, Anthony Maxwell, and Robert C. Liddington. Crystal structure of the breakage-reunion domain of DNA gyrase. *Nature*, 388(6645):903–906, 1997.

256. Alexandre Wohlkonig, Pan F Chan, Andrew P Fosberry, Paul Homes, Jianzhong Huang, Michael Kranz, Vaughan R Leydon, Timothy J Miles, Neil D Pearson, Rajika L Perera, Anthony J Shillings, Michael N Gwynn, and Benjamin D Bax. Structural basis of quinolone inhibition of type IIA topoisomerases and target-mediated resistance. *Nature Structural & Molecular Biology*, 17(99):1152–1153, 2010.

257. Ivan Laponogov, Maninder K Sohi, Dennis A Veselkov, Xiao-su Pan, Ritica Sawhney, Andrew W Thompson, Katherine E Mcauley, L Mark Fisher, and Mark R Sanderson. Structural insight into the quinoloneâDNA cleavage complex of type IIA topoisomerases. 16(6):667–669, 2009.

258. Katie J. Aldred, Heidi A. Schwanz, Gangqin Li, Sylvia A. McPherson, Charles L. Turnbough, Robert J. Kerns, and Neil Osheroff. Overcoming target-mediated quinolone resistance in topoisomerase IV by introducing metal-ion-independent drug-enzyme interactions. *ACS Chemical Biology*, 8(12):2660–2668, 2013.

259. Gerald L. Mandell and Elizabeth Coleman. Uptake, transport, and delivery of antimicrobial agents by human polymorphonuclear neutrophils. *Antimicrobial Agents and Chemotherapy*, 45(6):1794–1798, 2001.

260. Stéphane Carryn, Francoise Van Bambeke, Marie-Paule Mingeot-Leclercq, and Paul M Tulkens. Comparative Intracellular (THP-1 Macrophage) and Extracellular Activities of B-Lactams, Azithromycin, Gentamicin, and Fluoroquinolones against. *Society*, 46(7):2095–2103, 2002.

261. Natassja G Bush, Katherine Evans-Roberts, and Anthony Maxwell. DNA Topoisomerases. *EcoSal Plus*, 6(2), 2015.

262. Temilolu Idowu and Frank Schweizer. Ubiquitous nature of fluoroquinolones: The oscillation between antibacterial and anticancer activities. *Antibiotics*, 6(4), 2017.

263. Hiroaki Yoshida, Mayumi Bogaki, Mika Nakamura, and Shinichi Nakamura. Quinolone Resistance-Determining Region in the DNA Gyrase gyrA Gene of Escherichia coli. 34(6):1271–1272, 1990.

264. David C. Hooper and George A. Jacoby. Mechanisms of drug resistance: Quinolone resistance. *Annals of the New York Academy of Sciences*, 1354(1):12–31, 2015.

265. Arif M. Tanmoy, Emilie Westeel, Katrien De Bruyne, Johan Goris, Alain Rajoharison, Mohammad S.I. Sajib, Alex van Belkum, Samir K. Saha, Florence Komurian-Pradel, and Hubert P. Endtz. Salmonella enterica serovar typhi in Bangladesh: Exploration of genomic diversity and antimicrobial resistance. *mBio*, 9(6):1–17, 2018.

266. X. S. Pan and L. M. Fisher. Targeting of DNA gyrase in Streptococcus pneumoniae by sparfloxacin: Selective targeting of gyrase or topoisomerase IV by quinolones. *Antimicrobial Agents and Chemotherapy*, 41(2):471–474, 1997.

267. F Blanche, B Cameron, F X Bernard, L Maton, B Manse, L Ferrero, N Ratet, C Lecoq, A Goniot, D Bisch, and J Crouzet. Differential behaviors of Staphylococcus aureus and Escherichia coli type II DNA topoisomerases. *Antimicrobial agents and chemotherapy*, 40(12):2714–2720, dec 1996.

268. Tadesse G., Tessema T.S., Beyene G., and Aseffa A. Molecular epidemiology of fluoroquinolone resistant Salmonella in Africa: A systematic review and meta-analysis. *PLoS ONE*, 13(2):1–30, 2018.

269. David C. Hooper and George A. Jacoby. Topoisomerase inhibitors: Fluoroquinolone mechanisms of action and resistance. *Cold Spring Harbor Perspectives in Medicine*, 6(9):1–22, 2016.

270. Katie L. Hopkins, Robert H. Davies, and E. John Threlfall. Mechanisms of quinolone resistance in Escherichia coli and Salmonella: Recent developments. *International Journal of Antimicrobial Agents*, 25(5):358–373, 2005.

271. Isabelle Casin, Jacques Breuil, Jean Pierre Darchis, Claire Guelpa, and Ekkehard Collatz. Fluoroquinolone Resistance Linked to GyrA, GyrB, and ParC Mutations in Salmonella enterica Typhimurium Isolates in Humans. *Emerging Infectious Diseases*, 9(11):1455–1457, 2003.

272. Fernanda Almeida, Amanda Aparecida Seribelli, Marta Inês Cazentini Medeiros, Dália dos Prazeres Rodrigues, Alessandro De MelloVarani, Yan Luo, Marc W. Allard, and Juliana Pfrimer Falcão. Phylogenetic and antimicrobial resistance gene analysis of Salmonella Typhimurium strains isolated in Brazil by whole genome sequencing. *PLoS ONE*, 13(8):1–16, 2018.

273. S A Egorova, L A Kaftyreva, L V Suzhaeva, A V Zabrovskaia, E V Voitenkova, Z N Matveeva, Y V Ostankova, I V Likhachev, N V Satosova, R V Kitsbabashvili, E V Smirnova, L I Semchenkova, T E Bystraya, S E Sokol'nik, N P Utkina, and L Y Sikhando. [Antimicrobial resistance and clinical significant resistance mechanisms of Salmonella isolated in 2014-2018 in St.Petersburg, Russia.]. *Klinicheskaia laboratornaia diagnostika*, 64(10):620–626, 2019.

274. F Reyna, M Huesca, V González, and L Y Fuchs. Salmonella typhimurium gyrA mutations associated with fluoroquinolone resistance. *Antimicrobial agents and chemotherapy*, 39(7):1621–1623, jul 1995.

275. Susana Correia, Patrícia Poeta, Michel Hébraud, José Luis Capelo, and Gilberto Igrejas. Mechanisms of quinolone action and resistance: where do we stand? *Journal of Medical Microbiology*, 66(5):551–559, 2017.

276. George A Jacoby, Jacob Strahilevitz, and David C Hooper. <Plasmid-Mediated.pdf>. (October 2014):1–24, 2015.

277. Xizhou Guan, Xinying Xue, Yuxia Liu, Jing Wang, Yong Wang, Jianxin Wang, Kaifei Wang, Hong Jiang, Lina Zhang, Bing Yang, N. Wang, and Lei Pan. Plasmid-mediated quinolone resistance - Current knowledge and future perspectives. *Journal of International Medical Research*, 41(1):20–30, 2013.

278. Luis Martínez-Martínez, Maria Eliecer Cano, José Manuel Rodríguez-Martínez, Jorge Calvo, and Álvaro Pascual. Plasmid-mediated quinolone resistance. *Expert Review of Anti-Infective Therapy*, 6(5):685–711, oct 2008.

279. Patrice Nordmann and Laurent Poirel. Emergence of plasmid-mediated resistance to quinolones in Enterobacteriaceae. *Journal of Antimicrobial Chemotherapy*, 56(3):463–469, 2005.

280. Kathryn Gay, Ari Robicsek, Jacob Strahilevitz, Chi Hye Park, George Jacoby, Timothy J. Barrett, Felicita Medalla, Tom M. Chiller, and David C. Hooper. PlasmidâMediated Quinolone Resistance in NonâTyphi Serotypes of Salmonella enterica . *Clinical Infectious Diseases*, 2006.

281. Corinna Kehrenberg, Sonja Friederichs, Anno de Jong, Geovana Brenner Michael, and Stefan Schwarz. Identification of the plasmid-borne quinolone resistance gene qnrS in Salmonella enterica serovar Infantis. *Journal of Antimicrobial Chemotherapy*, 58(1):18–22, 2006.

282. Luis Martínez-martínez, Alvaro Pascual, and George A Jacoby. Quinolone resistance from a transferable plasmid. *The Lancet*, 351:797–799, 1998.

283. Jacob Strahilevitz, George A Jacoby, David C Hooper, and Ari Robicsek. Plasmid-Mediated Quinolone Resistance : a Multifaceted Threat. *Clinical Microbiology Reviews*, 22(4):664–689, 2009.

284. José Manuel Rodríguez-Martínez, Jesús Machuca, María Eliecer Cano, Jorge Calvo, Luis Martínez-Martínez, and Alvaro Pascual. Plasmid-mediated quinolone resistance: Two decades on. *Drug Resistance Updates*, 29:13–29, 2016.

285. Joaquim Ruiz. Mechanisms of resistance to quinolones: Target alterations, decreased accumulation and DNA gyrase protection. *Journal of Antimicrobial Chemotherapy*, 51(5):1109–1117, 2003.

286. Anna Fàbrega, Robert G Martin, Judah L Rosner, M Mar Tavio, and Jordi Vila. Constitutive SoxS expression in a fluoroquinolone-resistant strain with a truncated SoxR protein and identification of a new member of the marA-soxS-rob regulon, mdtG. *Antimicrobial agents and chemotherapy*, 54(3):1218–1225, mar 2010.

287. Lucía Fernández and Robert E.W. Hancock. Adaptive and mutational resistance: Role of porins and efflux pumps in drug resistance. *Clinical Microbiology Reviews*, 25(4):661–681, 2012.

288. Jean Michel Bolla, Sandrine Alibert-Franco, Jadwiga Handzlik, Jacqueline Chevalier, Abdallah Mahamoud, Gérard Boyer, Katarzyna Kieć-Kononowicz, and Jean Marie Pags. Strategies for bypassing the membrane barrier in multidrug resistant Gram-negative bacteria. *FEBS Letters*, 585(11):1682–1690, 2011.

289. Anne H. Delcour. Outer membrane permeability and antibiotic resistance. *Biochimica et Biophysica Acta - Proteins and Proteomics*, 1794(5):808–816, 2009.

290. Abeer Ahmed Rushdy, Mona Ibrahim Mabrouk, Ferialla Abdel Hamid Abu-Sef, Zeinab Hassan Kheiralla, Said Mohamed Abdel All, and Neveen Mohamed Saleh. Contribution of different mechanisms to the resistance to fluoroquinolones in clinical isolates of Salmonella enterica. *Brazilian Journal of Infectious Diseases*, 17(4):431–437, 2013.

291. Younes Smani, Anna FabÌrega, Ignasi Roca, Viviana Sańchez-Encinales, Jordi Vila, and Jerónimo Pachón. Role of OmpA in the multidrug resistance phenotype of Acinetobacter baumannii. *Antimicrobial Agents and Chemotherapy*, 58(3):1806–1808, 2014.

292. Jordi Vila, Anna Fábrega, Ignasi Roca, Alvaro Hernández, and José Luis Martínez. Efflux pumps as an important mechanism for quinolone resistance. *Advances in Enzymology and Related Areas of Molecular Biology*, 2010.

293. Jean Marie Pagès, Chloë E. James, and Mathias Winterhalter. The porin and the permeating antibiotic: A selective diffusion barrier in Gram-negative bacteria. *Nature Reviews Microbiology*, 6(12):893–903, 2008.

294. Ruchi Gupta, Rajni Gaind, Laishram Chandreshwor, Bianca Paglietti, and Monorama Deb. Detection of mutations in gyr B using denaturing high performance liquid chromatography (DHPLC) among Salmonella enterica serovar Typhi and Paratyphi A. *Transactions of the Royal Society of Tropical Medicine and Hygiene*, pages 684–689, 2017.

295. Bayer. CIPRO (ciprofloxacin hydrochloride) tablets. 2004.

296. R. Wise, D. Lister, C. A. M. McNulty, D. Griggs, and J. M. Andrews. The comparative pharmacokinetics of five quinolones. *Journal of Antimicrobial Chemotherapy*, 18(Supplement_D):71–81, 1986.

297. Niels Høiby, Jens Otto Jarløv, Michael Kemp, Michael Tvede, Jette Marie Bangsborg, Anne Kjerulf, Charlotte Pers, and Hanne Hansen. Excretion of ciprofloxacin in sweat and multiresistant Staphylococcus epidermidis. *Lancet*, 349(9046):167–169, 1997.

298. SJ Pamp, M Gjermansen, and T Tolker-Nielsen. The biofilm matrix: a sticky framework. In S Kjelleberg and M Givskow, editors, *The biofilm mode of life: mechanisms and adaptations*, pages 37–69. 2007.

299. Jing Yan and Bonnie L. Bassler. Surviving as a Community: Antibiotic Tolerance and Persistence in Bacterial Biofilms. *Cell Host and Microbe*, 26(1):15–21, 2019.

300. Luanne Hall-Stoodley, J. William Costerton, and Paul Stoodley. Bacterial biofilms: From the natural environment to infectious diseases. *Nature Reviews Microbiology*, 2(2):95–108, 2004.

301. E. Hauser, E. Junker, R. Helmuth, and B. Malorny. Different mutations in the oafA gene lead to loss of O5-antigen expression in Salmonella enterica serovar Typhimurium. *Journal of Applied Microbiology*, 110(1):248–253, 2011.

302. Bieke Tack, Marie-France Phoba, Barbara Barbé, Lisette M. Kalonji, Liselotte Hardy, Sandra Van Puyvelde, Brecht Ingelbeen, Dadi Falay, Dauly Ngonda, Marianne A. B. van der Sande, Stijn Deborggraeve, Jan Jacobs, and Octavie Lunguya. Non-typhoidal Salmonella bloodstream infections in Kisantu, DR Congo: Emergence of O5-negative Salmonella Typhimurium and extensive drug resistance. *PLOS Neglected Tropical Diseases*, 14(4):e0008121, 2020.

303. Gerald L. Murray, Stephen R. Attridge, and Renato Morona. Altering the length of the lipopolysaccharide O antigen has an impact on the interaction of Salmonella enterica serovar typhimurium with macrophages and complement. *Journal of Bacteriology*, 188(7):2735–2739, 2006.

304. Denisse Bravo, Cecilia Silva, Javier A. Carter, Anilei Hoare, Sergio A. Álvarez, Carlos J. Blondel, Mercedes Zaldívar, Miguel A. Valvano, and Inés Contreras. Growth-phase regulation of lipopolysaccharide O-antigen chain length influences serum resistance in serovars of Salmonella. *Journal of Medical Microbiology*, 57(8):938–946, 2008.

305. Sukhyun Ryu, Benjamin J Cowling, Peng Wu, Scott Olesen, Christophe Fraser, Daphne S Sun, Marc Lipsitch, and Yonatan H Grad. Case-based surveillance of antimicrobial resistance with full susceptibility profiles. *JAC-Antimicrobial Resistance*, 1(3):1–5, 2019.

306. Patricia S. Fontela, Shauna O'Donnell, and Jesse Papenburg. Can biomarkers improve the rational use of antibiotics? *Current Opinion in Infectious Diseases*, 31(4):347–352, 2018.

307. Roby P. Bhattacharyya, Nirmalya Bandyopadhyay, Peijun Ma, Sophie S. Son, Jamin Liu, Lorrie L. He, Lidan Wu, Rustem Khafizov, Rich Boykin, Gustavo C. Cerqueira, Alejandro Pironti, Robert F. Rudy, Milesh M. Patel, Rui Yang, Jennifer Skerry, Elizabeth Nazarian, Kimberly A. Musser, Jill Taylor, Virginia M. Pierce, Ashlee M. Earl, Lisa A. Cosimi, Noam Shoresh, Joseph Beechem, Jonathan Livny, and Deborah T. Hung. Simultaneous detection of genotype and phenotype enables rapid and accurate antibiotic susceptibility determination. *Nature Medicine*, 25(12):1858–1864, 2019.

308. Christiaan A Rees, Alison Burklund, Pierre-hugues Stefanuto, and D Joseph. Fungal Pathogen Groups. 12(2), 2019.

309. Katie Schelli, Joshua Rutowski, Julia Roubidoux, and Jiangjiang Zhu. Staphylococcus aureus methicillin resistance detected by HPLC-MS/MS targeted metabolic profiling. *Journal of Chromatography B: Analytical Technologies in the Biomedical and Life Sciences*, 1047:124–130, 2017.

310. Robert A Kingsley, Gemma Langridge, Sarah E Smith, Carine Makendi, Maria Fookes, Tom M Wileman, Moataz Abd El Ghany, A Keith Turner, Zoe A Dyson, Sushmita Sridhar, Derek Pickard, Sally Kay, Nicholas Feasey, Vanessa Wong, Lars Barquist, and Gordon Dougan. Functional analysis of Salmonella Typhi adaptation to survival in water. *Environmental microbiology*, 20(11):4079–4090, nov 2018.

311. Robert J. Nichols, Saunak Sen, Yoe Jin Choo, Pedro Beltrao, Matylda Zietek, Rachna Chaba, Sueyoung Lee, Krystyna M. Kazmierczak, Karis J. Lee, Angela Wong, Michael Shales, Susan Lovett, Malcolm E. Winkler, Nevan J. Krogan, Athanasios Typas, and Carol A. Gross. Phenotypic landscape of a bacterial cell. *Cell*, 144(1):143–156, 2011.

312. Jason H. Yang, Sarah N. Wright, Meagan Hamblin, Douglas McCloskey, Miguel A. Alcantar, Lars Schrübbers, Allison J. Lopatkin, Sangeeta Satish, Amir Nili, Bernhard O. Palsson, Graham C. Walker, and James J. Collins. A White-Box Machine Learning Approach for Revealing Antibiotic Mechanisms of Action. *Cell*, 177(6):1649–1661.e9, 2019.

313. Hui Yu, Wenwen Jing, Rafael Iriya, Yunze Yang, Karan Syal, Manni Mo, Thomas E. Grys, Shelley E. Haydel, Shaopeng Wang, and Nongjian Tao. Phenotypic Antimicrobial Susceptibility Testing with Deep Learning Video Microscopy. *Analytical Chemistry*, 90(10):6314–6322, 2018.

314. Michael Baym, Tami D Lieberman, Eric D Kelsic, Remy Chait, Rotem Gross, Idan Yelin, and Roy Kishony. Spatiotemporal microbial evolution on antibiotic landscapes. *Science (New York, N.Y.)*, 353(6304):1147–1151, sep 2016.

315. George Kritikos, Manuel Banzhaf, Lucia Herrera-Dominguez, Alexandra Koumoutsi, Morgane Wartel, Matylda Zietek, and Athanasios Typas. A tool named Iris for versatile high-throughput phenotyping in microorganisms. *Nature Microbiology*, 2(February), 2017.

316. Liselot Dewachter, Maarten Fauvart, and Jan Michiels. Bacterial Heterogeneity and Antibiotic Survival: Understanding and Combatting Persistence and Heteroresistance. *Molecular cell*, 76(2):255–267, oct 2019.

317. L. J.V. Piddock, R. N. Walters, and J. M. Diver. Correlation of quinolone MIC and inhibition of DNA, RNA, and protein synthesis and induction of the SOS response in Escherichia coli. *Antimicrobial Agents and Chemotherapy*, 34(12):2331–2336, 1990.

318. Antoine Grillon, Frédéric Schramm, Magali Kleinberg, and François Jehl. Comparative activity of ciprofloxacin, levofloxacin and moxifloxacin against Klebsiella pneumoniae, Pseudomonas aeruginosa and Stenotrophomonas maltophilia assessed by minimum inhibitory concentrations and time-kill studies. *PLoS ONE*, 11(6):1–10, 2016.

319. Sunniva Foerster, Magnus Unemo, Lucy J. Hathaway, Nicola Low, and Christian L. Althaus. Time-kill curve analysis and pharmacodynamic modelling for in vitro evaluation of antimicrobials against Neisseria gonorrhoeae. *BMC Microbiology*, 16(1):1–11, 2016.

320. Thomas M. Norman, Nathan D. Lord, Johan Paulsson, and Richard Losick. Stochastic Switching of Cell Fate in Microbes. *Annual Review of Microbiology*, 69(1):381–403, 2015.

321. Xiaofang Jiang, A Brantley Hall, Timothy D Arthur, Damian R Plichta, Christian T Covington, Mathilde Poyet, Jessica Crothers, Peter L Moses, Andrew C Tolonen, Hera Vlamakis, Eric J Alm, and Ramnik J Xavier. and Host Adaptation in the Gut. 187(January):181–187, 2019.

322. Jeongjin Kim, Ara Jo, Tian Ding, Hyeon Yong Lee, and Juhee Ahn. Assessment of altered binding specificity of bacteriophage for ciprofloxacin-induced antibiotic-resistant Salmonella Typhimurium. *Archives of Microbiology*, 198(6):521–529, 2016.

323. Rachid Menouni, Geoffrey Hutinet, Marie Agnès Petit, and Mireille Ansaldi. Bacterial genome remodeling through bacteriophage recombination. *FEMS Microbiology Letters*, 362(1):1–10, 2015.

324. Bradley L Bearson and Brian W Brunelle. Fluoroquinolone induction of phage-mediated gene transfer in multidrug-resistant Salmonella. *International Journal of Antimicrobial Agents*, 46(2):201–204, 2015.

325. Susana Campoy, Anna Hervàs, Núria Busquets, Ivan Erill, Laura Teixidó, and Jordi Barbé. Induction of the SOS response by bacteriophage lytic development in Salmonella enterica. *Virology*, 2006.

326. Sung Hee Jung, Choong Min Ryu, and Jun Seob Kim. Bacterial persistence: Fundamentals and clinical importance. *Journal of Microbiology*, 57(10):829–835, 2019.

327. T. Vogwill, A. C. Comfort, V. Furió, and R. C. MacLean. Persistence and resistance as complementary bacterial adaptations to antibiotics. *Journal of evolutionary biology*, 29(6):1223–1233, 2016.

328. David Helaine, Sophie; Cheverton, Angela; Watson, Kathryn; Faure, Laura; Matthews, Sophie; Holden. Internalization of Salmonella by. *Science*, 343(January):204–208, 2014.

329. Anaïs Soares, Valérie Roussel, Martine Pestel-Caron, Magalie Barreau, François Caron, Emeline Bouffartigues, Sylvie Chevalier, and Manuel Etienne. Understanding Ciprofloxacin Failure in Pseudomonas aeruginosa Biofilm: Persister Cells Survive Matrix Disruption. *Frontiers in Microbiology*, 10(November):1–10, 2019.

330. Samara Paula Mattiello Drescher, Stephanie Wagner Gallo, Pedro Maria Abreu Ferreira, Carlos Alexandre Sanchez Ferreira, and Sílvia Dias de Oliveira. Salmonella enterica persister cells form unstable small colony variants after in vitro exposure to ciprofloxacin. *Scientific Reports*, 9(1):1–11, 2019.

331. John P. Pribis, Libertad García-Villada, Yin Zhai, Ohad Lewin-Epstein, Anthony Z. Wang, Jingjing Liu, Jun Xia, Qian Mei, Devon M. Fitzgerald, Julia Bos, Robert H. Austin, Christophe Herman, David Bates, Lilach Hadany, P. J. Hastings, and Susan M. Rosenberg. Gamblers: An Antibiotic-Induced Evolvable Cell Subpopulation Differentiated by Reactive-Oxygen-Induced General Stress Response. *Molecular Cell*, 74(4):785–800.e7, 2019.

332. Minal Patkari and Sarika Mehra. Transcriptomic study of ciprofloxacin resistance in Streptomyces coelicolor A3(2). *Molecular BioSystems*, 9(12):3101–3116, 2013.

333. Lin Li, Xingyang Dai, Ying Wang, Yanfei Yang, Xia Zhao, Lei Wang, and Minghua Zeng. RNA-seq-based analysis of drug-resistant Salmonella enterica serovar Typhimurium selected in vivo and in vitro. *PLoS ONE*, 12(4):1–14, 2017.

334. Xiaoxue Wang, Younghoon Kim, Qun Ma, Seok Hoon Hong, Karina Pokusaeva, Joseph M. Sturino, and Thomas K. Wood. Cryptic prophages help bacteria cope with adverse environments. *Nature Communications*, 1(9), 2010.

335. Jesús Machuca, Esther Recacha, Alejandra Briales, Paula Díaz-de Alba, Jesús Blazquez, álvaro Pascual, and José Manuel Rodríguez-Martínez. Cellular response to ciprofloxacin in low-level quinolone-resistant Escherichia coli. *Frontiers in Microbiology*, 8(JUL):1–11, 2017.

336. A. Huguet, J. Pensec, and C. Soumet. Resistance in Escherichia coli: Variable contribution of efflux pumps with respect to different fluoroquinolones. *Journal of Applied Microbiology*, 114(5):1294–1299, 2013.

337. Takashi Yamane, Hideki Enokida, Hiroshi Hayami, Motoshi Kawahara, and Masayuki Nakagawa. Genome-wide transcriptome analysis of fluoroquinolone resistance in clinical isolates of Escherichia coli. *International Journal of Urology*, 19(4):360–368, 2012.

338. Farah J. Nassar, Elias A. Rahal, Ahmad Sabra, and Ghassan M. Matar. Effects of subinhibitory concentrations of antimicrobial agents on escherichia coli O157:H7 Shiga toxin release and role of the SOS response. *Foodborne Pathogens and Disease*, 10(9):805–812, 2013.

339. Edward Geisinger, Germán Vargas-Cuebas, Nadav J. Mortman, Sapna Syal, Yunfei Dai, Elizabeth L. Wainwright, David Lazinski, Stephen Wood, Zeyu Zhu, Jon Anthony, Tim van Opijnen, and Ralph R. Isberg. The landscape of phenotypic and transcriptional responses to ciprofloxacin in acinetobacter baumannii: Acquired resistance alleles modulate drug-induced sos response and prophage replication. *mBio*, 10(3):1–19, 2019.

340. Viviana Cafiso, Stefano Stracquadanio, Flavia Lo Verde, Giacoma Gabriele, Maria Lina Mezzatesta, Carla Caio, Giuseppe Pigola, Alfredo Ferro, and Stefania Stefani. Colistin resistant A. Baumannii: Genomic and transcriptomic traits acquired under colistin therapy. *Frontiers in Microbiology*, 9(January):1–20, 2019.

341. Christine J. Boinett, Amy K. Cain, Jane Hawkey, Nhu Tran Do Hoang, Nhu Nguyen Thi Khanh, Duy Pham Thanh, Janina Dordel, James I. Campbell, Nguyen Phu Huong Lan, Matthew Mayho, Gemma C. Langridge, James Hadfield, Nguyen Van Vinh Chau, Guy E. Thwaites, Julian Parkhill, Nicholas R. Thomson, Kathryn E. Holt, and Stephen Baker. Clinical and laboratory-induced colistin-resistance mechanisms in acinetobacter baumannii. *Microbial Genomics*, 5(2), 2019.

342. Vera Lućia Dias Siqueira, Rosilene Fressatti Cardoso, Katiany Rizzieri Caleffi-Ferracioli, Regiane Bertin De Lima Scodro, Maria Aparecida Fernandez, Adriana Fiorini, Tania Ueda-Nakamura, Benedito Prado Dias-Filho, and Celso Vataru Nakamura. Structural changes and differentially expressed genes in Pseudomonas aeruginosa exposed to meropenem-ciprofloxacin combination. *Antimicrobial Agents and Chemotherapy*, 58(7):3957–3967, 2014.

343. Marina Rusch, Astrid Spielmeyer, Holger Zorn, and Gerd Hamscher. Degradation and transformation of fluoroquinolones by microorganisms with special emphasis on ciprofloxacin. *Applied Microbiology and Biotechnology*, 103(17):6933–6948, 2019.

344. Kaitlyn R Kelly and Bryan W Brooks. Global Aquatic Hazard Assessment of Ciprofloxacin: Exceedances of Antibiotic Resistance Development and Ecotoxicological Thresholds. *Progress in molecular biology and translational science*, 159:59–77, 2018.

345. L. Guillier, A. I. Nazer, and F. Dubois-Brissonnet. Growth response of Salmonella typhimurium in the presence of natural and synthetic antimicrobials: Estimation of MICs from three different models. *Journal of Food Protection*, 70(10):2243–2250, 2007.

346. Elena N. Strukova, Yury A. Portnoy, Stephen H. Zinner, and Alexander A. Firsov. Predictors of bacterial resistance using in vitro dynamic models: Area under the concentration-time curve related to either the minimum inhibitory or mutant prevention antibiotic concentration. *Journal of Antimicrobial Chemotherapy*, 71(3):678–684, 2016.

347. Paul G. Ambrose, Brian VanScoy, Haley Conde, Jennifer McCauley, Christopher M. Rubino, and Sujata M. Bhavnani. Bacterial replication rate modulation in combination with antimicrobial therapy: Turning the microbe against itself. *Antimicrobial Agents and Chemotherapy*, 61(1):1–6, 2017.

348. Paul G. Ambrose, Brian D. VanScoy, John Adams, Steven Fikes, Justin C. Bader, Sujata M. Bhavnani, and Christopher M. Rubino. Norepinephrine in combination with antibiotic therapy increases both the bacterial replication rate and bactericidal activity. *Antimicrobial Agents and Chemotherapy*, 62(4):1–7, 2018.

349. G. C. Crumplin and J. T. Smith. Nalidixic acid: an antibacterial paradox. *Antimicrob.Agents Chemother.*, 8(3):251–261, 1975.

350. Gan Luan, Yuzhi Hong, Karl Drlica, and Xilin Zhaoa. Suppression of reactive oxygen species accumulation accounts for paradoxical bacterial survival at high quinolone concentration. *Antimicrobial Agents and Chemotherapy*, 62(3):1–13, 2018.

351. Deborah A. Siegele and James C. Hu. Gene expression from plasmids containing the araBAD promoter at subsaturating inducer concentrations represents mixed populations. *Proceedings of the National Academy of Sciences of the United States of America*, 94(15):8168–8172, 1997.

352. Sheryl S. Justice, David A. Hunstad, Patrick C. Seed, and Scott J. Hultgren. Filamentation by Escherichia coli subverts innate defenses during urinary tract infection. *Proceedings of the National Academy of Sciences of the United States of America*, 103(52):19884–19889, 2006.

353. S. Humphrey, T. Macvicar, A. Stevenson, M. Roberts, T. J. Humphrey, and M. A. Jepson. SulA-induced filamentation in Salmonella enterica serovar Typhimurium: Effects on SPI-1 expression and epithelial infection. *Journal of Applied Microbiology*, 111(1):185–196, 2011.

354. K. L. Mattick, F. Jørgensen, J. D. Legan, M. B. Cole, J. Porter, H. M. Lappin-Scott, and T. J. Humphrey. Survival and filamentation of Salmonella enterica serovar enteritidis PT4 and Salmonella enterica serovar typhimurium DT104 at low water activity. *Applied and Environmental Microbiology*, 66(4):1274–1279, 2000.

355. Karen L. Mattick, Robin J. Rowbury, and Tom J. Humphrey. Morphological changes to Escherichia coli O157:H7, commensal E. coli and Salmonella spp in response to marginal growth conditions, with special reference to mildly stressing temperatures. *Science progress*, 86(Pt 1-2):103–113, 2003.

356. Efstathios S. Giotis, Ian S. Blair, and David A. McDowell. Morphological changes in Listeria monocytogenes subjected to sublethal alkaline stress. *International Journal of Food Microbiology*, 120(3):250–258, 2007.

357. Sheryl S Justice, David A Hunstad, Lynette Cegelski, and Scott J Hultgren. Morphological plasticity as a bacterial survival strategy. *Nature reviews. Microbiology*, 6(2):162–168, feb 2008.

358. D R Phillips, C M Cullinane, and D M Crothers. An in vitro transcription assay for probing drug-DNA interactions at individual drug sites. *Molecular biotechnology*, 10(1):63–75, aug 1998.

359. Poochit Nonejuie, Michael Burkart, Kit Pogliano, and Joe Pogliano. Bacterial cytological profiling rapidly identifies the cellular pathways targeted by antibacterial molecules. *Proceedings of the National Academy of Sciences of the United States of America*, 110(40):16169–16174, 2013.

360. D. T. Quach, G. Sakoulas, V. Nizet, J. Pogliano, and K. Pogliano. Bacterial Cytological Profiling (BCP) as a Rapid and Accurate Antimicrobial Susceptibility Testing Method for Staphylococcus aureus. *EBioMedicine*, 4:95–103, 2016.

361. W. Ungphakorn, P. Lagerbäck, E. I. Nielsen, and T. Tängdén. Automated time-lapse microscopy a novel method for screening of antibiotic combination effects against multidrug-resistant Gram-negative bacteria. *Clinical Microbiology and Infection*, 24(7):778.e7–778.e14, 2018.

362. Theresa C. Barrett, Wendy W.K. Mok, Allison M. Murawski, and Mark P. Brynildsen. Enhanced antibiotic resistance development from fluoroquinolone persisters after a single exposure to antibiotic. *Nature Communications*, 10(1):1–11, 2019.

363. Joana Mourão, Sara Marçal, Paula Ramos, Joana Campos, Jorge Machado, Luísa Peixe, Carla Novais, and Patrícia Antunes. Tolerance to multiple metal stressors in emerging non-typhoidal MDR Salmonella serotypes: A relevant role for copper in anaerobic conditions. *Journal of Antimicrobial Chemotherapy*, 71(8):2147–2157, 2016.

364. Rebekah N. Whitehead, Tim W. Overton, Caroline L. Kemp, and Mark A. Webber. Exposure of salmonella enterica serovar Typhimurium to high level biocide challenge can select multidrug resistant mutants in a single step. *PLoS ONE*, 6(7):1–9, 2011.

365. Olachi Anuforom, Graham R Wallace, Michelle M C Buckner, and Laura J V Piddock. Ciprofloxacin and ceftriaxone alter cytokine responses, but not Toll-like receptors, to Salmonella infection in vitro. *The Journal of antimicrobial chemotherapy*, 71(7):1826–1833, jul 2016.

366. Mark A Webber, Vito Ricci, Rebekah Whitehead, Meha Patel, Maria Fookes, Alasdair Ivens, and J V Piddock. Clinically Relevant Mutant DNA Gyrase Alters Supercoiling , Changes the Transcriptome , and Confers Multidrug Resistance. *mBio*, 4(4):1–10, 2013.

367. Mark A Webber, Michelle M C Buckner, Liam S Redgrave, Gyles Ifill, Lesley A Mitchenall, Carly Webb, Robyn Iddles, Anthony Maxwell, and Laura J V Piddock. Quinolone-resistant gyrase mutants demonstrate decreased susceptibility to triclosan. *Journal of Antimicrobial Chemotherapy*, pages 2755–2763, 2017.

368. Nikko P Torres and Grant W Brown. A high-throughput confocal fluorescence microscopy platform to study DNA replication stress in yeast cells. *Methods in molecular biology (Clifton, N.J.)*, 1300:1–12, 2015.

369. Sandra Duffy and Vicky M Avery. Development and Optimization of a Novel 384-Well Anti-Malarial Imaging Assay Validated for High-Throughput Screening. *The American Journal of Tropical Medicine and Hygiene*, 86(1):84–92, 2012.

370. S K Hoiseth and B A Stocker. Aromatic-dependent Salmonella typhimurium are non-virulent and effective as live vaccines. *Nature*, 291(5812):238–239, may 1981.

371. Deborah J. Griggs, Karl Gensberg, and Laura J.V. Piddock. Mutations in gyrA gene of quinolone-resistant salmonella serotypes isolated from humans and animals. *Antimicrobial Agents and Chemotherapy*, 40(4):1009–1013, 1996.

372. Michael I. Love, Wolfgang Huber, and Simon Anders. Moderated estimation of fold change and dispersion for RNA-seq data with DESeq2. *Genome Biology*, 15(12), 2014.

373. Dries De Maeyer, Bram Weytjens, Joris Renkens, Luc De Raedt, and Kathleen Marchal. PheNetic: Network-based interpretation of molecular profiling data. *Nucleic Acids Research*, 43(W1):W244–W250, 2015.

374. Kirill Tsyganov, Andrew James Perry, Stuart Kenneth Archer, and David Powell. RNAsik: A Pipeline for complete and reproducible RNA-seq analysis that runs anywhere with speed and ease. *Journal of Open Source Software*, 3(28):583, 2018.

375. Matthew E. Ritchie, Belinda Phipson, Di Wu, Yifang Hu, Charity W. Law, Wei Shi, and Gordon K. Smyth. Limma powers differential expression analyses for RNA-sequencing and microarray studies. *Nucleic Acids Research*, 43(7):e47, 2015.

376. Kirill A. Datsenko and Barry L. Wanner. One-step inactivation of chromosomal genes in Escherichia coli K-12 using PCR products. *Proceedings of the National Academy of Sciences of the United States of America*, 97(12):6640–6645, 2000.

377. Lars Barquist, Matthew Mayho, Carla Cummins, Amy K. Cain, Christine J. Boinett, Andrew J. Page, Gemma C. Langridge, Michael A. Quail, Jacqueline A. Keane, and Julian Parkhill. The TraDIS toolkit: Sequencing and analysis for dense transposon mutant libraries. *Bioinformatics*, 32(7):1109–1111, 2016.

378. Emily A AU - Lees, Jessica L AU - Forbester, Sally AU - Forrest, Leanne AU - Kane, David AU - Goulding, and Gordon AU - Dougan. Using Human Induced Pluripotent Stem Cell-derived Intestinal Organoids to Study and Modify Epithelial Cell Protection Against Salmonella and Other Pathogens. *JoVE*, (147):e59478, 2019.

379. Alexandros Stamatakis. RAxML version 8: A tool for phylogenetic analysis and post-analysis of large phylogenies. *Bioinformatics*, 30(9):1312–1313, 2014.

380. Ivica Letunic and Peer Bork. Interactive tree of life (iTOL) v3: an online tool for the display and annotation of phylogenetic and other trees. *Nucleic acids research*, 44(W1):W242–W245, 2016.

381. Andrew J. Page, Carla A. Cummins, Martin Hunt, Vanessa K. Wong, Sandra Reuter, Matthew T.G. G Holden, Maria Fookes, Daniel Falush, Jacqueline A. Keane, and Julian Parkhill. Roary: rapid large-scale prokaryote pan genome analysis. *Bioinformatics (Oxford, England)*, 31(22):3691–3693, nov 2015.

382. Martin Hunt, Alison E. Mather, Leonor Sánchez-Busó, Andrew J. Page, Julian Parkhill, Jacqueline A. Keane, and Simon R. Harris. ARIBA: Rapid antimicrobial resistance genotyping directly from sequencing reads. *Microbial Genomics*, 3(10):1–11, 2017.

383. Brian P Alcock, Amogelang R Raphenya, Tammy T Y Lau, Kara K Tsang, Mégane Bouchard, Arman Edalatmand, William Huynh, Anna-Lisa V Nguyen, Annie A Cheng, Sihan Liu, Sally Y Min, Anatoly Miroshnichenko, Hiu-Ki Tran, Rafik E Werfalli, Jalees A Nasir, Martins Oloni, David J Speicher, Alexandra Florescu, Bhavya Singh, Mateusz Faltyn, Anastasia Hernandez-Koutoucheva, Arjun N Sharma, Emily Bordeleau, Andrew C Pawlowski, Haley L Zubyk, Damion Dooley, Emma Griffiths, Finlay Maguire, Geoff L Winsor, Robert G Beiko, Fiona S L Brinkman, William W L Hsiao, Gary V Domselaar, and Andrew G McArthur. CARD 2020: antibiotic resistome surveillance with the comprehensive antibiotic resistance database. *Nucleic Acids Research*, 48(D1):D517–D525, jan 2020.

384. Ea Zankari, Henrik Hasman, Salvatore Cosentino, Martin Vestergaard, Simon Rasmussen, Ole Lund, Frank M. Aarestrup, and Mette Voldby Larsen. Identification of acquired antimicrobial resistance genes. *Journal of Antimicrobial Chemotherapy*, 67(11):2640–2644, 2012.

385. Jonathan C. Craig, Gabrielle J. Williams, Mike Jones, Miriam Codarini, Petra Macaskill, Andrew Hayen, Les Irwig, Dominic A. Fitzgerald, David Isaacs, and Mary McCaskill. The accuracy of clinical symptoms and signs for the diagnosis of serious bacterial infection in young febrile children: Prospective cohort study of 15 781 febrile illnesses. *BMJ (Online)*, 340(7754):1015, 2010.

386. Erwin van Vliet, Mardas Daneshian, Mario Beilmann, Anthony Davies, Eugenio Fava, Roland Fleck, Yvon Julé, Manfred Kansy, Stefan Kustermann, Peter Macko, William R Mundy, Adrian Roth, Imran Shah, Marianne Uteng, Bob van de Water, Thomas Hartung,

and Marcel Leist. Current approaches and future role of high content imaging in safety sciences and drug discovery. *ALTEX*, 31(4):479–493, 2014.

387. Mark-Anthony Bray, Shantanu Singh, Han Han, Chadwick T Davis, Blake Borgeson, Cathy Hartland, Maria Kost-Alimova, Sigrun M Gustafsdottir, Christopher C Gibson, and Anne E Carpenter. Cell Painting, a high-content image-based assay for morphological profiling using multiplexed fluorescent dyes. *Nature protocols*, 11(9):1757–1774, sep 2016.

388. Alexandra Kiss, Arnold Péter Ráduly, Zsolt Regdon, Zsuzsanna Polgár, Szabolcs Tarapcsák, Isotta Sturniolo, Tarek El-Hamoly, László Virág, and Csaba HegedÅ±s. Targeting Nuclear NAD(+) Synthesis Inhibits DNA Repair, Impairs Metabolic Adaptation and Increases Chemosensitivity of U-2OS Osteosarcoma Cells. *Cancers*, 12(5):1180, may 2020.

389. Milan Esner, Felix Meyenhofer, and Marc Bickle. Live-Cell High Content Screening in Drug Development. *Methods in molecular biology (Clifton, N.J.)*, 1683:149–164, 2018.

390. Marion Vanneste, Qin Huang, Mengshi Li, Devon Moose, Lei Zhao, Mark A Stamnes, Michael Schultz, Meng Wu, and Michael D Henry. High content screening identifies monensin as an EMT-selective cytotoxic compound. *Scientific reports*, 9(1):1200, feb 2019.

391. Simon M. Bell, Katy Barnes, Hannah Clemmens, Aziza R. Al-Rafiah, Ebtisam A. Al-ofi, Vicki Leech, Oliver Bandmann, Pamela J. Shaw, Daniel J. Blackburn, Laura Ferraiuolo, and Heather Mortiboys. Ursodeoxycholic Acid Improves Mitochondrial Function and Redistributes Drp1 in Fibroblasts from Patients with Either Sporadic or Familial Alzheimer's Disease. *Journal of Molecular Biology*, 430(21):3942–3953, 2018.

392. M. Liu, J. Ylanko, E. Weekman, T. Beckett, D. Andrews, and J. McLaurin. Utilizing supervised machine learning to identify microglia and astrocytes in situ: implications for large-scale image analysis and quantification. *Journal of Neuroscience Methods*, 328(August):108424, 2019.

393. Alyssa J. Manning, Yulia Ovechkina, Amanda McGillivray, Lindsay Flint, David M. Roberts, and Tanya Parish. A high content microscopy assay to determine drug activity against intracellular Mycobacterium tuberculosis. *Methods*, 127:3–11, 2017.

394. Thierry Christophe, Fanny Ewann, Hee Kyoung Jeon, Jonathan Cechetto, and Priscille Brodin. High-content imaging of Mycobacterium tuberculosis-infected macrophages: an in vitro model for tuberculosis drug discovery. *Future medicinal chemistry*, 2(8):1283–1293, aug 2010.

395. Amy K. Barczak, Roi Avraham, Shantanu Singh, Samantha S. Luo, Wei Ran Zhang, Mark Anthony Bray, Amelia E. Hinman, Matthew Thompson, Raymond M. Nietupski, Aaron Golas, Paul Montgomery, Michael Fitzgerald, Roger S. Smith, Dylan W. White, Anna D. Tischler, Anne E. Carpenter, and Deborah T. Hung. Systematic, multiparametric analysis of Mycobacterium tuberculosis intracellular infection offers insight into coordinated virulence. *PLoS Pathogens*, 13(5):1–27, 2017.

396. Daniel J. Greenwood, Mariana Silva Dos Santos, Song Huang, Matthew R.G. Russell, Lucy M. Collinson, James I. MacRae, Andy West, Haibo Jiang, and Maximiliano G. Gutierrez. Subcellular antibiotic visualization reveals a dynamic drug reservoir in infected macrophages. *Science*, 364(6447):1279–1282, 2019.

397. Antony N. Antoniou, Simon J. Powis, and Janos Kriston-Vizi. High-content screening image dataset and quantitative image analysis of Salmonella infected human cells. *BMC Research Notes*, 12(1):1–4, 2019.

398. Sannah Zoffmann, Maarten Vercruysse, Fethallah Benmansour, Andreas Maunz, Luise Wolf, Rita Blum Marti, Tobias Heckel, Haiyuan Ding, Hoa Hue Truong, Michael Prummer, Roland Schmucki, Clive S. Mason, Kenneth Bradley, Asha Ivy Jacob, Christian Lerner, Andrea Araujo del Rosario, Mark Burcin, Kurt E. Amrein, and Marco Prunotto. Machine learning-powered antibiotics phenotypic drug discovery. *Scientific Reports*, 9(1):1–14, 2019.

399. Mailis Maes, Zoe A. Dyson, Sarah E. Smith, David A. Goulding, Catherine Ludden, Stephen Baker, Paul Kellam, Stephen T. Reece, Gordon Dougan, and Josefin Bartholdson Scott. A novel therapeutic antibody screening method using bacterial high-content imaging reveals functional antibody binding phenotypes of Escherichia coli ST131. *bioRxiv*, page 2020.05.22.110148, 2020.

400. Htut Htut Htoo, Lauren Brumage, Vorrapon Chaikeeratisak, Hannah Tsunemoto, Joseph Sugie, Chanwit Tribuddharat, Joe Pogliano, and Poochit Nonejuie. Bacterial Cytological Profiling as a Tool To Study Mechanisms of Action of Antibiotics That Are Active against Acinetobacter baumannii. *Antimicrobial Agents and Chemotherapy*, 63(4):1–11, 2019.

401. Anne Lamsa, Javier Lopez-Garrido, Diana Quach, Eammon P. Riley, Joe Pogliano, and Kit Pogliano. Rapid Inhibition Profiling in Bacillus subtilis to Identify the Mechanism of Action of New Antimicrobials. *ACS Chemical Biology*, 11(8):2222–2231, 2016.

402. Janet A. Hindler, Annie Wong-Beringer, Carmen L. Charlton, Shelley A. Miller, Theodoros Kelesidis, Marissa Carvalho, George Sakoulas, Poochit Nonejuie, Joseph Pogliano, Victor Nizet, and Romney Humphries. In vitro activity of daptomycin in combination with β-lactams, gentamicin, rifampin, and tigecycline against daptomycin-nonsusceptible enterococci. *Antimicrobial Agents and Chemotherapy*, 59(7):4279–4288, 2015.

403. Erlinda R. Ulloa, Nicholas Dillon, Hannah Tsunemoto, Joe Pogliano, George Sakoulas, and Victor Nizet. Avibactam Sensitizes Carbapenem-Resistant NDM-1-Producing Klebsiella pneumoniae to Innate Immune Clearance. *Journal of Infectious Diseases*, 220(3):484–493, 2019.

404. George Sakoulas, Joshua Olson, Juwon Yim, Niedita B. Singh, Monika Kumaraswamy, Diana T. Quach, Michael J. Rybak, Joseph Pogliano, and Victor Nizet. Cefazolin and ertapenem, a synergistic combination used to clear persistent Staphylococcus aureus Bacteremia. *Antimicrobial Agents and Chemotherapy*, 60(11):6609–6618, 2016.

405. Haroon Mohammad, Waleed Younis, Hany G. Ezzat, Christine E. Peters, Ahmed Abdelkhalek, Bruce Cooper, Kit Pogliano, Joe Pogliano, Abdelrahman S. Mayhoub,

and Mohamed N. Seleem. Bacteriological profiling of diphenylureas as a novel class of antibiotics against methicillin-resistant Staphylococcus aureus. *PLoS ONE*, 12(8):1–20, 2017.

406. Michal P. Wandel, Claudio Pathe, Emma I. Werner, Cara J. Ellison, Keith B. Boyle, Alexander von der Malsburg, John Rohde, and Felix Randow. GBPs Inhibit Motility of Shigella flexneri but Are Targeted for Degradation by the Bacterial Ubiquitin Ligase IpaH9.8. *Cell Host and Microbe*, 22(4):507–518.e5, 2017.

407. Stephanie K. Lathrop, Kelsey A. Binder, Tregei Starr, Kendal G. Cooper, Audrey Chong, Aaron B. Carmody, and Olivia Steele-Mortimer. Replication of Salmonella enterica serovar Typhimurium in human monocyte-derived macrophages. *Infection and Immunity*, 83(7):2661–2671, 2015.

408. Yu Liang Zheng, Yang Peng Sun, Hong Zhang, Wen Jing Liu, Rui Jiang, Wen Yu Li, You Hua Zheng, and Zhi Guang Zhang. Mesenchymal stem cells obtained from synovial fluid mesenchymal stem cell- Derived induced pluripotent stem cells on a matrigel coating exhibited enhanced proliferation and differentiation potential. *PLoS ONE*, 10(12):1–19, 2015.

409. Chun Yen Liu, Michiya Matsusaki, and Mitsuru Akashi. Three-Dimensional Tissue Models Constructed by Cells with Nanometer- or Micrometer-Sized Films on the Surfaces. *Chemical Record*, 16(2):783–796, 2016.

410. Dong Soo Hwang, Sung Bo Sim, and Hyung Joon Cha. Cell adhesion biomaterial based on mussel adhesive protein fused with RGD peptide. *Biomaterials*, 28(28):4039–4046, 2007.

411. Birendra AU - Singh, Maryam AU - Mostajeran, Yu-Ching AU - Su, Tamim AU - Al-Jubair, and Kristian AU - Riesbeck. Assays for Studying the Role of Vitronectin in Bacterial Adhesion and Serum Resistance. *JoVE*, (140):e54653, 2018.

412. Mattias Leino, Carolina Astrand, Nanayaa Hughes-Brittain, Brendan Robb, Robert McKean, and Véronique Chotteau. Human embryonic stem cell dispersion in electrospun PCL fiber scaffolds by coating with laminin-521 and E-cadherin-Fc. *Journal of Biomedical Materials Research - Part B Applied Biomaterials*, 106(3):1226–1236, 2018.

413. Kamalpreet Kaur, Rupinder Kaur Sodhi, Anju Katyal, Ritu Aneja, Upendra Kumar Jain, Om Prakash Katare, and Jitender Madan. Wheat germ agglutinin anchored chitosan microspheres of reduced brominated derivative of noscapine ameliorated acute inflammation in experimental colitis. *Colloids and Surfaces B: Biointerfaces*, 132:225–235, 2015.

414. Ryoko Sato-Nishiuchi, Shaoliang Li, Fumi Ebisu, and Kiyotoshi Sekiguchi. Recombinant laminin fragments endowed with collagen-binding activity: A tool for conferring laminin-like cell-adhesive activity to collagen matrices. *Matrix Biology*, 65:75–90, 2018.

415. Howard M. Shapiro. Microbial analysis at the single-cell level: Tasks and techniques. *Journal of Microbiological Methods*, 42(1):3–16, 2000.

416. Scott L. Burnett and Larry R. Beuchat. Comparison of methods for fluorescent detection of viable, dead, and total Escherichia coli O157:H7 cells in suspensions and on apples using confocal scanning laser microscopy following treatment with sanitizers. *International Journal of Food Microbiology*, 74(1-2):37–45, 2002.

417. Sruti Chattopadhyay, Avneet Kaur, Swati Jain, and Harpal Singh. Sensitive detection of food-borne pathogen Salmonella by modified PAN fibers-immunoassay. *Biosensors and Bioelectronics*, 45(1):274–280, 2013.

418. D. I. Hovanec and E. A. Gorzynski. Coagglutination as an expedient for grouping Escherichia coli associated with urinary tract infections. *Journal of Clinical Microbiology*, 11(1):41–44, 1980.

419. Rafal Kolenda, Maciej Ugorski, and Krzysztof Grzymajlo. Everything you always wanted to know about Salmonella type 1 fimbriae, but were afraid to ask. *Frontiers in Microbiology*, 10(MAY):1–18, 2019.

420. Markus Furter, Mikael E. Sellin, Gunnar C. Hansson, and Wolf Dietrich Hardt. Mucus Architecture and Near-Surface Swimming Affect Distinct Salmonella Typhimurium Infection Patterns along the Murine Intestinal Tract. *Cell Reports*, 27(9):2665–2678.e3, 2019.

421. Bruce L. Roth, Martin Poot, Stephen T. Yue, and Paul J. Millard. Bacterial viability and antibiotic susceptibility testing with SYTOX green nucleic acid stain. *Applied and Environmental Microbiology*, 63(6):2421–2431, 1997.

422. Karen McKenzie, Michelle Maclean, M. Helen Grant, Praveen Ramakrishnan, Scott J. MacGregor, and John G. Anderson. The effects of 405 nm light on bacterial membrane integrity determined by salt and bile tolerance assays, leakage of UV-absorbing material and SYTOX green labelling. *Microbiology (United Kingdom)*, 162(9):1680–1688, 2016.

423. P. Lebaron, P. Catala, and N. Parthuisot. Effectiveness of SYTOX green stain for bacterial viability assessment. *Applied and Environmental Microbiology*, 64(7):2697–2700, 1998.

424. Dieter Weichart, Diane Mcdougald, Daniel Jacobs, and Staffan Kjelleberg. In situ analysis of nucleic acids in cold-induced nonculturable Vibrio vulnificus. *Applied and Environmental Microbiology*, 63(7):2754–2758, 1997.

425. Fabien Joux, Philippe Lebaron, and Marc Trousselier. Succession of cellular states in a Salmonella typhimurium population during starvation in artificial seawater microcosms. *FEMS Microbiology Ecology*, 22:65–76, 1997.

426. A Keith Turner, Sabine E Eckert, Daniel J Turner, Muhammud Yasir, Mark A Webber, Ian G Charles, Julian Parkhill, and John Wain. A whole-genome screen identifies Salmonella enterica serovar Typhi genes involved in fluoroquinolone susceptibility. *Journal of Antimicrobial Chemotherapy*, jun 2020.

427. Chuan Zhen Zhang, Si Qi Ren, Man Xia Chang, Pin Xian Chen, Huan Zhong Ding, and Hong Xia Jiang. Resistance mechanisms and fitness of Salmonella Typhimurium and Salmonella Enteritidis mutants evolved under selection with ciprofloxacin in vitro. *Scientific Reports*, 7(1):1–9, 2017.

428. Yawei Sun, Menghong Dai, Haihong Hao, Yulian Wang, Lingli Huang, Yassir A. Almofti, Zhenli Liu, and Zonghui Yuan. The role of RamA on the development of ciprofloxacin resistance in Salmonella enterica serovar Typhimurium. *PLoS ONE*, 6(8), 2011.

429. Sebastian Braetz, Peter Schwerk, Arthur Thompson, Karsten Tedin, and Marcus Fulde. The role of ATP pools in persister cell formation in (fluoro) quinolone- susceptible and -resistant strains of Salmonella enterica ser . Typhimurium. *Veterinary Microbiology*, 210(September):116–123, 2017.

430. Robert A Fisher, Bridget Gollan, and Sophie Helaine. Persistent bacterial infections and persister cells. *Nature Publishing Group*, 15(8):453–464, 2017.

431. Yue Shan, Autumn Brown Gandt, Sarah E Rowe, Julia P Deisinger, Brian P Conlon, and Kim Lewis. ATP-Dependent Persister Formation in Escherichia coli. *mBio*, 8(1), feb 2017.

432. Brian P Conlon, Sarah E Rowe, Autumn Brown Gandt, Austin S Nuxoll, Niles P Donegan, Eliza A Zalis, Geremy Clair, Joshua N Adkins, Ambrose L Cheung, and Kim Lewis. Persister formation in Staphylococcus aureus is associated with ATP depletion. *Nature microbiology*, 1:16051, apr 2016.

433. Julia Bos, Qiucen Zhang, Saurabh Vyawahare, Elizabeth Rogers, Susan M. Rosenberg, and Robert H. Austin. Emergence of antibiotic resistance from multinucleated bacterial filaments. *Proceedings of the National Academy of Sciences of the United States of America*, 112(1):178–183, 2015.

434. Keith D. Mackenzie, Yejun Wang, Patrick Musicha, Elizabeth G. Hansen, Melissa B. Palmer, Dakoda J. Herman, Nicholas A. Feasey, and Aaron P. White. Parallel evolution leading to impaired biofilm formation in invasive Salmonella strains. *PLOS Genetics*, 15(6):e1008233, jun 2019.

435. Alison E Mather, Becki Lawson, Elizabeth de Pinna, Paul Wigley, Julian Parkhill, Nicholas R Thomson, Andrew J Page, Mark A Holmes, and Gavin K Paterson. Genomic Analysis of Salmonella enterica Serovar Typhimurium from Wild Passerines in England and Wales. *Applied and environmental microbiology*, 82(22):6728–6735, nov 2016.

436. Monique Ribeiro, Tiba Casas, Carlos Henrique, Flávia Barrosa, Wanderley Dias da Silveira, and Sueli Aparecida Fernandes. Presence of plasmid-mediated quinolone resistance determinants and mutations in gyrase and topoisomerase in Salmonella enterica isolates with resistance and reduced susceptibility to ciprofloxacin. *Diagnostic Microbiology and Infectious Disease*, 85(1):85–89, 2016.

437. Dai Kuang, Jianmin Zhang, Xuebin Xu, Weimin Shi, Sheng Chen, Xiaowei Yang, Xudong Su, Xianming Shi, and Jianghong Meng. Emerging high-level ciprofloxacin resistance and molecular basis of resistance in Salmonella enterica from humans, food and animals. *International journal of food microbiology*, 280:1–9, sep 2018.

438. Marcus H Wong, Edward W Chan, Li Z Liu, and Sheng Chen. PMQR genes oqxAB and aac(6')Ib-cr accelerate the development of fluoroquinolone resistance in Salmonella typhimurium. *Frontiers in microbiology*, 5:521, 2014.

439. Alexander A. Firsov, Elena N. Strukova, Darya S. Shlykova, Yury A. Portnoy, Varvara K. Kozyreva, Mikhail V. Edelstein, Svetlana A. Dovzhenko, Mikhail B. Kobrin, and Stephen H. Zinner. Bacterial resistance studies using in vitro dynamic models: The predictive power of the mutant prevention and minimum inhibitory antibiotic concentrations. *Antimicrobial Agents and Chemotherapy*, 57(10):4956–4962, 2013.

440. Jennifer M Andrews. Determination of minimum inhibitory concentrations. *Journal of Antimicrobial Chemotherapy*, 48(suppl_1):5–16, jul 2001.

441. Xiongwei Du, Ying Liu, Xiaojie Sun, Jianmei Zhao, Juan Wang, Jianping Li, Xuelian Liu, Junwei Wang, and Ye Li. The mRNA expression of ompF, invA and invE was associated with the ciprofloxacin-resistance in Salmonella. *Archives of microbiology*, 202(8):2263–2268, oct 2020.

442. Lyn-Fay Lee, Vanitha Mariappan, Kumutha Malar Vellasamy, Vannajan Sanghiran Lee, and Jamuna Vadivelu. Antimicrobial activity of Tachyplesin 1 against Burkholderia pseudomallei: an in vitro and in silico approach. *PeerJ*, 4:e2468, 2016.

443. Lena Dhara and Anusri Tripathi. Cinnamaldehyde: a compound with antimicrobial and synergistic activity against ESBL-producing quinolone-resistant pathogenic Enterobacteriaceae. *European Journal of Clinical Microbiology and Infectious Diseases*, 39(1):65–73, 2020.

444. Kannan Balaji, Ramalingam Thenmozhi, and Shunmugiah Karutha Pandian. Effect of subinhibitory concentrations of fluoroquinolones on biofilm production by clinical isolates of Streptococcus pyogenes. *The Indian journal of medical research*, 137(5):963–971, may 2013.

445. D C Hooper, J S Wolfson, E Y Ng, and M N Swartz. Mechanisms of action of and resistance to ciprofloxacin. *The American journal of medicine*, 82(4A):12–20, apr 1987.

446. S F Altschul, W Gish, W Miller, E W Myers, and D J Lipman. Basic local alignment search tool. *Journal of molecular biology*, 215(3):403–410, oct 1990.

447. Sinisa Vidovic, Ran An, and Aaron Rendahl. Molecular and Physiological Characterization of Fluoroquinolone-Highly Resistant Salmonella Enteritidis Strains. *Frontiers in microbiology*, 10:729, apr 2019.

448. Marta Albareda, Grant Buchanan, and Frank Sargent. Identification of a stable complex between a [NiFe]-hydrogenase catalytic subunit and its maturation protease. *FEBS Letters*, 591(2):338–347, 2017.

449. Lisa Bowman, Lindsey Flanagan, Paul K. Fyfe, Alison Parkin, William N. Hunter, and Frank Sargent. How the structure of the large subunit controls function in an oxygen-tolerant [NiFe]-hydrogenase. *Biochemical Journal*, 458(3):449–458, 2014.

450. Vito Ricci and Laura J V Piddock. Ciprofloxacin selects for multidrug resistance in Salmonella enterica serovar Typhimurium mediated by at least two different pathways. *The Journal of antimicrobial chemotherapy*, 63(5):909–916, may 2009.

451. Vito Ricci and Laura J V Piddock. Only for substrate antibiotics are a functional AcrAB-TolC efflux pump and RamA required to select multidrug-resistant Salmonella Typhimurium., sep 2009.

452. François Gravey, Vincent Cattoir, Frédéric Ethuin, Laetitia Fabre, Racha Beyrouthy, Richard Bonnet, Simon Le Hello, and François Guérin. ramR deletion in an Enterobacter hormaechei isolate as a consequence of therapeutic failure to key antibiotics in a long-term hospitalized patient. *Antimicrobial agents and chemotherapy*, aug 2020.

453. Clara Ballesté-delpierre, Mar Solé, Òscar Domènech, Jordi Borrell, Jordi Vila, and Anna Fàbrega. Molecular study of quinolone resistance mechanisms and clonal relationship of Salmonella enterica clinical isolates. *International Journal of Antimicrobial Agents*, 43(2):121–125, 2014.

454. Sheng Chen, Shenghui Cui, Patrick F. McDermott, Shaohua Zhao, David G. White, Ian Paulsen, and Jianghong Meng. Contribution of target gene mutations and efflux to decreased susceptibility of Salmonella enterica serovar typhimurium to fluoroquinolones and other antimicrobials. *Antimicrobial Agents and Chemotherapy*, 51(2):535–542, 2007.

455. Siân V. Owen, Rocío Canals, Nicolas Wenner, Disa L. Hammarlöf, Carsten Kröger, and Jay C. D. Hinton. A window into lysogeny: revealing temperate phage biology with transcriptomics. *Microbial Genomics*, 2020.

456. K Rutherford, J Parkhill, J Crook, T Horsnell, P Rice, M A Rajandream, and B Barrell. Artemis: sequence visualization and annotation. *Bioinformatics (Oxford, England)*, 16(10):944–945, oct 2000.

457. Kunihiko Nishino, Tammy Latifi, and Eduardo A. Groisman. Virulence and drug resistance roles of multidrug efflux systems of Salmonella enterica serovar Typhimurium. *Molecular Microbiology*, 59(1):126–141, jan 2006.

458. Eiji Nikaido, Akihito Yamaguchi, and Kunihiko Nishino. AcrAB multidrug efflux pump regulation in Salmonella enterica serovar Typhimurium by RamA in response to environmental signals. *Journal of Biological Chemistry*, 283(35):24245–24253, 2008.

459. Magdalena Ibanez-Ruiz, Véronique Robbe-Saule, Daniel Hermant, Séverine Labrude, and Françoise Norel. Identification of SoxS-regulated genes in Salmonella enterica serovar Typhimurium. *Journal of Bacteriology*, 182(1):23–29, 2000.

460. Martin W. Bader, William Wiley Navarre, Whitney Shiau, Hiroshi Nikaido, Jonathan G. Frye, Michael McClelland, Ferric C. Fang, and Samuel I. Miller. Regulation of Salmonella typhimurium virulence gene expression by cationic antimicrobial peptides. *Molecular Microbiology*, 50(1):219–230, 2003.

461. Nicholas R. Benson, Rita M.Y. Wong, and Michael McClelland. Analysis of the SOS response in Salmonella enterica serovar Typhimurium using RNA fingerprinting by arbitrarily primed PCR. *Journal of Bacteriology*, 182(12):3490–3497, 2000.

462. Noriko Motohashi and Yutaka Saito. Induction of SOS response in Salmonella typhimurium TA4107/pSK1002 by peroxynitrite-generating agent, N-morpholino sydnonimine. *Mutation Research - Fundamental and Molecular Mechanisms of Mutagenesis*, 502(1-2):11–18, 2002.

463. Jessica L. Kosa, Zoran Z. Zdraveski, Sophie Currier, Martin G. Marinus, and John M. Essigmann. RecN and RecG are required for Escherichia coli survival of Bleomycin-induced damage. *Mutation Research - Fundamental and Molecular Mechanisms of Mutagenesis*, 554(1-2):149–157, 2004.

464. Haiquan Li, Vagner A. Benedito, Michael K. Udvardi, and Patrick X. Zhao. TransportTP: A two-phase classification approach for membrane transporter prediction and characterization. *BMC Bioinformatics*, 10, 2009.

465. Qinghu Ren, Kaixi Chen, and Ian T. Paulsen. TransportDB: A comprehensive database resource for cytoplasmic membrane transport systems and outer membrane channels. *Nucleic Acids Research*, 35(SUPPL. 1), 2007.

466. J. W. Little, S. H. Edminston, L. Z. Pacelli, and D. Mount. Cleavage of the Escherichia coli lexA protein by the recA protease. *Proceedings of the National Academy of Sciences of the United States of America*, 77(6 I):3225–3229, 1980.

467. Yu Luo, Richard A. Pfuetzner, Steve Mosimann, Mark Paetzel, Elizabeth A. Frey, Maia Cherney, Baek Kim, John W. Little, and Natalie C.J. Strynadka. Crystal structure of LexA: A conformational switch for regulation of self-cleavage. *Cell*, 106(5):585–594, 2001.

468. Errol C Friedberg. Suffering in silence: the tolerance of DNA damage. *Nature Reviews Molecular Cell Biology*, 6(12):943–953, 2005.

469. Thuy Do Thi, Elena López, Alexandro Rodríguez-Rojas, Jerónimo Rodríguez-Beltrán, Alejandro Couce, Javier R. Guelfo, Alfredo Castañeda-García, and Jesús Blázquez. Effect of recA inactivation on mutagenesis of Escherichia coli exposed to sublethal concentrations of antimicrobials. *Journal of Antimicrobial Chemotherapy*, 66(3):531–538, 2011.

470. O Huisman and R D'Ari. An inducible DNA replication-cell division coupling mechanism in E. coli. *Nature*, 290(5809):797–799, apr 1981.

471. E Maguin, J Lutkenhaus, and R D'Ari. Reversibility of SOS-associated division inhibition in Escherichia coli. *Journal of bacteriology*, 166(3):733–738, jun 1986.

472. Haruo Ohmori, Errol C. Friedberg, Robert P.P. Fuchs, Myron F. Goodman, Fumio Hanaoka, David Hinkle, Thomas A. Kunkel, Christopher W. Lawrence, Zvi Livneh, Takehiko Nohmi, Louise Prakash, Satya Prakash, Takeshi Todo, Graham C. Walker, Zhigang Wang, and Roger Woodgate. The Y-Family of DNA Polymerases. 8:7–8, 2001.

473. Nina Bacher Reuven, Gali Arad, Ayelet Maor-Shoshani, and Zvi Livneh. The mutagenesis protein UmuC is a DNA polymerase activated by UmuD', RecA, and SSB and is specialized for translesion replication. *Journal of Biological Chemistry*, 1999.

474. Devin B Holman, Shawn M D Bearson, Bradley L Bearson, and Brian W Brunelle. Chlortetracycline and florfenicol induce expression of genes associated with pathogenicity in multidrug-resistant Salmonella enterica serovar Typhimurium. *Gut Pathogens*, pages 1–12, 2018.

475. T Kawarai, M Wachi, H Ogino, S Furukawa, K Suzuki, H Ogihara, and M Yamasaki. SulA-independent filamentation of Escherichia coli during growth after release from high hydrostatic pressure treatment. *Applied microbiology and biotechnology*, 64(2):255–262, apr 2004.

476. Nozomu Otsuji, Mutsuo Sekiguchi, Teiji Iijima, and Yasuyuki Takagi. Induction of phage formation in the lysogenic escherichia coli K-12 by mitomycin C. *Nature*, 184(4692):1079–1080, 1959.

477. Ingrid Smith-Kielland. The effect of mitomycin C on deoxyribonucleic acid and messenger ribonucleic acid in Escherichia coli. *BBA Section Nucleic Acids And Protein Synthesis*, 114(2):254–263, 1966.

478. Myron Levine. Effect of mitomycin C on interactions between temperate phages and bacteria. *Virology*, 13(4):493–499, 1961.

479. P. U. Giacomoni. Induction by mitomycin C of recA protein synthesis in bacteria and spheroplasts. *Journal of Biological Chemistry*, 257(24):14932–14936, 1982.

480. Elizabeth M. Grimsey, Natasha Weston, Vito Ricci, Jack W. Stone, and Laura J.V. Piddock. Over-expression of RamA, which regulates production of the MDR efflux pump AcrAB-TolC, increases mutation rate and influences drug-resistance phenotype. *Antimicrobial Agents and Chemotherapy*, jan 2020.

481. J B Chaires and G Kegeles. Sucrose density gradient sedimentation of E. coli ribosomes. *Biophysical Chemistry*, 7:173–178, 1977.

482. E Huff, H Oxley, and C S Silverman. Density-gradient patterns of Stapylococcus aureus cells and cell walls during growth and mechanical disruption. *Journal of bacteriology*, 88(4):1155–1162, oct 1964.

483. G Dougan, M Saul, A Twigg, R Gill, and D Sherratt. Polypeptides expressed in Escherichia coli K-12 minicells by transposition elements Tn1 and Tn3. *Journal of bacteriology*, 138(1):48–54, apr 1979.

484. G Dougan and D J Sherratt. Changes in protein synthesis on mitomycin C induction of wild-type and mutant CloDF13 plasmids. *Journal of bacteriology*, 130(2):846–851, may 1977.

485. Jeremy R. Ellermeier and James M. Slauch. Adaptation to the host environment: regulation of the SPI1 type III secretion system in Salmonella enterica serovar Typhimurium. *Current Opinion in Microbiology*, 10(1):24–29, 2007.

486. Don Walthers, Ronan K. Carroll, William Wiley Navarre, Stephen J. Libby, Ferric C. Fang, and Linda J. Kenney. The response regulator SsrB activates expression of diverse Salmonella pathogenicity island 2 promoters and counters silencing by the nucleoid-associated protein H-NS. *Molecular Microbiology*, 65(2):477–493, 2007.

487. Jonathan Frye, Joyce E Karlinsey, Heather R Felise, Bruz Marzolf, Naeem Dowidar, Michael Mcclelland, and Kelly T Hughes. Identification of New Flagellar Genes of Salmonella enterica Serovar Typhimurium. *Society*, 188(6):2233–2243, 2006.

488. Stuti K. Desai, Ricksen S. Winardhi, Saravanan Periasamy, Michal M. Dykas, Yan Jie, and Linda J. Kenney. The horizontally-acquired response regulator SsrB drives a Salmonella lifestyle switch by relieving biofilm silencing. *eLife*, 5(FEBRUARY2016):1–23, 2016.

489. Grace Yim, Joann McClure, Michael G. Surette, and Julian E. Davies. Modulation of Salmonella gene expression by subinhibitory concentrations of quinolones. *Journal of Antibiotics*, 64(1):73–78, 2011.

490. Matthew J. Dorman, Theresa Feltwell, David A. Goulding, Julian Parkhill, and Francesca L. Short. The capsule regulatory network of klebsiella pneumoniae defined by density-traDISort. *mBio*, 9(6), 2018.

491. Lars Barquist, Christine J. Boinett, and Amy K. Cain. Approaches to querying bacterial genomes with transposon-insertion sequencing, 2013.

492. Lauren A. Cowley, Alison S. Low, Derek Pickard, Christine J. Boinett, Timothy J. Dallman, Martin Day, Neil Perry, David L. Gally, Julian Parkhill, Claire Jenkins, and Amy K. Cain. Transposon insertion sequencing elucidates novel gene involvement in susceptibility and resistance to phages T4 and T7 in Escherichia coli O157. *mBio*, 2018.

493. Amy K. Cain, Lars Barquist, Andrew L. Goodman, Ian T. Paulsen, Julian Parkhill, and Tim van Opijnen. A decade of advances in transposon-insertion sequencing, 2020.

494. Tim van Opijnen and Andrew Camilli. Transposon insertion sequencing: a new tool for systems-level analysis of microorganisms sequencing: a new tool for systems-level analysis of microorganisms. Nature Reviews Microbiology, 11(7), 43. *Nature Reviews Microbiology*, 11(7):435–442, 2013.

495. A Keith Turner, Muhammad Yasir, Sarah Bastkowski, Andrea Telatin, Andrew J Page, Ian G Charles, and Mark A Webber. A genome-wide analysis of Escherichia coli responses to fosfomycin using TraDIS-Xpress reveals novel roles for phosphonate degradation and phosphate transport systems. *Journal of Antimicrobial Chemotherapy*, aug 2020.

496. Roy R. Chaudhuri, Eirwen Morgan, Sarah E. Peters, Stephen J. Pleasance, Debra L. Hudson, Holly M. Davies, Jinhong Wang, Pauline M. van Diemen, Anthony M. Buckley, Alison J. Bowen, Gillian D. Pullinger, Daniel J. Turner, Gemma C. Langridge, A. Keith Turner, Julian Parkhill, Ian G. Charles, Duncan J. Maskell, and Mark P. Stevens. Comprehensive Assignment of Roles for Salmonella Typhimurium Genes in Intestinal Colonization of Food-Producing Animals. *PLoS Genetics*, 9(4), 2013.

497. Eveline M. Weerdenburg, Abdallah M. Abdallah, Farania Rangkuti, Moataz Abd El Ghany, Thomas D. Otto, Sabir A. Adroub, Douwe Molenaar, Roy Ummels, Kars ter Veen, Gunny van Stempvoort, Astrid M. van der Sar, Shahjahan Ali, Gemma C.

Langridge, Nicholas R. Thomson, Arnab Pain, and Wilbert Bitter. Genome-wide transposon mutagenesis indicates that Mycobacterium marinum customizes its virulence mechanisms for survival and replication in different hosts. *Infection and Immunity*, 83(5):1778–1788, 2015.

498. Gemma C. Langridge, Minh Duy Phan, Daniel J. Turner, Timothy T. Perkins, Leopold Parts, Jana Haase, Ian Charles, Duncan J. Maskell, Sarah E. Peters, Gordon Dougan, John Wain, Julian Parkhill, and A. Keith Turner. Simultaneous assay of every Salmonella Typhi gene using one million transposon mutants. *Genome Research*, 19(12):2308–2316, 2009.

499. Prerna Vohra, Roy R Chaudhuri, Matthew Mayho, Christina Vrettou, Cosmin Chintoan-Uta, Nicholas R Thomson, Jayne C Hope, John Hopkins, and Mark P Stevens. Retrospective application of transposon-directed insertion-site sequencing to investigate niche-specific virulence of Salmonella Typhimurium in cattle. *BMC genomics*, 20(1):20, jan 2019.

500. Francesca L. Short, Gianna Di Sario, Nathalie T. Reichmann, Colin Kleanthous, Julian Parkhill, and Peter W. Taylor. Genomic Profiling Reveals Distinct Routes To Complement Resistance in Klebsiella pneumoniae. 88(8):1–19, 2020.

501. Michael S Sonnabend, Kristina Klein, Sina Beier, Angel Angelov, Robert Kluj, Christoph Mayer, Caspar Groß, Kathrin Hofmeister, Antonia Beuttner, Matthias Willmann, Silke Peter, Philipp Oberhettinger, Annika Schmidt, Ingo B Autenrieth, Monika Schutz, and Erwin Bohn. Identification of Drug Resistance Determinants in a Clinical Isolate of Pseudomonas aeruginosa by High-Density Transposon. 64(3):1–14, 2020.

502. Samuel Willcocks, Kristin K. Huse, Richard Stabler, Petra C.F. Oyston, Andrew Scott, Helen S. Atkins, and Brendan W. Wren. Genome-wide assessment of antimicrobial tolerance in yersinia pseudotuberculosis under ciprofloxacin stress. *Microbial Genomics*, 5(11), 2019.

503. Rocío Canals, Roy R. Chaudhuri, Rebecca E. Steiner, Siân V. Owen, Natalia Quinones-Olvera, Melita A. Gordon, Michael Baym, Michael Ibba, and Jay C.D. Hinton. The fitness landscape of the African Salmonella Typhimurium ST313 strain D23580 reveals unique properties of the pBT1 plasmid. *PLoS Pathogens*, 15(9):1–29, 2019.

504. Peter D Karp, Richard Billington, Ron Caspi, Carol A Fulcher, Mario Latendresse, Anamika Kothari, Ingrid M Keseler, Markus Krummenacker, Peter E Midford, Quang Ong, Wai Kit Ong, Suzanne M Paley, and Pallavi Subhraveti. The BioCyc collection of microbial genomes and metabolic pathways. *Briefings in Bioinformatics*, 20(4):1085–1093, aug 2017.

505. Ingrid M Keseler, Amanda Mackie, Alberto Santos-Zavaleta, Richard Billington, César Bonavides-Martínez, Ron Caspi, Carol Fulcher, Socorro Gama-Castro, Anamika Kothari, Markus Krummenacker, Mario Latendresse, Luis Muñiz-Rascado, Quang Ong, Suzanne Paley, Martin Peralta-Gil, Pallavi Subhraveti, David A Velázquez-Ramírez, Daniel Weaver, Julio Collado-Vides, Ian Paulsen, and Peter D Karp. The EcoCyc database: reflecting new knowledge about Escherichia coli K-12. *Nucleic Acids Research*, 45(D1):D543–D550, nov 2016.

506. Calvin A Henard and Andrés Vázquez-Torres. DksA-Dependent Resistance of Salmonella enterica Serovar Typhimurium against the Antimicrobial Activity of Inducible Nitric Oxide Synthase. *Infection and Immunity*, pages 1373–1380, 2012.

507. Calvin A Henard, Timothy Tapscott, Matthew A Crawford, Maroof Husain, Paschalisthomas Doulias, Steffen Porwollik, Lin Liu, Michael Mcclelland, Harry Ischiropoulos, and Andrés Vázquez-Torres. The 4-Cysteine Zinc-Finger Motif of the RNA Polymerase Regulator DksA serves as a Thiol Switch for Sensing Oxidative and Nitrosative Stress. *Molecular microbiology*, 91(4):790–804, 2015.

508. Sylvie Baucheron, Franck Coste, Sylvie Canepa, Marie Christine Maurel, Etienne Giraud, Françoise Culard, Bertrand Castaing, Alain Roussel, and Axel Cloeckaert. Binding of the RamR repressor to wild-type and mutated promoters of the ramA gene involved in efflux-mediated multidrug resistance in Salmonella enterica serovar typhimurium. *Antimicrobial Agents and Chemotherapy*, 56(2):942–948, 2012.

509. Masakazu Kaneko, Yoshiko Emoto, and Masashi Emoto. A Simple, Reproducible, Inexpensive, Yet Old-Fashioned Method for Determining Phagocytic and Bactericidal Activities of Macrophages. *Yonsei medical journal*, 57(2):283–290, mar 2016.

510. Jessica L Forbester, Emily A Lees, David Goulding, Sally Forrest, Amy Yeung, Anneliese Speak, Simon Clare, Eve L Coomber, Subhankar Mukhopadhyay, Judith Kraiczy, Fernanda Schreiber, Trevor D Lawley, Robert E W Hancock, Holm H Uhlig, Matthias Zilbauer, Fiona Powrie, and Gordon Dougan. Interleukin-22 promotes phagolysosomal fusion to induce protection against Salmonella enterica Typhimurium in human epithelial cells. *Proceedings of the National Academy of Sciences of the United States of America*, 115(40):10118–10123, oct 2018.

511. Yawei Sun, Guoyong Zhang, Xiaoqing Hou, Shuai Xiao, Xi Yang, Yali Xie, Xiyin Huang, Fan Wang, Xiangtao Mo, Xuezhi Ding, Liqiu Xia, and Shengbiao Hu. SrfABC Toxin from Xenorhabdus stockiae Induces Cytotoxicity and Apoptosis in HeLa Cells. *Toxins*, 11(12), nov 2019.

512. Lei Lei, Wenbiao Wang, Chuan Xia, and Fenyong Liu. Salmonella Virulence Factor SsrAB Regulated Factor Modulates Inflammatory Responses by Enhancing the Activation of NF-κB Signaling Pathway. *The Journal of Immunology*, 196(2):792 LP – 802, jan 2016.

513. E de Leeuw, D Poland, O Mol, I Sinning, C M ten Hagen-Jongman, B Oudega, and J Luirink. Membrane association of FtsY, the E. coli SRP receptor. *FEBS letters*, 416(3):225–229, oct 1997.

514. Markus Peschke, Mélanie Le Goff, Gregory M Koningstein, Alexandros Karyolaimos, Jan-Willem de Gier, Peter van Ulsen, and Joen Luirink. SRP, FtsY, DnaK and YidC Are Required for the Biogenesis of the E. coli Tail-Anchored Membrane Proteins DjlC and Flk. *Journal of molecular biology*, 430(3):389–403, feb 2018.

515. Bimal Jana, Amy K. Cain, William T. Doerrler, Christine J. Boinett, Maria C. Fookes, Julian Parkhill, and Luca Guardabassi. The secondary resistome of multidrug-resistant Klebsiella pneumoniae. *Scientific Reports*, 7(February):1–10, 2017.

516. Derek Pickard, Robert A. Kingsley, Christine Hale, Keith Turner, Karthikeyan Sivaraman, Michael Wetter, Gemma Langridge, and Gordon Dougan. A genomewide mutagenesis screen identifies multiple genes contributing to Vi capsular expression in Salmonella enterica serovar typhi. *Journal of Bacteriology*, 195(6):1320–1326, 2013.

517. Erik Wistrand-Yuen, Michael Knopp, Karin Hjort, Sanna Koskiniemi, Otto G. Berg, and Dan I. Andersson. Evolution of high-level resistance during low-level antibiotic exposure. *Nature Communications*, 9(1):1599, apr 2018.

518. Gábor Apjok, Gábor Boross, Ákos Nyerges, Gergely Fekete, Viktória Lázár, Balázs Papp, Csaba Pál, Bálint Csörgo, and Miriam Barlow. Limited Evolutionary Conservation of the Phenotypic Effects of Antibiotic Resistance Mutations. *Molecular Biology and Evolution*, 36(8):1601–1611, 2019.

519. Tugce Oz, Aysegul Guvenek, Sadik Yildiz, Enes Karaboga, Yusuf Talha Tamer, Nirva Mumcuyan, Vedat Burak Ozan, Gizem Hazal Senturk, Murat Cokol, Pamela Yeh, and Erdal Toprak. Strength of selection pressure is an important parameter contributing to the complexity of antibiotic resistance evolution. *Molecular biology and evolution*, 31(9):2387–2401, sep 2014.

520. Jeffrey B Stewart and Mark A Hermodson. Topology of RbsC, the Membrane Component of the. *Journal of bacteriology*, 185(17):5234–5239, sep 2003.

521. Yongkyu Park and Chankyu Park. Topology of RbsC, a membrane component of the ribose transporter, belonging to the AraH superfamily. *Journal of Bacteriology*, 181(3):1039–1042, 1999.

522. M S Kim, H Oh, C Park, and B H Oh. Crystallization and preliminary X-ray crystallographic analysis of Escherichia coli RbsD, a component of the ribose-transport system with unknown biochemical function. *Acta crystallographica. Section D, Biological crystallography*, 57(Pt 5):728–730, may 2001.

523. Chang jie Chen, Janice E. Chin, Kazumitsu Ueda, Douglas P. Clark, Ira Pastan, Michael M. Gottesman, and Igor B. Roninson. Internal duplication and homology with bacterial transport proteins in the mdr1 (P-glycoprotein) gene from multidrug-resistant human cells. *Cell*, 47(3):381–389, 1986.

524. Ming-Han Tsai, Sih-Ru Wu, Hao-Yuan Lee, Chyi-Liang Chen, Tzou-Yien Lin, Yhu-Chering Huang, and Cheng-Hsun Chiu. Recognition of mechanisms involved in bile resistance important to halting antimicrobial resistance in nontyphoidal Salmonella. *International journal of antimicrobial agents*, 40(2):151–157, aug 2012.

525. J A Yethon, J S Gunn, R K Ernst, S I Miller, L Laroche, D Malo, and C Whitfield. Salmonella enterica serovar typhimurium waaP mutants show increased susceptibility to polymyxin and loss of virulence In vivo. *Infection and immunity*, 68(8):4485–4491, aug 2000.

526. R J Roantree, T T Kuo, and D G MacPhee. The effect of defined lipopolysaccharide core defects upon antibiotic resistances of Salmonella typhimurium. *Journal of general microbiology*, 103(2):223–234, dec 1977.

527. K E Sanderson, T MacAlister, J W Costerton, and K J Cheng. Permeability of lipopolysaccharide-deficient (rough) mutants of Salmonella typhimurium to antibiotics, lysozyme, and other agents. *Canadian journal of microbiology*, 20(8):1135–1145, aug 1974.

528. David L Erickson, Cynthia S Lew, Brittany Kartchner, Nathan T Porter, S Wade McDaniel, Nathan M Jones, Sara Mason, Erin Wu, and Eric Wilson. Lipopolysaccharide Biosynthesis Genes of Yersinia pseudotuberculosis Promote Resistance to Antimicrobial Chemokines. *PloS one*, 11(6):e0157092, 2016.

529. Karl A. Hassan, Amy K. Cain, Taotao Huang, Qi Liu, Liam D.H. Elbourne, Christine J. Boinett, Anthony J. Brzoska, Liping Li, Martin Ostrowski, Nguyen Thi Khanh Nhu, Tran Do Hoang Nhu, Stephen Baker, Julian Parkhill, and Ian T. Paulsen. Fluorescence-based flow sorting in parallel with transposon insertion site sequencing identifies multidrug efflux systems in acinetobacter baumannii. *mBio*, 7(5):3–8, 2016.

530. Erika R. Vlieghe, Thong Phe, Birgit De Smet, Chhun H. Veng, Chun Kham, Sophie Bertrand, Raymond Vanhoof, Lut Lynen, Willy E. Peetermans, and Jan A. Jacobs. Azithromycin and Ciprofloxacin Resistance in Salmonella Bloodstream Infections in Cambodian Adults. *PLoS Neglected Tropical Diseases*, 6(12):e1933, 2012.

531. Balaji Veeraraghavan, Shalini Anandan, Dhiviya Prabaa Muthuirulandi Sethuvel, Nivetha Puratchiveeran, Kamini Walia, and Naveen Kumar Devanga Ragupathi. Molecular Characterization of Intermediate Susceptible Typhoidal Salmonella to Ciprofloxacin, and its Impact. *Molecular Diagnosis and Therapy*, 20(3):213–219, jun 2016.

532. Maha R. Farhat, Luca Freschi, Roger Calderon, Thomas Ioerger, Matthew Snyder, Conor J. Meehan, Bouke de Jong, Leen Rigouts, Alex Sloutsky, Devinder Kaur, Shamil Sunyaev, Dick van Soolingen, Jay Shendure, Jim Sacchettini, and Megan Murray. GWAS for quantitative resistance phenotypes in Mycobacterium tuberculosis reveals resistance genes and regulatory regions. *Nature Communications*, 10(1):2128, 2019.

533. Francesc Coll, Jody Phelan, Grant A. Hill-Cawthorne, Mridul B. Nair, Kim Mallard, Shahjahan Ali, Abdallah M. Abdallah, Saad Alghamdi, Mona Alsomali, Abdallah O. Ahmed, Stephanie Portelli, Yaa Oppong, Adriana Alves, Theolis Barbosa Bessa, Susana Campino, Maxine Caws, Anirvan Chatterjee, Amelia C. Crampin, Keertan Dheda, Nicholas Furnham, Judith R. Glynn, Louis Grandjean, Dang Minh Ha, Rumina Hasan, Zahra Hasan, Martin L. Hibberd, Moses Joloba, Edward C. Jones-López, Tomoshige Matsumoto, Anabela Miranda, David J. Moore, Nora Mocillo, Stefan Panaiotov, Julian Parkhill, Carlos Penha, João Perdigão, Isabel Portugal, Zineb Rchiad, Jaime Robledo, Patricia Sheen, Nashwa Talaat Shesha, Frik A. Sirgel, Christophe Sola, Erivelton Oliveira Sousa, Elizabeth M. Streicher, Paul Van Helden, Miguel Viveiros, Robert M. Warren, Ruth McNerney, Arnab Pain, and Taane G. Clark. Genome-wide analysis of multi- and extensively drug-resistant Mycobacterium tuberculosis. *Nature Genetics*, 50(2):307–316, 2018.

534. Magali Jaillard, Leandro Lima, Maud Tournoud, Pierre Mahé, Alex van Belkum, Vincent Lacroix, and Laurent Jacob. A fast and agnostic method for bacterial genome-wide association studies: Bridging the gap between k-mers and genetic events. *PLoS genetics*, 14(11):e1007758–e1007758, nov 2018.

535. Aurélia Caputo, Pierre Edouard Fournier, and Didier Raoult. Genome and pan-genome analysis to classify emerging bacteria. *Biology Direct*, 14(1):1–9, 2019.

536. Miriam Land, Loren Hauser, Se-Ran Ran Jun, Intawat Nookaew, Michael R. Leuze, Tae-Hyuk Hyuk Ahn, Tatiana Karpinets, Ole Lund, Guruprased Kora, Trudy Wassenaar, Suresh Poudel, and David W. Ussery. Insights from 20 years of bacterial genome sequencing. *Functional and Integrative Genomics*, 15(2):141–161, mar 2015.

537. Erol S. Kavvas, Edward Catoiu, Nathan Mih, James T. Yurkovich, Yara Seif, Nicholas Dillon, David Heckmann, Amitesh Anand, Laurence Yang, Victor Nizet, Jonathan M. Monk, and Bernhard O. Palsson. Machine learning and structural analysis of Mycobacterium tuberculosis pan-genome identifies genetic signatures of antibiotic resistance. *Nature Communications*, 9(1):4306, oct 2018.

538. Tulika Bhardwaj and Pallavi Somvanshi. Pan-genome analysis of Clostridium botulinum reveals unique targets for drug development. *Gene*, 623:48–62, aug 2017.

539. Hsuan Lin Her and Yu Wei Wu. A pan-genome-based machine learning approach for predicting antimicrobial resistance activities of the Escherichia coli strains. *Bioinformatics*, 34(13):i89–i95, 2018.

540. Chad Laing, Cody Buchanan, Eduardo N Taboada, Yongxiang Zhang, Andrew Kropinski, Andre Villegas, James E Thomas, and Victor P J Gannon. Pan-genome sequence analysis using Panseq: an online tool for the rapid analysis of core and accessory genomic regions. *BMC bioinformatics*, 11:461, sep 2010.

541. Gerry Tonkin-Hill, Neil MacAlasdair, Christopher Ruis, Aaron Weimann, Gal Horesh, John A Lees, Rebecca A Gladstone, Stephanie Lo, Christopher Beaudoin, R Andres Floto, Simon D W Frost, Jukka Corander, Stephen D Bentley, and Julian Parkhill. Producing polished prokaryotic pangenomes with the Panaroo pipeline. *Genome biology*, 21(1):180, jul 2020.

542. Ola Brynildsrud, Jon Bohlin, Lonneke Scheffer, and Vegard Eldholm. Rapid scoring of genes in microbial pan-genome-wide association studies with Scoary. *Genome biology*, 17(1):238, nov 2016.

543. Jared D Honeycutt, Nicolas Wenner, Yan Li, Susan M Brewer, Liliana M Massis, Sky W Brubaker, Phoom Chairatana, Siân V Owen, Rocío Canals, Jay C D Hinton, and Denise M Monack. Genetic variation in the MacAB-TolC efflux pump influences pathogenesis of invasive Salmonella isolates from Africa. *PLoS pathogens*, 16(8):e1008763, aug 2020.

544. Pham Thanh Duy, To Nguyen Thi Nguyen, Duong Vu Thuy, Hao Chung The, Felicity Alcock, Christine Boinett, Ho Ngoc Dan Thanh, Ha Thanh Tuyen, Guy E Thwaites, Maia A Rabaa, and Stephen Baker. Commensal Escherichia coli are a reservoir for the transfer of XDR plasmids into epidemic fluoroquinolone-resistant Shigella sonnei. *Nature microbiology*, 5(2):256–264, feb 2020.

545. Keith D. MacKenzie, Yejun Wang, Dylan J. Shivak, Cynthia S. Wong, Leia J.L. Hoffman, Shirley Lam, Carsten Kröger, Andrew D.S. Cameron, Hugh G.G. Townsend, Wolfgang Köster, and Aaron P. White. Bistable expression of CsgD in Salmonella

enterica serovar typhimurium connects virulence to persistence. *Infection and Immunity*, 83(6):2312–2326, 2015.

546. K. Papavasileiou, E. Papavasileiou, A. Tseleni-Kotsovili, S. Bersimis, C. Nicolaou, A. Ioannidis, and S. Chatzipanagiotou. Comparative antimicrobial susceptibility of biofilm versus planktonic forms of Salmonella enterica strains isolated from children with gastroenteritis. *European Journal of Clinical Microbiology & Infectious Diseases*, 29(11):1401–1405, 2010.

547. Chenxi Shi, Minmin Li, Ishfaq Muhammad, Xin Ma, Yicong Chang, Rui Li, Changwen Li, Jingshan He, and Fangping Liu. Combination of berberine and ciprofloxacin reduces multi-resistant Salmonella strain biofilm formation by depressing mRNA expressions of luxS, rpoE, and ompR. *Journal of veterinary science*, 19(6):808–816, nov 2018.

548. Anna Fàbrega, Sara M. Soto, Clara Ballesté-Delpierre, Dietmar Fernández-Orth, M. Teresa Jiménez de Anta, and Jordi Vila. Impact of quinolone-resistance acquisition on biofilm production and fitness in Salmonella enterica. *Journal of Antimicrobial Chemotherapy*, 69(7):1815–1824, 2014.

549. Francesca Micoli, Neil Ravenscroft, Paola Cescutti, Giuseppe Stefanetti, Silvia Londero, Simona Rondini, and Calman A. Maclennan. Structural analysis of O-polysaccharide chains extracted from different Salmonella Typhimurium strains. *Carbohydrate research*, 385:1–8, feb 2014.

550. Neeraj Dhar and John D. McKinney. Microbial phenotypic heterogeneity and antibiotic tolerance. *Current Opinion in Microbiology*, 10(1):30–38, 2007.

551. Beatrice Claudi, Petra Spröte, Anna Chirkova, Nicolas Personnic, Janine Zankl, Nura Schürmann, Alexander Schmidt, and Dirk Bumann. Phenotypic variation of salmonella in host tissues delays eradication by antimicrobial chemotherapy. *Cell*, 158(4):722–733, 2014.

552. Karl Gensberg, Yu Fang Jin, and Laura J V Piddock. A novel gyrB mutation in a fluoroquinolone-resistant clinical isolate of Salmonella Typhimurium. 132:57–60, 1995.

553. Łukasz Mąka, Elżbieta Maćkiw, Monika Stasiak, Tomasz Wołkowicz, Joanna Kowalska, Jacek Postupolski, and Magdalena Popowska. Ciprofloxacin and nalidixic acid resistance of Salmonella spp. isolated from retail food in Poland. *International journal of food microbiology*, 276:1–4, jul 2018.

554. Reetika Debroy, Sravan Kumar Miryala, Aniket Naha, Anand Anbarasu, and Sudha Ramaiah. Microbial Pathogenesis Gene interaction network studies to decipher the multi-drug resistance mechanism in Salmonella enterica serovar Typhi CT18 reveal potential drug targets. *Microbial Pthogenesis*, 142(February):104096, 2020.

555. Joseph Baker, Stephen H Wright, and Florence Tama. Simulations of substrate transport in the multidrug transporter EmrD. 80(6):1620–1632, 2013.

556. Kenneth P Smith, Sanath Kumar, and Manuel F Varela. Identification, cloning, and functional characterization of EmrD-3, a putative multidrug efflux pump of the major facilitator superfamily from Vibrio cholerae O395. *Archives of microbiology*, 191(12):903–911, dec 2009.

557. Kayo Matsumura, Soichi Furukawa, Hirokazu Ogihara, and Yasushi Morinaga. Roles of multidrug efflux pumps on the biofilm formation of Escherichia coli K-12. *Biocontrol science*, 16(2):69–72, jun 2011.

558. L M Weigel, C D Steward, and F C Tenover. gyrA mutations associated with fluoroquinolone resistance in eight species of Enterobacteriaceae. *Antimicrobial agents and chemotherapy*, 42(10):2661–2667, oct 1998.

559. Eirin Esaiassen, Erik Hjerde, Jorunn Pauline Cavanagh, Gunnar Skov Simonsen, Claus Klingenberg, and Norwegian Study Group on Invasive Bifidobacterial Infections. Bifidobacterium Bacteremia: Clinical Characteristics and a Genomic Approach To Assess Pathogenicity. *Journal of clinical microbiology*, 55(7):2234–2248, jul 2017.

560. Amit Katiyar, Priyanka Sharma, Sushila Dahiya, Harpreet Singh, Arti Kapil, and Punit Kaur. Genomic profiling of antimicrobial resistance genes in clinical isolates of Salmonella Typhi from patients infected with Typhoid fever in India. *Scientific reports*, 10(1):8299, may 2020.

561. Danesh Moradigaravand, Martin Palm, Anne Farewell, Ville Mustonen, Jonas Warringer, and Leopold Parts. Prediction of antibiotic resistance in Escherichia coli from large-scale pan-genome data. *PLoS computational biology*, 14(12):1–17, dec 2018.

562. Irani Rathnayake, Megan Hargreaves, and Flavia Huygens. SNP diversity of Enterococcus faecalis and Enterococcus faecium in a South East Queensland waterway, Australia, and associated antibiotic resistance gene profiles. *BMC microbiology*, 11:201, sep 2011.

563. K Fashae, P Leekitcharoenphon, and R S Hendriksen. Phenotypic and genotypic comparison of salmonellae from diarrhoeic and healthy humans and cattle, Nigeria. *Zoonoses and public health*, 65(1):e185–e195, feb 2018.

564. Handuo Shi, Alexandre Colavin, Timothy K Lee, and Kerwyn Casey Huang. Strain Library Imaging Protocol: high-throughput, automated single-cell microscopy for large bacterial collections arrayed on multi-well plates. *Nature protocols*, 12(2):429–438, feb 2018.

565. Jennifer Petitte, Michael Doherty, Jacob Ladd, Cassandra L Marin, Samuel Siles, Vanessa Michelou, Amanda Damon, Erin Quattrini Eckert, Xiang Huang, and John W Rice. Use of high-content analysis and machine learning to characterize complex microbial samples via morphological analysis. *PloS one*, 14(9):e0222528, 2019.

566. Benjamin P Bratton, Brody Barton, and Randy M Morgenstein. Three-dimensional Imaging of Bacterial Cells for Accurate Cellular Representations and Precise Protein Localization. *Journal of visualized experiments : JoVE*, (152), oct 2019.

567. Chen Wang, Peter W. Horby, Frederick G. Hayden, and George F. Gao. A novel coronavirus outbreak of global health concern. *The Lancet*, 395(10223):470–473, 2020.

568. Inna Grosheva, Danping Zheng, Maayan Levy, Omer Polansky, Ofra Golani, Mally Dori-bachash, Claudia Moresi, Hagit Shapiro, Del Mare-roumani, Rafael Valdes-mas, Yiming He, Hodaya Karbi, Minhu Chen, Alon Harmelin, Ravid Straussman, Nissan Yissachar, Eran Elinav, and Benjamin Geiger. High-Throughput Screen Identifies Host and Microbiota Regulators of Intestinal Barrier Function. *Gastroenterology*, 2020.

569. Joanna M Marshall, Alan D Flechtner, Krista M La Perle, and John S Gunn. Visualization of extracellular matrix components within sectioned Salmonella biofilms on the surface of human gallstones. *PloS one*, 9(2):e89243, 2014.

570. J M Goepfert and Ruthann Hicks. Immunofluorescent Staining of Salmonella Species with Flagellar Sera. *Applied Microbiology*, 18(4):612–617, 1969.

571. Shan E Ahmed Raza, Linda Cheung, Muhammad Shaban, Simon Graham, David Epstein, Stella Pelengaris, Michael Khan, and Nasir M Rajpoot. Micro-Net: A unified model for segmentation of various objects in microscopy images. *Medical image analysis*, 52:160–173, feb 2019.

572. Layla M Malt, Charlotte A Perrett, Suzanne Humphrey, and Mark A Jepson. Applications of microscopy in Salmonella research. *Methods in molecular biology (Clifton, N.J.)*, 1225:165–198, 2015.

573. Aravindan Varadarajan, Felix Oswald, and Yves J M Bollen. Single-Molecule Imaging of Escherichia coli Transmembrane Proteins BT - Single Molecule Analysis: Methods and Protocols. pages 135–144. Springer New York, New York, NY, 2018.

574. Anne Plochowietz, Ian Farrell, Zeev Smilansky, Barry S Cooperman, and Achillefs N Kapanidis. In vivo single-RNA tracking shows that most tRNA diffuses freely in live bacteria. *Nucleic acids research*, 45(2):926–937, jan 2017.

575. Kimberly M Davis and Ralph R Isberg. Defining heterogeneity within bacterial populations via single cell approaches. *BioEssays*, 38(8):782–790, aug 2016.

576. María Antonia Sánchez-Romero and Josep Casadesús. Contribution of phenotypic heterogeneity to adaptive antibiotic resistance. 111(1):355–360, 2014.

577. Linus Sandegren and Dan I Andersson. Bacterial gene amplification: implications for the evolution of antibiotic resistance. *Nature reviews. Microbiology*, 7(8):578–588, aug 2009.

578. R P Anderson and J R Roth. Tandem genetic duplications in phage and bacteria. *Annual review of microbiology*, 31:473–505, 1977.

579. Elisa Rodríguez Tarazona, José Ángel García Rodríguez, and Juan Luis Muñoz Bellido. Emergence of quinolone-resistant, topoisomerase-mutant Brucella after treatment with fluoroquinolones in a macrophage experimental infection model. *Enfermedades infecciosas y microbiologia clinica*, 33(4):248–252, apr 2015.

580. Maritza Barcia-Macay, Cristina Seral, Marie-Paule Mingeot-Leclercq, Paul M Tulkens, and Françoise Van Bambeke. Pharmacodynamic Evaluation of the Intracellular Activities of Antibiotics against Staphylococcus aureus in a Model of THP-1 Macrophages. *Antimicrobial Agents and Chemotherapy*, 50(3):841–851, 2006.

581. P Rajagopalan-Levasseur, E Dournon, G Dameron, J L Vilde, and J J Pocidalo. Comparative postantibacterial activities of pefloxacin, ciprofloxacin, and ofloxacin against intracellular multiplication of Legionella pneumophila serogroup 1. *Antimicrobial agents and chemotherapy*, 34(9):1733–1738, sep 1990.

582. Béatrice Marquez, Nancy E Caceres, Marie-Paule Mingeot-Leclercq, Paul M Tulkens, and Françoise Van Bambeke. Identification of the efflux transporter of the fluoroquinolone antibiotic ciprofloxacin in murine macrophages: studies with ciprofloxacin-resistant cells. *Antimicrobial agents and chemotherapy*, 53(6):2410–2416, jun 2009.

583. Coralie M Vallet, Béatrice Marquez, Naïma Nhiri, Ahalieyah Anantharajah, Marie-Paule Mingeot-Leclercq, Paul M Tulkens, Jean-Yves Lallemand, Eric Jacquet, and Françoise Van Bambeke. Modulation of the expression of ABC transporters in murine (J774) macrophages exposed to large concentrations of the fluoroquinolone antibiotic moxifloxacin. *Toxicology*, 290(2-3):178–186, dec 2011.

584. M S Sanchez, C W Ford, and R J Jr Yancey. Effect of tumor necrosis factor-alpha, interleukin-1 beta, and antibiotics on the killing of intracellular Staphylococcus aureus. *Journal of dairy science*, 77(5):1251–1258, may 1994.

585. Ricardo A Mosquera, Wilfredo De Jesus-Rojas, James M Stark, Aravind Yadav, Cindy K Jon, Constance L Atkins, Cheryl L Samuels, Traci R Gonzales, Katrina E McBeth, Syed S Hashmi, Roberto Garolalo, and Giuseppe N Colasurdo. Role of prophylactic azithromycin to reduce airway inflammation and mortality in a RSV mouse infection model. *Pediatric pulmonology*, 53(5):567–574, may 2018.

586. Henglin Yang, Jingyan Wang, Hui Liu, Xingliang Li, Renhua Nie, Chunfu Li, Hengye Wang, Qinghu Wang, Yaming Cao, and Liwang Cui. Randomized, Double-Blind, Placebo-Controlled Studies to Assess Safety and Prophylactic Efficacy of Naphthoquine-Azithromycin Combination for Malaria Prophylaxis in Southeast Asia. *Antimicrobial agents and chemotherapy*, 62(9), sep 2018.

587. J. D. Keenan, R. L. Bailey, S. K. West, A. M. Arzika, J. Hart, J. Weaver, K. Kalua, Z. Mrango, K. J. Ray, C. Cook, E. Lebas, K. S. O'Brien, P. M. Emerson, T. C. Porco, and T. M. Lietman. Azithromycin to reduce childhood mortality in sub-Saharan Africa. *New England Journal of Medicine*, 378(17):1583–1592, 2018.

588. Michael J Parnham, Vesna Erakovic Haber, Evangelos J Giamarellos-Bourboulis, Gianpaolo Perletti, Geert M Verleden, and Robin Vos. Azithromycin: mechanisms of action and their relevance for clinical applications. *Pharmacology & therapeutics*, 143(2):225–245, aug 2014.

589. Syh-Jae Lin, Ming-Ling Kuo, Hsiu-Shan Hsiao, and Pei-Tzu Lee. Azithromycin modulates immune response of human monocyte-derived dendritic cells and CD4(+) T cells. *International immunopharmacology*, 40:318–326, nov 2016.

590. Theodore J Cory, Susan E Birket, Brian S Murphy, Cynthia Mattingly, Jessica M Breslow-Deckman, and David J Feola. Azithromycin increases in vitro fibronectin production through interactions between macrophages and fibroblasts stimulated with Pseudomonas aeruginosa. *The Journal of antimicrobial chemotherapy*, 68(4):840–851, apr 2013.

591. Magali Meyer, François Huaux, Ximena Gavilanes, Sybille van den Brûle, Patrick Lebecque, Sandra Lo Re, Dominique Lison, Bob Scholte, Pierre Wallemacq, and Teresinha Leal. Azithromycin reduces exaggerated cytokine production by M1 alveolar macrophages in cystic fibrosis. *American journal of respiratory cell and molecular biology*, 41(5):590–602, nov 2009.

592. Tommi Mäklin, Teemu Kallonen, Sophia David, Christine J. Boinett, Ben Pascoe, Guillaume Méric, David M. Aanensen, Edward J. Feil, Stephen Baker, Julian Parkhill, Samuel K. Sheppard, Jukka Corander, and Antti Honkela. High-resolution sweep metagenomics using fast probabilistic inference. *Wellcome Open Research*, 5:14, 2020.

References for COVID-19

593. Xiaoquan Lai, Minghuan Wang, Chuan Qin, Li Tan, Lusen Ran, Daiqi Chen, Han Zhang, Ke Shang, Chen Xia, Shaokang Wang, Shabei Xu, and Wei Wang. Coronavirus Disease 2019 (COVID-2019) Infection Among Health Care Workers and Implications for Prevention Measures in a Tertiary Hospital in Wuhan, China. *JAMA network open*, 3(5):e209666–e209666, may 2020.

594. Hongzhou Lu, Charles W Stratton, and Yi-Wei Tang. Outbreak of pneumonia of unknown etiology in Wuhan, China: The mystery and the miracle. *Journal of Medical Virology*, 92(4):401–402, apr 2020.

595. Chen Wang, Peter W. Horby, Frederick G. Hayden, and George F. Gao. A novel coronavirus outbreak of global health concern. *The Lancet*, 395(10223):470–473, 2020.

596. Robert Verity, Lucy C Okell, Ilaria Dorigatti, Peter Winskill, Charles Whittaker, Natsuko Imai, Gina Cuomo-Dannenburg, Hayley Thompson, Patrick G T Walker, Han Fu, Amy Dighe, Jamie T Griffin, Marc Baguelin, Sangeeta Bhatia, Adhiratha Boonyasiri, Anne Cori, Zulma Cucunubá, Rich FitzJohn, Katy Gaythorpe, Will Green, Arran Hamlet, Wes Hinsley, Daniel Laydon, Gemma Nedjati-Gilani, Steven Riley, Sabine van Elsland, Erik Volz, Haowei Wang, Yuanrong Wang, Xiaoyue Xi, Christl A Donnelly, Azra C Ghani, and Neil M Ferguson. Estimates of the severity of coronavirus disease 2019: a model-based analysis. *The Lancet. Infectious diseases*, 20(6):669–677, jun 2020.

597. Susan Lee, Paula Meyler, Michelle Mozel, Tonia Tauh, and Richard Merchant. Asymptomatic carriage and transmission of SARS-CoV-2: What do we know? *Canadian journal of anaesthesia = Journal canadien d'anesthesie*, pages 1–7, jun 2020.

598. World Health Organization (WHO). Coronavirus Disease 2019 Situation Report 51 - 11th March 2020. *World Health Organization*, 2019(March):2633, 2020.

599. BMJ Best Practice. Coronavirus disease 2019 (COVID-19) Situation Report â23.03.2020. *World Health Organization*, 2019(March):2633, 2020.

600. Victor M Corman, Olfert Landt, Marco Kaiser, Richard Molenkamp, Adam Meijer, Daniel Kw Chu, Tobias Bleicker, Sebastian Brünink, Julia Schneider, Marie Luisa Schmidt, Daphne Gjc Mulders, Bart L Haagmans, Bas van der Veer, Sharon van den

Brink, Lisa Wijsman, Gabriel Goderski, Jean-Louis Romette, Joanna Ellis, Maria Zambon, Malik Peiris, Herman Goossens, Chantal Reusken, Marion Pg Koopmans, and Christian Drosten. Detection of 2019 novel coronavirus (2019-nCoV) by real-time RT-PCR. *Euro surveillance : bulletin Europeen sur les maladies transmissibles = European communicable disease bulletin*, 25(3):2000045, jan 2020.

601. Yi-Wei Tang, Jonathan E Schmitz, David H Persing, and Charles W Stratton. Laboratory Diagnosis of COVID-19: Current Issues and Challenges. *Journal of clinical microbiology*, 58(6), may 2020.

602. Yicheng Fang, Huangqi Zhang, Jicheng Xie, Minjie Lin, Lingjun Ying, Peipei Pang, and Wenbin Ji. Sensitivity of Chest CT for COVID-19: Comparison to RT-PCR. *Radiology*, 296(2):E115–E117, feb 2020.

603. Günter Mayer, Jens Müller, and Christina E Lünse. RNA diagnostics: real-time RT-PCR strategies and promising novel target RNAs. *WIREs RNA*, 2(1):32–41, jan 2011.

604. Public Health England. COVID-19: safe handling and processing for laboratories. pages 1–6, 2020.

605. Zhiruo Zhang, Shelan Liu, Mi Xiang, Shijian Li, Dahai Zhao, Chaolin Huang, and Saijuan Chen. Protecting healthcare personnel from 2019-nCoV infection risks: lessons and suggestions. *Frontiers of medicine*, 14(2):229–231, apr 2020.

606. Catherine F Houlihan, Nina Vora, Thomas Byrne, Dan Lewer, Gavin Kelly, Judith Heaney, Sonia Gandhi, Moira J Spyer, Rupert Beale, Peter Cherepanov, David Moore, Richard Gilson, Steve Gamblin, George Kassiotis, Laura E McCoy, Charles Swanton, Crick COVID-19 Consortium, Andrew Hayward, Eleni Nastouli, and SAFER Investigators. Pandemic peak SARS-CoV-2 infection and seroconversion rates in London frontline health-care workers. *Lancet (London, England)*, 396(10246):e6–e7, jul 2020.

607. Martina Ferioli, Cecilia Cisternino, Valentina Leo, Lara Pisani, Paolo Palange, and Stefano Nava. Protecting healthcare workers from SARS-CoV-2 infection: practical indications. *European respiratory review : an official journal of the European Respiratory Society*, 29(155), mar 2020.

608. John Willan, Andrew John King, Katie Jeffery, and Nicola Bienz. Challenges for NHS hospitals during covid-19 epidemic., mar 2020.

609. Alexandra Teslya, Thi Mui Pham, Noortje G Godijk, Mirjam E Kretzschmar, Martin C J Bootsma, and Ganna Rozhnova. Impact of self-imposed prevention measures and short-term government-imposed social distancing on mitigating and delaying a COVID-19 epidemic: A modelling study. *PLoS medicine*, 17(7):e1003166, jul 2020.

610. Lei Zhang, Yusha Tao, Mingwang Shen, Christopher K Fairley, and Yuming Guo. Can self-imposed prevention measures mitigate the COVID-19 epidemic? *PLoS medicine*, 17(7):e1003240, jul 2020.

611. R Boom, C J Sol, M M Salimans, C L Jansen, P M Wertheim-van Dillen, and J van der Noordaa. Rapid and simple method for purification of nucleic acids. *Journal of clinical microbiology*, 28(3):495–503, mar 1990.

612. Sushmita Sridhar, Sally Forrest, Iain Kean, Jamie Young, Josefin Bartholdson Scott, Mailis Maes, Joana Pereira-Dias, Surendra Parmar, Matthew Routledge, Lucy Rivett, Gordon Dougan, Michael Weekes, Martin Curran, Ian Goodfellow, and Stephen Baker. A blueprint for the implementation of a validated approach for the detection of SARS-Cov2 in clinical samples in academic facilities. *bioRxiv*, page 2020.04.14.041319, 2020.

613. Lucy Rivett, Sushmita Sridhar, Dominic Sparkes, Matthew Routledge, Nick K Jones, Sally Forrest, Jamie Young, Joana Pereira-Dias, William L Hamilton, Mark Ferris, M Estee Torok, Luke Meredith, Ravi Gupta, Paul A Lyons, Mark Toshner, Ben Warne, Josefin Bartholdson Scott, Claire Cormie, Harmeet Gill, Iain Kean, Mailis Maes, Nicola Reynolds, Michelle Wantoch, Sarah Caddy, Laura Caller, Theresa Feltwell, Grant Hall, Myra Hosmillo, Charlotte Houldcroft, Aminu Jahun, Fahad Khokhar, Anna Yakovleva, Helen Butcher, Daniela Caputo, Debra Clapham-Riley, Helen Dolling, Anita Furlong, Barbara Graves, Emma Le Gresley, Nathalie Kingston, Sofia Papadia, Hannah Stark, Kathleen E Stirrups, Jennifer Webster, Joanna Calder, Julie Harris, Sarah Hewitt, Jane Kennet, Anne Meadows, Rebecca Rastall, Criona O Brien, Jo Price, Cherry Publico, Jane Rowlands, Valentina Ruffolo, Hugo Tordesillas, Karen Brookes, Laura Canna, Isabel Cruz, Katie Dempsey, Anne Elmer, Naidine Escoffery, Heather Jones, Carla Ribeiro, Caroline Saunders, Angela Wright, Rutendo Nyagumbo, Anne Roberts, Ashlea Bucke, Simone Hargreaves, Danielle Johnson, Aileen Narcorda, Debbie Read, Christian Sparke, Lucy Warboys, Kirsty Lagadu, Lenette Mactavous, Tim Gould, Tim Raine, Claire Mather, Nicola Ramenatte, Anne-Laure Vallier, Mary Kasanicki, Penelope-Jane Eames, Chris McNicholas, Lisa Thake, Neil Bartholomew, Nick Brown, Surendra Parmar, Hongyi Zhang, Ailsa Bowring, Geraldine Martell, Natalie Quinnell, Jo Wright, Helen Murphy, Benjamin J Dunmore, Ekaterina Legchenko, Stefan Gräf, Christopher Huang, Josh Hodgson, Kelvin Hunter, Jennifer Martin, Federica Mescia, Ciara O'Donnell, Linda Pointon, Joy Shih, Rachel Sutcliffe, Tobias Tilly, Zhen Tong, Carmen Treacy, Jennifer Wood, Laura Bergamaschi, Ariana Betancourt, Georgie Bowyer, Aloka De Sa, Maddie Epping, Andrew Hinch, Oisin Huhn, Isobel Jarvis, Daniel Lewis, Joe Marsden, Simon McCallum, Francescsa Nice, Martin D Curran, Stewart Fuller, Afzal Chaudhry, Ashley Shaw, Richard J Samworth, John R Bradley, Gordon Dougan, Kenneth Gc Smith, Paul J Lehner, Nicholas J Matheson, Giles Wright, Ian G Goodfellow, Stephen Baker, and Michael P Weekes. Screening of healthcare workers for SARS-CoV-2 highlights the role of asymptomatic carriage in COVID-19 transmission. *eLife*, 9, may 2020.

614. Nick K Jones, Lucy Rivett, Dominic Sparkes, Sally Forrest, Sushmita Sridhar, Jamie Young, Joana Pereira-dias, Claire Cormie, Harmeet Gill, Nicola Reynolds, Michelle Wantoch, Matthew Routledge, Ben Warne, Jack Levy, William David Co, Michael Gill, The Citiid-nihr Covid-Bioresource Collaboration, John R Bradley, Gregory J Hannon, Ian G Goodfellow, Gordon Dougan, Stephen Baker, and Michael P Weekes. Effective control of SARS-CoV-2 transmission between healthcare workers during a period of diminished community prevalence of COVID-19. *eLife*, pages 1–10, 2020.

615. Luke W Meredith, William L Hamilton, Ben Warne, Charlotte J Houldcroft, Myra Hosmillo, Aminu S Jahun, Martin D Curran, Surendra Parmar, Laura G Caller, Sarah L Caddy, Fahad A Khokhar, Anna Yakovleva, Grant Hall, Theresa Feltwell, Sally Forrest, Sushmita Sridhar, Michael P Weekes, Stephen Baker, Nicholas Brown, Elinor Moore,

Ashley Popay, Iain Roddick, Mark Reacher, Theodore Gouliouris, Sharon J Peacock, Gordon Dougan, M Estée Török, Ian Goodfellow, M Estee Torok, and Ian Goodfellow. Rapid implementation of SARS-CoV-2 sequencing to investigate cases of healthcare associated COVID-19 : a prospective genomic surveillance study. *The Lancet. Infectious diseases*, 3099(20), jul 2020.

616. Mailis Maes, Ellen Higginson, Joana Pereira Dias, Martin D Curran, Surendra Parmar, Fahad Khokhar, Delphine Cuchet-Lourenço, Janine Lux, Sapna Sharma-Hajela, Benjamin Ravenhill, Razeen Mahroof, Amelia Solderholm, Sally Forrest, Sushmita Sridhar, Nicholas M Brown, Stephen Baker, Vilas Navapurkar, Gordon Dougan, Josefin Bartholdson Scott, and Andrew Conway Morris. Secondary pneumonia in critically ill ventilated patients with COVID-19. *medRxiv*, page 2020.06.26.20139873, jan 2020.

Supplementary Materials and Methods

The materials and methods described here expand on those introduced in Chapter 2.

DNA extractions using the Promega Wizard DNA Purification Kit

Bacterial pellets were resuspended in 600 μl Nucleic Lysis Solution, pipetted, incubated at 80°C, then cooled. 3 μl RNAse Solution was added, mixed, and incubated at 37°C for 15-60 m. After cooling, 200 μl of Protein Precipitation Solution was added and vortexed then incubated on ice for 5 m before centrifugation at 13,000 x g for 3 m. Supernatant was transferred to a tube of 600 μl isopropanol and mixed. Cells were centrifuged and supernatant decanted. 600 μl of 70% ethanol was added and mixed then centrifuged again. Ethanol was aspirated and pellets were air-dried for 10-15 m. Pellets were rehydrated for 1 h at 65°C in 100 μl Rehydration Solution.

***S.* Typhimurium D23580 bacteria grown for 24 h in ciprofloxacin medium for whole genome sequencing**

Detailed protocol of the three methods of bacterial growth of *S.* Typhimurium D23580 bacteria grown for 24 h in ciprofloxacin medium, following from **section 2.4**.

1. The first method used was intended to capture all bacterial DNA (from live and dead cells) in the culture at 24 h. One ml of each 0x or 1x ciprofloxacin MIC-treated culture was taken at time 0 and then after 24 h. Given a high density of bacteria, each 1 ml sample was spun down at 8000 x *g* for 3 min to collect bacteria before DNA was extracted as previously described . 10 ml of the 2x and 4x ciprofloxacin MIC-treated cultures were aliquoted into 50 ml Falcon tubes, and these were spun down at 4000 rpm for 7 min at 4°C. The supernatant was decanted, and the pellet was resuspended in the remaining medium. This was transferred to a 1.5 ml microfuge tube and spun again at 8000 rpm for 3 min, and then the supernatant was aspirated and pellet was ready for DNA extraction.

2. The second method of DNA extraction was intended to capture DNA from viable cells after 24 h growth as a population. For the 0x and 1x ciprofloxacin MIC 24 h cultures, 100 μl of the 24 h bacterial cultures were spread onto agar plates to do a plate sweep of all viable CFU[592]. For the 2x and 4x ciprofloxacin MIC cultures, 1000 μl was spread on agar plates. After overnight growth at 37°C, colonies were carefully scraped from the agar and resuspended in 1x PBS. This was spun down at 8000 rpm for 3 min, and the supernatant was aspirated off. The pellets were processed for DNA extraction.

3. The third method of 24 h growth was intended to identify and grow individual representative colonies viable to determine whether there are colony-specific stable genetic differences after ciprofloxacin-treatment. A dilution of 100 μl of each 24 h culture (1:100 of 0x and 1x, neat of 2x and 4x) was spread on agar plates. Plates were incubated at 37°C overnight. Three single colonies were taken from each plate and inoculated in 5 ml Isosensitest broth. Cultures were grown shaking at 200 rpm at 37°C for 6 h. 1 ml was removed and centrifuged at 8000 rpm for 3 min before the supernatant was aspirated. Pellets were processed for DNA extraction.

Whole genome sequencing: library creation and sequencing

Detailed protocol of library creation and sequencing at the Wellcome Sanger Institute, from **section 2.5**. Samples were quantified with Biotium Accuclear Ultra high sensitivity dsDNA Quantitative kit using the Mosquito LV liquid platform, Bravo WS and BMG FLUOstar Omega plate reader, and samples were cherrypicked to 200 ng /120 μl using Tecan liquid handling platform. Cherrypicked samples were sheared to 450 bp using a Covaris LE220 instrument. Post sheared samples were purified using Agencourt AMPure XP SPRI beads on the Agilent Bravo WS. Library construction was performed (ER, A-tailing and ligation) using 'NEB Ultra II custom kits' on an Agilent Bravo WS automation system. PCR was set up using KapaHiFi Hot start mix and IDT 96 iPCR tag barcodes on the Agilent Bravo WS automation system. The PCR cycles were as follows using 6 standard cycles:

- Incubate 95°C for 5 min
- Incubate 98°C for 30 sec
- Incubate 65°C for 30 sec

- 72°C for 1 min
- Cycle from 2, 5 more times
- Incubate 72°C for 10 min

The post PCR plate was purified using Agencourt AMPure XP SPRI beads (Beckman Coulter, A63882) on a Beckman BioMek NX96 liquid handling platform. Libraries were quantified with Biotium Accuclear Ultra high sensitivity dsDNA Quantitative kit using the Mosquito LV liquid handling platform, Bravo WS and BMG FLUOstar Omega plate reader. Libraries were pooled in equimolar amounts on a Beckman BioMek NX-8 liquid handling platform. Libraries were then normalised to 2.8nM ready for cluster generation on a c-BOT and loading on the requested Illumina sequencing platform.

Generation of *S.* Typhimurium D23580 single-gene knockout derivatives

Detailed methodology of *S.* Typhimurium D23580 single-gene knockout derivatives generation, from **section 2.11**. After primer design for the five single-gene knockouts (**Table 2.4**), copies of each gene were cloned independently into plasmid pKD4 carrying a kanamycin resistance cassette[376]. To amplify and purify the DNA fragments for each gene, AccuPrime Taq DNA Polymerase was used (Invitrogen, cat no. 12346094) for the PCR, with 30 cycles using an annealing temperature of 56°C for 5 cycles followed by an annealing temperature of 65°C for 25 cycles. This was followed by 10 minutes at 68°C. Once amplified, PCR products were purified by running on a 1% TAE agarose gel. DNA was extracted from gels using the Promega Wizard SV Gel and PCR Clean-Up System (Promega, cat no. A9281). The DNA pellet was washed in 70% ethanol and stored while semi-dry at -20°C or 4°C for subsequent use.

To produce electrocompetent *S.* Typhimurium D23580 cells, an overnight culture of D23580 was prepared in 5 ml LB and shaken at 37°C. 1 ml of the overnight culture was added the following day to 100 ml LB and incubated shaking at 37°C for $\sim$ 2 h until an OD600 of 0.3-0.5 was obtained. Cells were heat-shocked in a 42°C heat block for 15 min and then cooled on ice for 5 minutes. Cells were centrifuged at 4000 rpm for 10 min at 4°C. The cell pellets were resuspended in 100 ml of chilled 10% glycerol and centrifuged. The addition of glycerol and centrifugation were repeated before pellets were resuspended to a final volume of 180 μl in chilled 10% glycerol. The pSIM18 vector carrying the lambda

Red recombinase system was electroporated into *S.* Typhimurium D23580 using 200 ng pSIM18 DNA at 2.5 kV, 200 ohms, 25 μF (Ec2 on BioRad MicroPulser, using 0.2 gap cuvettes). 800 μl of warmed SOC medium was added to electroporation cuvettes, and cells were incubated for 2 h at 30°C to recover. Bacteria were then plated on L-agar containing 150 μg/ml hygromycin and incubated at 30°C overnight to grow. Six colonies were selected and re-grown on hygromycin plates. These colonies were stored at -80°C until use. The *S.* Typhimurium D23580::pSIM18 strain was used to create the mutant derivatives.

To prepare *S.* Typhimurium D23580::pSIM18 for electroporation, an overnight culture was grown overnight (in regular low-salt LB 10 ml with 150 μg/ml hygromycin) and then diluted 1:100 the next day in 200 ml of low salt LB plus 100 μg/ml Hygromycin B (Invitrogen) and incubated for 3 hrs, shaking at 30°C until the culture attained an OD590 of 0.4. To activate the recombinase, the culture was aliquoted into 4 x 50 ml volumes and placed at 42°C in a water bath for 15 minutes and then cooled on ice for 10 minutes. The culture was centrifuged for 10 min at 2500 x g (4000 rpm) and the pellet was washed twice in 50 ml aliquots of ice cold 10% glycerol (the culture was recentrifuged for 10 min at 2500 x g (4000 rpm)). The pellet was transferred to a 1.5 ml tube and the volume was increased to 1.4 ml with glycerol and spun for 20-30 sec at 8000 rpm. The cell pellet was finally resuspended in 320 μl of 10% glycerol and electroporated with 500 ng DNA for each mutant derivative in a precooled 2 mm electroporation cuvette under conditions specified above. Cells were then incubated in 700 μl of pre-warmed SOC outgrowth medium (New England Biolabs) at 37°C for 2 h. Separately, 20 μl of the cell pellet was incubated in 700 μl of SOC to use as a cellular control. 4 x 10 μl aliquots were plated onto 33 μg/ml Kanamycin (Km) and 50 μg/ml Chloramphenicol (Cm) (Life technologies)-containing L-agar plates and grown overnight at 37°C. The remaining volume was left at room temperature overnight and plated on 33 μg/ml Kanamycin (plus Chloramphenicol as before)-containing L agar plates (to allow more time for recombination overnight) and left to grow at 37°C.

Individual colonies that grew on the agar plates after approximately 18 hours were re-plated onto fresh plates and re-grown at 37°C. Upon growth, 6-12 colonies that grew well were inoculated in 10 ml L-agar for overnight growth at 42°C shaking at 200 rpm. The broth was plated out on Km Cm containing L-agar plates, and the same isolates were also streaked on hygromycin plates (600 μl of 50 mg/ml stock in 200 ml media). Plates were incubated overnight at 37°C. The following day, colonies should only have grown on Km Cm plates, and these colonies were re-inoculated for PCR. Colonies were prepared for PCR by boiling

for 5 min. The PCR master mix was as follows using the AccuPrime Taq DNA Polymerase (Invitrogen, 12346094):

- 5 μl of Accuprime High Fid Buffer I
- 1 μl of Forward Primer
- 1 μl of Reverse Primer
- 0.3 μl of Accuprime Taq DNA Polymerase
- 33 μl of sterile water

The PCR cycle used was: 94°C 3 min 1 cycle. 94°C 30 sec, 54°C 30 sec, 68°C 1 min- 30 cycles. 68°C 10 min 1 cycle.

4 μl of each sample was run on a 0.9% TAE agarose gel, and bands were assessed.

Intestinal organoid processing after infection with transposon mutant library

Detailed methodology of intestinal organoid processing, from **section 2.13**. Intestinal organoids were prepared as described previously by Lees *et al.*[378]. Using the same *S.* Typhimurium D23580 TraDIS library as described in section **section 2.12**, 50 μl of the library was inoculated in 10 ml LB containing 15 μg/ml Kanamycin and incubated shaking at 37°C overnight. The following day, the bacterial OD600 was measured, and bacterial concentration was adjusted to a multiplicity of infection of 10:1 in 1 ml PBS and 500 μl phenol red. For each biological replicate, 60 organoids were microinjected with bacteria and incubated at 37°C for 90 minutes. Media was aspirated from organoid plates after incubation and replaced with 3 ml cell recovery solution for 45 minutes at 4°C. Organoids in recovery solution were aspirated from plates into a 15 ml tube containing 5 ml PBS. Tubes of organoids were centrifuged for 3 minutes at 1500 rpm. The supernatant was aspirated, and organoids were resuspended in BMS media containing gentamicin and incubated at 37°C for 1 h. Organoids were centrifuged for 3 minutes at 1500 rpm, and the supernatant was aspirated. 50 μl of 1% Triton-X-100 was added to 5 ml PBS and warmed to dissolve before use as lysis buffer. The organoids were washed 1x with PBS and centrifuged again before resuspension in 500 μl lysis buffer and pipetting 20x to break up organoids. Cells were left

at room temperature for 5 minutes to further lyse. An additional 1 min spin at 1200 rpm was performed to separate organoids and bacteria. Serial dilutions were performed and plated to calculate CFU and grow bacteria for TraDIS screening.

Scanning electron microscopy (SEM) of bacteria grown under stress conditions

Detailed methodology of sample processing for scanning electron microscopy, from **section 2.17**. Colonies were first fixed on agar with 2.5% (1:10) GA and 2% (1:3) PFA in 0.05M sodium cacodylate buffer for 1 hour. Samples were rinsed in 0.05 M (or 0.1 M) sodium cacodylate buffer 3x 5 min. A secondary fix in osmium tetroxide solution in sodium cacodylate buffer for 3 hours was performed after removal of colony regions of interest. Alternation of osmium tetroxide and thiocarbohydrazide washes was then carried out:

- Buffer rinses 2x 20 min
- 1% aq thiocarbohydrazide 10 min
- Buffer rinses 3x 10min
- 1% osmium tetroxide 30 min
- dd.H_2O washes 3x 10 min
- 1% aq thiocarbohydrazide 10 min
- dd.H_2O washes 3x 10 min
- 1% osmium tetroxide 30 min
- dd.H_2O washes 3x 10 min

Samples were then dehydrated in an ethanol series of 30%, 50%, 70%, 90%, 3x 100% for 20 min each. A critical point dry then took place in a Leica CPD300. Samples were mounted onto aluminium stubs with silver dag, sputter coated in a Leica ACE600, and then dried in a vacuum drying cabinet. Samples were visualized using a Hitachi SU-8000 scanning electron microscope.

Isolate	Sanger Lane ID	Country	Year	MIC to ciprofloxacin (µg/ml)	Thesis chapter used in
D23580	Salmonella_enterica_subsp_enterica_serovar_Typhimurium_str_D23580_v1.2	Malawi	2004	0.03	3-7
SL1344		UK	1960s	0.015	3-5,7
VNS20081	7969_2#94	Vietnam	2009	1.0	3-5
5390_4	22709_8#181	DRC	2016	0.5	4,5,7
2735	22709_8#96	DRC	2008	0.25	7
10433_3	L10433_3_L001	DRC	2014	0.03	7
9412_3	L9412_3_L001	DRC	2014	0.03	7
2101	2101_R1_P_trim	DRC	2008	0.032	7
9266_3	9266_3_R1_P_trim	DRC	2014	0.032	7
12299_3	L12299_3_L001	DRC	2015	0.032	7
6948_3	26189_8#73	DRC	2002	0.032	7
10055_3	10055_3_R1_P_trim	DRC	2014	0.032	7
8866_3	8866_3_R1_P_trim	DRC	2014	0.023	7
12155_3	L12155_3_L001	DRC	2015	0.016	7
10393_3	10393_3_R1_P_trim	DRC	2014	0.032	7
8599_13	22709_8#227	DRC	2013	0.023	7
2643	22709_8#95	DRC	2008	0.023	7
319_8	25692_2#134	DRC	2008	0.25	7
10018	25692_2#162	DRC	2008	0.032	7
6452_11	22709_8#189	DRC	2011	0.5	7
453_08	22709_8#173	DRC	2008	0.023	7
1577	22709_8#86	DRC	2009	0.016	7
9085_3	22709_8#259	DRC	2014	0.016	7
1304	25692_2#149	DRC	2009	0.023	7
6088_3	22709_8#187	DRC	2012	0.032	7
6549_3	22709_8#190	DRC	2013	0.047	7
8314_12	22709_8#220	DRC	2012	0.19	7
9227_14	25692_2#79	DRC	2014	0.032	7
861	25692_2#141	DRC	2008	0.023	7
857	22709_8#76	DRC	2008	0.023	7
05_157	22709_8#243	DRC	2005	0.016	7
8429_3	22709_8#222	DRC	2014	0.023	7
8795_13	25692_2#71	DRC	2013	0.012	7
3382_3	22709_8#152	DRC	2011	0.023	7
7239_11	22709_8#198	DRC	2011	0.19	7
7236_11	25692_2#194	DRC	2011	0.032	7
6941_11	25692_2#188	DRC	2011	0.016	7
1303	25692_2#150	DRC	2009	0.012-0.016	7
5326_3	22709_8#179	DRC	2012	0.002	7

1563	25692_2#144	DRC	2009	0.023	7
1515	22709_8#84	DRC	2009	0.19	7
3484_3	25692_2#176	DRC	2011	0.023	7
P0494 S80	P0494_S80	Burkina Faso	2013	0.032	7
N0629	25692_2#82	Burkina Faso	2014	0.023	7
2407/N0487 H	25692_2#81	Burkina Faso	2014	0.023	7
P0114	25692_2#74	Burkina Faso	2013	0.032	7
N0084	25692_2#73	Burkina Faso	2013	0.047	7
AA00050	22709_8#65	Rwanda	1984	0.016	7
AA00279	22709_8#46	Rwanda	1984	0.016	7
AA00271	22709_8#47	Rwanda	1984	0.016	7
AA00065	25692_2#237	Rwanda	1984	0.023	7
AA00324	22709_8#44	Rwanda	1984	0.016	7
AA000104	25692_2#232	Rwanda	1984	0.016	7
N0442 S114	N0442_S114	Burkina Faso	2014	0.016	7
AA00512	22709_8#30	Rwanda	1984	0.023	7
AA00489	22709_8#36	Rwanda	1984	0.023	7
bkf00707	16404_4#76	Burkina Faso	2013	0.032	7
gnb00628	16404_4#79	Guinea-Bissau	2012	0.016	7
gnb00588	16404_4#43	Guinea-Bissau	2012	0.016	7
gha113848	16404_5#66	Ghana	2011	0.25	7
gnb01487	16399_1#19	Guinea-Bissau	2013	0.016	7
gha113018	16549_7#28	Ghana	2010	0.023	7
gha113289	16404_5#25	Ghana	2011	0.75	7
gha200597	16404_5#26	Ghana	2011	0.016	7
gha113988	16399_3#33	Ghana	2010	0.032	7
gha114575	16473_1#72	Ghana	2011	0.016	7
gha114348	16404_5#30	Ghana	2010	0.032	7
gha113920	16404_5#49	Ghana	2011	0.016	7

Table A.1 All *S.* Typhimurium isolates used in this thesis.

Isolate	Ciprofloxacin MIC
bkf00707	0.032
gnb00628	0.016
gnb00588	0.016
gha113848	0.25
gnb01487	0.016
gha113018	0.023
gha113289	0.75
gha200597	0.016
gha113988	0.032
gha114575	0.016
gha114348	0.032
gha113920	0.016
8599_13	0.023
2643	0.023
319_8	0.25
10018	0.032
6452_11	0.5
453_08	0.023
1577	0.016
9085_3	0.016
1304	0.023
6088_3	0.032
6549_3	0.047
8314_12	0.19

Table A.2 *S.* Typhimurium ST313 isolates phenotyped on the Opera Phenix.

Supplementary Information to Chapter 3 Opera Phenix phenotyping

The tables here provide details associated with **Chapter 3**.

Species	Isolate ID	Coating
S. Typhimurium	NCTC 13347	Thick Collagen
S. Typhimurium	NCTC 13348	Matrigel
S. Typhimurium	D23580	Vitronectin

Table B.1. Final plate coatings chosen for isolates used in Opera Phenix imaging.

Input Image	Input		
	Flatfield Correction: Basic Brightfield Correction **Stack Processing**: Maximum Projection (*for non-adherent isolates, individual planes were analysed*) **Min. Global Binning**: Dynamic		
Filter Image	Input	Method	Output
	Channel : DAPI	**Method** : Texture SER Filter : SER Ridge Scale : 1 px Normalization by : Kernel	Output Image : SER Ridge
Find Image Region	Input	Method	Output
	Channel: SER Ridge **ROI**: None	Method : Common Threshold Threshold : 0.4 Split into Objects Area : > 100 px²	Output Population : Image Region Output Region : Image Region
Calculate Intensity Properties	Input	Method	Output
	Channel : SER Ridge **Population** : Image Region **Region** : Image Region	**Method** : Standard Mean	Property Prefix : Intensity Image Region SER Ridge
Select Population	Input	Method	Output
	Population : Image Region	**Method** Filter by Property Intensity Image Region SER Ridge Mean : > 0.02	Output Population : Image Region Selected
Select Region	Input	Method	Output
	Population : Image Region Selected **Region** : Image Region	**Method** : Resize Region [µm/px] Outer Border : -4µm Restrictive Population : None Restrictive Region : Keep Image Border Inner Border : INF µm	Output Population : Image Region Resized
Select Region (2)	Input	Method	Output
	Population : Image Region Selected **Region** : Image Region Resized	**Method** : Standard Border Filled Region : INF µm²	Property Prefix : Image Region Resized

Select Region (3)	Input	Method	Output
	Population : Image Region Selected **Region** : Image Region Resized Filled	**Method** : Resize Region [µm/px] Outer Border : 4 px Restrictive Population : None Restrictive Region : Keep Image Border Inner Border : INF px	Output Population : Image Region Resized Filled Resized
Modify Population	Input	Method	Output
	Population : Image Region Selected Region : Image Region Resized Filled Resized	**Method** : Cluster by Distance Distance : 0 px Area : > 0 px²	Output Population : Modified Image Region Selected Output Region : Modified Image Region
Select Population (2)	Input	Method	Output
	Population : Modified Image Region Selected	**Method** : Common Filters Remove Border Objects Region : Modified Image Region	Output Population : Modified Image Region Selected Border Removed
Calculate Image	Input	Method	Output
		Method : By Formula Formula : 100*(A-300)+100*(B-300) Channel A : DAPI Channel B : FM4-64 Negative Values : Set to Zero Undefined Values : Set to Local Average	Output Image : Calculated Image
Find Spots	Input	Method	Output
	Channel : Calculated Image **ROI** : Modified Image Region Selected Border Removed **ROI Region** : Modified Image Region	**Method** : D Detection Sensitivity : 0.5 Splitting Sensitivity : 0.1 Background Correction : 0.5 Calculate Spot Properties	Output Population : Spots
Calculate Morphology Properties	Input	Method	Output
	Population : Spots **Region** : Spot	**Method** : Standard Area Roundness	Property Prefix : Spot
Select Population (3)	Input	Method	Output
	Population : Spot	**Method** Filter by Property Spot Area [px²] : > 1	Output Population : bacteria
Calculate Morphology Properties (2)	Input	Method	Output
	Population : bacteria **Region** : Spot	**Method** : Standard Area Roundness Width Length Ratio Width to Length	Property Prefix : bacteria
Calculate Morphology Properties (3)	Input	Method	Output
	Population : bacteria **Region** : Spot	**Method** : STAR Channel : DAPI Symmetry Threshold Compactness	Property Prefix : Bacteria DAPI

		Axial Radial Profile Profile Width : 3 px **Sliding Parabola** Curvature : 10 **Texture SER** Scale : 1 px Normalization by : Kernel	
Calculate Morphology Properties (4)	Input	Method	Output
	Population : bacteria **Region** : Spot	**Method** : STAR Channel : FM4-64 Symmetry Threshold Compactness Axial Radial Profile Profile Width : 3 px **Sliding Parabola** Curvature : 10 **Texture SER** Scale : 1 px Normalization by : Kernel	Property Prefix : Bacteria FM4-64
Calculate Morphology Properties (5)	Input	Method	Output
	Population : bacteria **Region** : Spot	**Method** : STAR Channel : SYTOX green Symmetry Threshold Compactness Axial Radial Profile Profile Width : 3 px **Sliding Parabola** Curvature : 10 **Texture SER** Scale : 1 px Normalization by : Kernel	Property Prefix : Bacteria SYTOX green
Calculate Intensity Properties (3)	Input	Method	Output
	Channel : SYTOX green **Population** : bacteria **Region** : Spot	**Method** : Standard Mean Standard Deviation	Property Prefix : Intensity Spot SYTOX green
Select Population (4)	Input	Method	Output
	Population : bacteria	**Method** Linear Classifier Number of Classes : 3 Relative Spot Intensity Corrected Spot Intensity Uncorrected Spot Peak Intensity Spot Contrast Spot Background Intensity Spot Area [px²] Region Intensity Spot to Region Intensity Spot Area [µm²] Spot Roundness bacteria Area [µm²] bacteria Roundness bacteria Width [µm] bacteria Length [µm] bacteria Ratio Width to Length Bacteria DAPI Symmetry 02 Bacteria DAPI Symmetry 03 Bacteria DAPI Symmetry 04 Bacteria DAPI Symmetry 05 Bacteria DAPI Symmetry 12 Bacteria DAPI Symmetry 13 Bacteria DAPI Symmetry 14	Output Population A : Single Cells Output Population B : Dividing Cells Output Population C : Other

		Bacteria DAPI Symmetry 15 Bacteria DAPI Threshold Compactness 30% Bacteria DAPI Threshold Compactness 40% Bacteria DAPI Threshold Compactness 50% Bacteria DAPI Threshold Compactness 60% Bacteria DAPI Axial Small Length Bacteria DAPI Axial Length Ratio Bacteria DAPI Radial Mean Bacteria DAPI Radial Relative Deviation Bacteria DAPI Profile 1/2 Bacteria DAPI Profile 2/2 Bacteria FM4-64 Symmetry 02 Bacteria FM4-64 Symmetry 03 Bacteria FM4-64 Symmetry 04 Bacteria FM4-64 Symmetry 05 Bacteria FM4-64 Symmetry 12 Bacteria FM4-64 Symmetry 13 Bacteria FM4-64 Symmetry 14 Bacteria FM4-64 Symmetry 15 Bacteria FM4-64 Threshold Compactness 30% Bacteria FM4-64 Threshold Compactness 40% Bacteria FM4-64 Threshold Compactness 50% Bacteria FM4-64 Threshold Compactness 60% Bacteria FM4-64 Axial Small Length Bacteria FM4-64 Axial Length Ratio Bacteria FM4-64 Radial Mean Bacteria FM4-64 Radial Relative Deviation Bacteria FM4-64 Profile 1/2 Bacteria FM4-64 Profile 2/2 Bacteria Sytox Symmetry 02 Bacteria Sytox Symmetry 03 Bacteria Sytox Symmetry 04 Bacteria Sytox Symmetry 05 Bacteria Sytox Symmetry 12 Bacteria Sytox Symmetry 13 Bacteria Sytox Symmetry 14 Bacteria Sytox Symmetry 15 Bacteria Sytox Threshold Compactness 30% Bacteria Sytox Threshold Compactness 40% Bacteria Sytox Threshold Compactness 50% Bacteria Sytox Threshold Compactness 60% Bacteria Sytox Axial Small Length Bacteria Sytox Axial Length Ratio Bacteria Sytox Radial Mean Bacteria Sytox Radial Relative Deviation Bacteria Sytox Profile 1/2 Bacteria Sytox Profile 2/2 Bacteria Sytox Symmetry 02 SP-Filter Bacteria Sytox Symmetry 03 SP-Filter Bacteria Sytox Symmetry 04 SP-Filter Bacteria Sytox Symmetry 05 SP-Filter Bacteria Sytox Symmetry 12 SP-Filter	

		Bacteria Sytox Symmetry 13 SP-Filter Bacteria Sytox Symmetry 14 SP-Filter Bacteria Sytox Symmetry 15 SP-Filter Bacteria Sytox Threshold Compactness 30% SP-Filter Bacteria Sytox Threshold Compactness 40% SP-Filter Bacteria Sytox Threshold Compactness 50% SP-Filter Bacteria Sytox Threshold Compactness 60% SP-Filter Bacteria Sytox Axial Small Length SP-Filter Bacteria Sytox Axial Length Ratio SP-Filter Bacteria Sytox Radial Mean SP-Filter Bacteria Sytox Radial Relative Deviation SP-Filter Bacteria Sytox Radial Mean Ratio SP-Filter Bacteria Sytox Profile 1/2 SP-Filter Bacteria Sytox Profile 2/2 SP-Filter Intensity Spot SYTOX green Mean Intensity Spot SYTOX green StdDev	

Table B.2. Gram-negative rods analysis pipeline (Harmony v4.9).

Species	ID	Ampicillin	Azithromycin	Trimethoprim-sulfamethoxazole	Ciprofloxacin	Gentamicin	Rifampicin	Meropenem	Tigecycline	Cefuroxime	Oxacillin	Vancomycin
***S.* Typhimurium**	NCTC 13347	0.5	2	0.25	0.012	2	16	0.125	0.19	3	ND	ND
***S.* Typhimurium**	NCTC 13348	>256*	3	0.25	0.012	3	24	0.064	0.19	3	ND	ND

Table B.3. Antimicrobials and determined MICs used for Opera Phenix imaging optimization.

Parameter	Z '
Single_cells - Bacteria_CSA Symmetry 14 - StdDev per Well	0.953
Single_cells - Bacteria_CSA Symmetry 04 - StdDev per Well	0.942
Single_cells - FITC_dead Radial Mean - Mean per Well	0.939
Single_cells - Bacteria_CSA Symmetry 15 - Mean per Well	0.938
Single_cells - Bacteria DAPI Symmetry 15 - Mean per Well	0.935
Single_cells - Bacteria_CSA Symmetry 04 - Mean per Well	0.934
Single_cells - Bacteria_CSA Radial Relative Deviation - Mean per Well	0.933
Single_cells - Bacteria_CSA Symmetry 02 - Mean per Well	0.93
Single_cells - Bacteria_CSA Symmetry 12 - Mean per Well	0.921
Single_cells - Bacteria_CSA Symmetry 14 - Mean per Well	0.918
Single_cells - Bacteria_CSA Threshold Compactness 60% - Mean per Well	0.918
Single_cells - Bacteria_CSA Threshold Compactness 40% - Mean per Well	0.917
Single_cells - Bacteria_CSA Axial Length Ratio - Mean per Well	0.916
Single_cells - Bacteria_CSA Threshold Compactness 30% - Mean per Well	0.913
Single_cells - Bacteria_CSA Radial Mean - Mean per Well	0.9
Single_cells - Bacteria_CSA Threshold Compactness 50% - Mean per Well	0.897
Single_cells - bacteria Roundness - Mean per Well	0.896
Single_cells - Spot Roundness - Mean per Well	0.896
Single_cells - Bacteria DAPI Symmetry 14 - StdDev per Well	0.893
Single_cells - FITC_dead Symmetry 04 - StdDev per Well	0.892
Single_cells - Bacteria DAPI Threshold Compactness 60% - Mean per Well	0.891
Single_cells - bacteria Length [µm] - Mean per Well	0.889
Single_cells - FITC_dead Symmetry 15 - Mean per Well	0.886
Single_cells - bacteria Ratio Width to Length - Mean per Well	0.878
Single_cells - Bacteria DAPI Symmetry 05 - Mean per Well	0.875
Single_cells - Bacteria DAPI Radial Mean - Mean per Well	0.874
Single_cells - Bacteria DAPI Symmetry 04 - StdDev per Well	0.871
Single_cells - Bacteria DAPI Threshold Compactness 40% - Mean per Well	0.869
Single_cells - Bacteria DAPI Threshold Compactness 50% - Mean per Well	0.862
Single_cells - FITC_dead Threshold Compactness 60% - Mean per Well	0.859
Single_cells - FITC_dead Radial Relative Deviation - Mean per Well	0.855
Single_cells - FITC_dead Symmetry 14 - StdDev per Well	0.838
Single_cells - Bacteria DAPI Symmetry 04 - Mean per Well	0.837
Single_cells - Bacteria DAPI Threshold Compactness 30% - Mean per Well	0.836
Single_cells - Bacteria DAPI Symmetry 14 - Mean per Well	0.827
Single_cells - Bacteria DAPI Symmetry 03 - Mean per Well	0.826
Single_cells - FITC_dead Symmetry 05 - StdDev per Well	0.823
Single_cells - Bacteria DAPI Axial Length Ratio - Mean per Well	0.818
Single_cells - Bacteria DAPI Radial Relative Deviation - Mean per Well	0.794
Single_cells - Bacteria DAPI Symmetry 12 - Mean per Well	0.792
Single_cells - Bacteria DAPI Symmetry 02 - Mean per Well	0.789
Single_cells - Bacteria_CSA Symmetry 05 - Mean per Well	0.767

Single_cells - FITC_dead Symmetry 14 - Mean per Well	0.763
Single_cells - FITC_dead Axial Length Ratio - Mean per Well	0.763
Single_cells - Bacteria DAPI Radial Relative Deviation - StdDev per Well	0.757
Single_cells - FITC_dead Symmetry 04 - Mean per Well	0.746
Single_cells - FITC_dead Threshold Compactness 50% - Mean per Well	0.745
Single_cells - bacteria Area [µm²] - Mean per Well	0.744
Single_cells - Spot Area [µm²] - Mean per Well	0.744
Single_cells - FITC_dead Symmetry 03 - StdDev per Well	0.724
Single_cells - FITC_dead Symmetry 05 - Mean per Well	0.723
Single_cells - FITC_dead Symmetry 12 - Mean per Well	0.719
Single_cells - FITC_dead Threshold Compactness 40% - Mean per Well	0.698
Single_cells - Bacteria DAPI Symmetry 15 - StdDev per Well	0.692
Single_cells - FITC_dead Symmetry 02 - Mean per Well	0.679
Single_cells - Bacteria_CSA Symmetry 15 - StdDev per Well	0.668
Single_cells - FITC_dead Radial Relative Deviation - StdDev per Well	0.659
Single_cells - bacteria Ratio Width to Length - StdDev per Well	0.653
Single_cells - FITC_dead Threshold Compactness 30% - Mean per Well	0.639
Single_cells - Bacteria_CSA Symmetry 02 - StdDev per Well	0.638
Single_cells - Bacteria DAPI Threshold Compactness 60% - StdDev per Well	0.59
Single_cells - Bacteria_CSA Threshold Compactness 60% - StdDev per Well	0.585
Single_cells - Bacteria_CSA Threshold Compactness 50% - StdDev per Well	0.556
Single_cells - Bacteria DAPI Threshold Compactness 50% - StdDev per Well	0.543
Single_cells - Bacteria DAPI Threshold Compactness 40% - StdDev per Well	0.499
Single_cells - Bacteria_CSA Radial Relative Deviation - StdDev per Well	0.486
Single_cells - Bacteria DAPI Symmetry 05 - StdDev per Well	0.47
Single_cells - FITC_dead Threshold Compactness 40% - StdDev per Well	0.436
Single_cells - FITC_dead Threshold Compactness 30% - StdDev per Well	0.427
Single_cells - Bacteria_CSA Symmetry 05 - StdDev per Well	0.425
Single_cells - Bacteria DAPI Threshold Compactness 30% - StdDev per Well	0.395
Single_cells - FITC_dead Threshold Compactness 60% - StdDev per Well	0.394
Single_cells - Spot Roundness - StdDev per Well	0.383
Single_cells - bacteria Roundness - StdDev per Well	0.383
Single_cells - Bacteria_CSA Threshold Compactness 30% - StdDev per Well	0.366
Single_cells - Bacteria_CSA Profile 1/2 - Mean per Well	0.351
Round_cells - Number of Objects	0.346
Single_cells - Bacteria_CSA Threshold Compactness 40% - StdDev per Well	0.34
Single_cells - FITC_dead Profile 2/2 - Mean per Well	0.314

Single_cells - Bacteria DAPI Symmetry 02 - StdDev per Well	0.269
Single_cells - Bacteria DAPI Profile 2/2 - Mean per Well	0.266
Single_cells - FITC_dead Symmetry 03 - Mean per Well	0.263
Single_cells - FITC_dead Threshold Compactness 50% - StdDev per Well	0.252
Single_cells - FITC_dead Symmetry 15 - StdDev per Well	0.184
Round_cells - bacteria Ratio Width to Length - Mean per Well	0.178
Single_cells - Bacteria_CSA Profile 2/2 - Mean per Well	0.049
Single_cells - FITC_dead Symmetry 02 - StdDev per Well	0.029
Single_cells - Bacteria DAPI Profile 1/2 - StdDev per Well	0.024
Single_cells - bacteria Area [µm²] - StdDev per Well	-0.018
Single_cells - Spot Area [µm²] - StdDev per Well	-0.018
Single_cells - bacteria Length [µm] - StdDev per Well	-0.038
Single_cells - Bacteria DAPI Symmetry 13 - Mean per Well	-0.055
Single_cells - Bacteria_CSA Symmetry 13 - Mean per Well	-0.06
Single_cells - Bacteria_CSA Profile 2/2 - StdDev per Well	-0.077
Single_cells - Intensity Spot Fluorescein (FITC) StdDev - StdDev per Well	-0.116
Spots Selected - Number of Objects	-0.123
Spots - Number of Objects	-0.158
Single_cells - Bacteria_CSA Axial Length Ratio - StdDev per Well	-0.238
Single_cells - Bacteria DAPI Profile 1/2 - Mean per Well	-0.259
Single_cells - FITC_dead Axial Length Ratio - StdDev per Well	-0.26
Single_cells - Bacteria_CSA Radial Mean - StdDev per Well	-0.381
Single_cells - Bacteria DAPI Profile 2/2 - StdDev per Well	-0.386
Single_cells - Bacteria_CSA Symmetry 03 - Mean per Well	-0.463
Single_cells - FITC_dead Profile 1/2 - Mean per Well	-0.494
Other (2) - Number of Objects	-0.505
Single_cells - FITC_dead Symmetry 13 - Mean per Well	-0.577
Single_cells - Bacteria DAPI Radial Mean - StdDev per Well	-0.589
Single_cells - Number of Objects	-0.638
Round_cells - bacteria Length [µm] - Mean per Well	-0.659
Single_cells - Bacteria_CSA Symmetry 12 - StdDev per Well	-0.713
Single_cells - Single_cells_live - Mean per Well	-0.719
Single_cells - Bacteria DAPI Axial Length Ratio - StdDev per Well	-0.755
Single_cells_live - Number of Objects	-0.755
Single_cells - Intensity Spot Fluorescein (FITC) Mean - StdDev per Well	-0.776
Single_cells - Bacteria_CSA Symmetry 03 - StdDev per Well	-0.793
Single_cells - bacteria Width [µm] - StdDev per Well	-0.797
Single_cells - Single_cells_live - StdDev per Well	-0.83
Single_cells - FITC_dead Profile 2/2 - StdDev per Well	-1.201
Single_cells - FITC_dead Radial Mean - StdDev per Well	-1.284
Single_cells - Intensity Spot DAPI StdDev - Mean per Well	-1.446
Round_cells - bacteria Ratio Width to Length - StdDev per Well	-1.684
Single_cells - Intensity Spot DAPI StdDev - StdDev per Well	-1.733

Single_cells - FITC_dead Symmetry 12 - StdDev per Well	-1.938
Single_cells - Bacteria_CSA Symmetry 13 - StdDev per Well	-2.106
Single_cells - Bacteria DAPI Symmetry 13 - StdDev per Well	-2.551
Round_cells - bacteria Length [µm] - StdDev per Well	-2.788
Single_cells - bacteria Width [µm] - Mean per Well	-2.998
Single_cells - Bacteria_CSA Profile 1/2 - StdDev per Well	-3.416
Single_cells - Intensity Spot DAPI Mean - StdDev per Well	-3.708
Single_cells - Bacteria DAPI Symmetry 03 - StdDev per Well	-3.92
Single_cells - Bacteria DAPI Axial Small Length - Mean per Well	-3.931
bacteria - Number of Objects	-3.98
Single_cells - FITC_dead Profile 1/2 - StdDev per Well	-4.04
Single_cells - FITC_dead Axial Small Length - Mean per Well	-4.552
Single_cells - FITC_dead Symmetry 13 - StdDev per Well	-4.962
Round_cells - bacteria Width [µm] - Mean per Well	-6.17
Round_cells - bacteria Area [µm²] - StdDev per Well	-6.651
Single_cells - Bacteria_CSA Axial Small Length - Mean per Well	-9.78
Round_cells - bacteria Width [µm] - StdDev per Well	-10.228
Round_cells - bacteria Area [µm²] - Mean per Well	-10.389
Single_cells - Intensity Spot Fluorescein (FITC) StdDev - Mean per Well	-13.553
Single_cells - Intensity Spot DAPI Mean - Mean per Well	-14.798
Single_cells - Bacteria_CSA Axial Small Length - StdDev per Well	-30.091
Single_cells - Bacteria DAPI Symmetry 12 - StdDev per Well	-50.256
Single_cells - Bacteria DAPI Axial Small Length - StdDev per Well	-53.794
Single_cells - Intensity Spot Fluorescein (FITC) Mean - Mean per Well	-844.663
Single_cells - FITC_dead Axial Small Length - StdDev per Well	-3258.365

Table B.4. Z' statistics of *S.* Typhimurium D23580 treated for 2 h with 2x MIC ciprofloxacin versus no treatment.